

Global Methane Budget 2000-2020

Marielle [Saunois](#)¹, [Adrien Martinez](#)¹, [Benjamin Poulter](#)², [Zhen Zhang](#)^{3,4}, [Peter A. Raymond](#)⁵, [Pierre Regnier](#)⁶, [Josep G. Canadell](#)⁷, [Robert B. Jackson](#)⁸, [Prabir K. Patra](#)^{9,10}, [Philippe Bousquet](#)¹, [Philippe Ciais](#)¹, [Edward J. Dlugokencky](#)¹¹, [Xin Lan](#)^{11,12}, [George H. Allen](#)¹³, [David Bastviken](#)¹⁴, [David J. Beerling](#)¹⁵, [Dmitry A. Belikov](#)¹⁶, [Donald R. Blake](#)¹⁷, [Simona Castaldi](#)¹⁸, [Monica Crippa](#)^{19,20}, [Bridget R. Deemer](#)²¹, [Fraser Dennison](#)²², [Giuseppe Etiope](#)^{23,24}, [Nicola Gedney](#)²⁵, [Lena Höglund-Jaksson](#)²⁶, [Meredith A. Holgerson](#)²⁷, [Peter O. Hopcroft](#)²⁸, [Gustaf Hugelius](#)²⁹, [Akihiko Ito](#)³⁰, [Atul K. Jain](#)³¹, [Rajesh Janardanan](#)³², [Matthew S. Johnson](#)³³, [Thomas Kleinen](#)³⁴, [Paul B. Krummel](#)²², [Ronny Lauerwald](#)³⁵, [Tingting Li](#)³⁶, [Xiangyu Liu](#)³⁷, [Kyle C. McDonald](#)³⁸, [Joe R. Melton](#)³⁹, [Jens Mühle](#)⁴⁰, [Jurek Müller](#)⁴¹, [Fabiola Murguía-Flores](#)⁴², [Yosuke Niwa](#)^{32,43}, [Sergio Noce](#)⁴⁴, [Shufen Pan](#)⁴⁵, [Robert J. Parker](#)⁴⁶, [Changhui Peng](#)^{47,48}, [Michel Ramonet](#)¹, [William J. Riley](#)⁴⁹, [Gerard Rocher-Ros](#)⁵⁰, [Judith A. Rosentretter](#)⁵¹, [Motoki Sasakawa](#)³², [Arjo Segers](#)⁵², [Steven J. Smith](#)^{53,54}, [Emily H. Stanley](#)⁵⁵, [Joël Thanwerdas](#)^{56,*}, [Hanqin Tian](#)⁵⁷, [Aki Tsuruta](#)⁵⁸, [Francesco N. Tubiello](#)⁵⁹, [Thomas S. Weber](#)⁶⁰, [Guido R. van der Werf](#)⁶¹, [Douglas E. J. Worthy](#)⁶², [Yi Xi](#)¹, [Yukio Yoshida](#)³², [Wenxin Zhang](#)⁶³, [Bo Zheng](#)^{64,65}, [Qing Zhu](#)⁴⁹, [Qian Zhu](#)⁶⁶, and [Qianlai Zhuang](#)³⁷

¹Laboratoire des Sciences du Climat et de l'Environnement, LSCE-IPSL (CEA-CNRS-UVSQ), Université Paris-Saclay 91191 Gif-sur-Yvette, France

²NASA Goddard Space Flight Center, Biospheric Science Laboratory, Greenbelt, MD 20771, USA

³National Tibetan Plateau Data Center (TPDC), State Key Laboratory of Tibetan Plateau Earth System, Environment and Resource (TPESER), Institute of Tibetan Plateau Research, Chinese Academy of Sciences, Beijing, 100101, China

⁴Earth System Science Interdisciplinary Center, University of Maryland, College Park, MD 20740, USA

⁵Yale School of the Environment, Yale University, New Haven, CT 06511, USA

⁶Department Geoscience, Environment & Society (BGEOSYS), Université Libre de Bruxelles, 1050 Bruxelles, Belgium

⁷Global Carbon Project, CSIRO Environment, Canberra, ACT 2601, Australia

⁸Department of Earth System Science, Woods Institute for the Environment, and Precourt Institute for Energy, Stanford University, Stanford, CA 94305-2210, USA

⁹Research Institute for Global Change, JAMSTEC, 3173-25 Showa-machi, Kanazawa, Yokohama, 236-0001, Japan

¹⁰Research Institute for Humanity and Nature, Kyoto 6038047, Japan

¹¹NOAA Global Monitoring Laboratory, 325 Broadway, Boulder, CO 80305, USA

¹²Cooperative Institute for Research in Environmental Sciences, University of Colorado Boulder, CO 80303, USA

¹³Department of Geosciences, Virginia Polytechnic Institute and State University, Blacksburg, VA, USA

¹⁴Department of Thematic Studies – Environmental Change, Linköping University, 581 83 Linköping, Sweden

¹⁵School of Biosciences, University of Sheffield, UK

¹⁶Center for Environmental Remote Sensing, Chiba University, Chiba, 263-8522, Japan

¹⁷Department of Chemistry, University of California Irvine, 570 Rowland Hall, Irvine, CA 92697, USA

¹⁸Dipartimento di Scienze Ambientali, Biologiche e Farmaceutiche, Università degli Studi della Campania Luigi

Définition du style ... [1]

Supprimé: The ...lobal Methane Budget 2000-2017 ... [2]

Supprimé: Saunois¹, Ann R. Stavert², Ben Poulter³, Philippe Bousquet¹, ...aunois¹, Adrien Martinez¹, Benjamin Poulter², Zhen Zhang^{3,4}, Peter A. Raymond⁵, Pierre Regnier⁶, Josep G. Canadell⁷, ...anadell⁷, Robert B. Jackson¹, Peter A. Raymond⁵, Edward J. Dlugokencky⁸, Sander Houweling^{7,8} ... [3]

Mis en forme : Police :12 pt

Supprimé: Ciais¹, Vivek K. Arora¹¹, ...ousquet¹, Philippe Ciais¹, Edward J. Dlugokencky¹¹, Xin Lan^{11,12}, George H. Allen¹³, David Bastviken¹², Peter Bergamaschi¹³, ...astviken¹⁴, David J. Beerling¹⁵, Dmitry A. Belikov¹⁶, Donald R. Blake¹⁴, Gordon Brailsford¹⁵, Lori Bruhwiler⁶, Kimberly M. Carlson^{16,17}, Mark Carrol³ ... [4]

Mis en forme ... [5]

Supprimé: 19

Mis en forme : Police :12 pt

Supprimé: Naveen Chandra⁹, Cyril Crevoisier²¹, Patrick M. Crill²², Kristofer Covey²³, Charles L. Curry²⁴, ...ridget R. Deemer²¹, Fraser Dennison²², Giuseppe Etiope^{25,26}, Christian ... [6]

Mis en forme : Police :12 pt

Supprimé: Aki Tsuruta⁶⁰ Nicolas Viovy¹, Apostolos ... [7]

Mis en forme : Police :10 pt

Supprimé: 2Global Carbon Project, CSIRO Oceans and ... [8]

Mis en forme ... [9]

Supprimé: 4Department

Mis en forme : Retrait : Gauche : 0 cm

Supprimé: 5School of Forestry and Environmental Studies, Yale ... [10]

Mis en forme ... [11]

Mis en forme : Police :10 pt

Supprimé: 10 Center

Mis en forme ... [12]

Supprimé: Remote Sensing, Chiba...ciences, University, Chiba ... [13]

Mis en forme : Police :8 pt

Supprimé: 11Canadian Centre for Climate Modelling and ... [14]

Mis en forme ... [15]

Supprimé: 13European Commission Joint Research Centre, Via ... [16]

Mis en forme ... [17]

Mis en forme ... [18]

Supprimé: Irvine

Mis en forme ... [19]

Supprimé: 15National Institute of Water and Atmospheric ... [20]

Mis en forme : Police :10 pt

204	Vanvitelli, via Vivaldi 43, 81100 Caserta, Italy	Mis en forme ... [21]
205	¹⁹ European Commission, Joint Research Centre (JRC), Ispra, Italy	Supprimé: ¹⁹ Department of Landscape Design and Sustainable...
206	²⁰ Unisystems S.A., Milan, Italy	Mis en forme ... [24]
207	²¹ U.S. Geological Survey, Southwest Biological Science Center, Flagstaff, AZ, USA	Supprimé: Sciences and Bolin Centre for Climate Research,...
208	²² CSIRO Environment, Aspendale, Victoria 3195, Australia	Mis en forme ... [26]
209	²³ Istituto Nazionale di Geofisica e Vulcanologia, Sezione Roma 2, via V. Murata 605 00143 Rome, Italy	Mis en forme ... [23]
210	²⁴ Faculty of Environmental Science and Engineering, Babes Bolyai University, Cluj-Napoca, Romania	Supprimé: ²⁴ School of Earth and Ocean Sciences, University of
211	²⁵ Met Office Hadley Centre, Joint Centre for Hydrometeorological Research, Maclean Building, Wallingford	Mis en forme ... [28]
212	OX10 8BB, UK	Supprimé: ²⁶ Faculty
213	²⁶ Pollution Management Group (PM), International Institute for Applied Systems Analysis (IIASA), 2361	Supprimé: ²⁷ Division of Geological and Planetary Sciences,...
214	Laxenburg, Austria	Supprimé: ³⁰ Department of Meteorology, University of ... [30]
215	²⁷ Department of Ecology & Evolutionary Biology, Cornell University, Ithaca, NY, USA	Mis en forme ... [31]
216	²⁸ School of Geography, Earth & Environmental Sciences, University of Birmingham, UK	Supprimé: ³² Department
217	²⁹ Department of Physical Geography and Bolin Centre for Climate Research, Stockholm University, 106 91	Mis en forme ... [32]
218	Stockholm, Sweden	Mis en forme ... [33]
219	³⁰ Graduate School of Agricultural and Life Sciences, The University of Tokyo, Tokyo, Japan	Supprimé: ³³ Center for Global Environmental Research
220	³¹ Department of Atmospheric Sciences, University of Illinois, Urbana, IL 61821, USA	Mis en forme ... [34]
221	³² Earth System Division, National Institute for Environmental Studies (NIES), Onogawa 16-2, Tsukuba, Ibaraki	Mis en forme ... [35]
222	305-8506, Japan	Supprimé: ³⁴ Department
223	³³ Earth Science Division, NASA Ames Research Center, Moffett Field, CA USA	Mis en forme ... [36]
224	³⁴ Max Planck Institute for Meteorology, Bundesstraße 53, 20146 Hamburg, Germany	Mis en forme ... [37]
225	³⁵ Université Paris-Saclay, INRAE, AgroParisTech, UMR EcoSys, Palaiseau, France	Supprimé: New York,
226	³⁶ LAPC, Institute of Atmospheric Physics, Chinese Academy of Sciences, Beijing, 100029, China	Mis en forme ... [38]
227	³⁷ Department of Earth, Atmospheric, and Planetary Sciences, Purdue University, West Lafayette, IN, USA	Supprimé: 10031
228	³⁸ Department of Earth and Atmospheric Sciences, City College of New York, City University of New York, NY, USA	Mis en forme ... [39]
229	³⁹ Climate Research Division, Environment and Climate Change Canada, Victoria, BC, V8W 2Y2, Canada	Supprimé: ³⁵ Climate
230	⁴⁰ Scripps Institution of Oceanography, University of California San Diego, La Jolla, CA, 92037, USA	Mis en forme ... [40]
231	⁴¹ Climate and Environmental Physics, Physics Institute and Oeschger Centre for Climate Change Research,	Supprimé: ³⁶ Max Planck Institute for Meteorology, ... [41]
232	University of Bern, Sidlerstr. 5, 3012 Bern, Switzerland	Supprimé: Earth, Atmospheric, Planetary Sciences, Department
233	⁴² Instituto de Investigaciones en Ecología y Sustentabilidad, Universidad Nacional Autónoma de México,	Supprimé: ⁴⁶ School of Chemistry, University of Bristol, ... [43]
234	Morelia, Mexico	Mis en forme ... [44]
235	⁴³ Department of Climate and Geochemistry Research, Meteorological Research Institute (MRI), Nagamine 1-1, Tsukuba,	Supprimé: ⁴⁸ Department
236	Ibaraki 305-0052, Japan	Supprimé: ⁴⁹ Sino-French Institute for Earth System Science, ... [45]
238	⁴⁴ CMCC Foundation - Euro-Mediterranean Center on Climate Change, Italy	Supprimé: ⁵⁰ CICERO Center for International Climate Research
239	⁴⁵ Department of Engineering and Environmental Studies Program, Boston College, Chestnut Hill, MA 02467,	Supprimé: ⁵⁴ Centre
240	USA	Mis en forme ... [47]
241	⁴⁶ National Centre for Earth Observation, School of Physics and Astronomy, University of Leicester, Leicester,	Supprimé: School...aculty of Environment, ... [48]
242	LE1 7RH, UK	Mis en forme ... [49]
243	⁴⁷ Department of Biology Sciences, Institute of Environment Science, University of Quebec at Montreal,	Supprimé: ⁵⁵ TNO
244	Montreal, QC H3C 3P8, Canada	
245	⁴⁸ School of Geographic Sciences, Hunan Normal University, Changsha 410081, China	
246	⁴⁹ Climate and Ecosystem Sciences Division, Lawrence Berkeley National Lab, 1 Cyclotron Road, Berkeley, CA	
247	94720, US	
248	⁵⁰ Department of Forest Ecology and Management, Swedish University of Agricultural Sciences, 90183 Umeå,	
249	Sweden	
250	⁵¹ Centre for Coastal Biogeochemistry, Faculty of Science and Engineering, Southern Cross University, Lismore,	
251	NSW 2480, Australia	
252	⁵² TNO, dep. of Climate Air & Sustainability, P.O. Box 80015, NL-3508-TA, Utrecht, The Netherlands	

406 ⁵³Joint Global Change Research Institute, Pacific Northwest National Lab, College Park, MD, USA
 407 ⁵⁴Center for Global Sustainability, University of Maryland, College Park, MD, USA
 408 ⁵⁵Center for Limnology, University of Wisconsin-Madison, Madison, WI, USA
 409 ⁵⁶Empa, Swiss Federal Laboratories for Materials Science and Technology, Dübendorf, Switzerland
 410 ⁵⁷Center for Earth System Science and Global Sustainability, Schiller Institute for Integrated Science and
 411 Society, Department of Earth and Environmental Sciences, Boston College, Chestnut Hill, MA 02467, USA
 412 ⁵⁸Finnish Meteorological Institute, P.O. Box 503, FI-00101, Helsinki, Finland
 413 ⁵⁹Statistics Division, Food and Agriculture Organization of the United Nations (FAO), Viale delle
 414 Terme di Caracalla, Rome 00153, Italy
 415 ⁶⁰Department of Earth and Environmental Sciences, University of Rochester, Rochester, NY 14627,
 416 USA
 417 ⁶¹Meteorology and Air Quality Group, Wageningen University and Research, Wageningen, the Netherlands
 418 ⁶²Environment and Climate Change Canada, 4905, Dufferin Street, Toronto, Canada
 419 ⁶³Department of Physical Geography and Ecosystem Science, Lund University, Sölvegatan 12, 223 62, Lund, Sweden
 420 ⁶⁴Institute of Environment and Ecology, Tsinghua Shenzhen International Graduate School, Tsinghua University,
 421 Shenzhen 518055, China
 422 ⁶⁵State Environmental Protection Key Laboratory of Sources and Control of Air Pollution Complex, Beijing 100084,
 423 China
 424 ⁶⁶College of Geography and Remote Sensing, Hohai University, Nanjing, 210098, China
 425
 426 *formerly at LSCE ¹
 427
 428 *Correspondence to:* Marielle Sauniois (marielle.sauniois@lsce.ipsl.fr)

429 **Abstract.** Understanding and quantifying the global methane (CH₄) budget is important for assessing realistic pathways to
 430 mitigate climate change. Emissions and atmospheric concentrations of CH₄ continue to increase, maintaining CH₄ as the
 431 second most important human-influenced greenhouse gas in terms of climate forcing after carbon dioxide (CO₂). The relative
 432 importance of CH₄ compared to CO₂ for temperature change is related to its shorter atmospheric lifetime, stronger radiative
 433 effect, and acceleration in atmospheric growth rate over the past decade, the causes of which are still debated. Two major
 434 challenges in reducing uncertainties in the factors explaining the well-observed atmospheric growth rate arise from diverse,
 435 geographically overlapping CH₄ sources and from the uncertain magnitude and temporal change in the destruction of CH₄
 436 by short-lived and highly variable hydroxyl radicals (OH). To address these challenges, we have established a consortium
 437 of multi-disciplinary scientists under the umbrella of the Global Carbon Project to improve, synthesise and update the global
 438 CH₄ budget regularly and to stimulate new research on the methane cycle. Following Sauniois et al. (2016, 2020), we present
 439 here the third version of the living review paper dedicated to the decadal CH₄ budget, integrating results of top-down CH₄
 440 emission estimates (based on in-situ and greenhouse gas observing satellite (GOSAT) atmospheric observations and an
 441 ensemble of atmospheric inverse-model results) and bottom-up estimates (based on process-based models for estimating
 442 land-surface emissions and atmospheric chemistry, inventories of anthropogenic emissions, and data-driven extrapolations).
 443 We present a budget for the most recent 2010-2019 calendar decade (the latest period for which full datasets are available),
 444 for the previous decade of 2000-2009 and for the year 2020.

- Supprimé: ⁵⁶International Center for Climate and Global ... [50]
- Supprimé: ⁵⁸Department of Atmospheric and Oceanic Science
- Déplacé (insertion) [1]
- Mis en forme ... [52]
- Mis en forme ... [51]
- Mis en forme ... [53]
- Déplacé vers le haut [1]: Meteorological Institute, P.O.
- Supprimé: ⁶⁰Finnish
- Mis en forme ... [54]
- Supprimé: ⁶¹Department of Physics, Imperial College ... [55]
- Supprimé: ⁶⁴KNMI, P.O. Box 201, 3730 AE, De Bilt
- Mis en forme ... [56]
- Supprimé: ⁶⁵Scripps Institution of Oceanography (SIO), ... [57]
- Mis en forme ... [58]
- Supprimé: rue
- Mis en forme ... [59]
- Supprimé: , Toronto, Canada[†] ... [60]
- Supprimé: ⁶⁶Department³Department of Geographical Science⁶¹
- Mis en forme ... [62]
- Supprimé: Maryland, United States
- Mis en forme ... [63]
- Mis en forme ... [64]
- Supprimé: America
- Mis en forme ... [65]
- Supprimé: ⁶⁹College⁶College of Hydrology...eography and... [66]
- Mis en forme ... [67]
- Mis en forme ... [68]
- Mis en forme ... [69]
- Supprimé: Atmospheric emissions...missions and atmospheric [70]
- Supprimé: ,
- Supprimé: depends on...or temperature change is related to its [71]
- Supprimé: variations...cceleration in atmospheric growth rate [72]
- Supprimé: the variety of
- Supprimé: difficulties
- Supprimé: synthesise
- Supprimé: aimed at improving and regularly updating the global [73]
- Supprimé: second...hird version of the living review paper ... [74]
- Supprimé: within
- Supprimé: modelling framework...odel results) and bottom-up [75]
- Supprimé:

550 The revision of the bottom-up budget in this edition benefits from important progress in estimating inland freshwater
 551 emissions, with better accounting of emissions from lakes and ponds, reservoirs, and streams and rivers. This budget also
 552 reduces double accounting across freshwater and wetland emissions and, for the first time, includes an estimate of the
 553 potential double accounting that still exists (average of 23 Tg CH₄ yr⁻¹). Bottom-up approaches show that the combined
 554 wetland and inland freshwater emissions average 248 [159-369] Tg CH₄ yr⁻¹ for the 2010-2019 decade. Natural fluxes are
 555 perturbed by human activities through climate, eutrophication, and land use. In this budget, we also estimate, for the first
 556 time, this anthropogenic component contributing to wetland and inland freshwater emissions. Newly available gridded
 557 products also allowed us to derive an almost complete latitudinal and regional budget based on bottom-up approaches.
 558 For the 2010-2019 decade, global CH₄ emissions are estimated by atmospheric inversions (top-down) to be 575 Tg CH₄ yr⁻¹
 559 (range 553-586, corresponding to the minimum and maximum estimates of the model ensemble). Of this amount, 369 Tg
 560 CH₄ yr⁻¹ or ~65% are attributed to direct anthropogenic sources in the fossil, agriculture and waste and anthropogenic
 561 biomass burning (range 350-391 Tg CH₄ yr⁻¹ or 63-68%). For the 2000-2009 period, the atmospheric inversions give a
 562 slightly lower total emission than for 2010-2019, by 32 Tg CH₄ yr⁻¹ (range 9-40). Since 2012, global direct anthropogenic
 563 CH₄ emission trends have been tracking scenarios that assume no or minimal climate mitigation policies proposed by the
 564 Intergovernmental Panel on Climate Change (shared socio-economic pathways SSP5 and SSP3). Bottom-up methods
 565 suggest 46% (94 Tg CH₄ yr⁻¹) larger global emissions (669 Tg CH₄ yr⁻¹, range 512-849) than top-down inversion methods
 566 for the 2010-2019 period. The discrepancy between the bottom-up and the top-down budgets has been greatly reduced
 567 compared to the previous differences (167 and 156 Tg CH₄ yr⁻¹ in Sauniois et al. (2016, 2020), respectively), and for the first
 568 time uncertainty in bottom-up and top-down budgets overlap. The latitudinal distribution from atmospheric inversion-based
 569 emissions indicates a predominance of tropical and southern hemisphere emissions (~65% of the global budget, <30°N)
 570 compared to mid (30°N-60°N, ~30% of emissions) and high-northern latitudes (60°N-90°N, ~4% of global emissions). This
 571 latitudinal distribution is similar in the bottom-up budget though the bottom-up budget estimates slightly larger contributions
 572 for the mid and high-northern latitudes, and slightly smaller contributions from the tropics and southern hemisphere than
 573 the inversions. Although differences have been reduced between inversions and bottom-up, the most important source of
 574 uncertainty in the global CH₄ budget is still attributable to natural emissions, especially those from wetlands and inland
 575 freshwaters.
 576 We identify five major priorities for improving the CH₄ budget: i) producing a global, high-resolution map of water-saturated
 577 soils and inundated areas emitting CH₄ based on a robust classification of different types of emitting ecosystems; ii) further
 578 development of process-based models for inland-water emissions; iii) intensification of CH₄ observations at local (e.g.,
 579 FLUXNET-CH₄ measurements, urban-scale monitoring, satellite imagery with pointing capabilities) to regional scales
 580 (surface networks and global remote sensing measurements from satellites) to constrain both bottom-up models and
 581 atmospheric inversions; iv) improvements of transport models and the representation of photochemical sinks in top-down
 582 inversions, and v) integration of 3D variational inversion systems using isotopic and/or co-emitted species such as ethane

Supprimé: 2008-2017...2010-2019 decade, global methane...H₄ emissions are estimated by atmospheric inversions (a...op-down approach... to be 576...75 Tg CH₄ yr⁻¹ (range 550-594... 53-586, corresponding to the minimum and maximum estimates of the model ensemble), of which 359... Of this amount, 369 Tg CH₄ yr⁻¹ or ~60...5% are attributed to direct anthropogenic sources, that is emissions caused by direct human activity ... [76]

Mis en forme : Anglais (G.B.)

Supprimé: 336-376

Mis en forme : Anglais (G.B.)

Supprimé: 50-65%). The updated...3-68%). For the 2000-2009 period, the atmospheric inversions give a slightly lower total emission is 29 Tg CH₄ yr⁻¹ larger...han our estimate for the period 2000-2009 and 24 Tg CH₄ yr⁻¹ larger than the one reported in the previous budget for 2003-2012 (Sauniois et al., 2016). ... [77]

Supprimé: CH₄ emissions...irect anthropogenic CH₄ emission trends have been tracking the warmest...enarios assessed...hat assume no or minimal climate mitigation policies proposed by the Intergovernmental Panel on Climate Change... (shared socio-economic pathways SSP5 and SSP3). Bottom-up methods suggest almost 30%...6% (94 Tg CH₄ yr⁻¹) larger global emissions (737...69 Tg CH₄ yr⁻¹, range 594-881...12-849) than top-down inversion methods. Indeed...for the 2010-2019 period. The discrepancy between the bottom-up estimates for natural sources such as natural wetlands, other inland water systems, and geological sources are higher than...nd the top-down estimates. The atmospheric constraints on the ... [78]

Supprimé: budget suggest that at least some of these bottom-up emissions are overestimated... The latitudinal distribution of...rom atmospheric observation...nversion-based emissions indicates a predominance of tropical and southern hemisphere emissions (~65% of the global budget, <30°N) compared to mid (~30%, ...30°N-60°N, ~30% of emissions) and high-northern latitudes (~4%, 60°N-90°N). The ... [79]

Supprimé: methane

Mis en forme : Indice

Supprimé: other inland waters. * Some of our global source estimates are smaller than those in previously published budgets (Sauniois et al. 2016; Kirschke et al. 2013), particularly for wetland emissions that are about 35 Tg CH₄ yr⁻¹ lower due to efforts to better partition wetlands and other inland waters. Emissions from geological sources are also found to be... [80]

Supprimé: methane

Mis en forme : Indice

Supprimé: include

Supprimé: methane

Supprimé: habitats...cosystems; ii) further development of process-based models for inland-water emissions; iii) intensification... [81]

Mis en forme : Indice

Mis en forme : Indice

Supprimé: scales...e.g., FLUXNET-CH₄ measurements and...urban-scale monitoring, satellite imagery with pointing capabilities... [82]

708 as well as information in the bottom-up inventories on anthropogenic super-emitters detected by remote sensing (mainly
709 oil and gas sector but also coal, agriculture and landfills) to improve source partitioning.

710 The data presented here can be downloaded from <https://doi.org/10.18160/GCP-CH4-2024/> (Martinez et al., 2024).

711 1 Introduction

712 The average surface dry air mole fraction of atmospheric methane (CH₄) reached 1912 ppb in 2022 (Fig. 1, Lan et
713 al., 2024), 2.6 times greater than its estimated pre-industrial value in 1750. This increase is attributable in large part to
714 increased anthropogenic emissions arising primarily from agriculture (e.g., livestock production, rice cultivation, biomass
715 burning), fossil fuel production and use, waste disposal, and alterations to natural CH₄ fluxes due to increased atmospheric
716 CO₂ concentrations, land use (Woodward et al., 2010, Fluet-Chouinard et al., 2023) and climate change (Ciais et al., 2013;
717 Canadell et al., 2021). Atmospheric CH₄ is a stronger absorber of Earth's emitted thermal infrared radiation than carbon
718 dioxide (CO₂), as assessed by its global warming potential (GWP) relative to CO₂. For a 100-yr time horizon and without
719 considering climate feedbacks the GWP of CH₄-fossil is 29.8 (CH₄-non fossil GWP is 27), whereas the values reach 82.5
720 over a 20-year horizon for CH₄-fossil and 79.7 for CH₄-non fossil (Forster et al., 2021). Although global anthropogenic
721 emissions of CH₄ are estimated at around 359 Tg CH₄ yr⁻¹ (Saunois et al., 2020), representing around 2.5% of the global
722 CO₂ anthropogenic emissions when converted to units of carbon mass flux for the recent decade, the emissions-based
723 effective radiative forcing of CH₄ concentrations has contributed ~31% (1.19 W m⁻²) to the additional radiative forcing
724 from anthropogenic emissions of greenhouse gases and their precursors (3.84 W m⁻²) over the industrial era (1750-2019)
725 (Forster et al., 2021). Changes in other chemical compounds such as nitrogen oxides (NO_x) or carbon monoxide (CO) also
726 influence atmospheric CH₄ through changes to its atmospheric lifetime. Emissions of CH₄ contribute to the production of
727 ozone, stratospheric water vapour, and CO₂, and most importantly affect its own lifetime (Myhre et al., 2013; Shindell
728 et al., 2012). CH₄ has a short lifetime in the atmosphere (about 9 years for the year 2010, Prather et al., 2012). Hence a
729 stabilisation or reduction of CH₄ emissions leads to the stabilisation or reduction of its atmospheric concentration (assuming
730 no change in the chemical oxidants), and therefore its radiative forcing, in only a few decades. While reducing CO₂ emissions
731 is necessary to stabilise long-term warming, reducing CH₄ emissions is recognized as an effective option to limit climate
732 warming in the near-term (Shindell et al., 2012; Jackson et al., 2020; Ocko et al., 2021; UNEP, 2021), because of its shorter
733 lifetime compared to CO₂.

734 The momentum around the potential of CH₄ to limit near-term warming has led to the launch of the Global Methane
735 Pledge at the November 2021 Conference of the Parties (COP 26). Signed by 150 countries, this collective effort aims at
736 reducing global CH₄ anthropogenic emissions at least 30 percent from 2020 levels by 2030 (Global Methane Pledge, 2023).
737 Given that global baseline CH₄ emissions are expected to grow through 2030 (by an additional 20-50 Million tons (Mt) of
738 CH₄, UNEP 2022), the CH₄ emission reductions currently needed to reach the Global Methane Pledge objective (UNEP,

Supprimé: <https://doi.org/10.18160/GCP-CH4-2019> (Saunois

Supprimé: 2019) and from the Global Carbon Project.

Supprimé: ¶

Mis en forme : Normal, Espace Avant : 24 pt, Après : 12 pt, Paragraphes solidaires, Bordure : Haut: (Pas de bordure), Bas: (Pas de bordure), Gauche: (Pas de bordure), Droite: (Pas de bordure), Entre : (Pas de bordure)

Mis en forme : Police :Gras, Couleur de police : Noir

Supprimé: The surface dry air mole fraction of atmospheric methane (CH₄) reached 1857 ppb in 2018 (Fig. 1), approximately 2.6 times greater than its estimated pre-industrial equilibrium value in 1750. This increase is attributable in large part to increased anthropogenic emissions arising primarily from agriculture (e.g., livestock production, rice cultivation, biomass burning), fossil fuel production and use, waste disposal, and alterations to natural methane fluxes due to increased atmospheric CO₂ concentrations and climate change (Ciais et al., 2013). Atmospheric CH₄ is a stronger absorber of Earth's emitted thermal infrared radiation than carbon dioxide (CO₂), as assessed by its global warming potential (GWP) relative to CO₂. For a 100-yr time horizon and without considering climate feedbacks GWP(CH₄) = 28 (IPCC AR5, Myhre et al., 2013). Although global anthropogenic emissions of CH₄ are estimated at around 366 Tg CH₄ yr⁻¹ (Saunois et al., 2016), representing only 3% of the global CO₂ anthropogenic emissions in units of carbon mass flux, the increase of atmospheric CH₄ concentrations has contributed ~23% (-0.62 W m⁻²) to the additional radiative forcing accumulated in the lower atmosphere since 1750 (Etminan et al., 2016). Changes in other chemical compounds (such as nitrogen oxides (NO_x) or carbon monoxide (CO)) also influence the forcing of atmospheric CH₄ through changes to its atmospheric lifetime. From an emission perspective, the total radiative forcing attributable to anthropogenic CH₄ emissions is currently about 0.97 W m⁻² (Myhre et al., 2013). Emissions of CH₄ contribute to the production of ozone, stratospheric water vapour, and CO₂, and most importantly affect its own lifetime (Myhre et al., 2013; Shindell et al., 2012). CH₄ has a short lifetime in the atmosphere (about 9 years for the year 2010 (Prather et al., 2012)) hence a stabilization or reduction of CH₄ emissions leads rapidly, in a few decades, to a stabilization or reduction of its atmospheric concentration and therefore its radiative forcing. Reducing CH₄ emissions is therefore recognized as an effective option for rapid climate change mitigation, especially on decadal timescales (Shindell et al., 2012), because of its shorter lifetime than CO₂. ¶ Of concern, the current anthropogenic methane emissions trajectory is estimated to lie between the two warmest IPCC-AR5 scenarios (Nisbet et al., 2016, 2019), i.e., the RCP8.5 and RCP6.0, corresponding to temperature increases above 3°C by the end of this century. This trajectory implies that large reductions of methane emissions are needed to meet the 1.5-2°C target of the Paris Agreement (Collins et al., 2013; Nisbet et al., 2019). Moreover, CH₄ is a precursor of important air pollutants such as ozone, and, as such, its emissions are covered by two international conventions: the United Nations Framework Convention on Climate Change (UNFCCC) and the Convention on Long Range Transport of Air Pollution (CLRTAP), another motivation to reduce its emissions. ¶ Changes in the magnitude and temporal variation (annual to inter-annual) of methane sources and sinks over the past decades are characterized by large uncertainties (Kirschke et al., 2013; Saunois et al., 2017; Turner et al., 2019). Also, the decadal budget suggests relative uncertainties (hereafter reported as min-max ranges) of 20-31

866 2022) correspond to 36% of the projected baseline emissions in 2030 (ie. if no further emission reductions were
867 implemented). This implies that large reductions of CH₄ emissions are needed to meet the Global Methane Pledge that is
868 consistent also with the 1.5-2°C target of the Paris Agreement (UNEP, 2022). Moreover, because CH₄ is a precursor of
869 important air pollutants such as ozone, CH₄ emissions reductions are required by two international conventions: the United
870 Nations Framework Convention on Climate Change (UNFCCC) and the Convention on Long Range Transport of Air
871 Pollution (CLRTAP), making this global CH₄ budget assessment all the more critical.

872 Changes in the magnitude and temporal variation (annual to inter-annual) of CH₄ sources and sinks over the past
873 decades are characterised by large uncertainties (e.g., Kirschke et al., 2013; Sauniois et al., 2017; Turner et al., 2019). Also,
874 the decadal budget suggests relative uncertainties (hereafter reported as min-max ranges) of 20-35% for inventories of
875 anthropogenic emissions in specific sectors (e.g., agriculture, waste, fossil fuels (Tibrewal et al., 2024)), 50% for biomass
876 burning and natural wetland emissions, and up to 100% for other natural sources (e.g., inland waters, geological sources).
877 The uncertainty in the chemical loss of CH₄ by OH, the predominant sink of atmospheric CH₄, has been s estimated using
878 Prather et al. (2012) and Rigby et al. (2017) estimated this uncertainty at ~10% from the uncertainty in the reaction rate
879 between CH₄ and OH, or using methyl-chloroform measurements. Bottom-up approaches (chemistry transport models)
880 estimate the uncertainty of the chemical loss by OH at around 15-20% (Sauniois et al., 2016, 2020). This uncertainty on the
881 OH induced loss translates, in the top-down methods, into the minimum relative uncertainty associated with global CH₄
882 emissions, as other CH₄ sinks (atomic oxygen and chlorine oxidations, soil uptake) are much smaller and the atmospheric
883 growth rate is well-defined (Dlugokencky et al., 2009). Globally, the contribution of natural CH₄ emissions to total emissions
884 can be quantified by combining lifetime estimates with reconstructed pre-industrial atmospheric CH₄ concentrations from
885 ice cores (assuming natural emissions have not been perturbed during the anthropocene) (e.g., Ehhalt et al., 2001).
886 Regionally or nationally, uncertainties in emissions may reach 40-60% (e.g., for South America, Africa, China, and India,
887 see Sauniois et al., 2016).

888 To monitor emission reductions, for example to help conduct the Paris Agreement's stocktake, sustained and long-
889 term monitoring of anthropogenic emissions per sector is needed in particular for hotspots of emissions that may be missed
890 in inventories (Bergamaschi et al., 2018a; Pacala, 2010; Lauvaux et al., 2022). At the same time, reducing uncertainties in
891 all individual CH₄ sources, and thus in the overall CH₄ budget remains challenging for at least four reasons. First, CH₄ is
892 emitted by multiple processes, including natural and anthropogenic sources, point and diffuse sources, and sources
893 associated with at least three different production origins (i.e., microbial, thermogenic, and pyrogenic). These multiple
894 sources and processes require the integration of data from diverse scientific communities and across multiple temporal and
895 spatial scales. The production of accurate bottom-up estimates is complicated by the fact that anthropogenic emissions result
896 from leakage from fossil fuel production with large differences between countries depending on technologies and practices,
897 the fact that many large leak events are sporadic, and the location of many emissions hotspots is not well known, and from
898 uncertain emission factors used to summarise complex microbial processes in the agriculture and waste sectors. For the

899 latter, examples include difficulties in upscaling methane emissions from livestock without considering the variety of animal
900 weight, diet and environment, and difficulties in assessing emissions from landfills depending on waste type and waste
901 management technology. Second, atmospheric CH₄ is removed mainly by chemical reactions in the atmosphere involving
902 OH and other radicals that have very short lifetimes (typically ~1s). Due to the short lifetime of OH, the spatial and temporal
903 distributions of OH are highly variable. While OH can be measured locally, calculating global CH₄ loss through OH
904 measurements requires high-resolution global OH measurements (typically half an hour to integrate cloud cover, and 1 km
905 spatially to consider OH high reactivity and heterogeneity) which is impossible from direct OH observations. As a result,
906 OH can only be calculated through large scale atmospheric chemistry modelling. Those simulated OH concentrations from
907 transport-chemistry models prescribed with emissions of precursor species affecting OH still show uncertain spatio-temporal
908 distribution from regional to global scales (Zhao et al., 2019). Third, only the net CH₄ budget (sources minus sinks) is well
909 constrained by precise observations of atmospheric growth rates (Dlugokencky et al., 2009), leaving the sum of sources and
910 the sum of sinks uncertain. One distinctive feature of CH₄ sources compared to CO₂ fluxes is that the oceanic contribution
911 to the global CH₄ budget is small (~1-3%), making CH₄ source estimation predominantly a terrestrial endeavour (USEPA,
912 2010b). Finally, we lack comprehensive observations to constrain 1) the areal extent of different types of wetlands and
913 inland freshwater (Kleinen et al., 2012, 2020, 2021, 2023; Stocker et al., 2014; Zhang et al., 2021), 2) models of wetland
914 and inland freshwater emission rates (Melton et al., 2013; Poulter et al., 2017; Wania et al., 2013; Bastviken et al., 2011;
915 Wik et al., 2016a; Rosentreter et al., 2021; Bansal et al., 2023; Lauerwald et al., 2023a; Stanley et al. 2023), 3) inventories
916 of anthropogenic emissions (Höglund-Isaksson et al., 2020; Crippa et al., 2023; USEPA, 2019), and 4) atmospheric
917 inversions, which aim to estimate CH₄ emissions from global to regional scales (Houweling et al., 2017; Jacob et al., 2022).

918 The global CH₄ budget inferred from atmospheric observations by atmospheric inversions relies on regional
919 constraints from atmospheric sampling networks, which are relatively dense for northern mid-latitudes, with various high-
920 precision and high-accuracy surface stations, but are sparser at tropical latitudes and in the Southern Hemisphere
921 (Dlugokencky et al., 2011). Recently, the density of atmospheric observations has increased in the tropics due to satellite-
922 based platforms that provide column-average CH₄ mixing ratios. Despite continuous improvements in the precision and
923 accuracy of space-based measurements (e.g., Buchwitz et al., 2016), systematic errors greater than several ppb on total
924 column observations can still limit the usage of such data to constrain surface emissions (e.g., Jacob et al., 2022). The
925 development of robust bias corrections on existing data can help overcome this issue (e.g., Inoue et al., 2016) and satellite
926 data are now widely used in atmospheric inversions where they provide more global information on the distribution of fluxes
927 and highly complement the surface networks (e.g., Lu et al., 2021).

928 In this context, the Global Carbon Project (GCP) seeks to develop a complete picture of the carbon cycle by
929 establishing common, consistent scientific knowledge to support policy development and actions to mitigate greenhouse gas
930 emissions to the atmosphere (www.globalcarbonproject.org). The objective of this paper is to analyse and synthesise the
931 current knowledge of the global CH₄ budget, by gathering results of observations and models, to better understand and

Mis en forme : Retrait : Première ligne : 1,27 cm

Supprimé : debate

Supprimé : synthesize

Supprimé : methane

Supprimé : in order

936 quantify the main robust features of this budget, its remaining uncertainties, and to make recommendations for improvement.
 937 We combine results from a large ensemble of bottom-up approaches (e.g., process-based models for natural wetlands, data-
 938 driven approaches for other natural sources, inventories of anthropogenic emissions and biomass burning, and atmospheric
 939 chemistry models), and top-down approaches (including CH₄ atmospheric observing networks, atmospheric inversions
 940 inferring emissions and sinks from the assimilation of atmospheric observations into models of atmospheric transport and
 941 chemistry). The focus of this work is to update the previous assessment made for the period 2000-2017 (Saunois et al.,
 942 2020) to the more recent 2000-2020 period. More in-depth analyses of trends and year-to-year changes are left to future
 943 publications. Our current paper is a living review, published at about four-year intervals, to provide an update and new
 944 synthesis of available observational, statistical, and model data for the overall CH₄ budget and its individual components.
 945 Kirschke et al. (2013) was the first CH₄ budget synthesis followed by Saunois et al. (2016) and Saunois et al.
 946 (2020), with companion papers by Stavert et al. (2021) on regional CH₄ budgets and Jackson et al. (2020) focusing on the
 947 last year of the budget (2017). Saunois et al. (2020) covered 2000-2017 and reported CH₄ emissions and sinks for three time
 948 periods: 1) the latest calendar decade at that time (2000-2009), 2) data for the latest available decade (2008-2017), and 3)
 949 the latest available year (2017) at the time. Here, the Global Methane Budget (GMB) covers 2000-2020 split into the 2000-
 950 2009 decade, the 2010-2019 decade (where data are available), the year 2020 affected by COVID induced changes in human
 951 activity, and briefly for 2021-2023 as per data availability (Section 6). The CH₄ budget is presented at global, latitudinal,
 952 and regional scales and data can be downloaded from <https://doi.org/10.18160/GCP-CH4-2024/> (Martinez et al., 2024).
 953 Six sections follow this introduction. Section 2 presents the methodology used in the budget: units, definitions of
 954 source categories, regions, data analysis; and discusses the delay between the period of study of the budget and the release
 955 date. Section 3 presents the current knowledge about CH₄ sources and sinks based on the ensemble of bottom-up approaches
 956 reported here (models, inventories, data-driven approaches). Section 4 reports atmospheric observations and top-down
 957 atmospheric inversions gathered for this paper. Section 5, based on Sections 3 and 4, provides the updated analysis of the
 958 global CH₄ budget by comparing bottom-up and top-down estimates and highlighting differences. Section 6 discusses the
 959 recent changes in atmospheric CH₄ in relation with changes in CH₄ sources and sinks. Finally, Section 7 discusses future
 960 developments, missing components, and the most critical remaining uncertainties based on our update to the global CH₄
 961 budget.

962 2 Methodology

963 2.1 Units used

964 Unless specified, fluxes are expressed in teragrams of CH₄ per year (1 Tg CH₄ yr⁻¹ = 10¹² g CH₄ yr⁻¹), while atmospheric
 965 mixing ratios are expressed as dry air mole fractions, in parts per billion (ppb), with atmospheric CH₄ annual increases,
 966 G_{ATM}, expressed in ppb yr⁻¹. In the tables, we present mean values and ranges for the two decades 2000-2009, and 2010-

Supprimé :

Supprimé : methane

Supprimé : on decadal budgets and on the update of the previous assessment made for the period 2003-2012 to the more recent 2008-2017 decade. More in-depth analysis of trends and year-to-year changes are left to future publications. The regional budget is further discussed in Stavert et al. (2020). Our current paper is a living review, published at about three-year intervals, to provide an update and new synthesis of available observational, statistical

Supprimé : Kirschke et al. (2013) was the first CH₄ budget synthesis and was followed by Saunois et al. (2016). Kirschke et al. (2013) reported decadal mean CH₄ emissions and sinks from 1980 to 2009 based on bottom-up and top-down approaches. Saunois et al. (2016) reported methane emissions for three time periods: 1) the last calendar decade (2000-2009), 2) the last available decade (2003-2012), and 3) the last available year (2012) at the time. Here, we update reporting methane emissions and sinks for 2000-2009 decade, for the most recent 2008-2017 decade where data are available, and for the year 2017, reducing the time lag between the last reported year and analysis. The methane budget is presented here at global and latitudinal scales and data can be downloaded from <https://doi.org/10.18160/GCP-CH4-2019> (Saunois et al., 2019). ¶ Five

Mis en forme : Retrait : Première ligne : 1,27 cm

Supprimé : of

Supprimé : methane

Supprimé : methane

Supprimé : 6

Supprimé : methane

Mis en forme : Police : Gras, Couleur de police : Noir

Mis en forme : Normal, Espace Avant : 24 pt, Après : 12 pt, Paragraphes solidaires, Bordure : Haut: (Pas de bordure), Bas: (Pas de bordure), Gauche: (Pas de bordure), Droite: (Pas de bordure), Entre : (Pas de bordure)

Supprimé : lTg

Supprimé : =

Supprimé : gCH₄

Supprimé : concentrations

Supprimé : methane

Supprimé :

Supprimé : 2008-2017

1002 2019, together with results for the most recent available year (2020). Results obtained from previous syntheses (i.e., Saunois
1003 et al., 2020 and Saunois et al., 2016) are also given for the decade 2000-2009. Following Saunois et al. (2016) and
1004 considering that the number of studies is often relatively small for many individual source and sink estimates, uncertainties
1005 are reported as minimum and maximum values of the available studies, given in brackets. In doing so, we acknowledge that
1006 we do not consider the uncertainty of the individual estimates, and we express uncertainty as the range of available mean
1007 estimates, i.e., differences across measurements/methodologies considered. These minimum and maximum values are those
1008 presented in Section 2.5 and exclude identified outliers.

1009 The CH₄ emission estimates are provided with up to three significant digits, for consistency across all budget flux
1010 components and to ensure the accuracy of aggregated fluxes. Nonetheless, given the values of the uncertainties in the CH₄
1011 budget, we encourage the reader to consider not more than two digits as significant for the global total budget.

1012 2.2 Period of the budget and availability of data

1013 The bottom-up estimates rely on global anthropogenic emission inventories, an ensemble of process-based models for
1014 wetlands emissions, and published estimates in the literature for other natural sources. The global gridded anthropogenic
1015 inventories (see Section 3.1.1) are updated irregularly, generally every 3 to 5 years. The last reported years of available
1016 inventories were 2018 or 2019 when we started the top-down modelling activity. In order to cover the period 2000-2020, it
1017 was necessary to extrapolate the anthropogenic inventory EDGARv6 (Crippa et al., 2021) to 2020 to use it as prior
1018 information for the anthropogenic emissions in the atmospheric inversion systems as explained in the supplementary
1019 material. The land surface (wetland) models were run over the full period 2000-2020 using dynamical wetland areas derived
1020 by remote sensing data or other models of flooded area variability (Sect. 3.2.1).

1021 The atmospheric inversions run until mid-2021, but the last year of reported inversion results is 2020, which represents a
1022 three-year lag with the present. This is due to the long time period it takes to acquire atmospheric in-situ data and integrate
1023 models. Even though satellite observations are processed operationally and are generally available with a latency of days to
1024 weeks, by contrast surface observations can lag from months to years because of the time for flask analyses and data quality
1025 checks in (mostly) non-operational chains. In addition, the final six months of inversions must be generally ignored because
1026 the estimated fluxes are not constrained by as many observations as the previous periods. Lastly, this budget presents an
1027 extended synthesis of the most recent development regarding inland water emissions (Sect. 3.2.2) and corrections associated
1028 with double counting with wetlands.

1029 2.3 Definition of regions

1030 Geographically, emissions are reported globally and for three latitudinal bands (90°S-30°N, 30-60°N, 60-90°N, only for
1031 gridded products). When extrapolating emission estimates forward in time (see Sect. 3.1.1), and for the regional budget
1032 presented by Stavert et al. (2021), a set of 19 regions (oceans and 18 continental regions, see supplementary Fig. S3) were

Supprimé: 2017

Supprimé: .

Supprimé: methane

Mis en forme : Police :Gras, Couleur de police : Noir

Mis en forme : Normal, Espace Avant : 12 pt, Après : 12 pt, Paragraphes solidaires, Bordure : Haut: (Pas de bordure), Bas: (Pas de bordure), Gauche: (Pas de bordure), Droite: (Pas de bordure), Entre : (Pas de bordure)

Supprimé: surface land

Supprimé: 2012, 2014

Supprimé: 2016

Supprimé: this study. For this budget, in

Supprimé: reported

Supprimé: (

Supprimé: 2017),

Supprimé: some of these datasets as

Supprimé: Sect. 3.1.1.

Supprimé: land

Supprimé: 2017

Supprimé: (Sect.

Supprimé: For the top-down estimates, we use

Supprimé: covering 2000-2017. The simulations

Supprimé: 2018

Supprimé: 2017

Supprimé: two and a half

Supprimé: , a two-year shorter lag than for the last release (Saunois et al., 2016). Satellite

Supprimé: linked to operational data chains

Supprimé: after the recording of the spectra. Surface

Supprimé: The

Supprimé: are

Supprimé: (spin down)

Mis en forme : Police :Gras, Couleur de police : Noir

Mis en forme : Normal, Espace Avant : 12 pt, Après : 12 pt, Paragraphes solidaires, Bordure : Haut: (Pas de bordure), Bas: (Pas de bordure), Gauche: (Pas de bordure), Droite: (Pas de bordure), Entre : (Pas de bordure)

Supprimé:

Mis en forme : Police :Gras, Couleur de police : Noir

Supprimé: Geographically, emissions are reported globally and for three latitudinal bands (90°S-30°N, 30-60°N, 60-90°N, only for gridded products). When extrapolating emission estimates forward in time

1079 used. As anthropogenic emissions are often reported by country, we define these regions based on a country list (Table S1).
 1080 This approach was compatible with all top-down and bottom-up approaches considered. The number of regions was chosen
 1081 to be close to the widely used TransCom inter-comparison map (Gurney et al., 2004) but with subdivisions to separate the
 1082 contribution from important countries or regions for the CH₄ cycle (China, South Asia, Tropical America, Tropical Africa,
 1083 United States of America, and Russia). The resulting region definition is the same as that used for the Global Carbon Project
 1084 (GCP) N₂O budget (Tian et al., 2020). Compared to Saunois et al. (2020), the Oceania region has been replaced by
 1085 Australasia including only Australia and New Zealand. Other territories formerly in Oceania were included in Southeast
 1086 Asia.

1087 2.4 Definition of source and sink categories

1088 CH₄ is emitted by different processes (i.e., biogenic, thermogenic, or pyrogenic) and can be of anthropogenic or natural
 1089 origin. Biogenic CH₄ is the final product of the decomposition of organic matter by methanogenic *Archaea* in anaerobic
 1090 environments, such as water-saturated soils, swamps, rice paddies, marine and freshwater sediments, landfills, sewage and
 1091 wastewater treatment facilities, or inside animal digestive systems. Thermogenic methane is formed on geological time
 1092 scales by the breakdown of buried organic matter due to heat and pressure deep in the Earth's crust. Thermogenic CH₄
 1093 reaches the atmosphere through marine and land geological gas seeps. These CH₄ emissions are increased by human
 1094 activities, for instance, the exploitation and distribution of fossil fuels. Pyrogenic CH₄ is produced by the incomplete
 1095 combustion of biomass and other organic materials. Peat fires, biomass burning in deforested or degraded areas, wildfires,
 1096 and biofuel burning are the largest sources of pyrogenic CH₄. CH₄ hydrates, ice-like cages of frozen CH₄ found in continental
 1097 shelves and slopes and below sub-sea and land permafrost, can be of either biogenic or thermogenic origin. Each of these
 1098 three process categories has both anthropogenic and natural components.

1099 In the following, we present the different CH₄ sources depending on their anthropogenic or natural origin, which is relevant
 1100 to climate policy. Compared to the previous budgets, marginal changes have been made regarding source categories (naming
 1101 and grouping), to reflect the improved estimates for inland water sources and their indirect anthropogenic component. In the
 1102 previous Global Methane Budgets (Saunois et al., 2016, 2020), natural and anthropogenic emissions were split in a way that
 1103 did not correspond exactly to the definition used by the UNFCCC following the IPCC guidelines (IPCC, 2006), where, for
 1104 pragmatic reasons, all emissions from managed land are typically reported as anthropogenic. For instance, we considered
 1105 all wetlands as natural emissions, despite some wetlands being on managed land and their emissions being partly reported
 1106 as anthropogenic in UNFCCC national communications. The human induced perturbation of climate, atmospheric CO₂, and
 1107 nitrogen and sulfur deposition may cause changes in wetland sources we classified as natural. Following our previous
 1108 definition, emissions from wetlands, inland freshwaters, thawing permafrost, or geological leaks are accountable for
 1109 "natural" emissions, even though we acknowledge that climate change and other human perturbations (e.g. eutrophication)
 1110 may cause changes in those emissions. CH₄ emissions from reservoirs were also considered as natural even though reservoirs

Mis en forme : Police :Gras, Couleur de police : Noir

Supprimé:

Mis en forme : Normal, Espace Avant : 12 pt, Après : 12 pt, Paragraphes solidaires, Bordure : Haut: (Pas de bordure), Bas: (Pas de bordure), Gauche: (Pas de bordure), Droite: (Pas de bordure), Entre : (Pas de bordure)

Mis en forme : Police :Gras, Couleur de police : Noir

Mis en forme : Police :Gras, Couleur de police : Noir

Supprimé: Methane

Supprimé: methane

Supprimé: methane

Supprimé: methane

Supprimé: methane

Supprimé: material

Supprimé: methane. Methane

Supprimé: trapped methane

Supprimé: methane

Supprimé: for

Supprimé: Here, "natural sources" refer to pre-agricultural emissions even if they are perturbed by anthropogenic climate change.

Supprimé: "anthropogenic sources" are caused by direct human activities since pre-industrial/pre-agricultural time (3000-2000 BC, Nakazawa et al., 1993) including agriculture, waste management and fossil fuel related activities. Natural emissions are split between "wetland" and "other natural" emissions (e.g., non-wetland inland waters, wild animals, termites, land geological sources, oceanic geological and biogenic sources, and terrestrial permafrost). ... [85]

Supprimé: 1 ... [86]

Supprimé: (IPCC, 2006),

Supprimé: , which is not the case here.

Supprimé: consider

Mis en forme : Indice

Supprimé: the

Supprimé: water or

Supprimé: will be

Supprimé: in

Supprimé: ,

Supprimé: – a

Supprimé: perturbation –

Supprimé: increasing

Supprimé: from these sources. Methane

Supprimé: are

159 are human-made. Indeed, since the 2019 refinement to the IPCC guidelines (IPCC, 2019) emissions from reservoirs and
160 other flooded lands are considered to be anthropogenic by the UNFCCC and should be reported as such. However these
161 estimates are not provided by inventories and not systematically reported by all countries (especially non Annex-I countries).
162 In this budget we rename “natural sources” to “natural and indirect anthropogenic sources” to acknowledge that CH₄
163 emissions from reservoirs, as well as from water bodies that were perturbed by agricultural activities (drainage,
164 eutrophication, land use change) are indirect anthropogenic emissions. As a result, here, “natural and indirect anthropogenic
165 sources” refer to “emissions that do not directly originate from fossil, agricultural, waste, and biomass burning sources”
166 even if they are perturbed by anthropogenic activities and climate change. Natural and indirect anthropogenic emissions are
167 split between “Wetlands and Inland Freshwaters” and “Other natural” emissions (e.g., wild animals, termites, land
168 geological sources, oceanic geological and biogenic sources, and terrestrial permafrost). “Anthropogenic direct sources” are
169 caused by direct human activities since pre-industrial/pre-agricultural time (3000-2000 BC, Nakazawa et al., 1993) including
170 agriculture, waste management, fossil fuel-related activities and biofuel and biomass burning (yet we acknowledge that a
171 small fraction of wildfires are naturally ignited). Direct anthropogenic emissions are split between: “Agriculture and waste
172 emissions”, “Fossil fuel emissions”, and “Biomass and biofuel burning emissions”, assuming that all types of fires are caused
173 by anthropogenic activities. To conclude, this budget reports “direct anthropogenic”, and “natural and indirect
174 anthropogenic” methane emissions for the five main source categories explained above for both bottom-up and top-down
175 approaches.
176 The sinks of methane are split into the soil uptake that can be derived from land-surface models in the bottom-up budget,
177 and the chemical sinks. The chemical sinks are estimated by either chemistry climate or chemistry transport models in the
178 bottom-up budget, and are further detailed in terms of vertical distribution (troposphere and stratosphere) and oxidants.
179 Bottom-up estimates of CH₄ emissions for some processes are derived from process-oriented models (e.g., biogeochemical
180 models for wetlands, models for termites), inventory models (agriculture and waste emissions, fossil fuel emissions, biomass
181 and biofuel burning emissions), satellite-based models (large scale biomass burning), or observation-based upscaling models
182 for other sources (e.g., inland water, geological sources). From these bottom-up approaches, it is possible to provide
183 estimates for more detailed source subcategories inside each main category described above (see budget in Table 3).
184 However, the total CH₄ emission derived from the sum of independent bottom-up estimates remains unconstrained.
185 For atmospheric inversions (top-down approach), atmospheric methane concentration observations provide a constraint on
186 the global methane total source if we assume the global sink is known (OH and other oxidant prescribed), or inversions are
187 optimising also for the chemical sink. OH estimates are constrained by methyl chloroform-inversion (Montzka et al., 2011;
188 Rigby et al., 2017; Patra et al., 2021). The inversions reported in this work solve for the total net CH₄ flux at the surface
189 (sum of sources minus soil uptake) (e.g., Pison et al., 2013), or a limited number of source categories (e.g., Bergamaschi et
190 al., 2013). In most of the inverse systems the atmospheric oxidant concentrations were prescribed with pre-optimized or
191 scaled OH fields, and thus the atmospheric sink is not optimised. The assimilation of CH₄ observations alone, as reported in

Supprimé: , and

Supprimé: (IPCC, 2006, 2019)

Supprimé: by UNFCCC.¶
Following Saunois et al. (2016), we report

Supprimé: and natural methane

Supprimé: for

Supprimé:

Supprimé: methane

Supprimé: sub-categories

Supprimé: GCP

Supprimé: methane

Supprimé: For atmospheric inversions (top-down approach) the situation is different. Atmospheric observations provide a constraint on the global total source and a reasonable constraint on the global sink derived from methyl chloroform (Montzka et al., 2011; Rigby et al., 2017). The inversions reported in this work solve either for a total methane flux (e.g. Pison et al., 2013), or for a limited number of source categories (e.g. Bergamaschi et al., 2013). In most of the inverse systems the atmospheric oxidant concentrations are prescribed with pre-optimized or scaled OH fields, and thus the atmospheric sink is not solved. The assimilation of CH₄ observations alone, as reported in this synthesis, can help to separate sources with different locations or temporal variations but cannot fully separate individual sources as they often overlap in space and time in some regions. Top-down global and regional methane emissions per source category were obtained directly from gridded optimized fluxes, wherever an inversion had solved for the separate five main GCP categories. Alternatively, if an inversion only solved for total emissions (or for categories other than the main five described above), then the prior contribution of each source category at the spatial resolution of the inversion was scaled by the ratio of the total (or embedding category) optimized flux divided by the total (or embedding category) prior flux (Kirschke et al., 2013). In other words, the prior relative mix of sources at model resolution is kept while updating total emissions with atmospheric observations. The soil uptake was provided separately in order to report total gross surface emissions instead of net fluxes (sources minus soil uptake).¶

1229 this synthesis, can help to separate sources with different locations or temporal variations but cannot fully separate individual
1230 sources where they overlap in space and time in some regions. Top-down global and regional CH₄ emissions per source
1231 category were nevertheless obtained from gridded optimised fluxes, for the inversions that separated emissions into the five
1232 main GCP categories. Alternatively, for the inversion that only solved for total emissions (or for other categories other than
1233 the five described above), the prior contribution of each source category at the spatial resolution of the inversion was scaled
1234 by the ratio of the total (or embedding category) optimised flux divided by the total (or embedding category) prior flux
1235 (Kirschke et al., 2013). In other words, the prior relative mix of sources at model resolution is kept in each grid cell while
1236 total emissions are given by the atmospheric inversions. The soil uptake was provided separately to report total gross surface
1237 emissions instead of net fluxes (sources minus soil uptake).

1238 In summary, bottom-up models and inventories emissions are presented for all relevant source processes and grouped if
1239 needed into the five main categories defined above. Top-down inversion emissions are reported globally and, for the five
1240 main emission categories.

1241 2.5 Processing of emission maps and box-plot representation of emission budgets

1242 Common data analysis procedures have been applied to the different bottom-up models, inventories and atmospheric
1243 inversions whenever gridded products exist. Gridded emissions from atmospheric inversions, land-surface models for
1244 wetland or biomass burning were provided at the monthly scale. Emissions from anthropogenic inventories are usually
1245 available as yearly estimates. These monthly or yearly fluxes were provided on a 1°x1° grid or re-gridded to 1°x1°, then
1246 converted into units of Tg CH₄ per grid cell. Inversions with a resolution coarser than 1° were downscaled to 1° by each
1247 modelling group. Land fluxes in coastal pixels were reallocated to the neighbouring land pixel according to our 1° land-sea
1248 mask, and vice-versa for ocean fluxes. Annual and decadal means used for this study were computed from the monthly or
1249 yearly gridded 1°x1° maps.

1250 Budgets are presented as boxplots with quartiles (25%, median, 75%), outliers, and minimum and maximum values without
1251 outliers. Outliers were determined as values below the first quartile minus three times the interquartile range, or values above
1252 the third quartile plus three times the interquartile range. Mean values reported in the tables are represented as “+” symbols
1253 in the corresponding figures.

1254 3 Methane sources and sinks: bottom-up estimates

1255 For each source category, a short description of the relevant processes, original data sets (measurements, models) and related
1256 methodology are given. More detailed information can be found in original publication references, in Annex A2 where the
1257 sources of data used to estimate the different sources and sinks are summarised and compared with those used in Sauniois et
1258 al. (2020) and in the Supplementary Material of this study, when specified in the text. The emission estimates for each source

Supprimé : for

Supprimé : globally

Supprimé : inversions

Supprimé : only

Mis en forme : Police :Gras, Couleur de police : Noir

Mis en forme : Normal, Espace Avant : 12 pt, Après : 12 pt, Paragraphes solidaires, Bordure : Haut: (Pas de bordure), Bas: (Pas de bordure), Gauche: (Pas de bordure), Droite: (Pas de bordure), Entre : (Pas de bordure)

Supprimé : modeling

Supprimé : inter-quartile

Supprimé : inter-quartile

Mis en forme : Police :Gras, Couleur de police : Noir

Mis en forme : Normal, Espace Avant : 24 pt, Après : 12 pt, Paragraphes solidaires, Bordure : Haut: (Pas de bordure), Bas: (Pas de bordure), Gauche: (Pas de bordure), Droite: (Pas de bordure), Entre : (Pas de bordure)

Mis en forme : Police :Gras, Couleur de police : Noir

Supprimé : and

Supprimé : supplementary material

Supprimé : .

1269 category are compared with Saunois et al. (2020) in Table 3 and with Saunois et al. (2016) in Table S12 for the decade 2000-
1270 2009.

1271 **3.1 Anthropogenic direct sources**

1272 **3.1.1 Global inventories**

1273 The main bottom-up global inventory datasets covering direct anthropogenic emissions from all sectors (Table 1) are from
1274 the United States Environmental Protection Agency (USEPA, 2019), the Greenhouse gas and Air pollutant Interactions and
1275 Synergies (GAINS) model developed by the International Institute for Applied Systems Analysis (IIASA) (Höglund-
1276 Isaksson et al., 2020) and the Emissions Database for Global Atmospheric Research (EDGARv6 and v7, Crippa et al., 2021,
1277 2023) compiled by the European Commission Joint Research Centre (EC-JRC) and Netherlands Environmental Assessment
1278 Agency (PBL). We also used the Community Emissions Data System for historical emissions (CEDS) (Hoesly et al., 2018)
1279 developed for climate modelling and the Food and Agriculture Organization (FAO) FAOSTAT emission database (Tubiello
1280 et al., 2022), which covers emissions from agriculture and land use (including peatland fires and biomass fires). These
1281 inventories are not independent as they may use the same activity data or emission factors, as discussed below.

1282 These inventory datasets report emissions from fossil fuel production, transmission, and distribution; livestock enteric
1283 fermentation; manure management and application; rice cultivation; solid waste and wastewater. Since the level of detail
1284 provided by country and by sector varies among inventories, the data were reconciled into common categories according to
1285 Table S2. For example, agricultural waste burning emissions treated as a separate category in EDGAR, GAINS and FAO,
1286 are included in the biofuel sector in the USEPA inventory and in the agricultural sector in CEDS. The GAINS, EDGAR and
1287 FAO estimates of agricultural waste burning were excluded from this analysis (these amounted to 1-3 Tg CH₄ yr⁻¹ in recent
1288 decades) to prevent any potential overlap with separate estimates of biomass burning emissions (e.g. GFEDv4.1s, Gioglio et
1289 al. (2013); van der Werf et al (2017)). In the inventories used here, emissions for a given region/country and a given sector
1290 are usually calculated following IPCC methodology (IPCC, 2006), as the product of an activity factor and its associated
1291 emission factor. An abatement coefficient may also be used, to account for any regulations implemented to control emissions
1292 (see e.g., Höglund-Isaksson et al., 2015). These datasets differ in their assumptions and data used for the calculation;
1293 however, they are not completely independent because they often use the same activity data and some of them follow the
1294 same IPCC guidelines (IPCC, 2006). While the USEPA inventory adopts emissions reported by the countries to the
1295 UNFCCC, other inventories (FAOSTAT, EDGAR and the GAINS model) produce their own estimates using a consistent
1296 approach for all countries, typically IPCC Tier 1 methods or deriving IPCC Tier 2 emission factors from country-specific
1297 information using a consistent methodology. These other inventories compile country-specific activity data and emission
1298 factor information or, if not available, adopt IPCC default factors (Tibrewal et al., 2024; Oreggioni et al., 2021; Höglund-
1299 Isaksson et al., 2020; Tubiello, 2019). CEDS takes a different approach (Hoesly et al., 2018) and combines data from
1300 GAINS, EDGAR and FAO depending on the sector. Then their first estimates are scaled to match other individual or region-

Mis en forme : Police :Gras, Couleur de police : Noir

Mis en forme : Normal, Espace Avant : 12 pt, Après : 12 pt, Paragraphes solidaires, Bordure : Haut: (Pas de bordure), Bas: (Pas de bordure), Gauche: (Pas de bordure), Droite: (Pas de bordure), Entre : (Pas de bordure)

Mis en forme : Police :Gras, Couleur de police : Noir

Supprimé: gathered

Mis en forme : Police :Gras, Couleur de police : Noir

Supprimé: The main bottom-up global inventory datasets covering anthropogenic emissions from all sectors (Table 1) are from the United States Environmental Protection Agency (USEPA, 2012), the Greenhouse gas and Air pollutant Interactions and Synergies (GAINS) model developed by the International Institute for Applied Systems Analysis (IIASA) (Gomez Sanabria et al., 2018; Höglund-Isaksson, 2012, 2017) and the Emissions Database for Global Atmospheric Research (EDGARv3.2.2, Janssens-Maenhout et al., 2019) compiled by the European Commission Joint Research Centre (EC-JRC) and Netherland's Environmental Assessment Agency (PBL). We also used the Community Emissions Data System for historical emissions (CEDS) (Hoesly et al., 2018) developed for climate modelling and the Food and Agriculture Organization (FAO) dataset emission database (Tubiello, 2019), which only covers emissions from agriculture and land use (including peatland and biomass fires).[†]

Supprimé: and

Supprimé:

Supprimé: inadvertent

Supprimé: .

Supprimé:).

Supprimé: (IPCC, 2006),

Supprimé: an

Supprimé: for this activity.

Supprimé: is

Supprimé: additionally

Supprimé: (see e.g. Höglund-Isaksson et al., 2015).

Supprimé: (IPCC, 2006), and, at least for agriculture, use the same FAOSTAT activity data.

Supprimé: .

Supprimé: (Höglund-Isaksson, 2012; Janssens-Maenhout et al., 2019; Tubiello, 2019).

Supprimé: starting

Supprimé: pre-existing default emission estimates; for methane, a combination of

Supprimé: is used,

1338 specific inventory values when available. This process maintains the spatial information in the default emission inventories
 1339 while preserving consistency with country level data. The FAOSTAT dataset (hereafter FAO-CH₄) provides estimates at
 1340 the country level and is limited to agriculture (CH₄ emissions from enteric fermentation, manure management, rice
 1341 cultivation, energy usage, burning of crop residues, and prescribed burning of savannahs) and land-use (peatland fires and
 1342 biomass burning). FAO-CH₄ uses activity data mainly from the FAOSTAT crop and livestock production database, as
 1343 reported by countries to FAO (Tubiello et al., 2013), and applies mostly the Tier 1 IPCC methodology for emissions factors
 1344 (IPCC, 2006), which depends on geographic location and development status of the country. For manure, the country-scale
 1345 temperature was obtained from the FAO global agro-ecological zone database (GAEZv3.0, 2012). Although country
 1346 emissions are reported annually to the UNFCCC by annex I countries, and episodically by non-annex I countries, data gaps
 1347 of those national inventories do not allow the inclusion of these estimates in this analysis.

1348 In this budget, we use the following versions of these inventories that were available at the start and during the analysis (see
 1349 Table 1):

- 1350 • EDGARv6 which provides yearly gridded emissions by sectors from 1970 to 2018 (Crippa et al., 2021; Oreggioni
 1351 et al., 2021; EDGARv6 website https://edgar.jrc.ec.europa.eu/dataset_ghg60; Monforti Ferrario et al., 2021).
- 1352 • EDGARv7, which provides yearly gridded emissions by sectors from 1970 to 2020 (monthly for some sectors),
 1353 but emissions from fossil fuel energy are not separated (oil and gas, and coal are lumped together - see Table S2)
 1354 (EDGARv7 website https://edgar.jrc.ec.europa.eu/dataset_ghg70; Crippa et al., 2023).
- 1355 • GAINS model scenario version 4.0 (Höglund-Isaksson et al., 2020) which provides an annual sectorial gridded
 1356 product from 1990 to 2020 both by country and gridded. USEPA (USEPA, 2019), which provides 5-year sectorial
 1357 totals by country from 1990 to 2020 (estimates from 2015 onward are a projection), with no gridded distribution
 1358 available. The USEPA dataset was linearly interpolated to provide yearly values from 1990-2020.
- 1359 • CEDS version v 2021_04_21 which provides gridded monthly and annual country-based emissions by sectors
 1360 from 1970 to 2019 (Hoesly et al., 2018; O'Rourke et al., 2021). Fossil fuel emissions for 2020 have been updated
 1361 using the methodology described for CO in Zheng et al. (2023).
- 1362 • FAO-CH₄ (database accessed in December 2022, FAO, 2022) containing annual country level data for the period
 1363 1961-2020, for rice, manure, and enteric fermentation; and 1990-2020 for burning savannah, crop residue and non-
 1364 agricultural biomass burning.

1365 3.1.2 Total anthropogenic direct emissions

1366 We calculated separately the total anthropogenic emissions for each inventory by adding its values for "Agriculture and
 1367 waste", "Fossil fuels" and "Biofuels" with additional large-scale biomass burning emissions data (Sect. 3.1.5). This method
 1368 avoids double counting and ensures consistency within each inventory. This approach was used for the EDGARv6 and v7,
 1369 CEDS and GAINS inventories, but we kept the USEPA inventory as originally reported because it includes its own estimates

Supprimé: FAOSTATdataset

Supprimé: was used to provide

Supprimé: of methane emissions

Supprimé: but

Supprimé: (Tubiello et al., 2013),

Supprimé: (IPCC, 2006),

Supprimé: depend

Supprimé: necessary

Supprimé: (GAEZv3.0, 2012).

Supprimé: databases

Supprimé: <#>EDGARv4.3.2 which provides yearly gridded emissions by sectors from 1970 to 2012 (Janssens-Maenhout et al., 2019).[†]

<#>GAINS model scenario ECLIPSE v6 (Gomez Sanabria et al., 2018; Höglund-Isaksson, 2012, 2017) which provides both annual sectoral totals by country from 1990 to 2015 and a projection for 2020 (that assumes current emission legislation for the future) and an annual sectorial gridded product from 1990 to 2015.[†]

Mis en forme : Hiérarchisation + Niveau : 1 + Style de numérotation : Puce + Alignement : 0,63 cm + Retrait : 1,27 cm

Supprimé: (USEPA, 2012),

Supprimé: 2005

Supprimé: ,

Supprimé: <#>CEDS version 2017-05-18 which provides both gridded monthly and annual country-based emissions by sectors from 1970 to 2014 (Hoesly et al., 2018).[†]

Mis en forme : Hiérarchisation + Niveau : 1 + Style de numérotation : Puce + Alignement : 0,63 cm + Retrait : 1,27 cm

Supprimé: February 2019, (FAO, 2019))

Supprimé: 2016

Supprimé: 2016

Supprimé: In order to report emissions for the period 2000-2017, we extended and interpolated some of the datasets as explained in [87]

Mis en forme ... [88]

Mis en forme : Police :Gras, Couleur de police : Noir

Mis en forme : Police :Gras, Couleur de police : Noir

Mis en forme ... [89]

Supprimé: In order to avoid double counting and ensure ... [90]

Supprimé: biofuels

Supprimé: the range of available

Supprimé: .

Supprimé: EGDARv4.3.2

1443 of biomass burning emissions. FAO-CH₄ was only included in the range reported for the “Agriculture and waste” category.
1444 For the latter, we calculated the range and mean value as the sum of the mean and range of the three anthropogenic
1445 subcategory estimates “Enteric fermentation and Manure”, “Rice”, and “Landfills and Waste”. The values reported for the
1446 upper-level anthropogenic categories (“Agriculture and waste”, “Fossil fuels” and “Biomass burning & biofuels”) are
1447 therefore consistent with the sum of their subcategories, although there might be small percentage differences between the
1448 reported total anthropogenic emissions and the sum of the three upper-level categories. This approach provides a more
1449 accurate representation of the range of emission estimates, avoiding an artificial expansion of the uncertainty attributable to
1450 subtle differences in the definition of sub-sector categorisations between inventories.

1451 Based on the ensemble of databases detailed above, total direct anthropogenic emissions were 358 [329-387] Tg CH₄ yr⁻¹
1452 for the decade 2010-2019 (Table 3, including biomass and biofuel burning) and 331 [305-365] Tg CH₄ yr⁻¹ for the decade
1453 2000-2009. Our estimate for the 2000-2009 decade is within the range of Sauniois et al. (2020) (334 [321-358]), Sauniois et
1454 al. (2016) (338 Tg CH₄ yr⁻¹ [329-342]) and Kirschke et al. (2013) (331 Tg CH₄ yr⁻¹ [304-368]) for the same period. The
1455 slightly larger range reported herein with respect to previous estimates is due to the USEPA lower estimate for agriculture,
1456 waste and fossil emissions associated with the lowest estimate of biomass burning.

1457 Figure 2 (left) summarises or projects global CH₄ emissions of anthropogenic sources (including biomass and biofuel
1458 burning) by different datasets between 2000 and 2050. The datasets consistently estimate total anthropogenic emissions of
1459 ~300 Tg CH₄ yr⁻¹ in 2000. For the Sixth Assessment Report of the IPCC, seven main Shared Socioeconomic Pathways
1460 (SSPs) were defined for future climate projections in the Coupled Model Intercomparison Project 6 (CMIP6) (Gidden et al.,
1461 2019; O’Neill et al., 2016) ranging from 1.9 to 8.5 W m⁻² radiative forcing by the year 2100 (as shown by the number in the
1462 SSP names). For the 1970-2015 period, historical emissions used in CMIP6 (Feng et al., 2019) combine anthropogenic
1463 emissions from CEDS (Hoesly et al., 2018) and a climatological value from the GFEDv4.1s biomass burning inventory (van
1464 Marle et al., 2017). The harmonised scenarios used for CMIP6 activities start in 2015 at 388 Tg CH₄ yr⁻¹, which corresponds
1465 to the higher range of our estimates. Since CH₄ emissions continue to track scenarios that assume no or minimal climate
1466 policies (SSP5 and SSP3), it may indicate that climate policies, when present, have not yet produced sufficient results to
1467 change the emissions trajectory substantially (Nisbet et al., 2019). After 2015, the SSPs span a range of possible outcomes,
1468 but current emissions appear likely to follow the higher-emission trajectories over the next decade in terms of trend, and the
1469 peak year has not yet been reached. This illustrates the challenge of methane mitigation that lies ahead to help reach the
1470 goals of the Paris Agreement. In addition, estimates of methane atmospheric concentrations (Meinshausen et al., 2017, 2020)
1471 from the harmonised scenarios (Riahi et al., 2017) indicate that observations of global CH₄ concentrations fall well within
1472 the range of scenarios (Fig. 2 right). The CH₄ concentrations are estimated using a simple exponential decay with inferred
1473 natural emissions (Meinshausen et al., 2011), and the emergence of any trend between observations and scenarios needs to
1474 be confirmed in the following years. However, the current observed concentrations and emissions estimates lie in the upper
1475 range of the former RCPs scenarios starting in 2005 (Fig. S1). In the future, it will be important to monitor the trends from

Supprimé: Based on the ensemble of databases detailed above, total anthropogenic emissions were 366 [349-393] Tg CH₄ yr⁻¹ for the decade 2008-2017 (Table 3, including biomass and biofuel burning) and 334 [321-358] Tg CH₄ yr⁻¹ for the decade 2000-2009. Our estimate for the preceding decade is statistically consistent with Sauniois et al. (2016) (338 Tg CH₄ yr⁻¹ [329-342]) and Kirschke et al. (2013) (331 Tg CH₄ yr⁻¹ [304-368]) for the same period. The slightly larger range reported herein with respect to previous estimates is mainly due to a larger range in the biomass burning estimates, as more biomass burning products are included in this update. The range associated with our estimates (~10-12%) is smaller than the range reported in Höglund-Isaksson et al. (2015) (~20%), perhaps because they analysed data from a wider range of inventories and projections, plus this study was referenced to one year only (2005) rather than averaged over a decade, as done here.⁴ Figure 2 (top panels) summarizes global methane emissions of anthropogenic sources (including biomass and biofuel burning) by different datasets between 2000 and 2050. The datasets consistently estimate total anthropogenic emissions of ~300 Tg CH₄ yr⁻¹ in 2000. The main discrepancy between the inventories is their trend after 2005, with the lowest emissions projected by GAINS and the largest by CEDS. For the Sixth Assessment Report of the IPCC, seven main Shared Socioeconomic Pathways (SSPs) were defined for future climate projections in the Coupled Model Intercomparison Project 6 (CMIP6) (Gidden et al., 2019; O’Neill et al., 2016) ranging from 1.9 to 8.5 W m⁻² radiative forcing by the year 2100 (as shown by the number in the SSP names). The trends in methane emissions from 2010 estimated by current inventories track the pathways with the highest radiative forcing in 2100 (based on the unharmonized scenarios developed by Integrated Assessment Models, top left panel). For the 1970-2015 period, historical emissions used in CMIP6 (Feng et al., 2019) combine anthropogenic emissions from CEDS (Hoesly et al., 2018) and a climatological value from the GFEDv4.1s biomass burning inventory (van Marle et al., 2017). The CEDS anthropogenic emissions estimates, based on EDGARv4.2, are 10-20 Tg higher than the more recent EDGARv4.3.2 (van Marle et al., 2017). Harmonized scenarios used for CMIP6 activities start in 2015 at 388 Tg CH₄ yr⁻¹. Since methane emissions continue to track scenarios that assume no or minimal climate policies, it may indicate that climate policies, when present, have not yet produced sufficient results to change the emissions trajectory substantially (Nisbet et al., 2019). After 2015, the SSPs span a range of possible outcomes, but current emissions appear likely to follow the higher-emission trajectories over the next decade. This illustrates the challenge of methane mitigation that lies ahead to help reach the goals of the Paris agreement. In addition, estimates of methane atmospheric concentrations from the unharmonized scenarios (Riahi et al., 2017) indicate that observations of global methane concentrations fall well within the range of scenarios (Fig. 2 bottom). The methane concentrations are estimated using a simple exponential decay with inferred natural emissions (Meinshausen et al., 2011), and the emergence of any trend between observations and scenarios needs to be confirmed in the following years. In the future, it will be important to monitor the trends from year 2015 (the Paris agreement) estimated in inventories and from atmospheric observations, and compare them to various scenarios.⁴

532 2015 (the Paris Agreement) and from 2020 (Global Methane Pledge) estimated in inventories and from atmospheric
533 observations, and compare them to various scenarios.

534 **3.1.3 Fossil fuel production and use**

535 Most anthropogenic CH₄ emissions related to fossil fuels come from the exploitation, transportation, and usage of coal, oil,
536 and natural gas. Additional emissions reported in this category include small industrial contributions such as the production
537 of chemicals and metals, fossil fuel fires (e.g., underground coal mine fires and the Kuwait oil and gas fires), and transport
538 (road and non-road transport). CH₄ emissions from the oil processing industry (e.g., refining) and production of charcoal
539 are estimated to be a few Tg CH₄ yr⁻¹ only and are included in the transformation industry sector in the inventory. Fossil
540 fuel fires are included in the subcategory "Oil & Gas". Emissions from industries, road and non-road transport are reported
541 apart from the two main subcategories "Oil & Gas" and "Coal", as in Saunois et al. (2020) and contrary to Saunois et al.
542 (2016); each of these amounts to about 2 to 5 Tg CH₄ yr⁻¹ (Table 3). The large range (1-9 Tg CH₄ yr⁻¹) is attributable to
543 difficulties in allocating some sectors to these sub-sectors consistently among the different inventories (See Table S2). The
544 spatial distribution of CH₄ emissions from fossil fuels is presented in Fig. 3 based on the mean gridded maps provided by
545 CEDS, EDGARv6, and GAINS for the 2010-2019 decade; USEPA lacks a gridded product.

546 Global mean emissions from fossil fuel-related activities, other industries and transport are estimated from the four global
547 inventories (Table 1) to be of 120 [117-125] Tg CH₄ yr⁻¹ for the 2010-2019 decade (Table 3), but with large differences in
548 the rate of change during this period across inventories. The sector accounts on average for 34% (range 31-42%) of total
549 global anthropogenic emissions.

550 **Coal mining.**

551 During mining, CH₄ is emitted primarily from ventilation shafts, where large volumes of air are pumped in and out of the
552 mine to keep the CH₄ mixing ratio below 0.5% to avoid accidental ignition, and from dewatering operations. In countries of
553 the Organization for Economic Co-operation and Development (OECD), coalbed CH₄ is often extracted as fuel up to ten
554 years before the coal mine starts operation, thereby reducing the CH₄ channelled through ventilation shafts during mining.
555 In many countries, large quantities of ventilation air CH₄ are still released to the atmosphere or flared, despite efforts to
556 extend coal mine gas recovery under the UNFCCC Clean Development Mechanisms (<http://cdm.unfccc.int>). CH₄ leaks also
557 occur during post-mining handling, processing, and transportation. Some CH₄ is released from coal waste piles and
558 abandoned mines; while emissions from these sources were believed to be low (IPCC, 2000), recent work has estimated
559 these at 22 billion m³ (compared to 103 billion m³ from functioning coal mines) in 2010 with emissions projected to increase
560 into the future (Kholod et al., 2020).

561 In 2020, more than 35% (IEA, 2023a) of the world's electricity is still produced from coal. This contribution grew in the
562 2000s at the rate of several percent per year, driven by Asian economic growth where large reserves exist, but global coal
563

- Mis en forme : Police :Gras, Couleur de police : Noir
- Mis en forme : Police :Gras, Couleur de police : Noir, Motif : Transparente (Orange clair)
- Mis en forme : Normal, Espace Avant : 12 pt, Après : 12 pt, Paragraphes solidaires, Bordure : Haut: (Pas de bordure), Bas: (Pas de bordure), Gauche: (Pas de bordure), Droite: (Pas de bordure), Entre : (Pas de bordure)
- Supprimé: methane
- Supprimé: Methane
- Supprimé: .
- Supprimé: sub-category
- Supprimé: and
- Supprimé: sub-categories
- Supprimé: theses
- Supprimé: 0-12
- Supprimé: methane
- Supprimé: EDGARv4.3.2
- Supprimé: 2008-2017
- Supprimé:
- Supprimé: 128 [113-154]
- Supprimé: 2008-2017
- Supprimé: 35
- Supprimé: 30
- Supprimé: methane
- Supprimé: into
- Supprimé: methane released from
- Supprimé: is in principle used as fuel, but in
- Supprimé: it is
- Supprimé: emitted into
- Supprimé: the
- Supprimé: for coalmine
- Supprimé: Methane
- Supprimé: (IPCC, 2000),
- Supprimé: against
- Supprimé: (Kholod et al., 2020).
- Mis en forme : Anglais (G.B.)
- Supprimé: In 2017, almost 40% (IEA, 2019b)
- Supprimé: per cent

1594 consumption declined between 2014 and 2020. In 2020, the top ten largest coal producing nations accounted for ~90% of
1595 total world CH₄ emissions from coal mining; among them, the top three producers (China, United States of America, and
1596 India) produced almost two-thirds (66%) of the world's coal (IEA, 2021).

1597 Global estimates of CH₄ emissions from coal mining show a reduced range of 37-44 Tg CH₄ yr⁻¹ for 2010-2019, compared
1598 to the previous estimate for 2008-2017 in Sauniois et al. (2020) reporting a range of 29-61 Tg CH₄ yr⁻¹ for 2008-2017. This
1599 reduced range probably results from using similar activity data (mostly from IEA statistics) in the different inventories. The
1600 highest value of the range in Sauniois et al. (2020) came from the CEDS inventory while the lowest came from USEPA.
1601 CEDS seems to have revised downward their estimate compared to the previous version used in Sauniois et al. (2020). There
1602 were previously large discrepancies in Chinese coal emissions, with a large overestimation from EDGARv4.2 on which
1603 CEDS was based. As highlighted by Liu et al. (2021a), a county-based inventory of Chinese methane emissions also
1604 confirms the overestimation of previous EDGAR inventories and estimated total anthropogenic Chinese emissions at
1605 38.2±5.5 Tg CH₄ yr⁻¹ for 2000-2008 (Liu et al., 2021a). Coal mining emission factors depend strongly on the type of coal
1606 extraction (underground mining emits up to 10 times more than surface mining), the geological underground structure
1607 (region-specific), history (basin uplift), and the quality of the coal (brown coal (lignite) emits more than hard coal
1608 (anthracite)). Finally, the different emission factors derived for coal mining is the main reason for the differences between
1609 inventories globally (Fig. 2).

1610 For the 2010-2019 decade, methane emissions from coal mining represent 33% of total fossil fuel-related emissions of CH₄
1611 (40 [37-44] Tg CH₄ yr⁻¹). An additional very small source corresponds to fossil fuel fires (mostly underground coal fires,
1612 ~0.15 Tg yr⁻¹ any year in EDGARv7).

1613 ▲ Oil and natural gas systems.

1615 This sub-category includes emissions from both conventional and shale oil and gas exploitation. Natural gas is composed
1616 primarily of CH₄, so both fugitive and planned emissions during the drilling of wells in gas fields, extraction, transportation,
1617 storage, gas distribution, end use, and incomplete combustion in gas flares emit CH₄ (Lamb et al., 2015; Shorter et al., 1996).
1618 Persistent fugitive emissions (e.g., due to leaky valves and compressors) should be distinguished from intermittent emissions
1619 due to maintenance (e.g., purging and draining of pipes) or incidents. During transportation, fugitive emissions can occur in
1620 oil tankers, fuel trucks and gas transmission pipelines, attributable to corrosion, manufacturing, and welding faults.
1621 According to Lelieveld et al. (2005), CH₄ fugitive emissions from gas pipelines should be relatively low, however, old
1622 distribution networks in some cities may have higher rates, especially those with cast-iron and unprotected steel pipelines
1623 (Phillips et al., 2013). Measurement campaigns in cities within the USA (e.g., McKain et al., 2015) and Europe (e.g.,
1624 Defratyka et al., 2021) revealed that significant emissions occur in specific locations (e.g., storage facilities, city natural gas
1625 fueling stations, well and pipeline pressurisation/depressurisation points, sewage systems, and furnaces of buildings) along
1626 the distribution networks (e.g., Jackson et al., 2014a; McKain et al., 2015; Wunch et al., 2016). However, CH₄ emissions

Supprimé: since

Supprimé: 2018

Supprimé: methane

Supprimé: for

Supprimé: USA

Supprimé:

Supprimé: 64

Supprimé: (IEA, 2019a).

Supprimé: Global estimates of CH₄ emissions from coal mining show a large range of 29-61 Tg CH₄ yr⁻¹ for 2008-2017, in part due to the lack of comprehensive data from all major producing countries. The highest value of the range comes from the CEDS inventory while the lowest comes from USEPA. CEDS seems to have overestimated coal mining emissions from China by almost a factor of 2, most likely due to its dependence on the EDGARv4.2 emission inventory. As highlighted by Sauniois et al. (2016), a county-based inventory of Chinese methane emissions also confirms the overestimate of about +38% with total anthropogenic emissions estimated at 43±6 Tg CH₄ yr⁻¹ (Peng et al., 2016). EDGARv4.2 inventory follows the IPCC guidelines and uses European averaged emission factor for CH₄ from coal production to substitute missing data for China, which appears to be overestimated by a factor of approximately two. These differences highlight significant errors resulting from the use of emission factors, and that applying "Tier 1" approaches for coal mine emissions is not sufficiently accurate as stated by the IPCC guidelines. The newly released version of EDGARv4.3.2 used here has revised China coal methane emission factors downwards and distributed them to more than 80 times more coal mining locations in China. Coal mining emission factors depend strongly on the type of coal extraction (underground mining emits up to 10 times more than surface mining), the geological underground structure (region-specific), history (basin uplift), and the quality of the coal (brown coal emits more than hard coal). Finally, coal mining is the main source explaining the differences between inventories globally (Fig. 2).†

Supprimé: 2008-2017

Supprimé:

Supprimé: methane (42

Supprimé: , range of 29-61

Supprimé: 2012, EDGARv4.3.2).

Mis en forme : Police :Gras

Supprimé: Natural gas is comprised primarily of methane, so both fugitive and planned emissions during the drilling of wells in gas fields, extraction, transportation, storage, gas distribution, end use, and incomplete combustion of gas flares emit methane (Lamb et al., 2015; Shorter et al., 1996). Persistent fugitive emissions (e.g., due to leaky valves and compressors) should be distinguished from intermittent emissions due to maintenance (e.g. purging and draining of pipes). During transportation, fugitive emissions can occur in oil tankers, fuel trucks and gas transmission pipelines, attributable to corrosion, manufacturing and welding faults. According to Lelieveld et al. (2005), CH₄ fugitive emissions from gas pipelines should be relatively low, however distribution networks in older cities may have higher rates, especially those with cast-iron and unprotected†[91]

723 vary significantly from one city to another depending, in part, on the age of city infrastructure and the quality of its
724 maintenance, making urban emissions difficult to scale-up from measurement campaigns, although attempts have been made
725 (e.g., Defratyka et al., 2021). In many facilities, such as gas and oil fields, refineries, and offshore platforms, most of the
726 associated and other waste gas generated will be flared for security reasons with almost complete conversion to CO₂,
727 however, due to the large quantities of waste gas generated, small fractions of gas still being vented make up relatively large
728 quantities of methane. These two processes are usually considered together in inventories of oil and gas industries. In
729 addition, single-point failure of natural gas infrastructure can leak CH₄ at high rate for months, such as at the Aliso Canyon
730 blowout in the Los Angeles, CA (Conley et al., 2016) or the shale gas well blowout in Ohio (Pandey et al., 2019), thus
731 hampering emission control strategies. Production of natural gas from the exploitation of hitherto unproductive rock
732 formations, especially shale, began in the 1970s in the US on an experimental or small-scale basis, and then, from the early
733 2000s, exploitation started at a large commercial scale. The shale gas contribution to total dry natural gas production in the
734 United States reached 82% in 2023, growing rapidly from 48% in 2013 (IEA, 2023b). The possibly larger emission factors
735 from shale gas compared to conventional gas, have been widely debated (e.g., Cathles et al., 2012; Howarth, 2019; Lewan,
736 2020). However, the latest studies tend to infer similar emission factors in a narrow range of 1-3% (Alvarez et al., 2018;
737 Peischl et al., 2015; Zavala-Araiza et al., 2015), different from the widely spread rates of 3-17% from previous studies (e.g.,
738 Caulton et al., 2014; Schneising et al., 2014).

739 CH₄ emissions from oil and natural gas systems vary greatly in different global inventories (67 to 80 Tg yr⁻¹ in 2020, Table
740 3). The inventories generally rely on the same sources and magnitudes for activity data, with the derived differences
741 therefore resulting primarily from different methodologies and parameters used, including emission factors. Those factors
742 are country- or even site-specific and the few field measurements available often combine oil and gas activities (Brandt et
743 al., 2014), resulting in high uncertainty in emission estimates for many major oil and gas producing countries. Depending
744 on the region, the IPCC 2006 default emission factors may vary by two orders of magnitude for oil production and one order
745 for gas production. For instance, the GAINsv4.0 estimate of CH₄ emissions from US oil and gas systems in 2015 is 16
746 Tg, which is almost twice as high as EDGARv8.0 at 8.4 Tg and USEPA (UNFCCC, 2023) at 9.5 Tg. The difference can
747 partly be explained by GAINS using a bottom-up methodology to derive country- and year-specific flows of associated
748 petroleum gas and attributing these to recovery/reinjection, flaring or venting (Höglund-Isaksson, 2017), and partly to
749 GAINS using a higher emission factor for unconventional gas production (Höglund-Isaksson et al., 2020). Recent
750 quantifications using satellite observations and inversion estimate a relatively stable trend for US oil and gas systems
751 emissions since 2010, with Lu et al. (2023) estimating 14.6 Tg for 2010, 15.9 Tg for 2014 and 15.6 Tg for 2019, Shen et al.
752 (2022) estimating a mean of 12.6 Tg for 2018-2020, and Maasackers et al (2021) a mean of 11.1 Tg for 2010 to 2015. The
753 stable top-down trend for the US appears not well captured in the bottom-up inventories from GAINS and EDGAR, which
754 tend to show an increasing trend driven by increase in production volumes.

Supprimé: Methane emissions from oil and natural gas systems vary greatly in different global inventories (72 to 97 Tg yr⁻¹ in 2017, Table 3). The inventories generally rely on the same sources and magnitudes for activity data, with the derived differences therefore resulting primarily from different methodologies and parameters used, including emission factors. Those factors are country- or even site-specific and the few field measurements available often combine oil and gas activities (Brandt et al., 2014) and remain largely unknown for most major oil- and gas-producing countries. Depending on the country, the reported emission factors may vary by two orders of magnitude for oil production and by one order of magnitude for gas production (Table SI-5.1 of Höglund-Isaksson (2017)). The GAINS estimate of methane emissions from oil production, for instance, is twice as high as EDGARv4.3.2. For natural gas, the uncertainty is of a similar order of magnitude. During oil extraction, natural gas generated can be either recovered (re-injected or utilized as an energy source) or not recovered (flared or vented to the atmosphere). The recovery rates vary from one country to another (being much higher in the USA, Europe and Canada than elsewhere), and from one type of oil to another: flaring is less common for heavy oil wells than for conventional ones (Höglund-Isaksson et al., 2015). Considering recovery rates could lead to two-times-higher methane emissions accounting for country-specific rates of generation and recovery of associated gas than when using default values (Höglund-Isaksson, 2012). This difference in methodology explains, in part, why GAINS estimates are higher than those of EDGARv4.3.2.†

Most studies (Alvarez et al., 2018; Brandt et al., 2014; Jackson et al., 2014b; Karion et al., 2013; Moore et al., 2014; Olivier and Janssens-Maenhout, 2014; Pétron et al., 2014; Zavala-Araiza et al., 2015), albeit not all (Allen et al., 2013; Cathles et al., 2012; Peischl et al., 2015), suggest that methane emissions from oil and gas industry are underestimated by inventories and agencies, including the USEPA. Zavala-Araiza et al. (2015) showed that a few high-emitting facilities, i.e., super-emitters, neglected in the inventories, dominated USA emissions. These high emitting points, located on the conventional part of the facility, could be avoided through better operating conditions and repair of malfunctions. As USA production increases, absolute methane emissions almost certainly increase, as well USA crude oil production doubled over the last decade and natural gas production rose more than 50% (EIA, 2019). However, global implications of the rapidly growing shale gas activity in the US remains to be determined precisely.†

798 Most studies (Alvarez et al., 2018; Brandt et al., 2014; Jackson et al., 2014b; Karion et al., 2013; Moore et al., 2014; Olivier
 799 and Janssens-Maenhout, 2014; Pétron et al., 2014; Zavala-Araiza et al., 2015), albeit not all (Allen et al., 2013; Cathles et
 800 al., 2012; Peischl et al., 2015), suggest that the methane emissions from oil and gas industry are underestimated by
 801 inventories, industries, and agencies, including the USEPA. Lauvaux et al. (2022) showed that emissions from a few high-
 802 emitting facilities, i.e., super-emitters ($> 20 \text{ t hr}^{-1}$), which are usually sporadic in nature, and not accounted for in the
 803 inventories, could represent 8-12% of global oil & gas emissions, or around $8 \text{ Tg CH}_4 \text{ yr}^{-1}$. These high emitting points,
 804 located on the conventional part of the facilities, could be avoided through better operating conditions and repair of
 805 malfunctions. Over the last decade, absolute CH_4 emissions almost certainly increased, since USA crude oil production
 806 doubled and natural gas production rose by about 50% (IEA, 2023a). However, global implications of the rapidly growing
 807 shale gas activity in the US remain to be determined precisely.

808 For the 2010-2019 decade, CH_4 emissions from upstream and downstream oil and natural gas sectors are estimated to
 809 represent about 56% of total fossil CH_4 emissions ($67 [57-74] \text{ Tg CH}_4 \text{ yr}^{-1}$, Table 3) based on global inventories, with a
 810 lower uncertainty range than for coal emissions for most countries. However, it is worth noting that $8 \text{ Tg CH}_4 \text{ yr}^{-1}$ should
 811 be added on top of this estimate to acknowledge the ultra-emitters contribution, as done in Tibrewal et al (2024).

812 3.1.4 Agriculture and waste sector

813 This main category includes CH_4 emissions related to livestock production (i.e., enteric fermentation in ruminant animals
 814 and manure management), rice cultivation, landfills, and wastewater handling. Of these activities, globally and in most
 815 countries, livestock is by far the largest source of CH_4 , followed by waste handling and rice cultivation. Conversely, field
 816 burning of agricultural residues is a minor source of CH_4 reported in emission inventories, (a few Tg at the global scale).
 817 The spatial distribution of CH_4 emissions from agriculture and waste handling is presented in Fig. 3 based on the mean
 818 gridded maps provided by CEDS, EDGARv6 and GAINS over the 2010-2019 decade.

819 Global emissions from agriculture and waste for the period 2010-2019 are estimated to be $211 [195-231] \text{ Tg CH}_4 \text{ yr}^{-1}$ (Table
 820 3), representing 60% of total direct anthropogenic emissions. Agriculture emissions amount to $144 \text{ Tg CH}_4 \text{ yr}^{-1}$, 40% of the
 821 direct anthropogenic emissions, with the rest coming from the fossil fuel sector (34%), waste (19%) and biomass (5%) and
 822 biofuel (3%) burning.

823 **Livestock: Enteric fermentation and manure management.** Domestic ruminants such as cattle, buffalo, sheep, goats, and
 824 camels emit CH_4 as a by-product of the anaerobic microbial activity in their digestive systems (Johnson et al., 2002). The
 825 very stable temperatures (about 39°C) and pH (6.5-6.8) within the rumen of domestic ruminants, along with a constant plant
 826 matter flow from grazing (cattle graze many hours per day), allow methanogenic *Archaea* residing within the rumen to
 827 produce CH_4 . CH_4 is released from the rumen mainly through the mouth of multi-stomached ruminants (eructation, ~90%
 828 of emissions) or absorbed in the blood system. The CH_4 produced in the intestines and partially transmitted through the
 829 rectum is only ~10%.

- Supprimé: 2008-2017
- Supprimé: methane
- Supprimé: 63
- Supprimé: $80 \text{ Tg CH}_4 \text{ yr}^{-1}$, range of 68-92
- Supprimé:),
- Supprimé: sectors
- Mis en forme : Police :Gras, Couleur de police : Noir
- Mis en forme : Police :Gras, Couleur de police : Noir, Motif : Transparente (Orange clair)
- Mis en forme : Normal, Espace Avant : 12 pt, Après : 12 pt, Paragraphes solidaires, Bordure : Haut: (Pas de bordure), Bas: (Pas de bordure), Gauche: (Pas de bordure), Droite: (Pas de bordure), Entre : (Pas de bordure)
- Supprimé: methane
- Mis en forme : Non Exposant/ Indice
- Supprimé: .
- Supprimé: methane
- Supprimé: EDGARv4.3.2
- Supprimé: 2008-2017
- Supprimé: 2008-2017
- Supprimé: 206
- Supprimé: range 191-223,
- Supprimé: 56
- Supprimé: methane
- Supprimé: (Johnson et al., 2002).
- Supprimé: values
- Supprimé: methane. Methane
- Supprimé: 87
- Supprimé: methane
- Supprimé: 13

852 The total number of livestock continues to grow steadily. There are currently (2020) about 1.5 billion cattle globally, almost
853 1.3 billion sheep, and nearly as many goats (<http://www.fao.org/faostat/en/#data/GE>). Livestock numbers are linearly related
854 to CH₄ emissions in inventories using the Tier 1 IPCC approach such as FAOSTAT. In practice, some non-linearity may
855 arise due to dependencies of emissions on the total weight of the animals and their diet, which are better captured by Tier 2
856 and higher approaches. Cattle, due to their large population, large individual size, and particular digestive characteristics,
857 account for the majority of enteric fermentation CH₄ emissions from livestock worldwide (Tubiello, 2019; FAO, 2022),
858 particularly in intensive agricultural systems in wealthier and emerging economies, including the United States (USEPA,
859 2016). CH₄ emissions from enteric fermentation also vary from one country to another as cattle may experience diverse
860 living conditions that vary spatially and temporally, especially in the tropics (Chang et al., 2019).
861 Anaerobic conditions often characterise manure decomposition in a variety of manure management systems globally (e.g.,
862 liquid/slurry treated in lagoons, ponds, tanks, or pits), with the volatile solids in manure producing CH₄. In contrast, when
863 manure is handled as a solid (e.g., in stacks or dry-lots) or deposited on pasture, range, or paddock lands, it tends to
864 decompose aerobically and to produce little or no CH₄. However aerobic decomposition of manure tends to produce nitrous
865 oxide (N₂O), which has a larger global warming impact than CH₄. Ambient temperature, moisture, energy contents of the
866 feed, manure composition, and manure storage or residency time affect the amount of CH₄ produced. Despite these
867 complexities, most global datasets used herein apply a simplified IPCC Tier 1 approach, where amounts of manure treated
868 depend on animal numbers and simplified climatic conditions by country.

869 Global CH₄ emissions from enteric fermentation and manure management are estimated in the range of 114-124 Tg CH₄ yr⁻¹
870 for the year 2020, in the GAINS model and CEDS, USEPA, FAO-CH₄ and EDGARv7 inventories. Using the Tier 2
871 method adopted from the 2019 Refinement to 2006 IPCC guidelines, a recent study (Zhang et al., 2022) estimated that
872 global CH₄ emissions from livestock increased from 31.8 [26.5–37.1] (mean [minimum–maximum of 95% confidence
873 interval) Tg CH₄ yr⁻¹ in 1890 to 131.7 [109.6–153.7] Tg CH₄ yr⁻¹ in 2019, a fourfold increase in the past 130 years. Chang
874 et al. (2021) estimates enteric fermentation and manure management emissions based on mixed Tier 1&2 and Tier1
875 approaches and calculate livestock emissions being 120±13 and 136±15 Tg CH₄ yr⁻¹ respectively for 2018. Chang et al.
876 (2021) and Zhang et al. (2022) estimates for 2018 or 2019 are on average a bit higher than the inventories estimates but in
877 agreement considering the uncertainties.

878 For the period 2010-2019, we estimated total emissions of 112 [107-118] Tg CH₄ yr⁻¹ for enteric fermentation and manure
879 management, about one third of total global anthropogenic emissions.

880 **Rice cultivation.** Most of the world's rice is grown in flooded paddy fields (Baicich, 2013). The water management systems,
881 particularly flooding, used to cultivate rice are one of the most important factors influencing CH₄ emissions and one of the
882 most promising approaches for CH₄ emission mitigation: periodic drainage and aeration not only cause existing soil CH₄ to
883 oxidise, but also inhibit further CH₄ production in soils (Simpson et al., 1995; USEPA, 2016; Zhang, 2016). Upland rice
884 fields are not typically flooded, and therefore are not a significant source of CH₄. Other factors that influence CH₄ emissions

Supprimé: 2017

Supprimé: (Tubiello, 2019),

Supprimé: (USEPA, 2016). Methane

Supprimé: (Chang et al., 2019).

Supprimé: characterize

Supprimé: Global methane emissions from enteric fermentation and manure management are estimated in the range of 99-115 Tg CH₄ yr⁻¹, for the year 2010, in the GAINS model and CEDS, USEPA, FAO-CH₄ and EDGARv4.3.2 inventories. These values are slightly higher than the IPCC Tier 2 estimate of Dangal et al. (2017) (95.7 Tg CH₄/yr for 2010) and the IPCC Tier 3 estimates of Herrero et al. (2013) (83.2 Tg CH₄ yr⁻¹ for 2000), but in agreement with the recent IPCC Tier 2 estimate of Chang et al. (2019) (99± 12 Tg CH₄ yr⁻¹ for 2012).[¶]

Supprimé: 2008-2017

Supprimé: 111 [106-116

Supprimé: Most of the world's rice is grown in flooded paddy fields (Baicich, 2013). The water management systems, particularly flooding, used to cultivate rice are one of the most important factors influencing CH₄ emissions and one of the most promising approaches for CH₄ emission mitigation: periodic drainage and aeration not only cause existing soil CH₄ to oxidize, but also inhibit further CH₄ production in soils (Simpson et al., 1995; USEPA, 2016; Zhang, 2016). Upland rice fields are not typically flooded, and therefore are not a significant source of CH₄. Other factors that influence CH₄ emissions from flooded rice fields include fertilization practices (i.e. the use of urea and organic fertilizers), soil temperature, soil type (texture and aggregated size), rice variety and cultivation practices (e.g. tillage, seeding, and weeding practices) (Conrad et al., 2000; Kai et al., 2011; USEPA, 2011; Yan et al., 2009). For instance, methane emissions from rice paddies increase with organic amendments (Cai et al., 1997) but can be mitigated by applying other types of fertilizers (mineral, composts, biogas residues) or using wet seeding (Wassmann et al., 2000).

1919 from flooded rice fields include fertilisation practices (i.e., the use of urea and organic fertilisers), soil temperature, soil type
1920 (texture and aggregated size), rice variety and cultivation practices (e.g., tillage, seeding, and weeding practices) (Conrad et
1921 al., 2000; Kai et al., 2011; USEPA, 2011; Yan et al., 2009). For instance, CH₄ emissions from rice paddies increase with
1922 organic amendments (Cai et al., 1997) but can be mitigated by applying other types of fertilisers (mineral, composts, biogas
1923 residues) or using wet seeding (Wassmann et al., 2000).

1924 The geographical distribution of rice emissions has been assessed by global (e.g., Janssens-Maenhout et al., 2019; Tubiello,
1925 2019; USEPA, 2012) and regional (e.g., Castelań-Ortega et al., 2014; Chen et al., 2013; Chen and Prinn, 2006; Peng et al.,
1926 2016; Yan et al., 2009; Zhang and Chen, 2014) inventories and land surface models (Li et al., 2005; Pathak et al., 2005; Ren
1927 et al., 2011; Spahni et al., 2011; Tian et al., 2010, 2011; Zhang, 2016). The emissions show a seasonal cycle, peaking in the
1928 summer months in the extra-tropics associated with monsoons and land management. Emissions from rice paddies are
1929 influenced not only by the extent of rice field area, but also by changes in the productivity of plants (Jiang et al., 2017) as
1930 these alter the CH₄ emission factor used in inventories. However, the inventories considered herein are largely based on
1931 IPCC Tier 1 methods, which mainly scale with cultivated areas and include regional specific emission factors but do not
1932 account for changes in plant productivity and detailed cultivation practices.

1933 The largest emissions from rice cultivation are found in Asia accounting for 30 to 50% of global emissions (Fig. 3). The
1934 decrease of CH₄ emissions from rice cultivation over recent decades is confirmed in most inventories, because of the
1935 decrease in rice cultivation area, changes in agricultural practices, and a northward shift of rice cultivation since the 1970s,
1936 as in China (e.g., Chen et al., 2013).

1937 Based on the global inventories considered in this study, global CH₄ emissions from rice paddies are estimated to be 32 [25-
1938 37] Tg CH₄ yr⁻¹ for the 2010-2019 decade (Table 3), or about 9% of total global anthropogenic emissions of CH₄. These
1939 estimates are consistent with the 29 Tg CH₄ yr⁻¹ estimated for the year 2000 by Carlson et al. (2017).

1940 **Waste management.** This sector includes emissions from managed and non-managed landfills (solid waste disposal on
1941 land), and wastewater handling, where all kinds of waste are deposited. CH₄ production from waste depends on the pH,
1942 moisture, and temperature of the material. The optimum pH for CH₄ emission is between 6.8 and 7.4 (Thorneloe et al.,
1943 2000). The development of carboxylic acids leads to low pH, which limits methane emissions. Food or organic waste, such
1944 as leaves and grass clippings, ferment quite easily, while wood and wood products generally ferment slowly, and cellulose
1945 and lignin even more slowly (USEPA, 2010a).

1946 Waste management was responsible for about 11% of total global direct anthropogenic CH₄ emissions in 2000 (Kirschke et
1947 al., 2013). A recent assessment of CH₄ emissions in the USA found landfills to account for almost 26% of total USA
1948 anthropogenic CH₄ emissions in 2014, the largest contribution of any single CH₄ source in the United States of America
1949 (USEPA, 2016). In Europe, gas control has been mandatory on all landfills since 2009, and more importantly for CH₄
1950 emissions, the EU Landfill Directive (1999) with subsequent amendments, has diverted most biodegradable waste away

Supprimé: The geographical distribution of rice emissions has been assessed by global (e.g. Janssens-Maenhout et al., 2019; Tubiello, 2019; USEPA, 2012) and regional (e.g. Castelań-Ortega et al., 2014; Chen et al., 2013; Chen and Prinn, 2006; Peng et al., 2016; Yan et al., 2009; Zhang and Chen, 2014) inventories or land surface models (Li et al., 2005; Pathak et al., 2005; Ren et al., 2011; Spahni et al., 2011; Tian et al., 2010, 2011; Zhang, 2016). The emissions show a seasonal cycle, peaking in the summer months in the extra-tropics associated with monsoons and land management. Similar to emissions from livestock, emissions from rice paddies are influenced not only by extent of rice field area (analogous to livestock numbers), but also by changes in the productivity of plants (Jiang et al., 2017) as these alter the CH₄ emission factor used in inventories. Nonetheless, the inventories considered herein are largely based on IPCC Tier 1 methods, which largely scale with cultivated areas but include regional specific emission factors.¶ The largest emissions from rice cultivation are found in Asia accounting for 30 to 50% of global emissions (Fig. 3). The decrease of CH₄ emissions from rice cultivation over recent decades is confirmed in most inventories, because of the decrease in rice cultivation area, changes in agricultural practices, and a northward shift of rice cultivation since the 1970s, as in China (e.g. Chen et al., 2013).¶ Based on the global inventories considered in this study, global methane emissions from rice paddies are estimated to be 30 [25-38] Tg CH₄ yr⁻¹ for the 2008-2017 decade (Table 3), or about 8% of total global anthropogenic emissions of methane. These estimates are consistent with the 29 Tg CH₄ yr⁻¹ estimated for the year 2000 by Carlson et al. (2017).¶

Supprimé: Methane

Supprimé: methane emission is between 6.8 and 7.4 (Thorneloe et al., 2000).

Supprimé: (USEPA, 2010a).

Supprimé: Waste management was responsible for about 11% of total global anthropogenic methane emissions in 2000 (Kirschke et al., 2013). A recent assessment of methane emissions in the U.S. found landfills to account for almost 26% of total U.S. anthropogenic methane emissions in 2014, the largest contribution of any single CH₄ source in the United States (USEPA, 2016). In Europe, gas control has been mandatory on all landfills since 2009, following the ambitious objective raised in the EU Landfill Directive (1999) to reduce landfilling of biodegradable waste to 65% below the 1990 level by 2016. This mitigation is attempted through source separation and treatment of separated biodegradable waste in composts, biogas, and paper recycling.¶

1996 from landfills towards source separation, recycling, composting and energy recovery, and with a legally binding target not
1997 to landfill more than 10% of municipal solid waste by 2035.

1998 Wastewater from domestic and industrial sources is treated in municipal sewage treatment facilities and private effluent
1999 treatment plants. The principal factor in determining the CH₄ generation potential of wastewater is the amount of degradable
2000 organic material in the wastewater. Wastewater with high organic content is treated anaerobically, which leads to increased
2001 emissions (André et al., 2014). Excessive and rapid urban development worldwide, especially in Asia and Africa, could
2002 enhance methane emissions from waste unless adequate mitigation policies are designed and implemented rapidly.

2003 The GAINS model and CEDS and EDGAR inventories give robust emission estimates from solid waste in the range of 37-
2004 42 Tg CH₄ yr⁻¹ for the year 2019, and more uncertain wastewater emissions in the range 20-45 Tg CH₄ yr⁻¹.

2005 In our study, the global emission of CH₄ from waste management is estimated in the range of 56-80 Tg CH₄ yr⁻¹ for the
2006 2010-2019 period with a mean value of 69 Tg CH₄ yr⁻¹, about 19% of total global anthropogenic emissions.

2007 3.1.5 Biomass and biofuel burning

2008 This category includes CH₄ emissions from biomass burning in forests, savannahs, grasslands, peats, agricultural residues,
2009 as well as, from the burning of biofuels in the residential sector (stoves, boilers, fireplaces). Biomass and biofuel burning
2010 emit CH₄ under incomplete combustion conditions (i.e., when oxygen availability is insufficient for complete combustion),
2011 for example in charcoal manufacturing and smouldering fires. The amount of CH₄ emitted during the burning of biomass
2012 depends primarily on the amount of biomass, burning conditions, fuel moisture and the specific material burned.

2013 In this study, we use large-scale biomass burning (forest, savannah, grassland, and peat fires) from five biomass burning
2014 inventories (described below) and the biofuel burning contribution from anthropogenic emission inventories (EDGARv6
2015 and v7, CEDS, GAINS and USEPA). The spatial distribution of emissions from the burning of biomass and biofuel over
2016 the 2010-2019 decade is presented in Fig. 3 based on data listed in Table 1.

2017 At the global scale, during the period of 2010-2019, biomass and biofuel burning generated CH₄ emissions of 28 [21-39] Tg
2018 CH₄ yr⁻¹ (Table 3), of which 30-50% is from biofuel burning.

2019 ▼
2020 Biomass burning. Fire is an important disturbance event in terrestrial ecosystems globally (van der Werf et al., 2010), and
2021 can be of either natural (typically ~10% of fires, ignited by lightning strikes or started accidentally) or anthropogenic origin
2022 (~90%, human initiated fires) (USEPA, 2010b, chapter 9.1). As previously noted all fires are accounted as anthropogenic in
2023 Table 3. Anthropogenic fires are concentrated in the tropics and subtropics, where forests, savannahs and grasslands may
2024 be burned to clear land for agricultural purposes or to maintain pastures and rangelands. Small fires associated with
2025 agricultural activity, such as field burning and agricultural waste burning, are often not well detected by remote sensing
2026 methods and are instead estimated based on cultivated area.

Supprimé: (André et al., 2014).

Supprimé: 29-41

Supprimé: 2005

Supprimé: 14-33

Supprimé: methane

Supprimé: 60-69

Supprimé: 2008-2017

Supprimé: 65

Supprimé: 12

Mis en forme : Police :Gras, Couleur de police : Noir

Mis en forme : Normal, Espace Avant : 12 pt, Après : 12 pt, Paragraphes solidaires, Bordure : Haut: (Pas de bordure), Bas: (Pas de bordure), Gauche: (Pas de bordure), Droite: (Pas de bordure), Entre : (Pas de bordure)

Supprimé: methane

Supprimé: emits methane

Supprimé: methane

Supprimé: EDGARv4.3.2

Supprimé: 2008-2017

Supprimé: 2008-2017

Supprimé: methane

Supprimé: 30 [26-40

Supprimé:

Supprimé: ¶

Biomass burning. Fire is an important disturbance event in terrestrial ecosystems globally (van der Werf et al., 2010), and can be of either natural (typically ~10% of fires, ignited by lightning strikes or started accidentally) or anthropogenic origin (~90%, human initiated fires) (USEPA (2010b) chapter 9.1). Anthropogenic fires are concentrated in the tropics and subtropics, where forests, savannahs and grasslands may be burned to clear land for agricultural purposes or to maintain pastures and rangelands. Small fires associated with agricultural activity, such as field burning and agricultural waste burning, are often not well detected by remote sensing methods and are instead estimated based on cultivated area. ¶ Emission rates of biomass burning vary with biomass loading (depending on the biomes) at the location of the fire, the efficiency of the fire (depending on the vegetation type), the fire type (smouldering

1060 Emission rates of biomass burning vary with biomass loading (depending on the biomes) at the location of the fire, the
1061 efficiency of the fire (depending on the vegetation type), the fire type (smouldering or flaming) and emission factor (mass
2062 of the considered species / mass of biomass burned). Depending on the approach, these parameters can be derived using
2063 satellite data and/or biogeochemical model, or through simpler IPCC default approaches.

2064 In this study, we use five products to estimate biomass burning emissions. The Global Fire Emission Database (GFED) is
2065 the most widely used global biomass burning emission dataset and provides estimates from 1997 onwards. Here, we use
2066 GFEDv4.1s (van der Werf et al., 2017), based on the Carnegie-Ames-Stanford-Approach (CASA) biogeochemical model
2067 (van der Werf et al., 2010) driven by satellite derived vegetation characteristics and burned area mostly from the MODerate
2068 resolution Imaging Sensor, MODIS (Giglio et al., 2013). GFEDv4.1s (with small fires) is available at a 0.25° resolution and
2069 on a daily basis from 1997 to 2020. One characteristic of the GFEDv4.1s burned area is that small fires are better accounted
2070 for compared to GFEDv4.1 (Randerson et al., 2012), increasing carbon emissions by approximately 35% at the global scale.
2071 The latest version GFEDv5 (Chen et al., 2023) suggest 61% higher burned area than GFEDv4.1s, in closer agreement with
2072 burned area products from higher resolution satellite sensors. The next budget would benefit from GFEDv5 to revisit the
2073 estimates of biomass burning emissions (which would likely go up) based on more specific comparison studies.

2074 The Quick Fire Emissions Dataset (QFED) is calculated using the fire radiative power (FRP) approach, in which the thermal
2075 energy emitted by active fires (detected by MODIS) is converted to an estimate of CH₄ flux using biome specific emissions
2076 factors and a unique method of accounting for cloud cover. Further information related to this method and the derivation of
2077 the biome specific emission factors can be found in Darnenov and da Silva (2015). Here we use the historical QFEDv2.5
2078 product available daily on a 0.1x0.1 grid for 2000 to 2020.

2079 The Fire INventory from the National Center for Atmospheric Research (FINNv2.5, Wiedinmyer et al., 2023) provides
2080 daily, 1 km resolution estimates of gas and particle emissions from open burning of biomass (including wildfire, agricultural
2081 fires and prescribed burning) over the globe for the period 2002-2020. FINNv2.5 uses MODIS and VIIRS satellite
2082 observations for active fires, land cover and vegetation density.

2083 We use v1.3 of the Global Fire Assimilation System (GFAS, Kaiser et al., 2012), which calculates emissions of biomass
2084 burning by assimilating Fire Radiative Power (FRP) observations from MODIS at a daily frequency and 0.5° resolution and
2085 is available for 2000-2020.

2086 The FAO-CH₄ yearly biomass burning emissions are based on the most recent MODIS 6 burned area products, (Prosperi et
2087 al., 2020), coupled with a pixel level (500 m) implementation of the IPCC Tier 1 approach, and are available from 1990 to
2088 2020 (Table 1).

2089 The differences in emission estimates for biomass burning arise from specific geographical and meteorological conditions
2090 and fuel composition, which strongly impact combustion completeness and emission factors. The latter vary greatly
2091 according to fire type, ranging from 2.2 g CH₄ kg⁻¹ dry matter burned for savannah and grassland fires up to 21 g CH₄ kg⁻¹
2092 dry matter burned for peat fires (van der Werf et al., 2010). Biomass burning emissions encountered large inter annual

Supprimé : Here, we use GFEDv4.1s (van der Werf et al., 2017), based on the Carnegie-Ames-Stanford-Approach (CASA) biogeochemical model and satellite derived estimates of burned area (from MODerate resolution Imaging Sensor, MODIS), fire activity and plant productivity. GFEDv4.1s (with small fires) is available at 0.25° resolution and on a daily basis from 1997 to 2017. One characteristic of the GFEDv4.1s burned area is that small fires are better accounted compared to GFEDv4.1 (Randerson et al., 2012), increasing carbon emissions by approximately 35% at the global scale

Supprimé : methane

Supprimé : (Darnenov and da Silva, 2015). Here we use the historical QFEDv2.5 product available daily on a 0.1x0.1 grid for 2000 to 2017

Supprimé : The Fire Inventory from NCAR (FINN, Wiedinmyer et al., 2011) provides daily, 1km resolution estimates of gas and particle emissions from open burning of biomass (including wildfire, agricultural fires and prescribed burning) over the globe for the period 2002-2018. FINNv1.5 uses MODIS satellite observations for active fires, land cover and vegetation density. ¶

Supprimé : (GFAS, Kaiser et al., 2012),

Supprimé : 2016

Supprimé : ,

Supprimé : 500m

Supprimé : 2016

Supprimé : The differences in emission estimates for biomass burning arise from specific geographical and meteorological conditions and fuel composition, which strongly impact combustion completeness and emission factors. The latter vary greatly according to fire type, ranging from 2.2 g CH₄ kg⁻¹ dry matter burned for savannah and grassland fires up to 21 g CH₄ kg⁻¹ dry matter burned for peat fires (van der Werf et al., 2010). ¶

1125 variability related to meteorological conditions, with generally higher emissions during El-Nino periods as in 2019 (20 [14-
1126 28] Tg CH₄ yr⁻¹), 2015 (22 [15-28] Tg CH₄ yr⁻¹) and 2010 to a lesser extent (18 [15-29] Tg CH₄ yr⁻¹).

1127 In this study, based on the five aforementioned products, biomass burning emissions are estimated at 17 Tg CH₄ yr⁻¹ [12-
1128 24] for 2010-2019, representing about 5% of total global anthropogenic CH₄ emissions.

1130 **Biofuel burning.** Burning of biomass to produce energy for domestic, industrial, commercial, or transportation purposes is
1131 hereafter called biofuel burning. A largely dominant fraction of CH₄ emissions from biofuel burning comes from domestic
1132 cooking or heating in stoves, boilers, and fireplaces, mostly in open cooking fires where wood, charcoal, agricultural
1133 residues, or animal dung are burned. It is estimated that more than two billion people, mostly in developing countries, use
1134 solid biofuels to cook and heat their homes daily (André et al., 2014), and yet CH₄ emissions from biofuel combustion have
1135 received relatively little attention. Biofuel burning estimates are gathered from the CEDS, USEPA, GAINS and EDGAR
1136 inventories. Due to the sectoral breakdown of the EDGAR and CEDS inventories the biofuel component of the budget has
1137 been estimated as equivalent to the “RCO - Energy for buildings” sector as defined in Worden et al. (2017) and Hoesly et
1138 al. (2018) (Table S2). This is equivalent to the sum of the IPCC 1A4a_Commercial-institutional, 1A4b_Residential,
1139 1A4c_Agriculture-forestry-fishing and 1A5_Other-unspecified reporting categories. This definition is consistent with that
1140 used in Saunio et al. (2016) and Kirschke et al. (2013). While this sector incorporates biofuel use, it also includes the use
1141 of other combustible materials (e.g., coal or gas) for small-scale heat and electricity generation within residential and
1142 commercial premises. Data provided by the GAINS inventory suggests that this approach may overestimate biofuels
1143 emissions by between 5 and 50%. Further study into this category would be needed to better disentangle biofuels from fossil
1144 combustibles.

1145 In our study, biofuel burning is estimated to contribute 1.1 [0.8-1.4] Tg CH₄ yr⁻¹ to the global CH₄ budget, about 3% of total
1146 global anthropogenic CH₄ emissions for 2010-2019.

1147 **3.1.6 Other anthropogenic sources (not explicitly included in this study)**

1148 Other anthropogenic sources not included in this study are related to agriculture and land-use management. In particular,
1149 increases in agricultural areas (such as global palm oil production) have led to the clearing of natural peat forests, reducing
1150 natural peatland area and associated natural CH₄ emissions. Peatlands planted to forests (like in Northern Europe) also lead
1151 to reduced CH₄ emissions. While studies have long suggested that CH₄ emissions from peatland drainage ditches are likely
1152 to be significant (e.g., Minkinen and Laine, 2006, Peacock et al., 2021), CH₄ emissions related to palm oil plantations have
1153 yet to be properly quantified (e.g., Manning et al. 2019). Taylor et al. (2014) have quantified global palm oil wastewater
1154 treatment fluxes to be 4 ± 32 Tg CH₄ yr⁻¹ for 2010-2013. This currently represents a small and highly uncertain source of
1155 methane but one potentially growing in the future.

Supprimé: 14-26

Supprimé: 2008-2017

Supprimé: methane

Supprimé: Biomass that is used

Supprimé: methane

Supprimé: biofuels

Supprimé: (André et al., 2014), and yet methane

Supprimé: (2017) and Hoesly et al. (2018) (See Table S2).

Supprimé: .

Supprimé:

Supprimé: 12

Supprimé: [10-14]

Supprimé: methane

Supprimé: methane

Supprimé: 2008-2017

Mis en forme : Police :Gras, Couleur de police : Noir

Mis en forme : Normal, Espace Avant : 12 pt, Après : 12 pt, Paragraphes solidaires, Bordure : Haut: (Pas de bordure), Bas: (Pas de bordure), Gauche: (Pas de bordure), Droite: (Pas de bordure), Entre : (Pas de bordure)

Mis en forme : Police :Gras, Couleur de police : Noir

Supprimé: In particular, increases in global palm oil production have led to the clearing of natural peat forests, reducing natural peatland area and associated natural CH₄ emissions. While studies have long suggested that CH₄ emissions from peatland drainage ditches are likely to be significant (e.g. Minkinen and Laine, 2006), CH₄ emissions related to palm oil plantations have yet to be properly quantified. Taylor et al. (2014) have quantified global palm oil wastewater treatment fluxes to be 4 ± 32 Tg CH₄ yr⁻¹ for 2010-2013.

1179 **3.2 Natural and indirect anthropogenic sources**

1180 As introduced in section 2.4, natural and indirect anthropogenic sources refer to pre-agricultural CH₄ emissions even if they
 1181 are perturbed by anthropogenic climate change or other global change factors (e.g., eutrophication), and indirect emissions
 1182 resulting from anthropogenic perturbation of the landscape (reservoirs) and the biogeochemical characteristics of soil. They
 1183 include vegetated wetland emissions and inland freshwater systems (lakes, small ponds, reservoirs, and rivers), land
 1184 geological sources (gas-oil seeps, mud volcanoes, microseepage, geothermal manifestations, and volcanoes), wild animals,
 1185 wildfires, termites, thawing terrestrial and marine permafrost, and coastal and oceanic sources (biogenic, geological and
 1186 hydrate). In water-saturated or flooded ecosystems, the decomposition of organic matter gradually depletes most of the
 1187 oxygen in the soil or the sediment zone, resulting in anaerobic conditions and CH₄ production. Once produced, CH₄ can
 1188 reach the atmosphere through a combination of three processes: (1) diffusive loss of dissolved CH₄ across the air-water
 1189 boundary; (2) ebullition flux from sediments; and (3) flux mediated by emergent aquatic macrophytes and terrestrial plants
 1190 (plant transport). On its way to the atmosphere, in the soil or water columns, CH₄ can be partly or completely oxidised by
 1191 microorganisms, which use CH₄ as a source of energy and carbon (USEPA, 2010b). Concurrently, methane from the
 1192 atmosphere can diffuse into the soil column and be oxidised (See Sect. 3.3.4 on soil uptake).

1193 **3.2.1 Wetlands**

1194 Wetlands are generally defined as ecosystems in which mineral or peat soils are water-saturated at some depth or where
 1195 surface inundation (permanent or not) has a dominating influence on the soil biogeochemistry and determines the ecosystem
 1196 species composition (USEPA, 2010b). To refine such an overly broad definition for CH₄ emissions, we define wetlands as
 1197 ecosystems with inundated or saturated soils or peats where anaerobic conditions below the water table lead to CH₄
 1198 production (Matthews and Fung, 1987; USEPA, 2010b). Brackish water emissions are discussed separately in Sect. 3.2.6.
 1199 Our definition of wetlands includes ombrotrophic and minerotrophic peatlands (i.e., bogs and fens), mineral soil wetlands
 2200 (swamps and marshes), and seasonal or permanent floodplains. It excludes exposed water surfaces without emergent
 2201 macrophytes, such as lakes, rivers, estuaries, ponds, and reservoirs (addressed in the next section), as well as rice agriculture
 2202 (see Sect. 3.1.4, rice cultivation paragraph), and wastewater ponds. It also excludes coastal vegetated ecosystems
 2203 (mangroves, seagrasses, salt marshes) with salinities usually >0.5 (See Sect. 3.2.6). Even with this definition, some wetlands
 2204 could be considered as anthropogenic systems, being affected by human land-use changes such as impoundments, drainage,
 2205 or restoration (Woodward et al., 2012). In the following, we retain the generic denomination “wetlands” for natural and
 2206 human-influenced wetlands, as discussed in Sect. 2.2.

2207 The three most important factors influencing CH₄ production in wetlands are the spatial and temporal extent of anoxia
 2208 (linked to water saturation), temperature, and substrate availability (Valentine et al., 1994; Wania et al., 2010; Whalen, 2005;
 2209 Delwiche et al., 2021; Knox et al., 2021).

Mis en forme : Police :Gras, Couleur de police : Noir

Mis en forme : Normal, Espace Avant : 12 pt, Après : 12 pt, Paragraphes solidaires, Bordure : Haut: (Pas de bordure), Bas: (Pas de bordure), Gauche: (Pas de bordure), Droite: (Pas de bordure), Entre : (Pas de bordure)

Mis en forme : Police :Gras, Couleur de police : Noir

Supprimé : Natural methane

Supprimé : water

Supprimé : methane

Supprimé : methane

Supprimé : methane

Supprimé : oxidized

Supprimé : a group of bacteria called methanotrophs

Supprimé : methane

Supprimé : their only

Supprimé : (USEPA, 2010b).

Supprimé : oxidized

Mis en forme : Police :Gras, Couleur de police : Noir

Mis en forme : Normal, Retrait : Première ligne : 0 cm, Espace Avant : 12 pt, Après : 12 pt, Paragraphes solidaires, Bordure : Haut: (Pas de bordure), Bas: (Pas de bordure), Gauche: (Pas de bordure), Droite: (Pas de bordure), Entre : (Pas de bordure)

Supprimé : or peats

Supprimé :

Supprimé : dominates

Supprimé : (USEPA, 2010b). In order to

Supprimé : methane

Supprimé : methane

Supprimé : (Matthews and Fung, 1987; USEPA, 2010b).

Supprimé : psu

Supprimé : (Woodward et al., 2012).

Supprimé : 2.

Supprimé : The three most important factors influencing methane production in wetlands are the spatial and temporal extent of anoxia (linked to water saturation), temperature and substrate availability (Valentine et al., 1994; Wania et al., 2010; Whalen, 2005). Land-surface models estimate CH₄ emissions through a series of processes, including CH₄ production, oxidation and transport. The models are then forced with inputs accounting for changing environmental factors (Melton et al., 2013; Poulter et al., 2017; Tian et al., 2010; Wania et al., 2013; Xu et al., 2010). Methane emissions from wetlands are computed as the product of an emission flux density and a methane producing area or surface extent (see Supplementary Material; Bohn et al., 2015; Melton et al., 2013). Wetland extent appears to be a primary contributor to uncertainty.

3300 [Land surface models estimate CH₄ emissions through a series of processes, including CH₄ production, oxidation, and](#)
3301 [transport. The models are then forced with inputs accounting for changing environmental factors \(Melton et al., 2013;](#)
3302 [Poulter et al., 2017; Tian et al., 2010; Wania et al., 2013; Xu et al., 2010\). CH₄ emissions from wetlands are computed as](#)
3303 [the product of an emission flux density and a CH₄ producing area or surface extent \(see Supplementary Material; Bohn et](#)
3304 [al., 2015; Melton et al., 2013\). The areal extent of different wetland types \(having large differences in areal CH₄ emission](#)
3305 [rates\) appears to be a primary contributor to uncertainties in the absolute flux of CH₄ emissions from wetlands, with](#)
3306 [meteorological response being the main source of uncertainty for seasonal and interannual variability \(Poulter et al., 2017;](#)
3307 [Kuhn et al., 2021; Parker et al., 2022; McNicol et al., 2023; Karlson and Bastviken 2023\).](#)
3308 [In this work, sixteen land surface models computing net CH₄ emissions \(Table 2\) were run under a common protocol with](#)
3309 [a spin-up using repeated climate data from 1901-1920 to pre-industrial conditions followed by a transient simulation through](#)
3310 [the end of 2020. Of the 16 models, 13 previously contributed to Saunio et al. \(2020\), and three models were new to this](#)
3311 [release \(CH4MOD_{wetland} \(Li et al., 2010\), ISAM \(Shu et al., 2020; Xu et al., 2021\), and SDGVM \(Beerling and Woodward,](#)
3312 [2001; Hopcroft et al., 2011; Hopcroft et al., 2020 \)\) \(Table 2, see also in the Supplementary Material Table S3 for a history](#)
3313 [of the contributing models\). Climatic forcing uncertainties are considered in the ensemble estimate by using two climate](#)
3314 [datasets, CRU/CRU-JRA55 \(Harris, 2014\) and GSWP3-W5E5 \(Dirmeyer et al., 2006; Kim 2017; Lange, 2019; Cucchi et](#)
3315 [al., 2020\). Atmospheric CO₂ was also prescribed in the models. For all models, two wetland area dynamic schemes were](#)
3316 [applied: a diagnostic scheme using a remote sensing-based wetland area and dynamics dataset called WAD2M \(Wetland](#)
3317 [Area Dynamics for Methane Modeling; Zhang et al., 2021a; 2021b\) available at 0.25 degree of horizontal resolution, as in](#)
3318 [Saunio et al. \(2020\), and a prognostic scheme using internal model-specific hydrologic models.](#)
3319 [The diagnostic wetland extent product WAD2Mv1.0 \(Zhang et al., 2021a\) has been updated since Saunio et al. \(2020\) to](#)
3320 [WAD2Mv2.0 \(Zhang et al., 2021b\) and extended to 2020. It uses the same Surface Water Microwave Product Series](#)
3321 [\(SWAMPSv3.2\) for capturing inundation dynamics \(Jenson and McDonald, 2019\), which was extended to 2020. To reduce](#)
3322 [potential double-counting with the freshwater budget, the surface areas of rivers/streams and lakes/ponds are excluded by](#)
3323 [using the products Global River Widths from Landsat \(GRWL\) database v01.01 \(Allen and Pavelsky, 2018\) and HydroLakes](#)
3324 [v1.0 \(Messenger et al., 2016\), instead of the Global Surface Water \(GSW\) product \(Pekel et al., 2016\) used in WAD2Mv1.0.](#)
3325 [The GRWL and Hydrolakes are also the datasets used separately in the upscaling of the freshwater budget allowing for a](#)
3326 [more consistent approach between the wetland and freshwater CH₄ budgets \(Sect. 3.2.2\). This update in WAD2M leads to](#)
3327 [a downward revised annual average wetland extent by 0.5 Mkm² for the mid-high latitudes \(mainly due to larger lake extent](#)
3328 [in HydroLakes than in the GSW dataset\) with small impacts in other regions. However, since HydroLakes includes only](#)
3329 [vectorized lakes larger than 0.1 km², smaller lakes/ponds under 0.1 km² are implicitly still included as wetlands in](#)
3330 [WAD2Mv2.0. For the high-latitude region, the recent peatland extent product from Hugelius et al. \(2020\) is applied, which](#)
3331 [indicates a slightly higher peatland area by 0.2 Mkm² primarily in regions above 60°N, compared to the Northern](#)
3332 [Circumpolar Soil Carbon Database \(NCSCD\) product \(Hugelius et al., 2013\) used in WAD2Mv1.0. Rice agriculture was](#)

333 removed using the Monthly Irrigated and Rainfed Crop Areas (MIRCA2000, Portmann et al. (2010)) dataset from circa
 334 2000, as a fixed distribution.

335 The combined remote-sensing and inventory WAD2Mv2.0 product leads to a maximum wetland area of 13.6 Mkm² during
 336 the peak season (7.9 Mkm² on annual average, with a range of 7.5 to 8.4 Mkm² from 2000-2020, about 5.2% of the global
 337 land surface). The largest wetland areas in WAD2Mv2.0 are in Amazonia, the Congo Basin, and the Western Siberian
 338 Lowlands, which in previous studies were underestimated by inventories (Bohn et al., 2015). However, the SWAMPS v3.2
 339 dataset which serves as a proxy of temporal variations of wetland extent, has discontinuity issues over a few tropical hotspots
 340 since 2015 and hence affects the temporal variations of WAD2M. Consequently, this affects CH₄ emissions estimates for a
 341 subset of land surface models that are particularly sensitive to inundation in these hotspots. Meanwhile, prognostic estimates
 342 show moderate consistency in capturing the spatial distribution of wetland area with WAD2M, with an annual average
 343 wetland area of 8.0±2.0 Mkm² during the peak season for 2000-2020. The ensemble mean of annual wetland area anomaly
 344 by the prognostic models show reasonable agreement with satellite-based estimates in capturing the response of wetland
 345 area to climate variations (Zhang et al., in review), with higher agreement over temperate and boreal regions than in the
 346 tropics.

347 For the wetland methane emissions estimate, we use the decadal mean from the prognostic runs and adjust these flux
 348 estimates for double counting from inland waters (described in next section) given the reliance of the prognostic models on
 349 satellite flooded area data like WAD2Mv2 to parameterize maximum wetland extent (Zhang et al., in review). The average
 350 emission from wetlands for 2010-2019 for the 16 models is plotted in Fig. 3. The zones with the largest emissions are the
 351 Amazon basin, equatorial Africa and Asia, Canada, western Siberia, eastern India, and Bangladesh. Regions where CH₄
 352 emissions have high inter-model agreement (defined as regions where mean flux is larger than the standard deviation of the
 353 models, on a decadal mean) represent 72% of the total CH₄ flux due to natural wetlands. The different sensitivities of the
 354 models to temperature, vapour pressure, precipitation, and radiation can generate substantially different patterns, such as in
 355 India. Emission estimates over regions with lower emissions (in total) are also consistently inferred between models, (e.g.,
 356 Scandinavia, Continental Europe, Eastern Siberia, Central United States of America, and Southern Africa).

357 The resulting global flux range for vegetated wetland emissions from the prognostic runs is 117-195 Tg CH₄ yr⁻¹ for the
 358 2000-2020 period, with an average of 157 Tg CH₄ yr⁻¹ and a one-sigma standard deviation of 24 Tg CH₄ yr⁻¹. Using the
 359 prognostic set of simulations, the average ensemble emissions were 159 [119-203] Tg CH₄ yr⁻¹ for the 2010-2019 period
 360 (Table 3). The estimated average ensemble annual total from the two sets of simulations by CRU/CRU-JRA55 and GSWP3-
 361 W5E5 are 158 [126-193] and 158 [118-203] for 2010-2019, respectively. Generally, the magnitude and interannual
 362 variability agree between these two sets of simulations (Zhang et al., in review). Wetland emissions represent about 25% of
 363 the total (natural plus anthropogenic) CH₄ sources estimated by bottom-up approaches. The large range in the estimates of
 364 wetland CH₄ emissions results from difficulties in defining wetland CH₄ producing areas as well as in parameterizing
 365 terrestrial anaerobic conditions that drive sources and the oxidative conditions leading to sinks (Melton et al., 2013; Poulter

Supprimé: methane

Supprimé: are robustly inferred

Supprimé: 61

Supprimé: methane

Supprimé: This contribution is 80% lower than found in Sauniois et al. (2016) probably due to the different ensemble of models gathered here and the more stringent exclusion of inland waters.

Supprimé: main primary emission zones are consistent between models, which is clearly favoured by the prescribed common wetland extent. However, the

Supprimé: Some secondary

Supprimé: magnitude) emission zones

Supprimé: :

Supprimé: USA

Supprimé: tropical

Supprimé: :

Supprimé: The resulting global flux range for natural wetland emissions is 101-179 Tg CH₄ yr⁻¹ for the 2000-2017 period, with an average of 148 Tg CH₄ yr⁻¹ and a one-sigma standard deviation of 25 Tg CH₄ yr⁻¹. For the last decade, 2008-2017, the average ensemble emissions were 149 Tg CH₄ yr⁻¹ with a range of 102-182 (Table 3). Using a prognostic set of simulations, where models used their own internal approach to estimate wetland area and dynamics, the average ensemble emissions were 161 Tg CH₄ yr⁻¹ with a range of 125-218 for the 2008-2017 period. The greater range of uncertainty from prognostic area models is due to unconstrained wetland area, but generally the magnitude and interannual variability agree between diagnostic and prognostic area approaches. Wetland emissions represent about 20% of the total (natural plus anthropogenic) methane sources estimated by bottom-up approaches. The large range in the estimates of wetland CH₄ emissions results from difficulties in defining wetland CH₄ producing areas as well as in parameterizing terrestrial anaerobic conditions that drive sources and the oxidative conditions leading to sinks (Melton et al., 2013; Poulter et al., 2017; Wania et al., 2013). The ensemble mean emission using diagnostic wetland extent in the models is lower by ~35 Tg CH₄ yr⁻¹ than the one previously reported (see Table 3, for 2000-2009 with comparison to Sauniois et al. 2016). This difference results from a reduction in double counting due to i) decreased wetland area in WAD2M, especially for high-latitude regions where inland waters, i.e., lakes, small ponds and lakes, were removed, and ii) to some extent, an improved removal of rice agriculture area using the MIRCA-2000 database.

For the last decade, 2008-2017, the average ensemble emissions were 149 Tg CH₄ yr⁻¹ with a range of 102-182.

3.2.2 Other inland water systems (lakes, ponds, reservoirs, streams, rivers)

This category includes methane emissions from freshwater systems (lakes, ponds, reservoirs, streams and rivers). To date, very few process-based models exist for these fluxes, relying on data driven approaches and extrapolations. Meta-data analyses are hampered for methane due to a mix of methodological approaches, which capture different components of emissions, and different scales in space and time, depending on method and time of deployment and data processing (Stanley et al., 2016). Altogether, this inconsistency in

1494 [et al., 2017; Wania et al., 2013](#)). The ensemble mean emission using the same simulation setup (i.e., diagnostic wetland
1495 extent and CRU/CRU-JRA55) in the models is 163 [117-195] Tg CH₄ yr⁻¹, higher by ~22 Tg CH₄ yr⁻¹ than the one previously
1496 reported (see Table 3, for 2000-2009 with comparison to Sauniois et al., 2020). This difference is mainly due to the updated
1497 model structure and parameterizations in the wetland CH₄ models compared to the versions in the previous budget and the
1498 inclusion of three new land surface models.
1499 For the last decade 2010-2019, we report in this budget an average ensemble estimate of 159 Tg CH₄ yr⁻¹ with a range of
1500 119-203 (based on prognostic wetland extent runs).

1501 **3.2.2 Inland freshwater systems (lakes, ponds, reservoirs, streams, rivers)**

1502 [This category includes CH₄ emissions from freshwater systems \(lakes, ponds, reservoirs, streams, and rivers\). Numerous](#)
1503 [advances have been made in the freshwater greenhouse gases knowledge base in the last few years \(Lauerwald et al., 2023a\).](#)
1504 [These advances include improvements in the underlying databases used to estimate inland water surface areas and model](#)
1505 [their dynamics, a rapidly growing number of direct measurements of methane fluxes, and improvements in our process-](#)
1506 [based understanding of methane biogeochemistry. Despite this, aspects of global freshwater methane estimates remain rather](#)
1507 [crude and continue to have large uncertainties. This includes the overall temperature dependency of methane emissions, the](#)
1508 [relative role of ebullition \(i.e., bubble flux, which may represent the most important, but most difficult-to-capture emission](#)
1509 [path in many standing water bodies\), fluxes from the smallest standing water bodies \(sometimes referred to as ponds\) having](#)
1510 [large emissions per m² but uncertain area extent, and the magnitude of anthropogenic influence on emissions, all which are](#)
1511 [discussed below.](#)

1512
1513 **Streams and rivers.** [The last global CH₄ budget used an estimate of 27 Tg CH₄ yr⁻¹ for global streams and rivers based](#)
1514 [largely on a data compilation by Stanley et al. \(2016\). This estimate was scaled from a simple data compilation without a](#)
1515 [spatial component or an estimate of ebullition. More recently, Rosentreter et al. \(2021\) performed a new data compilation](#)
1516 [of 652 flux estimates, including diffusive and ebullitive fluxes, coupled to an ice corrected surface area estimate of ~625,000](#)
1517 [km² that was aggregated to 5 latitudinal bands to come up with a global estimate of 6 and 31± 17 Tg CH₄ yr⁻¹ \(respectively](#)
1518 [for the median and mean ± c.i. 95%\). We believe, due to better data representation in underlying datasets, that the mean](#)
1519 [estimate of Rosentreter et al. \(2021\) is more representative statistically because the median does not capture hotspots and](#)
1520 [hot moments of intense ebullitive fluxes. Finally, Rocher-Ros et al. \(2023\) used a new Global River Methane \(GRiMeDB\)](#)
1521 [database \(Stanley et al., 2023\) with > 24,000 observations of CH₄ concentrations to predict ~28±17 Tg CH₄ yr⁻¹ \(±c.i. 95%\)](#)
1522 [river emissions globally. This approach used machine learning methods coupled to the latest spatially and temporally explicit](#)
1523 [mapping of monthly stream surface area \(the smallest streams are still extrapolated\) which incorporates drying and freezing](#)
1524 [effects \(yearly average 672,000 km², Liu et al., 2022\) and includes an ebullitive flux estimated from a correlation between](#)
1525 [measured diffusive and ebullitive emissions in the GRiMeDB database \(Stanley et al., 2023\). Thus, for this study we use an](#)

526 estimate of 29±17 (±c.i. 95%) Tg CH₄ yr⁻¹ for streams and rivers, which averages the mean estimate of Rosentreter et al.
527 (2021) and Rocher-Ros et al. (2023). Currently, ebullitive fluxes remain a major unknown quantity in streams and rivers but
528 appear to be coarsely linearly correlated in a log-space to diffusive fluxes and of similar magnitude (Rocher-Ros et al.,
529 2023). Methodologically, the high-water velocity of many streams and rivers make measurement of ebullitive fluxes
530 challenging (Robison et al., 2021). Effluxes are also linked to hydrology (Aho et al., 2021) although very few studies have
531 sampled over a representative hydrograph. Plant-mediated effluxes of CH₄ in running waters also remain difficult to
532 constrain, with a recent compilation highlighting very few measurements (Bodmer et al. 2024). Connected adjacent wetlands
533 is a common source of CH₄ to streams and rivers (Borges et al., 2019) which may be important for the regulation of running
534 water emissions but is currently difficult to assess at the global scale. Overall, the poor representation of sites and deficient
535 mechanistic understanding make it difficult to model and predict methane evasion from streams and rivers using process-
536 based models.

537
538 **Lakes and ponds.** The previous global CH₄ budget used an estimate of 71 Tg CH₄ yr⁻¹ for lakes and 18 Tg CH₄ yr⁻¹ for
539 reservoirs. These estimates were based on an early study by Bastviken et al. (2011) coupled with a newer estimate for lakes
540 north of 50°N (Wik et al., 2016b). There have been three new lake studies that have published their data with global estimates
541 of 56 and 151± 73 (Rosentreter et al. (2021); (±c.i. 95%) ; respectively for the median and mean ± c.i. 95%), 22±8 (Zhuang
542 et al., 2023; ±lake-area-weighted normalised RMSE for all parameterized lake types), process-based model), and 41±36
543 Tg CH₄ yr⁻¹ (Johnson et al., 2022, mean ±c.i. 95%). This large range in estimated emissions can be attributed to the
544 differences in the datasets and methods used to calculate the surface area of small waterbodies, as well as the differences
545 between how the flux data were analyzed and extrapolated between studies. For instance, total surface areas of all lakes and
546 ponds of 3712-5688 × 10³ km² (Rosentreter et al., 2021) and 2806 × 10³ km² (Johnson et al., 2022) were used along with
547 measurement data from 198 and 575 individual lake systems, respectively. In contrast, Zhuang et al. (2023) generated
548 estimates using higher temporal resolution data from just 54 lakes to build a process-based model, which generated much
549 lower flux estimates from tropical lakes than previously implemented statistical approaches, but in line with the most recent
550 assessments by Borges et al. (2022). For this study, we explicitly excluded lakes <0.1 km² which are treated separately (see
551 below). If we re-assess these three studies for only lakes greater than 0.1 km², we obtain global effluxes of 17 and 42.9±20.8
552 Tg CH₄ yr⁻¹ (Rosentreter et al. (2021); median and mean (±95% C.I.) of global flux), 21.9±8.0. (Zhuang et al., 2023, ±lake-
553 area-weighted normalised RMSE for all parameterized lake types), and 35.3±31.0 Tg CH₄ yr⁻¹ (Johnson et al. 2022, ±95%
554 C.I.) (with areas of 2556-3468 ×10³, 2640×10³, and 2676×10³ km² respectively). Thus, for lakes >0.1 km², we propose an
555 efflux of ~33±26 Tg CH₄ yr⁻¹ (an average of the mean from Rosentreter et al., 2021 Zhuang et al., 2023, and Johnson et al.,
556 2022, with the average 95% C.I. from Rosentreter et al., 2021 and Johnson et al. 2022).
557 Small waterbody emissions, hereafter small lakes and ponds<0.1 km², remain difficult to assess. Evidence is emerging that
558 there is a lower limit to the power scaling laws that early studies used to extrapolate the surface area of these small systems

1559 (Bastviken et al., 2023; Kyzivat et al., 2022). Thus, for small lakes and ponds < 0.1 km² (and >0.001 km²), we disregard the
1560 higher end surface area used in Rosentreter et al., 2021 which relied on these earlier estimates and scale their numbers to
1561 the evasion estimates to the lower end surface area of 1,002x10³ to obtain a mean flux of 33 Tg CH₄ yr⁻¹ (Rosentreter et al.,
1562 2021). Johnson et al. (2022) estimated a surface area of only 166,000 km² for this size class to obtain an efflux of 6.3
1563 Tg CH₄ yr⁻¹, which we acknowledge as a lower limit. Averaging these two values provide a conservative estimate of ~20
1564 [6-33] Tg CH₄ yr⁻¹, which is close to the number proposed by Holgerson and Raymond (2016) for diffusion effluxes only
1565 for this size class. The experts involved in this assessment have low confidence in this estimate. This also does not include
1566 artificial ponds, which we discuss below. As a result, CH₄ emissions from both large lakes (>0.1 km²) and small lakes and
1567 ponds (<0.1km²) are estimated at 53 [19-86] Tg CH₄ yr⁻¹, on average lower than the 71 Tg estimated in the previous budget.

1568
1569 **Reservoirs.** New mean estimates of diffusive + ebullitive CH₄ emissions from reservoirs include 15 and 24±8 (the median
1570 and mean±95% C.I. from Rosentreter et al., 2021), 10±4 (Johnson et al., 2021, mean±95% C.I.), 10 (Harrison et al., 2021,
1571 low and high 95% CI 7 and 22, respectively), and 2.1 Tg CH₄ yr⁻¹ (Zhuang et al., 2023). We compile the first three estimates
1572 to a direct efflux of ~14 Tg CH₄ yr⁻¹ (with ±95% C.I. of 9 and 23). We note the fourth estimate as a lower bound, but exclude
1573 it from this budget given that it was generated via a model that only included data from six reservoir systems (Zhuang et al.,
1574 2023). We also add in an additional 12 Tg CH₄ yr⁻¹ (95% C.I. 7 and 37) that is estimated to degas in dam turbines (Harrison
1575 et al., 2021), which was not addressed in the studies by Rosentreter et al. (2021), Zhuang et al. (2023), or Johnson et al.
1576 (2021). Rocher-Ros et al. (2023) also excluded river observations below dams when executing their statistical model, and
1577 so did not capture downstream dam emissions. Thus, we use a direct reservoir emission here of ~13 [6-28] Tg CH₄ yr⁻¹ and
1578 estimate an additional ~12 [7-37] Tg CH₄ yr⁻¹ from dam turbine degassing fluxes, giving a total of 25 [13-65] Tg CH₄ yr⁻¹
1579 from reservoirs.

1580
1581 **Uncertainties and confidence levels.** The emission estimates of lakes, reservoirs and ponds described above are limited by
1582 several uncertainties. First, a major unknown for lakes remains the size cut off and the representation of small lakes and
1583 ponds (Deemer and Holgerson, 2021), which are also more variable than larger water bodies in their CH₄ concentrations
1584 and fluxes (Rosentreter et al. 2021, Ray et al., 2023). Interestingly, there is also a lack of methane data representation from
1585 large lakes that are a large component of global lake surface area (Deemer and Holgerson, 2021; Messenger et al., 2016).
1586 There is also a growing knowledge base on the importance of high CH₄ fluxes from lake littoral zones that is not yet well
1587 incorporated into global scaling efforts (e.g., Grinham et al., 2011; Natchimuthu et al., 2016), and emergent vegetation
1588 (Bastviken et al., 2023; Kyzivat et al., 2022). Ebullition is more constrained in lakes/reservoirs compared to streams/rivers
1589 but is still difficult to measure and model accurately. Finally, for all aquatic systems a greater scrutiny of the regulation
1590 (including the impact of ice-cover and seasonality) of different CH₄ emission pathways is needed.

2591 The majority of the inland water CH₄ estimates are from a limited number of studies, some without spatial representation or
2592 reported statistical uncertainties. Furthermore, as mentioned above the knowledge base of the surface area of these
2593 ecosystems is new and rapidly expanding, but not standardised between studies leading to uncertainty (but see Lauerwald
2594 et al. 2023b), particularly for ponds. For this study, we are able to provide confidence intervals from the original studies for
2595 all fluxes except the smallest lake/pond size class.

2596
2597 **The Surface Area of Inland Freshwaters.** For all of these ecosystems, determining their surface area remains a central
2598 challenge. Since the last GMB, several methodological advances have reduced the uncertainty associated with the surface
2599 area estimates of rivers, streams, lakes, and reservoirs. Using a single geospatial dataset that includes both lakes and
2600 reservoirs (Messenger et al., 2016) has decreased double counting of lakes and reservoirs (Johnson et al., 2022; Rosentreter
2601 et al., 2021). For rivers and streams, high-resolution global streamflow simulations, informed by satellite observations,
2602 enabled a much finer scale estimate of surface areas for rivers with a new temporal component (Allen and Pavelsky, 2018;
2603 Lin et al., 2019; Liu et al., 2022), although the surface for the smaller streams are still estimated indirectly, and mapping of
2604 human-created drainage ditches and canals is lacking. Seasonal ice cover and melt turnover corrections also have been newly
2605 incorporated into rivers, streams, lakes, and reservoirs (Harrison et al., 2021; Johnson et al., 2022; Lauerwald et al., 2023b;
2606 Rocher-Ros et al., 2023; Rosentreter et al., 2021; Zhuang et al., 2023). Finally, removing open water body surface areas
2607 from wetland surface areas based on geographic location has reduced double counting between these two land cover types,
2608 as described in the wetlands section of the GMB. Yet, the surface area of small lakes and ponds (<0.1 km²) is still highly
2609 uncertain, and new techniques for counting these systems and determining the overlap with wetland data bases is paramount.

2610
2611 **Anthropogenic Contributions to Inland Freshwater Emissions.** We argue that all reservoirs should be categorised as an
2612 direct anthropogenic source of emissions. Most of the surface area of reservoirs are human-made and reservoir construction
2613 leads to anoxic sediments and/or bottom waters with labile organic matter sourced from the watershed and to in-situ nutrient
2614 augmented phytoplankton production (Deemer et al., 2016; Maavara et al., 2017; Prairie et al., 2018). It is also clear that the
2615 cultural eutrophication of natural lakes is augmenting CH₄ emissions (DelSontro et al., 2018; Li et al., 2021), with shallow
2616 lakes particularly likely to experience eutrophication (Qin et al., 2020). For instance, Beaulieu et al. (2019) modelled a 15%
2617 reduction in lake CH₄ with a 25% reduction in lake phosphorus concentrations. Several recent studies have estimated that
2618 anywhere between 30 and 50% of lakes are eutrophic (Cael et al., 2022; Qin et al., 2020; Sayers et al., 2015; Wu et al.,
2619 2022). These studies estimate numerical percentages (one by depth class: Qin et al., 2020), but none have estimated the
2620 percent of lake surface area that is eutrophic nor have any determined the extent of anthropogenic vs. natural eutrophication.
2621 Still, numerous studies have noted widespread increases in eutrophication indicators across lakes due to nutrient loading
2622 and warming (Griffiths et al., 2022; Ho et al., 2019; Taranu et al., 2015), thus we estimate that 1/3, or 11 Tg CH₄ yr⁻¹ of
2623 CH₄ emissions from lakes >0.1 km² could be anthropogenic. Similarly, CH₄ emissions from small lakes and ponds are

1624 influenced by human factors, with emissions increasing with eutrophication (Deemer and Holgerson, 2021), erosion and
1625 runoff in agricultural landscapes (Heathcote et al., 2013), and warming, the latter likely to have a disproportionately greater
1626 effect in small, shallow systems (Woolway et al., 2016). Thus, we adopt the same 1/3 number as for lakes for the proportion
1627 of anthropogenic emissions in small lakes and ponds (<0.1 km²), which amounts to 6 Tg CH₄ yr⁻¹.
1628 There are also human-made small lakes and ponds, notably for agriculture, aquaculture, and recreation, that generally have
1629 conditions favourable for high CH₄ emissions (Downing, 2010; Holgerson and Raymond, 2016; Malerba et al., 2022;
1630 Ollivier et al., 2019; Zhao et al., 2021; Dong et al., 2023). Downing (2010) estimated that farm ponds comprise a global
1631 surface area of ~77,000 km²; using a conservative emission rate of 265 mg CH₄ m⁻² d⁻¹ and an ice correction factor of 0.6
1632 leads to an emission of 4.5 Tg yr⁻¹ that is anthropogenically sourced from farm ponds. Here the value is rounded to 5 Tg yr⁻¹.
1633 Clearly, more work is required to assess the anthropogenic component of CH₄ emissions from lakes and ponds.
1634 It remains difficult to parse out an anthropogenic component to stream and river CH₄ fluxes. Although some studies have
1635 noticed a temperature dependence with stream sediments (Comer-Warner et al., 2018; Zhu et al., 2020), Rocher-Ros et al.
1636 (2023) noted a small temperature dependence of CH₄ emissions in streams and rivers compared to other freshwater
1637 ecosystems, potentially due to the many other external processes affecting fluxes in these dynamic flowing ecosystems.
1638 Urbanisation can lead to elevated river CH₄ emissions, particularly in regions with elevated organic matter and nutrient
1639 loading due to limited wastewater treatment (Begum et al., 2021; Nirmal Rajkumar et al., 2008; Wang et al., 2021a). Some
1640 studies have found agricultural streams and ditches can have higher effluxes due to inputs of fine sediments (Comer-Warner
1641 et al., 2018; Crawford and Stanley, 2016), organic carbon, and nutrients (Borges et al., 2018) that lead to in-situ methane
1642 production. Furthermore, the creation of drainage ditches in organic soils tap CH₄ rich waters from water-logged horizons
1643 and heighten emissions from ex-situ sources (Peacock et al., 2021), although limitations in both the geographic scope of
1644 existing ditch emission estimates our ability to estimate global surface area of ditches precludes their inclusion in this budget.
1645 Finally, extremely high rates of CH₄ emission have been linked to ongoing permafrost thaw in Asia's Qinghai–Tibet Plateau
1646 (Zhang et al., 2020). However, the loss and disconnection of wetlands to rivers may have resulted in a decrease in the input
1647 of dissolved CH₄ from this source. A recent expert elicitation (Rosentreter, et al. submitted) reported that 35% of all inland
1648 freshwater sources were anthropogenic and given that some of the river flux is from upstream reservoirs, we assign a 30%
1649 anthropogenic contribution to the stream and river flux (9 Tg CH₄ yr⁻¹), which approximates the expert elicitation via the
1650 impact of eutrophication and urban influences.
1651
1652 **Combination (lakes, ponds, reservoirs, streams and rivers, farm ponds).** Combining the aforementioned emissions from
1653 lakes >0.1 km² (~33 [13-53] Tg CH₄ yr⁻¹), small lakes and ponds < 0.1 km² (20 [6-33] Tg CH₄ yr⁻¹), reservoirs (25 [13-65]
1654 Tg CH₄ yr⁻¹), streams and rivers (29 [12-46] Tg CH₄ yr⁻¹) and farm ponds (5 Tg CH₄ yr⁻¹), leads to a total of ~112 Tg CH₄
1655 yr⁻¹ from freshwater systems, with a range of [49-202] Tg CH₄ yr⁻¹. This estimate is about 50 Tg lower than in Sauniois et
1656 al. (2020) and is broadly consistent with the recent regionalized estimate by Lauerwald et al. (2023b) compiled for the

1657 Regional Carbon Cycle Assessment and Processes (RECCAP2, <https://www.globalcarbonproject.org/reccap/>; 103 Tg CH₄
1658 yr⁻¹, IQR= 82.1–134.8). The updated budget from these ecosystems and their anthropogenic components are represented on
1659 Fig 4. The gridded products for emissions from lakes and ponds by Johnson et al. (2022), from reservoirs by Johnson et al.
1660 (2021) and from streams and rivers by Rocher-Ros et al. (2023) have been combined into a single map presented in Fig. 5.

1661
1662 **Double-counting aquatic systems in the bottom-up estimates.** To address the differences found between bottom-up and
1663 top-down CH₄ budgets, and to acknowledge advances in addressing the central issue of double counting CH₄ emissions for
1664 inland ecosystems, we introduce here a new correction term. Historically, the bottom-up estimate of global CH₄ emissions
1665 has been higher than the top-down estimate, first recognized in Kirschke et al. (2013) and confirmed in Saunio et al. (2016,
1666 2020). The larger bottom-up emissions estimate has been partly attributed to double-counting vegetated wetland emissions
1667 with inland freshwater emissions (including lakes, ponds, rivers, streams, and reservoirs) and also the emissions of CH₄
1668 produced in vegetated wetlands and then transported via aquatic processes and emitted from inland freshwaters (Pangala et
1669 al., 2017; Kirk and Cohen, 2023). The Saunio et al. (2020) CH₄ budget addressed the issue of double counting through the
1670 use of a revised vegetated wetland area dataset, WAD2M v1.0 (Zhang et al., 2021), that removed inland waters from the
1671 SWAMPS (Jenson and McDonald, 2019) surface-inundation dataset, allowing for independent vegetated wetlands and
1672 inland freshwater CH₄ emissions to be compiled. Yet, the Saunio et al. (2020) CH₄ budget still had a ~150 Tg CH₄ yr⁻¹
1673 difference between bottom-up and top-down estimates. In this budget, we refined the vegetated wetland area dataset with
1674 WAD2M v2.0 (see section 3.2.1, where HydroLakes is used to remove lakes and ponds >0.1 km²). Additionally, we applied
1675 numbers from peer-reviewed publications and expert elicitation to account for lateral CH₄ flux emissions. This most recent
1676 BU budget estimates 159 [119–203] Tg CH₄ yr⁻¹ from vegetated wetlands for 2010–2019 and 112 Tg CH₄ yr⁻¹ from inland
1677 freshwaters that includes 83 Tg CH₄ yr⁻¹ from lakes, ponds, and reservoirs and 29 Tg CH₄ yr⁻¹ from rivers and streams,
1678 leading to a combined wetland and inland freshwater flux of 271 Tg CH₄ yr⁻¹. Here, we propose a correction of 20 Tg CH₄
1679 yr⁻¹ to account for double counting of small lakes and ponds (< 0.1 km²) that are likely included in our vegetated wetlands
1680 estimate, and removing 1–3 Tg CH₄ yr⁻¹ from river emissions due to lateral transport of CH₄ originating in adjacent vegetated
1681 wetlands. The river flux correction arises from assuming that for catchments with >10% wetlands, rivers provide 5–10% of
1682 vegetated CH₄ emissions. The total double-counting correction term of 23 Tg CH₄ reduces the BU budget for combined
1683 wetlands and inland waters from 271 Tg CH₄ yr⁻¹ to 248 Tg CH₄ yr⁻¹ (see Fig. 4 and Table 3). Comparing the 2000–2009
1684 decadal emissions from wetlands and inland freshwater ecosystems across the last three previous assessments of the budget
1685 shows a significant downward revision with 305 (183+122) Tg CH₄ yr⁻¹, 356 (147+209) Tg CH₄ yr⁻¹ and 248 (159+112–23)
1686 Tg CH₄ yr⁻¹ (respectively from Saunio et al. (2016; 2020) and this work).

1687 Finally, it is worth noting that inland freshwater ecosystems can overlap with geological seepage systems in some areas,
1688 i.e., they may occur in correspondence with geological structures that emit fossil (microbial, thermogenic, or abiotic)
1689 CH₄ generated in the Earth’s crust. Examples have been documented in the Fisherman Lake in Canada (Smith et al., 2005),

1690 in the Baikal lake (Schmid et al., 2007), and in rice paddies in Japan (Etiopie et al., 2011). Thus, some gas emissions in
1691 freshwater environments, particularly as bubble plumes, can be incorrectly attributed to modern biological (ecosystem)
1692 activities if appropriate isotopic and molecular analyses are not performed.

1693 3.2.3 Onshore and offshore geological sources.

1694 Significant amounts of CH_4 , produced within the Earth's crust, naturally migrate to the atmosphere through tectonic faults
1695 and fractured rocks. Major emissions are related to hydrocarbon formation in sedimentary basins (microbial and thermogenic
1696 methane), through continuous or episodic exhalations from onshore and shallow marine hydrocarbon seeps and through
1697 diffuse soil microseepage (Etiopie, 2015). Specifically, five source categories have been considered. Four are onshore
1698 sources: gas-oil seeps, mud volcanoes, diffuse microseepage, and geothermal manifestations including volcanoes. One
1699 source is offshore: submarine seepage, which may include the same types of gas manifestations occurring on land. Etiopie
1700 et al. (2019) have produced the first gridded maps of geological CH_4 emissions and their isotopic signature for these five
1701 categories, with a global total of $37.4 \text{ Tg } CH_4 \text{ yr}^{-1}$ (reproduced in Fig. 5). However, these maps are based on incomplete
1702 data on geological sites due to missing information and difficulties in defining all current geological emitting sites.
1703 Combining the best estimates for the five categories of geological sources (from grid maps or from previous statistical and
1704 process-based models), the breakdown by category reveals that onshore microseepage dominate ($24 \text{ Tg } CH_4 \text{ yr}^{-1}$), the other
1705 categories having similar smaller contributions: as mean values, $4.7 \text{ Tg } CH_4 \text{ yr}^{-1}$ for geothermal manifestations, about $7 \text{ Tg } CH_4 \text{ yr}^{-1}$
1706 for submarine seepage and $9.6 \text{ Tg } CH_4 \text{ yr}^{-1}$ for onshore seeps and mud volcanoes. These values lead to a global
1707 bottom-up geological emission mean of $45 [27-63] \text{ Tg } CH_4 \text{ yr}^{-1}$ (Etiopie and Schwietzke, 2019).

1708 While all bottom-up and some top-down estimates, following different and independent techniques from different authors,
1709 consistently suggest a global geo- CH_4 emission in the order of $40-50 \text{ Tg } CH_4 \text{ yr}^{-1}$, the radiocarbon ($^{14}C-CH_4$) data in ice cores
1710 reported by Hmiel et al. (2020) appear to give a much lower estimate, with a minimum of about $1.6 \text{ Tg } CH_4 \text{ yr}^{-1}$ and a
1711 maximum value of $5.4 \text{ Tg } CH_4 \text{ yr}^{-1}$ (95 percent confidence) for the pre-industrial period. The discrepancy between Hmiel et
1712 al. (2020) and all other estimates has been discussed in Thornton et al. (2021), which demonstrated that the global near-zero
1713 geologic CH_4 emission estimate in Hmiel et al. (2020) is incompatible with the sum of multiple independent bottom-up
1714 estimates, based on a wide variety of methodologies, from individual natural geological seepage areas: for example, from
1715 the Black Sea (up to $1 \text{ Tg } CH_4 \text{ yr}^{-1}$), the Eastern Siberian Arctic Shelf (ESAS, up to $4.6 \text{ Tg } CH_4 \text{ yr}^{-1}$, referring mostly to
1716 thermogenic gas), onshore Alaska (up to $1.4 \text{ Tg } CH_4 \text{ yr}^{-1}$) and a single seepage site in Indonesia (releasing $0.1 \text{ Tg } CH_4 \text{ yr}^{-1}$
1717 as estimated by satellite measurement) (see Thornton et al. (2021) and references therein). Jackson et al. (2020) expressed
1718 doubt about the low Hmiel et al. (2020) estimates, noting that they are difficult to reconcile with the results of many other
1719 researchers and with bottom-up approaches in general. This discrepancy highlights another main unresolved uncertainty in
1720 the methane budget. Waiting for further investigation to better understand discrepancies between radiocarbon approaches
1721 and other studies, we decided to keep the estimates from Etiopie and Shwietzke (2019) for the mean values, and associate it

Mis en forme : Police :Gras, Couleur de police : Noir

Mis en forme : Normal, Espace Avant : 12 pt, Après : 12 pt, Paragraphes solidaires, Bordure : Haut: (Pas de bordure), Bas: (Pas de bordure), Gauche: (Pas de bordure), Droite: (Pas de bordure), Entre : (Pas de bordure)

Mis en forme : Police :Gras, Couleur de police : Noir

Supprimé : methane

Supprimé : production

Supprimé : (Etiopie, 2015). Specifically, five source categories have been considered.

Supprimé : (2019) have produced the first gridded maps of geological methane

Supprimé : 4). According to them, the grid maps do not represent, however, the actual global geological- CH_4 emission because the datasets used for the spatial gridding (developed for modelling purposes) were not complete or did not contain the information necessary for improving all previous estimates.

Supprimé : average

Supprimé : These values lead to a global bottom-up geological emission mean of $45 [27-63] \text{ Tg } CH_4 \text{ yr}^{-1}$ (Etiopie and Schwietzke, 2019).

Supprimé : While all bottom-up and some top-down estimates, following different and independent techniques from different authors, consistently suggest a global geo- CH_4 emission in the order of $40-50 \text{ Tg } CH_4 \text{ yr}^{-1}$, the radiocarbon ($^{14}C-CH_4$) data in ice cores reported by Hmiel et al. (2020) appear to lower the estimate, with a minimum of about $1.6 \text{ Tg } CH_4 \text{ yr}^{-1}$ and a maximum estimated value of $5.4 \text{ Tg } CH_4 \text{ yr}^{-1}$ (95 percent confidence) for the pre-industrial period. The discrepancy between Hmiel et al. (2020) and all other estimates continue to feed the debate. Eastern Siberian Arctic Shelf (ESAS) emissions have been estimated at $\sim 3 \text{ Tg } CH_4 \text{ yr}^{-1}$ based on current atmospheric surface observations (Thornton et al., 2020), corresponding to the same order of magnitude of the estimate from Hmiel et al. (2020) for global geological emissions. However, ESAS emissions are likely from both thermogenic and biogenic origins (e.g. Berchet et al., 2019). More investigation and confrontation between top-down and bottom-up results are needed to reduce this discrepancy.

Waiting for further investigation on this topic, we decided to keep the best estimates from Etiopie and Shwietzke (2019) for the mean values, and associate it to the lowest estimates reported in Etiopie et al. (2019). Thus, we report a total global geological emission of $45 [18-63] \text{ Tg } CH_4 \text{ yr}^{-1}$, with a breakdown between offshore emissions of $7 [5-10] \text{ Tg } CH_4 \text{ yr}^{-1}$ and onshore emissions of $38 [13-53] \text{ Tg } CH_4 \text{ yr}^{-1}$. The updated bottom-up estimate is slightly lower than the previous budget mostly due to a reduction of estimated emissions of onshore and offshore seeps (see Sect. 3.2.6 for more offshore contribution explanations).

3.2.4 Termites

Termites are an infraorder of insects (isoptera), which occur predominantly in the tropical and subtropical latitudes (Abe et al., 2000). CH_4 is released during the anaerobic decomposition of plant biomass in their gut (Sanderson, 1996). The uncertainty related to this CH_4 source is very high as CH_4 emissions from termites in different ecosystem types can vary and are driven by a range of factors, which

1843 to the lowest estimates reported in Etiope et al. (2019), as in Saunois et al. (2020). Thus, we report a total global geological
1844 emission of 45 [18-63] Tg CH₄ yr⁻¹, with a breakdown between offshore emissions of 7 [5-10] Tg CH₄ yr⁻¹ and onshore
1845 emissions of 38 [13-53] Tg CH₄ yr⁻¹, similar to Saunois et al. (2020). This bottom-up estimate is slightly lower than in the
1846 Saunois et al. (2016) budget mostly due to a reduction of estimated emissions of onshore and offshore seeps (see Sect. 3.2.6
1847 for more offshore contribution explanations).

1848 **3.2.4 Termites**

1849 Termites are decomposers playing a central role in ecosystem nutrient fluxes at tropical and subtropical latitudes, in
1850 particular (Abe et al., 2000). Termites represent a natural CH₄ source due to methanogenesis occurring in their hindgut
1851 during the symbiotic metabolic breakdown of lignocellulose (Sanderson, 1996; Brune, 2014). The upscaling of CH₄
1852 emissions from termites from site to global level is characterised by high uncertainty (Sanderson, 1996; Kirschke et al.,
1853 2013; Saunois et al., 2016) due to the combination of factors that need to be considered and the scarcity of information for
1854 each of these factors for global upscaling. Needed data include termite biomass density (Sanderson, 1996), species
1855 distribution within and among ecosystems (Sugimoto et al., 1998), variation of termite CH₄ emission rates per species and
1856 dietary group (Sanderson, 1996), the role played by the termite mound structure in affecting the fraction of produced CH₄
1857 that is effectively released into the atmosphere (Sugimoto et al., 1998; Nauer et al., 2018). In Kirschke et al. (2013) and
1858 Saunois et al. (2016) a global upscaling of termite CH₄ emissions was proposed, where CH₄ emissions, E_{CH₄} (kg CH₄ ha⁻¹yr⁻¹
1859), were estimated as the product of three terms: termite biomass (Bi_{TERM} g fresh weight m⁻²), a scalar correction factor
1860 (LU) expressing the effect of land use/cover change on termite biomass density, a termite CH₄ emission factor (EF_{TERM}, μg
1861 CH₄ g⁻¹ Bi_{TERM} h⁻¹). The approach between the two re-analyses of CH₄ emissions varied only for the data sources of gross
1862 primary productivity (GPP) and land use which were used to attribute biomass values of termite per ecosystem surface unit,
1863 in order to cover different time spans, 1980s, 1990s and 2000s in Kirschke et al. (2013) and 2000-2007 and 2010-2016 in
1864 Saunois et al. (2016). For the present update, additional changes have been introduced compared with the previous versions.
1865 Here we summarise the key data used for the new upscaling. CH₄ fluxes were modelled between 45°S and 45°N and within
1866 35°S and 35°N. The termite biomass density, Bi_{TERM} for tropical ecosystems was estimated as function (Kirschke et al.,
1867 2013; Bi_{TERM}=1.21·e^{0.0008·GPP}) of the gross primary production (GPP, g C m⁻² yr⁻¹) using the 0.25° native resolution
1868 VODCA2GPP dataset covering the period 2001-2020 (Wild et al., 2022). Wetlands, barren areas, water bodies and artificial
1869 surfaces were excluded from this estimation and set as no data (no emissions). The scalar correction factor LU of 0.4 (60%)
1870 for agricultural areas (i.e., croplands) (Kirschke et al., 2013) was applied to the GPP value of the nearest natural areas to
1871 account for anthropic disturbance. The annual (2001-2020) land cover information was obtained from the MODIS
1872 Terra+ Aqua Combined Land Cover product (MCD12C1v006; <https://lpdaac.usgs.gov/products/mcd12c1v006/>), using the
1873 International Geosphere-Biosphere Programme (IGP) classification with a 0.05° spatial resolution. For desert and arid lands,
1874 within 35°S and 35°N, a fixed Bi_{TERM} value of 1.56 g m⁻² was instead used (Sanderson, 1996; Heděnc et al., 2022).

1875 Similarly, fix values from the few available studies reported in literature were used to estimate Bio_{TERM} between 35°- 45° N
1876 and 35°- 45° S as follows: 1.83 g m⁻² for temperate forests and grasslands (Wood and Sands, 1978; Petersen and Luxton,
1877 1982; Sanderson, 1996; Bignell and Eggleton, 2000; King et al., 2013; conversion factor from dry to fresh biomass is 0.27
1878 from Petersen and Luxton, 1982), 5.3 g m⁻² for scrublands and Mediterranean areas of Australia (Sanderson, 1996), 1.09 g
1879 m⁻² for the other Mediterranean shrubland ecosystems (Heděnc et al., 2022). Other climates and land covers were set as no
1880 data. Climate zoning was defined using the Climate Zones Köppen-Geiger dataset (Beck et al., 2018), this product is
1881 representative for the 1980-2016 time period and has a 0.0083° native resolution. The EF_{TERM} was revised compared with
1882 previous estimates (Kirschke et al., 2013; Saunois et al., 2016), in order to consider the different distribution of termite
1883 families and subfamilies in the different continents and ecosystems, characterised by different feeding habits and nest
1884 typologies, as reported by Sugimoto et al. (1998), which might influence the EF. The species of each family and subfamily
1885 of the two major groups of lower and higher termites, listed by Sugimoto et al. (1998) were associated with EF values based
1886 on emissions from in-vitro experiments as reported by Sanderson (1996) and Eggleton et al. (1999), to which a correction
1887 factor (cf_{MOUND}) of 0.5 (Nauer et al., 2018) was applied in order to take into account the mound effect on the CH₄ produced
1888 by termites, once inside the nest. The average EF_{TERM} for tropical and temperate areas was hence estimated as the weighted
1889 EF_{TERM} derived from the product of the percentage weight of each family or subfamily of termites in the “community
1890 composition” in each geographical area and ecosystem (Sugimoto et al. (1998, Table 6), the respective calculated EF of
1891 each family or subfamily, a scalar or correction factor which considers the nest type (as in Table 5 from Sugimoto et al.
1892 1998). For desert and arid lands and temperate areas, which were not reported in Sugimoto et al. (1998), EF rates were
1893 calculated directly from data reported in literature for the most representative species which were the genus *Amitermes* for
1894 the former (EF from data by Sanderson 1996, Eggleton et al. 1999, Jamali et al. 2011) and the genus *Reticulitermes* (family
1895 Rhinotermitidea) for the latter (EF from data by Odelson and Breznak, 1983; Sanderson, 1996; Eggleton et al., 1999; Myer
1896 et al., 2021). The following EF_{TERMS} were hence obtained to scale up emissions: $3.26 \pm 1.79 \mu\text{g CH}_4 \text{ g}^{-1} \text{ termite h}^{-1}$ (28.56
1897 $\text{mg CH}_4 \text{ g}^{-1} \text{ termite year}^{-1}$) for tropical ecosystems, $1.82 \pm 1.54 \mu\text{g CH}_4 \text{ g}^{-1} \text{ termite h}^{-1}$ for temperate forests, grasslands, and
1898 Mediterranean areas, $1.24 \pm 1.22 \mu\text{g CH}_4 \text{ g}^{-1} \text{ termite h}^{-1}$ for deserts and arid lands (warm climate). Annual CH₄ fluxes were
1899 computed for all the years from 2001 to 2020 producing 20 global maps at 0.05° resolution of yearly total emissions. A
1900 further map of the estimated error representative of the entire time period was elaborated at the same resolution as the
1901 emissions dataset.

1902 Termite CH₄ emissions over the period 2001-2020 varied between 9.7-10.8 Tg CH₄ yr⁻¹, with an average of $10.2 \pm 6.2 \text{ Tg}$
1903 $\text{CH}_4 \text{ yr}^{-1}$. Considering a 20-year average, tropical and subtropical moist broadleaf forests contributed to 46% of the total
1904 average flux, while tropical and subtropical grasslands, savannas, and shrublands to another 36%. In terms of regional
1905 contribution, 37.2% of fluxes were attributed to South America, 31.5% to Africa, 18.1% to Asia, 5.5% to Australia, 7.4%
1906 to North America and less than 1% to Europe. The present estimate value is within the range of previous up-scaling studies.

spanning from 2 to 22 Tg CH₄ yr⁻¹ (Ciais et al., 2013). In this study, we report a decadal value of 10 Tg CH₄ yr⁻¹ with a range of [4-16].

3.2.5 Wild animals

Wild ruminants emit CH₄ through microbial fermentation that occurs in their rumen, similarly to domesticated livestock species (USEPA, 2010b). Using a total animal population of 100-500 million, Crutzen et al. (1986) estimated the global emissions of CH₄ from wild ruminants to be in the range of 2-6 Tg CH₄ yr⁻¹. More recently, Pérez-Barbería (2017) lowered this estimate to 1.1-2.7 Tg CH₄ yr⁻¹ using a total animal population estimate of 214 million (range of 210-219), arguing that the maximum number of animals (500 million) used in Crutzen et al. (1986) was poorly justified. Moreover Pérez-Barbería (2017) also stated that the value of 15 Tg CH₄ yr⁻¹ found in the last IPCC reports is much higher than their estimate because this value comes from an extrapolation of Crutzen's work for the last glacial maximum when the population of wild animals was much larger, as originally proposed by Chappellaz et al. (1993). Recently, based on the modelling of grassland extent, Kleinen et al. (2023) also suggest that the population of wild animal during the last glacial maximum proposed by Crutzen et al. (1986) and further used by Chappellaz et al. (1993) were overestimated.

Based on these findings, the range adopted in this updated CH₄ budget is 2 [1-3] Tg CH₄ yr⁻¹ (Table 3).

3.2.6 Coastal and ocean sources

Coastal and oceanic sources comprise CH₄ release from estuaries, coastal vegetated habitats, as well as marine waters including seas and oceans. Possible sources of coastal and oceanic CH₄ include (1) in-situ biogenic production through various pathways in oxygenated sea-surface waters (Oremland, 1979; Karl et al., 2008; Lenhart et al., 2016; Repeta et al., 2016), a flux that can be enhanced in the coastal ocean because of submarine groundwater discharge (USEPA, 2010b); (2) production from shallow and marine (bare and vegetated) sediments including free gas or destabilised hydrates and thawing subsea permafrost containing modern (¹⁴C-bearing) microbial gas; (3) geological marine seepage (see also Sect. 3.2.3), including hydrates, containing fossil (¹⁴C-free) microbial or thermogenic CH₄. CH₄ produced in marine sediments and seabed CH₄ seepage can be transported across the water column to the sea-surface by upwelling waters (once at the surface methane can cross the sea-air interface via diffusion) and gas bubble plumes (for instance from geological marine seeps; e.g., Judd, 2004; Etiope et al., 2019). Gas bubble plumes can generally (but not exclusively, as described below) reach the atmosphere in relatively shallow waters (<400 m) of continental shelves and coastal zones. In coastal vegetated habitats CH₄ can also be transported to the atmosphere through the aerenchyma of emergent aquatic plants (Purvaia et al., 2004). We distinguish between coastal and oceanic "geological" and "modern biogenic" CH₄ sources. Coastal and oceanic "geological" emissions refer to CH₄ seepage from the Earth's crust (mostly in hydrocarbon-rich sedimentary basins), which is typically evaluated by combining geochemical analyses (isotopic and molecular, including radiocarbon, ¹⁴C, analyses) and geological observations (degassing along faults, seeps, mud volcanoes). Geological emissions do not contain modern

Mis en forme : Police :Gras, Couleur de police : Noir

Mis en forme : Normal, Espace Avant : 12 pt, Après : 12 pt, Paragraphes solidaires, Bordure : Haut: (Pas de bordure), Bas: (Pas de bordure), Gauche: (Pas de bordure), Droite: (Pas de bordure), Entre : (Pas de bordure)

Mis en forme : Police :Gras, Couleur de police : Noir

Supprimé: Wild ruminants emit methane through the microbial fermentation process occurring in their rumen, similarly to domesticated livestock species (USEPA, 2010b). Using a total animal population of 100-500 million, Crutzen et al. (1986) estimated the global emissions of CH₄ from wild ruminants to be in the range of 2-6 Tg CH₄ yr⁻¹. More recently, Pérez-Barbería (2017) lowered this estimate to 1.1-2.7 Tg CH₄ yr⁻¹ using a total animal population estimate of 214 million (range of 210-219), arguing that the maximum number of animals (500 million) used in Crutzen et al. (1986) was poorly justified. Moreover Pérez-Barbería (2017) also stated that the value of 15 Tg CH₄ yr⁻¹ found in the last IPCC reports is much higher than their estimate because this value comes from an extrapolation of Crutzen's work for the last glacial maximum when the population of wild animals was much larger, as originally proposed by Chappellaz et al. (1993).

Supprimé: methane

Supprimé: Oceanic

Mis en forme : Police :Gras, Couleur de police : Noir

Mis en forme : Police :Gras, Couleur de police : Noir

Mis en forme : Police :Gras, Couleur de police : Noir

Mis en forme ... [95]

Supprimé: Oceanic

Supprimé: coastal ocean and open ocean methane

Supprimé: .

Supprimé: .

Supprimé: from marine (bare and vegetated) sediments or thawing

Supprimé: the water column, especially

Supprimé: (USEPA, 2010b);

Supprimé: leaks from

Supprimé:); and (4) emission from the destabilisation of marine

Supprimé: , methane

Supprimé: through

Supprimé: in a dissolved form (especially in the upwelling zone)

Supprimé:), for instance, in shallow waters

Supprimé: .

Supprimé: methane

Mis en forme : Police :Non Italique

Supprimé: Ramachandran

1977 biogenic gas that is fossil (^{14}C -free). Coastal and oceanic “biogenic” CH_4 refers to CH_4 formed *in situ* in coastal and marine
1978 sediments and in the water column by recent or modern microbial activity (therefore with measurable amounts of
1979 radiocarbon (^{14}C)). To avoid double-counting, we assume that all diffusive CH_4 emissions outside of geological seepage
1980 regions (identified in global grid maps; Etiope et al., 2019) are fuelled by biogenic CH_4 . Finally, we briefly discuss the case
1981 of CH_4 hydrates, which can be considered either a “geological” source when they host fossil CH_4 or a “biogenic” source
1982 when they host modern CH_4 .

Coastal and oceanic modern biogenic methane emissions. Area-integrated diffusive modern biogenic CH_4 emissions
1984 from coastal ecosystems are 1-2 magnitudes lower than from inland freshwaters but significantly higher than biogenic
1985 emissions from the open ocean (Rosentreter et al., 2021; Rosentreter et al., 2023; Weber et al., 2019). Particularly the shallow
1986 vegetated coastline fringed by mangroves, salt marshes, and seagrasses is a CH_4 hotspot in the coastal ocean, characterised
1987 by significantly higher flux densities than other coastal settings such as estuaries or the continental shelves (Rosentreter et
1988 al., 2021; Rosentreter et al., 2023). Coastal ecosystems are thus being increasingly recognized as weak global sources to the
1989 atmosphere (Weber et al., 2019; Saunois et al., 2020; Rosentreter et al., 2021). Hydrogenotrophic and acetoclastic
1990 methanogenesis are largely outcompeted by sulphate reduction in coastal/marine sediments, which is often shown by a
1991 decreasing trend of CH_4 concentrations with increasing salinity from upper tidal (low salinity) to marine (high salinity)
1992 regions. Much of the CH_4 produced below the sulfate-reduction zone is indeed re-oxidized by sedimentary anaerobic
1993 methane oxidation or re-oxidized in the water column, leading to small emissions despite much larger production (Knittel
1994 and Boetius 2009; Regnier et al., 2011). Methylated compounds such as methylamines and methyl sulphides are non-
1995 competitive substrates that are exclusively used by methanogens, therefore methylated methanogenesis can occur in coastal
1996 regions with high sulphate concentrations, for example, in organic-rich (Maltby et al., 2018), vegetated (Schorn et al., 2022),
1997 and hypersaline coastal sediments (Xiao et al., 2018). Coastal CH_4 can be driven by the exchange of pore water or
1998 groundwater (high in CH_4) with coastal surface waters in tidal systems, referred to as tidal pumping (Ovalle et al., 1990;
1999 Call et al., 2015). Anthropogenic impacts such as wastewater pollution and land-use change can increase CH_4 fluxes in
2000 estuaries (Wells et al., 2020). A large increase of CH_4 emissions follows the conversion of natural coastal habitats to
2001 aquaculture farms (Yuan et al., 2019; Yang et al., 2022).

Currently available global modern biogenic CH_4 flux data show high spatiotemporal variability within and between coastal
2002 systems, but also because of the overall global paucity of data. Therefore, global estimates have high uncertainties and show
2003 large ranges in both empirical (Rosentreter et al., 2021) and machine-learning based approaches (Weber et al., 2019).
2004 According to a recent data-driven meta-data analysis, global estuaries, including tidal systems and deltas, lagoons, and
2005 fjords, are estimated to emit median (Q1-Q3) 0.25 (0.07-0.46) $\text{Tg CH}_4 \text{ yr}^{-1}$ (Rosentreter et al., 2023). Coastal vegetation,
2006 including mangrove forests, salt marshes, and seagrasses are estimated to emit 0.77 (0.47-1.41) $\text{Tg CH}_4 \text{ yr}^{-1}$, which is 3
2007 times more than global estuaries (Rosentreter et al., 2023). The combined median (Q1-Q3) emission of 1.01 (0.54-1.87) Tg
2008 $\text{CH}_4 \text{ yr}^{-1}$ for coastal vegetation and estuaries by Rosentreter et al. (2023) is lower than the recent observation-based global
2009

3010 synthesis including tidal flats and aquaculture ponds (median 1.49 (0.22-6.48) Tg CH₄ yr⁻¹) by Rosentreter et al. (2021).
3011 Total shallow coastal modern biogenic CH₄ emissions based on existing data including emissions from estuaries, coastal
3012 vegetation (Rosentreter et al., 2023), tidal flats, and man-made coastal aquaculture ponds (Rosentreter et al., 2021) amount
3013 to median (Q1-Q3) 1.8 (0.59-5.57) Tg CH₄ yr⁻¹. This range is about 3-4 times lower than the earlier global assessment by
3014 Borges and Abril (2011) and also lower than the value of 4-5 Tg CH₄ yr⁻¹ reported in the previous CH₄ budget for inner and
3015 outer estuaries including marshes and mangroves (Saunois et al., 2020), which was based on a significantly smaller dataset
3016 (n=80) and larger estuarine surface areas (Laruelle et al., 2013) than used here (Laruelle et al., 2023).
3017 The near-shore (0-50 m), inner shelf diffusive modern biogenic CH₄ flux of median (Q1-Q3) 1.33 (0.93-2.10) Tg CH₄ yr⁻¹
3018 by Weber et al. (2019) based on machine-learning is similar to the combined shallow coastal (estuaries and coastal
3019 vegetation) median by Rosentreter et al. (2021, 2023). Adding the diffusive modern biogenic CH₄ flux for the outer shelf
3020 (50-200 m) (median (Q1-Q3) of 0.54 (0.40-0.73) Tg CH₄ yr⁻¹) and for the slope (200-2000m) (median (Q1-Q3) of 0.28
3021 (0.22-0.37) Tg CH₄ yr⁻¹) (Weber et al., 2019), and excluding geological seepage regions (Etiopie et al., 2019; see below),
3022 gives a total median (Q1-Q3) of 3.95 (2.14-8.77) Tg CH₄ yr⁻¹ for combined coastal shallow, near-shore, outer shelf and
3023 slope diffusive modern biogenic CH₄ emissions. The previous budget by Saunois (2020) also included poorly constrained
3024 emissions (upper bound value: 1-2 Tg CH₄ yr⁻¹) from large river plumes protruding onto the shelves. However, here we
3025 assume that emissions from large river plumes are accounted for in the near-shore and outer shelf estimates by Weber et al.
3026 (2019). Area-integrated diffusive CH₄ emissions from the open ocean and deep seas (>2000 m) are much lower than from
3027 other coastal systems but amount to median (Q1-Q3) 0.91 (0.75-1.12) Tg CH₄ yr⁻¹ because of the large surface area of the
3028 open ocean (>300 x 10⁶ km²) (Weber et al., 2019). Overall, these marine biogenic emissions are sustained by a mixture of
3029 sedimentary production and in-situ production in the sea-surface layers, as shown by, e.g., Karl et al. (2008) and Repeta et
3030 al. (2016). The total coastal and ocean diffusive modern biogenic emissions retained here amount to 5 (3-10) Tg CH₄ yr⁻¹.
3031
3032 **Coastal and oceanic geological methane emissions** Submarine geological CH₄ emission is the offshore component of the
3033 general geological emissions of natural gas from the Earth's crust (Judd, 2004; Etiopie, 2009; Etiopie et al., 2019). The
3034 onshore components include terrestrial seeps, mud volcanoes, microseepage, and geothermal manifestations, addressed in
3035 Sect. 3.2.3. Natural gas seeping at the seabed as bubble plumes can reach the surface, generally occurs in relatively shallow
3036 waters (<400 m), but CH₄-rich bubble plumes reaching the atmosphere from depths >500 m have been observed in some
3037 cases (e.g., Solomon et al., 2009), and upwelling of bottom marine waters can, in theory, transport geological
3038 CH₄ (dissolved) to the surface from any depth. This represents, however, a small and poorly known fraction of geological
3039 CH₄ emission. Geological CH₄ can be either microbial or thermogenic, produced throughout diverse geological periods in
3040 hydrocarbon source rocks in sedimentary basins (therefore it is always fossil, ¹⁴C-free). The seepage at the seafloor is
3041 typically related to tectonic faults, sometimes forming mud diapirs and mud volcanoes (Mazzini and Etiopie, 2017).

3042 Published estimates of geological CH₄ submarine emissions range from 3 to 20 Tg yr⁻¹, with a best guess of 7 Tg yr⁻¹ (Etiopie
3043 and Schwietzke, 2019; Etiopie et al., 2019 and references therein).

3044 Here, the diffusive geological CH₄ emissions are estimated at 0.16 (0.11-0.24) Tg CH₄ yr⁻¹ for near-shore (0-50 m), 0.03
3045 (0.02-0.05) Tg CH₄ yr⁻¹ for outer shelf (50-200 m), and 0.02 (0.01-0.03) Tg CH₄ yr⁻¹ for slope (200-2000 m) by calculating
3046 the fraction of the Weber et al. (2019) diffusive fluxes that occur within the identified geological seepage regions from
3047 Etiopie et al. (2019). No geological seepage regions were identified in the open ocean and deep seas (> 2000 m).

3048 In this study, we consider the ebullitive flux as geologically sourced CH₄. While modern biogenic CH₄ gas production
3049 appears ubiquitous in shallow sediments (Fleischer et al., 2001; Best et al., 2006), no global dataset is currently available to
3050 estimate the biogenic ebullitive CH₄ flux to the atmosphere. Omission of this flux thus constitutes a significant knowledge
3051 gap in the coastal and oceanic CH₄ budget. Global geological CH₄ ebullition from continental shelf and slope, referring only
3052 to depths <200 m, were estimated at 5.06 (1.99-8.16) Tg CH₄ yr⁻¹ (Weber et al., 2019). This estimate is based on prior
3053 estimates of the geological flux from the seafloor (Hovland et al., 1993) and bubble transfer efficiency to the ocean surface
3054 (McGinnis et al., 2006). Etiopie et al. (2019) estimated a partial fraction of geological emissions in the form of gas bubbles
3055 of 3.9 (1.8-6) Tg CH₄ yr⁻¹, only referring to the sum of published estimates from 15 geological seepage regions, which are
3056 also deeper than 200 m. Global extrapolation including other 16 identified seepage zones (where flux data are not available)
3057 was suggested to be at least 7 (3-10) Tg CH₄ yr⁻¹ (Etiopie et al., 2019), and this value coincides with the mean emission value
3058 (best guess) derived by combining literature data, see Etiopie and Schwietzke (2019) for further details. It is worth noting
3059 that the Weber et al. (2019) estimate of 5.06 (1.99-8.16) Tg CH₄ yr⁻¹, which considers only the continental shelf at depths
3060 <200 m, is compatible with the overall submarine emission of 7 (3-10) Tg CH₄ yr⁻¹ (including seeps > 200 m deep) indicated
3061 in Etiopie and Schwietzke (2019) and Etiopie et al. (2019). Although 300-400 m is considered a general depth limit for
3062 efficient transport (with limited oxidation and dissolution) of CH₄ bubbles to the atmosphere (e.g., Judd, 2004; Schmale et
3063 al., 2005; Etiopie et al., 2019), in some cases oil coatings on bubbles inhibit gas dissolution so that CH₄-rich bubbles can
3064 reach the atmosphere from depths >500 m (e.g., Solomon et al., 2009). As mentioned above, a fraction of geological CH₄
3065 released in deep seas (such as in the areas with gas-charged sediments inventoried in Fleischer et al., 2001) can also be
3066 transported to the surface by upwelling bottom waters. Further research is needed to better evaluate the atmospheric impact
3067 of such deep seeps.

3068 Geological submarine emissions, thus, would amount to 0.21 (0.14-0.32) Tg CH₄ yr⁻¹ in the form of a diffusive flux while
3069 the ebullitive flux would be 5.06 (3.01-7.88) Tg CH₄ yr⁻¹, considering only < 200 m deep seepage, and 7 (3-10) Tg CH₄ yr⁻¹
3070 considering all data available (Etiopie and Schwietzke, 2019). Here, we select the Etiopie and Schwietzke (2019) assessment
3071 in order to account for all potential seepage areas, including those located at water depths > 200m.

3072

3073 As a result, here we report a (rounded) median of 12 Tg CH₄ yr⁻¹ with a range of 6-20 Tg CH₄ yr⁻¹ for all coastal and ocean
3074 sources.

1075
1076 Methane emissions from gas hydrates. Among the different origins of coastal and oceanic CH₄, hydrates have attracted a
1077 lot of attention. CH₄ hydrates (or clathrates) are ice-like crystals formed under specific temperature and pressure conditions
1078 (Milkov, 2005). Hydrates may host either modern microbial CH₄, containing ¹⁴C and formed *in situ* in shallow sediments
1079 (this type of hydrates is also called “autochthonous”) or fossil, microbial or thermogenic CH₄, migrated from deeper
1080 sediments, generally from reservoirs in hydrocarbon-rich sedimentary basins (this type of hydrates is also called
1081 “allochthonous”; Milkov, 2005; Foschi et al., 2023). The total stock of marine CH₄ hydrates is large but uncertain, with
1082 global estimates ranging from hundreds to thousands of Pg CH₄ (Klauda and Sandler, 2005; Wallmann et al., 2012). Note
1083 that the highly climate-sensitive subsea permafrost reservoir beneath Arctic Ocean shelves also contributes to the hydrate
1084 inventory (Ruppel and Kassler, 2017).

1085 Concerning more specifically atmospheric emissions from marine hydrates, Etiopie (2015) points out that current estimates
1086 of CH₄ air-sea flux from hydrates (2–10 Tg CH₄ yr⁻¹ in Ciais et al., 2013, or Kirschke et al., 2013) originate from the
1087 hypothetical values of Cicerone and Oremland (1988). No experimental data or estimation procedures have been explicitly
1088 described along the chain of references since then (Denman et al., 2007; IPCC, 2001; Kirschke et al., 2013; Lelieveld et al.,
1089 1998). It was estimated that ~473 Tg CH₄ has been released into the water column over 100 years (Kretschmer et al., 2015).
1090 Those few teragrams per year become negligible once consumption within the water column has been accounted for. While
1091 events such as submarine slumps may trigger local releases of considerable amounts of CH₄ from hydrates that may reach
1092 the atmosphere (Etiopie, 2015; Paull et al., 2002), on a global scale, present-day atmospheric CH₄ emissions from hydrates
1093 do not appear to be a significant source to the atmosphere, and at least formally, we should consider 0 (< 0.1) Tg CH₄ yr⁻¹
1094 emissions.

3.2.7 Terrestrial permafrost

1096 Permafrost is defined as frozen soil, sediment, or rock having temperatures at or below 0°C for at least two consecutive
1097 years (Harris et al., 1988). The total extent of permafrost in the Northern Hemisphere is about 14 million km² or 15% of the
1098 exposed land surface (Obu et al., 2019). As the climate warms, a rise in soil temperatures has been observed across the
1099 permafrost region, and permafrost thaw occurs when temperatures pass 0°C, often associated with melting of ice in the
1100 ground (Biskaborn et al., 2019). Permafrost thaw is most pronounced in southern and spatially isolated permafrost zones,
1101 but also occurs in northern continuous permafrost (Obu et al., 2019). Thaw occurs either as a gradual, often widespread,
1102 deepening of the active layer (surface soils that thaw every summer) or as more rapid localised thaw associated with loss of
1103 massive ground ice (thermokarst) (Turetsky et al., 2020). A total of 1000 ± 200 Pg of carbon can be found in the upper 3
1104 meters of permafrost region soils, or 1400-2000 Pg C for all permafrost (Hugelius et al., 2014; Strauss et al., 2021).

Supprimé: Biogenic emissions from open and coastal ocean. The most common biogenic ocean emission value found in the literature is 10 Tg CH₄ yr⁻¹ (Rhee et al., 2009b). It appears that most studies rely on the work of Ehhalt (1974), where the value was estimated on the basis of the measurements done by Swinnerton and co-workers (Lamontagne et al., 1973; Swinnerton and Linnenbom, 1967) for the open ocean, combined with purely speculated emissions from the continental shelf. Based on basin-wide observations using updated methodologies, three studies found estimates ranging from 0.2 to 3 Tg CH₄ yr⁻¹ (Bates et al., 1996; Conrad and Seiler, 1988; Rhee et al., 2009b), associated with super-saturations of surface waters that are an order of magnitude smaller than previously estimated, both for the open ocean (saturation anomaly ~0.04, see Rhee et al. (2009a), equation 4) and for continental shelf (saturation anomaly ~0.2). In their synthesis, indirectly referring to the original observations from Lambert and Schmidt (1993), Wuebbles and Hayhoe (2002), they use a value of 5 Tg CH₄ yr⁻¹. Proposed explanations for discrepancies regarding sea-to air methane emissions in the open ocean rely on experimental biases in the former studies of Swinnerton and Linnenbom (Rhee et al., 2009b). This may explain why the Bange et al. (1994) compilation cites a global source of 11-18 Tg CH₄ yr⁻¹ with a dominant contribution of coastal regions. Here, we report a range of 0-5 Tg CH₄ yr⁻¹, with a mean value of 2 Tg CH₄ yr⁻¹ for biogenic emissions from open and coastal ocean (excluding estuaries). Biogenic emissions from brackish waters (estuaries, coastal wetlands) were not reported in the previous budget (Saunois et al., 2016). Methane emissions from estuaries were originally estimated by Bange et al. (1994), Upstill-Goddard et al. (2000) and Middelburg et al. (2002) to be comprised between 1 and -3 Tg CH₄ yr⁻¹. This range was later revised upwards by Borges and Abril (2011) to about 7 Tg CH₄ yr⁻¹ based on a methodology distinguishing between different estuarine types and accounting for the contribution of tidal flats, marshes and mangroves, for a total of 39 systems and a global “inner” estuarine surface area of 1.1 10⁶ km² (Laruelle et al., 2013). The same methodology as in Laruelle et al. (2013) has been applied here to the same systems using an expanded database of local and regional measurements (72 systems) and suggests however that global estuarine CH₄ emissions were overestimated and may actually not surpass 3-3.5 Tg CH₄ yr⁻¹. Despite this overall reduction, the specific contribution of sediment and water emissions from mangrove ecosystems is however higher and contributes <0.1 to 1.7 Tg CH₄ yr⁻¹ globally (Rosentretter et al., 2018). This estuarine estimate does not include the uncertain contribution from large river plumes (Dore

Supprimé: and hydrates

Mis en forme : Normal, Espace Avant : 12 pt, Après : 12 pt, Paragraphes solitaires, Bordure : Haut: (Pas de bordure), Bas: (Pas de bordure), Gauche: (Pas de bordure), Droite: (Pas de bordure), Entre : (Pas de bordure)

Mis en forme : Police :Gras, Couleur de police : Noir

Mis en forme : Police :Gras, Couleur de police : Noir

Supprimé: Permafrost is defined as frozen soil, sediment, or rock having temperatures at or below 0°C for at least two consecutive years (Harris et al., 1988). The total extent of permafrost in the Northern Hemisphere is about 14 million km² or 15% of the exposed land surface (Obu et al., 2019). As the climate warms, large areas of permafrost are also warming, and if soil temperatures pass 0°C, thawing of the permafrost occurs. Permafrost thaw is most pronounced in southern and spatially isolated permafrost zones, but also occurs in northern continuous permafrost (Obu et al., 2019)

3268 The thawing permafrost can generate direct and indirect CH₄ emissions. Direct CH₄ emissions are from the release of
3269 CH₄ contained within the thawing permafrost. This flux to the atmosphere is small and estimated to be a maximum of 1 Tg
3270 CH₄ yr⁻¹ at present (USEPA, 2010b). Increased seepage of geogenic CH₄ gas seeps along permafrost boundaries and lake
3271 beds may also be considered a direct flux, and this is estimated to be 2±0.4 Tg CH₄ yr⁻¹ (Walter Anthony et al., 2012).
3272 Indirect CH₄ emissions are probably more important. They are caused by 1) methanogenesis induced when the organic
3273 matter contained in thawing permafrost becomes available for microbial decomposition; 2) thaw induced soil wetting and
3274 changes in land surface hydrology possibly enhancing CH₄ production (McCalley et al., 2014; Schuur et al., 2022); and 3)
3275 the landscape topography changes driven by abrupt thaw processes and loss of ground ice, including the formation of
3276 thermokarst lakes, hill-slope thermokarst, and wetland thermokarst (Turetsky et al., 2020). Such CH₄ production is probably
3277 already significant today and is likely to become more important in the future associated with climate change and strong
3278 positive feedback from thawing permafrost (Schuur et al., 2022). However, indirect CH₄ emissions from permafrost thawing
3279 are difficult to estimate at present, with very few data to refer to, and in any case largely overlap with wetland and freshwater
3280 emissions occurring above or around thawing areas. In a recent synthesis of full permafrost region CH₄ budgets for the
3281 period 2000-2017, Hugelius et al. (2023) compared CH₄ budgets from bottom-up and top-down (atmospheric inversion
3282 models) approaches. They estimate an integrated bottom-up budget of 50 (23, 53; mean upper and lower 95% CI) Tg CH₄
3283 yr⁻¹ while the top-down estimate is 19 (15, 24) Tg CH₄ yr⁻¹. The bottom-up estimate is based on a combination of data-
3284 driven upscaling reported by Ramage et al. (2023) and process-based model estimates for wetland CH₄ flux calculated from
3285 model ensembles used in Saunio et al. (2020). The top-down estimate is calculated from ensembles of atmospheric
3286 inversion models used in Saunio et al. (2020). Although it is difficult with direct process-attribution, fluxes of ca. 20-30 Tg
3287 CH₄ yr⁻¹ in the bottom-up budget are caused by land cover types affected by previous permafrost thaw (thermokarst lakes,
3288 wetlands, hillslope). Because pre-thaw land cover types often have near neutral CH₄ balances (Ramage et al. 2023), these
3289 fluxes can largely be seen as driven by permafrost thaw, however the thaw may have occurred decades, or even centuries,
3290 before today.

3291 Here, we choose to report only the direct emission range of 0-1 Tg CH₄ yr⁻¹, keeping in mind that current wetland,
3292 thermokarst lakes and other freshwater methane emissions already likely include a significant indirect contribution
3293 originating from thawing permafrost.

3294 3.2.8 Vegetation

3295 Three distinct pathways for the production and emission of CH₄ by living vegetation are considered here (see Covey and
3296 Megonigal (2019) and Bastviken et al. (2023) for extensive reviews). Firstly, plants produce CH₄ through an abiotic
3297 photochemical process induced by stress (Keppler et al., 2006). This pathway was initially questioned (e.g., Dueck et al.,
3298 2007; Nisbet et al., 2009), and although numerous studies have since confirmed aerobic emissions from plants and better
3299 resolved its physical drivers (Fraser et al., 2015), global estimates still vary by two orders of magnitude (Liu et al., 2015).

Mis en forme : Police :Gras, Couleur de police : Noir

Mis en forme : Normal, Espace Avant : 12 pt, Après : 12 pt, Paragraphes solidaires, Bordure : Haut: (Pas de bordure), Bas: (Pas de bordure), Gauche: (Pas de bordure), Droite: (Pas de bordure), Entre : (Pas de bordure)

Supprimé: Three distinct pathways for the production and emission of methane by living vegetation are considered here (see Covey and Megonigal (2019) for an extensive review). Firstly, plants produce methane through an abiotic photochemical process induced by stress (Keppler et al., 2006). This pathway was initially criticized (e.g. Dueck et al., 2007; Nisbet et al., 2009), and although numerous studies have since confirmed aerobic emissions from plants and better resolved its physical drivers (Fraser et al., 2015), global estimates still vary by two orders of magnitude (Liu et al., 2015). This plant source has not been confirmed in-field however, and although the potential implication for the global methane budget remains unclear, emissions from this source are certainly much smaller than originally estimated in Keppler et al. (2006) (Bloom et al., 2010; Fraser et al., 2015). Second, and of clearer significance, plants act as "straws", drawing up and releasing microbially produced methane from anoxic soils (Cicerone and Shetter, 1981; Rice et al., 2010). For instance, in the forested wetlands of Amazonia, tree stems are the dominant ecosystem flux pathway for soil-produced methane, therefore, including stem emissions in ecosystem budgets can reconcile regional bottom-up and top-down estimates (Pangala et al., 2017). Third, the stems of both living trees (Covey et al., 2012) and dead wood (Covey et al., 2016) provide an environment suitable for microbial methanogenesis. Static chambers demonstrate locally significant through-bark flux from both soil- (Pangala et al., 2013, 2015), and tree stem-based methanogens (Pitz and Megonigal, 2017; Wang et al., 2016). A recent synthesis indicates stem CH₄ emissions significantly increase the source strength of forested wetlands, and modestly decrease the sink strength of upland forests (Covey and Megonigal, 2019). The scientific activity covering CH₄ emissions in forested ecosystems reveals a far more complex story than previously thought, with an interplay of, productive/consumptive, aerobic/anaerobic, biotic/abiotic, processes occurring between upland/wetland soils, trees, and atmosphere. Understanding the complex processes that regulate CH₄ source-sink dynamics in forests and estimating their contribution to the global methane budget requires cross-disciplinary research, more observations, and new models that can overcome the classical binary classifications of wetland versus upland forest and of emitting versus uptaking soils (Barba et al., 2019; Covey and Megonigal, 2019). Although we recognize these emissions are potentially large (particularly tree transport from inundated soil), global estimates for each of these pathways remain highly uncertain and/or are currently ascribed here to other flux categories sources (e.g. inland waters, wetlands, upland soils).

3.3 Methane sinks and lifetime

Methane is the most abundant reactive trace gas in the troposphere and its reactivity is important to both tropospheric and stratospheric chemistry. The main atmospheric sink of methane (~90% of the total sink mechanism) is oxidation by the hydroxyl radical (OH), mostly in the troposphere (Ehhalt, 1974). Other losses are by photochemistry in the stratosphere (reactions with chlorine atoms (Cl) and excited atomic oxygen (O(¹D))), oxidation in soils (Curry, 2007; Dutaur and Verchot, 2007), and by photochemistry in the marine boundary layer (reaction with Cl; Allan et al. (2007), Thornton et al. (2010)). Uncertainties in the total sink of methane as estimated by atmospheric chemistry models are in the order of 20-40% (Saunio et al., 2015).

3418 This plant source has not been confirmed in-field however, and although the potential implication for the global CH₄ budget
3419 remains unclear, emissions from this source are certainly much smaller than originally estimated in Keppler et al. (2006)
3420 (Bloom et al., 2010; Fraser et al., 2015). Second, and of clearer significance, plants act as “straws”, drawing up and releasing
3421 microbially produced CH₄ from anoxic soils (Cicerone and Shetter, 1981; Rice et al., 2010). For instance, in the forested
3422 wetlands of Amazonia, tree stems are the dominant ecosystem flux pathway for soil-produced CH₄, therefore, including
3423 stem emissions in ecosystem budgets can reconcile regional bottom-up and top-down estimates (Pangala et al., 2017; Gauci
3424 et al., 2021). Third, the stems of both living trees (Covey et al., 2012) and dead wood (Covey et al., 2016) provide an
3425 environment suitable for microbial methanogenesis. Static chambers demonstrate locally significant through-bark flux from
3426 both soil- (Pangala et al., 2013, 2015), and tree stem-based methanogens (Pitz and Megonigal, 2017; Wang et al., 2016). A
3427 recent synthesis indicates stem CH₄ emissions significantly increase the source strength of forested wetlands, and modestly
3428 decrease the sink strength of upland forests (Covey and Megonigal, 2019). The scientific activity covering CH₄ emissions
3429 in forested ecosystems reveals a far more complex story than previously thought, with an interplay of
3430 productive/consumptive, aerobic/anaerobic, and biotic/abiotic processes occurring between upland/wetland soils, trees, and
3431 atmosphere. Understanding the complex processes that regulate CH₄ source–sink dynamics in forests and estimating their
3432 contribution to the global CH₄ budget requires cross-disciplinary research, more observations, and new models that can
3433 overcome the classical binary classifications of wetland versus upland forest and of emitting versus uptaking soils (Barba et
3434 al., 2019; Covey and Megonigal, 2019). Although we recognize these emissions are potentially large (particularly tree
3435 transport from inundated soil), global estimates for each of these pathways remain highly uncertain and/or are currently
3436 included here within other flux category sources (e.g. inland waters, wetlands, upland soils).

3437 **3.3 Methane sinks and lifetime**

3438 CH₄ is the most abundant reactive trace gas in the troposphere and its reactivity is important to both tropospheric and
3439 stratospheric chemistry. The main atmospheric sink of CH₄ (~90% of the total sink mechanism) is oxidation by the hydroxyl
3440 radical (OH), mostly in the troposphere (Ehhalt, 1974). Other losses are by photochemistry in the stratosphere (reactions
3441 with chlorine atoms (Cl) and excited atomic oxygen (O(¹D))), oxidation in soils (Curry, 2007; Dutaur and Verchot, 2007),
3442 and by photochemistry in the marine boundary layer (reaction with Cl; Allan et al. (2007), Thornton et al. (2010)).
3443 Uncertainties in the total sink of CH₄ as estimated by atmospheric chemistry models are in the order of 20–40% (Saunio et
3444 al., 2016). It is much less (10–20%) when using atmospheric proxy methods (e.g., methyl chloroform, see below) as in
3445 atmospheric inversions (Saunio et al., 2016). In the present release of the global CH₄ budget, we estimate bottom-up
3446 CH₄ chemical sinks and lifetime mainly based on global model results from the Chemistry Climate Model Initiative (CCMI)
3447 2022 activity (Plummer et al., 2021) and CMIP6 simulations (Collins et al., 2017).

3448 **3.3.1 Tropospheric OH oxidation**

3449 OH radicals are produced following the photolysis of ozone (O₃) in the presence of water vapour. OH is destroyed by
 3450 reactions with **carbon monoxide (CO)**, CH₄, and non-methane volatile organic compounds.

3451 Following the Atmospheric Chemistry and Climate Model Intercomparison Project (ACCMIP), which studied the long-term
 3452 changes in atmospheric composition between 1850 and 2100 (Lamarque et al., 2013), a new series of experiments was
 3453 conducted by several chemistry-climate models and chemistry-transport models participating in the Chemistry-Climate
 3454 Model Initiative (CCMI) (Plummer et al., 2021). Mass-weighted OH tropospheric concentrations do not directly represent
 3455 CH₄ loss, as the spatial and vertical distributions of OH affect this loss through, in particular, the temperature dependency
 3456 and the distribution of CH₄ (e.g., Zhao et al., 2019). However, estimating OH concentrations and, spatial and vertical
 3457 distributions is a key step in estimating methane loss through OH. Over the period 2000-2010, the global mass-weighted
 3458 OH tropospheric concentration is estimated at 13.3 [11.7-18.2] x 10⁵ molecules cm⁻³ by 8 CCMI-2022 models and at 11.5
 3459 [7.9-13.5] x 10⁵ molecules cm⁻³ by 10 models contributing CMIP6 (see supplementary Table S4). The ranges calculated
 3460 here are larger than the ones proposed previously in Saunio et al. (2020), where the multi-model mean (11 models) global
 3461 mass-weighted OH tropospheric concentration was 11.7±1.0 x 10⁵ molecules cm⁻³ (range 9.9-14.4 x 10⁵ molecules cm⁻³,
 3462 Zhao et al. (2019)) consistent with the previous estimates from ACCMIP (11.7±1.0 x 10⁵ molecules cm⁻³, with a range of
 3463 10.3-13.4 x 10⁵ molecules cm⁻³, Voulgarakis et al. (2013) for year 2000) and the estimates of Prather et al. (2012) of 11.2±1.3
 3464 x 10⁵ molecules cm⁻³. Nicely et al. (2017) attribute the differences in OH simulated by different chemistry transport models
 3465 to, in decreasing order of importance, different chemical mechanisms, various treatments of the photolysis rate of O₃, and
 3466 modelled O₃ and CO. Besides the uncertainty on global OH concentrations, there is an uncertainty in the spatial and temporal
 3467 distribution of OH. Models often simulate higher OH in the northern hemisphere (NH) than in the southern hemisphere
 3468 (SH), leading to a NH/SH OH ratio greater than 1 (Naik et al., 2013; Zhao et al., 2019). However, there is evidence for
 3469 parity in inter-hemispheric OH concentrations (Patra et al., 2014), which needs to be confirmed by other observational and
 3470 model-derived estimates. The analysis of the latest CCMI (Plummer et al., 2021) and CMIP6 (Collins et al., 2021) model
 3471 outputs show that structural uncertainties in the atmospheric chemistry models remain large, probably due to inherent biases
 3472 in OH precursors. Based on OH precursor observations and a chemical box model, Zhao et al. (2023) corrected the OH 3D
 3473 fields simulated by two atmospheric chemistry models, resulting in tropospheric OH mean concentrations lowered by 2 · 10⁵
 3474 molecules cm⁻³, leading to around 10 x 10⁵ molecules cm⁻³, and a NH/SH OH ratio closer to 1, in better agreement with
 3475 methyl chloroform (MCF)-based approaches. This study highlights the need for further improvement of the atmospheric
 3476 chemistry model.

3477 OH concentrations and their changes can be sensitive to climate variability (Dlugokencky et al., 1996; Holmes et al., 2013;
 3478 Turner et al., 2018), biomass burning (Voulgarakis et al., 2015), and anthropogenic activities. For instance, the increase of
 3479 the oxidizing capacity of the troposphere in South and East Asia associated with increasing NO_x emissions (Mijling et al.,
 3480 2013) and decreasing CO emissions (Yin et al., 2015), possibly enhances CH₄ oxidation and therefore limits the atmospheric

Mis en forme : Police :Gras, Couleur de police : Noir

Mis en forme : Police :Gras, Couleur de police : Noir

Mis en forme : Normal, Espace Avant : 12 pt, Après : 12 pt, Paragraphes solitaires, Bordure : Haut: (Pas de bordure), Bas: (Pas de bordure), Gauche: (Pas de bordure), Droite: (Pas de bordure), Entre : (Pas de bordure)

Supprimé:

Supprimé :

Supprimé: Following the Atmospheric Chemistry and Climate Model Intercomparison Project (ACCMIP), which studied the long-term changes in atmospheric composition between 1850 and 2100 (Lamarque et al., 2013), a new series of experiments was conducted by several chemistry-climate models and chemistry-transport models participating in the Chemistry-Climate Model Initiative (CCMI) (Morgenstern et al., 2017). Mass-weighted OH tropospheric concentrations do not directly represent methane loss, as the spatial and vertical distributions of OH affect this loss, through, in particular, the temperature dependency and the distribution of methane (e.g. Zhao et al., 2019). However, estimating OH concentrations and, spatial and vertical distributions is a key step in estimating methane loss through OH. Over the period 2000-2010, the multi-model mean (11 models) global mass-weighted OH tropospheric concentration was 11.7±1.0 x 10⁵ molecules cm⁻³ (range 9.9-14.4 x 10⁵ molecules cm⁻³, Zhao et al. (2019)) consistent with the previous estimates from ACCMIP (11.7±1.0 x 10⁵ molecules cm⁻³, with a range of 10.3-13.4 x 10⁵ molecules cm⁻³, Voulgarakis et al. (2013) for year 2000) and the estimates of Prather et al. (2012) at 11.2±1.3 x 10⁵ molecules cm⁻³. Nicely et al. (2017) attribute the differences in OH simulated by different chemistry transport models to, in decreasing order of importance, different chemical mechanisms, various treatment of the photolysis rate of ozone, and modeled ozone and carbon monoxide. Besides the uncertainty on global OH concentrations, there is an uncertainty in the spatial and temporal distribution of OH. Models often simulate higher OH in the northern hemisphere leading to a NH/SH OH ratio greater than 1 (Naik et al., 2013; Zhao et al., 2019). However, there is evidence for parity in inter-hemispheric OH concentrations (Patra et al., 2014), which needs to be confirmed by other observational and model-derived estimates. OH concentrations and their changes can be sensitive to climate variability (Dlugokencky et al., 1996; Holmes et al., 2013; Turner et al., 2018), biomass burning (Voulgarakis et al., 2015), and anthropogenic activities. For instance, the increase of the oxidizing capacity of the troposphere in South and East Asia associated with increasing NO_x emissions (Mijling et al., 2013) and decreasing CO emissions (Yin et al., 2015), possibly enhances CH₄ oxidation and therefore limits the atmospheric impact of increasing emissions (Dalsoren et al., 2009). Despite such large regional changes, the global mean OH concentration was suggested to have changed only slightly over the past 150 years (Naik et al., 2013). This is due to the compensating effects of the concurrent increases of positive influences on OH (water vapour, tropospheric ozone, nitrogen oxides (NO_x) emissions, and UV radiation due to decreasing stratospheric ozone), and of OH sinks (methane burden, carbon monoxide and non-methane volatile organic compound emissions and burden). CCMI models show OH inter-annual variability ranging from 0.4% to 1.8% (Zhao et al., 2019) over 2000-2010, lower than the value deduced from methyl chloroform measurements (proxy, top-down approach). However, these simulations consider meteorology variability but not emission interannual variability (e.g., from biomass burning) and

3599 impact of increasing emissions (Dalsøren et al., 2009). Despite such large regional changes, the global mean OH
3600 concentration was suggested to have changed only slightly over the past 150 years (Naik et al., 2013). This is due to the
3601 compensating effects of the concurrent increases of positive influences on OH (water vapour, tropospheric ozone, nitrogen
3602 oxides (NO_x) emissions, and UV radiation due to decreasing stratospheric O₃), and of OH sinks (CH₄ burden, CO and non-
3603 CH₄ volatile organic compound emissions and burden). CCMI models show OH inter-annual variability ranging from 0.4%
3604 to 1.8% (Zhao et al., 2019) over 2000-2010 (similar values are derived in the latest CCMI and CMIP6 activities - see
3605 supplementary Table S4), lower than the value deduced from methyl chloroform measurements (proxy, top-down approach).
3606 However, these simulations consider meteorology variability but not emission interannual variability (e.g., from biomass
3607 burning) and thus are expected to simulate lower OH inter annual variability than in reality. Using an empirical model
3608 constrained by global observations of O₃, water vapour, CH₄, and temperature as well as the simulated effects of changing
3609 NO_x emissions and tropical expansion, Nicely et al. (2017) found an inter-annual variability in OH of about 1.3-1.6%
3610 between 1980 and 2015, in agreement with methyl chloroform based estimates (Montzka et al., 2011).
3611 Over 2000-2009, the tropospheric loss (tropopause height at 200 hPa) of CH₄ by OH oxidation derived from the ten and
3612 CCMI modelling activities (see supplementary Table S5) is estimated at of 546 [446-663] Tg CH₄ yr⁻¹, which is similar to
3613 the one reported previously in Saunois et al. (2020) from CCMI model (553 [476-677] Tg CH₄ yr⁻¹) and still slightly higher
3614 than the one from the ACCMIP models (528 [454-617] Tg CH₄ yr⁻¹ reported in Kirschke et al. (2013) and Saunois et al.
3615 (2016).
3616 For the recent 2010-2019 decade, we report a climatological value based on five models that contributed to CMIP6 runs
3617 (historic followed by SSP3-7.0 projections starting in 2015, Collins et al. (2021)) to acknowledge the impact of the rise in
3618 atmospheric methane on the methane chemical sink. Hence, for 2010-2019, we report the climatological value of 563 [510-
3619 663] Tg CH₄ yr⁻¹

3.3.2 Stratospheric loss

3621 In the stratosphere, CH₄ is lost through reactions with excited atomic oxygen O(¹D), atomic chlorine (Cl), atomic fluorine
3622 (F), and OH (Brasseur and Solomon, 2005; le Texier et al., 1988). Uncertainties in the chemical loss of stratospheric CH₄ are
3623 large, due to uncertain inter-annual variability in stratospheric transport as well as its chemical interactions and feedbacks
3624 with stratospheric O₃ (Portmann et al., 2012). Particularly, the fraction of stratospheric loss due to the different oxidants is
3625 still uncertain, with possibly 20-35% due to halons, about 25% due to O(¹D) mostly in the high stratosphere and the rest due
3626 to stratospheric OH (McCarthy et al., 2003).

3627 In this study, ten chemistry climate models that contributed to CMIP6 and CCMI modelling activities (Table S5) are used
3628 to provide estimates of CH₄ chemical loss, including reactions with OH, O(¹D), and Cl; CH₄ photolysis is also included but
3629 occurs only above the stratosphere. Considering a 200 hPa tropopause height, the CMIP6 and CCMI results suggest an

Mis en forme : Police :Gras, Couleur de police : Noir

Mis en forme : Normal, Espace Avant : 12 pt, Après : 12 pt, Paragraphes solidaires, Bordure : Haut: (Pas de bordure), Bas: (Pas de bordure), Gauche: (Pas de bordure), Droite: (Pas de bordure), Entre : (Pas de bordure)

Supprimé: In the stratosphere, CH₄ is lost through reactions with excited atomic oxygen O(¹D), atomic chlorine (Cl), atomic fluorine (F), and OH (Brasseur and Solomon, 2005; le Texier et al., 1988). Uncertainties in the chemical loss of stratospheric methane are large, due to uncertain inter-annual variability in stratospheric transport as well as its chemical interactions and feedbacks with stratospheric ozone (Portmann et al., 2012). Particularly, the fraction of stratospheric loss due to the different oxidants is still uncertain, with possibly 20-35% due to halons, about 25% due to O(¹D) mostly in the high stratosphere and the rest due to stratospheric OH (McCarthy et al., 2003).⁴
In this study, seven chemistry climate models from the CCMI project (Table S4) are used to provide estimates of methane chemical loss, including reactions with OH, O(¹D), and Cl; CH₄ photolysis is also included but occurs only above the stratosphere. Considering a 200 hPa tropopause height, the CCMI models suggest an estimate of 31 [12-37] Tg CH₄ yr⁻¹ for the methane stratospheric sink for the period 2000-2010 (Table S4). The 20 Tg difference compared to the mean value reported by Kirschke et al. (2013) and Saunois et al. (2016) for the same period (51 [16-84] Tg CH₄ yr⁻¹), is probably due to the plausible double-counting of O(¹D) and Cl oxidations in our previous calculation, as the chemistry-climate models usually report the total chemical loss of methane (not OH oxidation only).⁴
We

3654 estimate of 34 [10-51]Tg CH₄ yr⁻¹ for the CH₄ stratospheric sink for the 2000-2009 decade (Table S5), similar to the value
3655 derived from the previous CCMI activity reported in Saunois et al. (2020) (31 [12-41] Tg CH₄ yr⁻¹).
3656 For 2010-2019, we report here a climatological range of 1-43 Tg CH₄ yr⁻¹ associated with a mean value of 33 Tg CH₄ yr⁻¹
3657 based on five models that contributed to CMIP6 runs (historic followed by SSP3-7.0 projections starting in 2015; Table S5).

3.3.3 Tropospheric reaction with Cl

3659 Halogen atoms can also contribute to the oxidation of CH₄ in the troposphere. Allan et al. (2005) measured mixing ratios of
3660 methane and δ¹³C-CH₄ at two stations in the southern hemisphere from 1991 to 2003, and found that the apparent kinetic
3661 isotope effect (KIE) of the atmospheric CH₄ sink was significantly larger than that explained by OH alone. A seasonally
3662 varying sink due to Cl in the marine boundary layer of between 13 and 37 Tg CH₄ yr⁻¹ was proposed as the explanatory
3663 mechanism (Allan et al., 2007; Platt et al., 2004). This sink was estimated to occur mainly over coastal and marine regions,
3664 where sodium chloride (NaCl) from evaporated droplets of seawater react with NO₂ to eventually form Cl₂, which then UV-
3665 dissociates to Cl. However significant production of nitryl chloride (ClNO₂) at continental sites has been recently reported
3666 (Riedel et al., 2014) and suggests the broader presence of Cl, which in turn would expand the significance of the Cl sink in
3667 the troposphere. Recently, Hossaini et al. (2016), Sherwen et al. (2016), and Wang et al. (2019b, 2021b) have made
3668 significant improvements in tropospheric chemistry modelling and they conclude to an oxidation contribution of 2.6%, 2%,
3669 1% and 0.8%, respectively. These values correspond to a tropospheric CH₄ loss of around 12-13 Tg CH₄ yr⁻¹, 9 Tg CH₄ yr⁻¹,
3670 5 Tg yr⁻¹, and 3 Tg CH₄ yr⁻¹ respectively, much lower than the first estimates by Allan et al. (2007). The recent work of
3671 Wang et al. (2021b) is the most comprehensive modelling study and based upon Sherwen et al. (2016) and Wang et al.
3672 (2019b). Both the KIE approach and chemistry transport model simulations carry uncertainties (extrapolations based on
3673 only a few sites and use of indirect measurements, for the former and missing sources, coarse resolution, underestimation
3674 of some anthropogenic sources for the latter). However, Gromov et al. (2018) found that Cl can contribute only 0.23% the
3675 tropospheric sink of CH₄ (about 1 Tg CH₄ yr⁻¹) in order to balance the global ¹³C(CO) budget (see their Table S1). While
3676 tropospheric Cl has a marginal impact on the total CH₄ sink (few percents), it influences more significantly the atmospheric
3677 isotopic δ¹³C-CH₄ signal and improved estimates of the tropospheric Cl amount should be used for isotopic CH₄ modelling
3678 studies (Strode et al., 2020; Thanwerdas et al., 2022b).
3679 Each recent Cl estimate suggests a reduced contribution to the methane loss than previously reported by Allen et al. (2007).
3680 As a result, we suggest here to use the mean, minimum and maximum of the last five estimates published since 2016, leading
3681 to a climatological value of 6 [-13] Tg CH₄ yr⁻¹, thus reducing both the magnitude and the uncertainty range compared to
3682 Saunois et al. (2020).

Supprimé: 12-37

Supprimé: to

Supprimé: 31

Mis en forme : Police :Gras, Couleur de police : Noir

Mis en forme : Normal, Espace Avant : 12 pt, Après : 12 pt, Paragraphes solidaires, Bordure : Haut: (Pas de bordure), Bas: (Pas de bordure), Gauche: (Pas de bordure), Droite: (Pas de bordure), Entre : (Pas de bordure)

Supprimé: Halogen atoms can also contribute to the oxidation of methane in the troposphere. Allan et al. (2005) measured mixing ratios of methane and δ¹³C-CH₄ at two stations in the southern hemisphere from 1991 to 2003, and found that the apparent kinetic isotope effect (KIE) of the atmospheric methane sink was significantly larger than that explained by OH alone. A seasonally varying sink due to atomic chlorine (Cl) in the marine boundary layer of between 13 and 37 Tg CH₄ yr⁻¹ was proposed as the explanatory mechanism (Allan et al., 2007; Platt et al., 2004). This sink was estimated to occur mainly over coastal and marine regions, where NaCl from evaporated droplets of seawater react with NO₂ to eventually form Cl₂, which then UV-dissociates to Cl. However significant production of nitryl chloride (ClNO₂) at continental sites has been recently reported (Riedel et al., 2014) and suggests the broader presence of Cl, which in turn would expand the significance of the Cl sink in the troposphere. Recently, using a chemistry transport model, Hossaini et al. (2016) suggest a chlorine sink in the lower range of Allan et al. (2007), ~12-13 Tg CH₄ yr⁻¹ (about 2.5 % of the tropospheric sink). They also estimate that ClNO₂ yields a 1 Tg yr⁻¹ sink of methane. Another modelling study (Wang et al., 2019b) produced a more comprehensive analysis of global tropospheric chlorine chemistry and found a chlorine sink of 5 Tg yr⁻¹, representing only 1% of the total methane tropospheric sink. Both the KIE approach and chemistry transport model simulations carry uncertainties (extrapolations based on only a few sites and use of indirect measurements, for the former; missing sources, coarse resolution, underestimation of some anthropogenic sources for the latter). However, Gromov et al. (2018) found that chlorine can contribute only 0.23% the tropospheric sink of methane (about 1 Tg CH₄ yr⁻¹) in order to balance the global ¹³C(CO) budget. Awaiting further work to better assess the magnitude of the chlorine sink in the methane budget, we suggest a lower estimate but a larger range than in Saunois et al. (2016) and used the following climatological value for the 2000s: 11 [-13] Tg CH₄ yr⁻¹.

3.3.4 Soil uptake

Unsaturated oxic soils are sinks of atmospheric CH₄ due to the presence of methanotrophic bacteria, which consume CH₄ as a source of energy. Dutaur and Verchot (2007) conducted a comprehensive meta-analysis of field measurements of CH₄ uptake spanning a variety of ecosystems. Extrapolating to the global scale, they reported a range of 36 ± 23 Tg CH₄ yr⁻¹, but also showed that stratifying the results by climatic zone, ecosystem, and soil type led to a narrower range (and lower mean estimate) of 22 ± 12 Tg CH₄ yr⁻¹. Modelling studies, employing meteorological data as external forcing, have also produced a considerable range of estimates. Using a soil depth-averaged formulation based on Fick's law with parameterizations for diffusion and biological oxidation of CH₄, Ridgwell et al. (1999) estimated the global sink strength at 38 Tg CH₄ yr⁻¹, with a range 20-51 Tg CH₄ yr⁻¹ reflecting the model structural uncertainty in the base oxidation parameter. Curry (2007) improved on the latter by employing an exact solution of the one-dimensional diffusion-reaction equation in the near-surface soil layer (i.e., exponential decrease in CH₄ concentration below the surface), a land surface hydrology model, and calibration of the oxidation rate to field measurements. This resulted in a global estimate of 28 Tg CH₄ yr⁻¹ (9-47 Tg CH₄ yr⁻¹), the result reported by Zhuang et al. (2013), Kirschke et al. (2013) and Saunio et al. (2016). Ito and Inatomi (2012) used an ensemble methodology to explore the variation in estimates produced by these parameterizations and others, which spanned the range 25-35 Tg CH₄ yr⁻¹. For the period 2000-2020, as part of the wetland emissions modelling activity, JSBACH (Kleinen et al., 2020) and VISIT (Ito and Inatomi, 2012) models compute a global CH₄ soil uptake to 18 and 35 Tg CH₄ yr⁻¹, respectively. Murguia-Flores et al. (2018) further refined the Curry (2007) model's structural and parametric representations of key drivers of soil methanotrophy, demonstrating good agreement with the observed latitudinal distribution of soil uptake (Dutaur and Verchot, 2007). Their model (MeMo) simulates a CH₄ soil sink of 37.5 Tg CH₄ yr⁻¹ for the period 2010-2019 (Fig. S4), compared to 39.5 and 31.3 Tg CH₄ yr⁻¹ using the Ridgwell et al. (1999) and Curry (2007) parameterizations, respectively, under the same meteorological forcing, run specifically for this study. For the 2000s period, the simulations estimate the soil uptake at 30.4, 36.7 and 38.3 Tg CH₄ yr⁻¹ based on the parameterization of Curry, MeMo, and Ridgwell, respectively. As part of a more comprehensive model accounting for a range of CH₄ sources and sinks, Tian et al. (2010, 2015, 2016) computed vertically-averaged CH₄ soil uptake including the additional mechanisms of aqueous diffusion and plant-mediated (*aerenchyma*) transport, arriving at the estimate 30±19 Tg CH₄ yr⁻¹ (Tian et al., 2016) for the 2000s. The still more comprehensive biogeochemical model of Riley et al. (2011) included vertically resolved representations of the same processes considered by Tian et al. (2016), in addition to grid cell fractional inundation and, importantly, the joint limitation of uptake by both CH₄ and O₂ availability in the soil column. Riley et al. (2011) estimated a global CH₄ soil sink of 31 Tg CH₄ yr⁻¹ with a structural uncertainty of 15-38 Tg CH₄ yr⁻¹ (a higher upper limit resulted from an elevated gas diffusivity to mimic convective transport; as this is not usually considered, we adopt the lower upper bound associated with no limitation of uptake at low soil moisture). A model of this degree of complexity is required to explicitly simulate situations where the soil water content increases enough to inhibit the diffusion of oxygen, and the soil becomes a methane source

Mis en forme : Police :Gras, Couleur de police : Noir

Mis en forme : Normal, Espace Avant : 12 pt, Après : 12 pt, Paragraphes solidaires, Bordure : Haut: (Pas de bordure), Bas: (Pas de bordure), Gauche: (Pas de bordure), Droite: (Pas de bordure), Entre : (Pas de bordure)

Supprimé: Unsaturated oxic soils are sinks of atmospheric methane due to the presence of methanotrophic bacteria, which consume methane as a source of energy. Dutaur and Verchot (2007) conducted a comprehensive meta-analysis of field measurements of CH₄ uptake spanning a variety of ecosystems. Extrapolating to the global scale, they reported a range of 36 ± 23 Tg CH₄ yr⁻¹, but also showed that stratifying the results by climatic zone, ecosystem and soil type led to a narrower range (and lower mean estimate) of 22 ± 12 Tg CH₄ yr⁻¹. Modelling studies, employing meteorological data as external forcing, have also produced a considerable range of estimates. Using a soil depth-averaged formulation based on Fick's law with parameterizations for diffusion and biological oxidation of CH₄, Ridgwell et al. (1999) estimated the global sink strength at 38 Tg CH₄ yr⁻¹, with a range 20-51 Tg CH₄ yr⁻¹ reflecting the model structural uncertainty in the base oxidation parameter. Curry (2007) improved on the latter by employing an exact solution of the one-dimensional diffusion-reaction equation in the near-surface soil layer (i.e., exponential decrease in CH₄ concentration below the surface), a land surface hydrology model, and calibration of the oxidation rate to field measurements. This resulted in a global estimate of 28 Tg CH₄ yr⁻¹ (9-47 Tg CH₄ yr⁻¹), the result reported by Zhuang et al. (2013), Kirschke et al. (2013) and Saunio et al. (2016). Ito and Inatomi (2012) used an ensemble methodology to explore the variation in estimates produced by these parameterizations and others, which spanned the range 25-35 Tg CH₄ yr⁻¹. Murguia-Flores et al. (2018) further refined the Curry (2007) model's structural and parametric representations of key drivers of soil methanotrophy, demonstrating good agreement with the observed latitudinal distribution of soil uptake (Dutaur and Verchot, 2007). Their model simulated a methane soil sink of 32 Tg CH₄ yr⁻¹ for the period 2000-2017 (Fig. 4), compared to 38 and 29 Tg CH₄ yr⁻¹ using the Ridgwell et al. (1999) and Curry (2007) parameterizations, respectively, under the same meteorological forcing. As part of a more comprehensive model accounting for a range of methane sources and sinks, Tian et al. (2010, 2015, 2016) computed vertically-averaged CH₄ soil uptake including the additional mechanisms of aqueous diffusion and plant-mediated (*aerenchyma*) transport, arriving at the estimate 30±19 Tg CH₄ yr⁻¹ (Tian et al., 2016). The still more comprehensive biogeochemical model of Riley et al. (2011) included vertically resolved representations of the same processes considered by Tian et al. (2016), in addition to grid cell fractional inundation and, importantly, the joint limitation of uptake by both CH₄ and O₂ availability in the soil column. Riley et al. (2011) estimated a global CH₄ soil sink of 31 Tg CH₄ yr⁻¹ with a structural uncertainty of 15-38 Tg CH₄ yr⁻¹ (a higher upper limit resulted from an elevated gas diffusivity to mimic convective transport; as this is not usually considered, we adopt the lower upper bound associated with no limitation of uptake at low soil moisture). A model of this degree of complexity is required to explicitly simulate situations where the soil water content increases enough to inhibit the diffusion of oxygen, and the soil becomes a methane source (Lohila et al., 2016). This transition can be rapid, thus creating areas (for example, seasonal wetlands) that can be either a source or a sink of methane depending on the season. †
The previous Curry (2007) estimate can be revised upward based on subsequent work and the increase in CH₄ concentration since 1940. †

3870 (Lohila et al., 2016). This transition can be rapid, thus creating areas (for example, seasonal wetlands) that can be either
3871 source or a sink of methane depending on the season.
3872 The previous Curry (2007) estimate can be revised upward slightly based on subsequent work and the increase in CH₄
3873 concentration since that time. Considering the latest estimates (based on VISIT, JSBACH, and Memo models, Table S6 in
3874 the supplementary) we report here a mean estimate of 31 [17-39] Tg CH₄ yr⁻¹ for 2000-2009 and 32 [18-40] for 2010-2019
3875 Tg CH₄ yr⁻¹.

3.3.5 CH₄ lifetime

3877 The atmospheric lifetime of a given gas in steady state may be defined as the global atmospheric burden (Tg) divided by the
3878 total sink (Tg yr⁻¹) (IPCC, 2001). Global models provide an estimate of the loss of the gas due to individual sinks, which
3879 can then be used to derive lifetime due to a specific sink. For example, the tropospheric lifetime of CH₄ is determined as the
3880 global atmospheric CH₄ burden divided by the loss from OH oxidation in the troposphere, sometimes called “chemical
3881 lifetime”. The total lifetime of CH₄ corresponds to the global burden divided by the total loss including tropospheric loss
3882 from OH oxidation, stratospheric chemistry and soil uptake. The CCMI (Plummer et al., 2021) and CMIP6 (Collins et al.,
3883 2021) runs estimate the tropospheric methane lifetime at about 9.2 years (average over years 2000-2009), with a range of
3884 7.5-11 years (see Table S5). This range agrees with previous values found in ACCMIP and CCMI (9.3 [7.1-10.6] years,
3885 Voulgarakis et al. (2013), 9 [7.2-10.1] years, Saunio et al. (2020)). Adding 31 Tg to account for the soil uptake to the total
3886 chemical loss of the CMIP6 and CCMI models, we derive a total CH₄ lifetime of 8.2 years (average over 2000-2009 with a
3887 range of 6.8-9.7 years). The lifetime calculated over 2010-2019 based on CMIP6 simulations is similar (Table S5). These
3888 updated model estimates of total CH₄ lifetime agree with the previous estimates from ACCMIP (8.2 [6.4-9.2] years for year
3889 2000, Voulgarakis et al. (2013)) and Saunio et al. (2020) based CCMI models. Reducing the large spread in CH₄ lifetime
3890 (between models, and between models and observation-based estimates) would 1) bring an improved constraint on global
3891 total methane emissions, and 2) ensure an accurate forecast of future climate.

4 Atmospheric observations and top-down inversions

4.1 Atmospheric observations

3894 Systematic atmospheric CH₄ observations began in 1978 (Blake et al., 1982) with infrequent measurements from discrete
3895 air samples collected in the Pacific at a range of latitudes from 67°N to 53°S. Because most of these air samples were from
3896 well-mixed oceanic air masses and the measurement technique was precise and accurate, they were sufficient to establish
3897 an increasing trend and the first indication of the latitudinal gradient of methane. Spatial and temporal coverage was greatly
3898 improved soon after (Blake and Rowland, 1986) with the addition of the Earth System Research Laboratory from US
3899 National Oceanic and Atmospheric Administration (NOAA/GML) flask network (Steele et al. (1987); Lan et al. (2024), Fig.

Mis en forme : Police :Gras, Couleur de police : Noir

Mis en forme : Normal, Espace Avant : 12 pt, Après : 12 pt, Paragraphes solidaires, Bordure : Haut: (Pas de bordure), Bas: (Pas de bordure), Gauche: (Pas de bordure), Droite: (Pas de bordure), Entre : (Pas de bordure)

Supprimé: The atmospheric lifetime of a given gas in steady state may be defined as the global atmospheric burden (Tg) divided by the total sink (Tg/yr) (IPCC, 2001). Global models provide an estimate of the loss of the gas due to individual sinks, which can then be used to derive lifetime due to a specific sink. For example, methane's tropospheric lifetime is determined as global atmospheric methane burden divided by the loss from OH oxidation in the troposphere, sometimes called “chemical lifetime”. Methane total lifetime corresponds to the global burden divided by the total loss including tropospheric loss from OH oxidation, stratospheric chemistry and soil uptake. The CCMI models (described in Morgenstein et al. (2017)) estimate the tropospheric methane lifetime at about 9 years (average over years 2000-2009), with a range of 7.2-10.1 years (see Table S4). While this range agrees with previous values found in ACCMIP (9.3 [7.1-10.6] years, Voulgarakis et al. (2013)), the mean value reported here is lower than previously reported, probably due to a smaller and different ensemble of climate models. Adding 30 Tg to account for the soil uptake to the total chemical loss of the CCMI models, we derive a total methane lifetime of 7.8 years (average over 2000-2009 with a range of 6.5-8.8 years). These updated model estimates of total methane lifetime agree with the previous estimates from ACCMIP (8.2 [6.4-9.2] years for year 2000, Voulgarakis et al. (2013)). Reducing the large spread in methane lifetime (between models, and between models and observation-based estimates) would 1) bring an improved constraint on global total methane emissions, and 2) ensure an accurate forecast of future climate.†

4 Atmospheric observations and top-down inversions†

4.1 Atmospheric observations†

Systematic atmospheric CH₄ observations began in 1978 (Blake et al., 1982) with infrequent measurements from discrete air samples collected in the Pacific at a range of latitudes from 67°N to 53°S. Because most of these air samples were from well-mixed oceanic air masses and the measurement technique was precise and accurate, they were sufficient to establish an increasing trend and the first indication of the latitudinal gradient of methane. Spatial and temporal coverage was greatly improved soon after (Blake and Rowland, 1986) with the addition of the Earth System Research Laboratory from US National Oceanic and Atmospheric Administration (NOAA/ESRL) flask network (Steele et al. (1987), Fig. 1), and of the Advanced Global Atmospheric Gases Experiment (AGAGE) (Cunnold et al., 2002; Prinn et al., 2000), the Commonwealth Scientific and Industrial Research Organisation (CSIRO, Francey et al. (1999)), the University of California Irvine (UCI, Simpson et al. (2012)) and in situ and flask measurements from regional networks, such as ICOS (Integrated Carbon Observation System) network in Europe (<https://www.icos-ri.eu/>). The combined datasets provide the longest time series of globally averaged CH₄ abundance. Since the early-2000s, CH₄ column-averaged mole fractions have been retrieved through passive remote sensing from space (Buchwitz et al., 2005a, 2005b; Butz et al., 2011; Crevoisier et al., 2009; Frankenberg et al., 2005; Hu et al., 2018). Ground-based Fourier transform infrared (FTIR) measurements at fixed locations also provide time-resolved methane column observations during daylight hours, and a validation dataset against which to evaluate the satellite measurements such as TCCON network (e.g. Pollard et al., 2011, 2014).

1), and the Advanced Global Atmospheric Gases Experiment (AGAGE) (Cunnold et al., 2002; Prinn et al., 2018), the Commonwealth Scientific and Industrial Research Organisation (CSIRO, Francey et al. (1999)), the University of California Irvine (UCI, Simpson et al., 2012) and in situ and flask measurements from regional networks, such as ICOS (Integrated Carbon Observation System) in Europe (<https://www.icos-ri.eu/>). The combined datasets provide the longest time series of globally averaged CH₄ abundances. Since the early-2000s, CH₄ column-averaged mole fractions have been retrieved through passive remote sensing from space (Buchwitz et al., 2005a, 2005b; Butz et al., 2011; Crevoisier et al., 2009; Frankenberg et al., 2005; Hu et al., 2018). Ground-based Fourier transform infrared (FTIR) measurements at fixed locations also provide time-resolved CH₄ column observations during daylight hours, and a validation dataset against which to evaluate the satellite measurements such as the Total Carbon Column Observing Network (TCCON) network (e.g., Pollard et al., 2017; Wunch et al., 2011), or Network for Detection of Atmospheric Composition Change (NDACC) (e.g., Bader et al., 2017).

In this budget, in-situ observations from the different networks were used in the top-down atmospheric inversions to estimate CH₄ sources and sinks over the period 2000-2020. Satellite observations from the TANSO/FTS instrument on board the satellite GOSAT were used to estimate CH₄ sources and sinks over the period 2010-2020. Other atmospheric data (FTIR, airborne measurements, AirCore, isotopic measurements, etc.) have been used for validation by some groups, but not specifically in this study. However, further information is provided in Tables S7, S8, S9, S10, and S11 and a more comprehensive validation of the inversions is planned to use some of these data.

4.1.1 In situ CH₄ observations and atmospheric growth rate at the surface

We use globally averaged CH₄ mole fractions at the Earth's surface from the four observational networks (NOAA/GML, AGAGE, CSIRO and UCI). The data are archived at the World Data Centre for Greenhouse Gases (WDCGG) of the WMO Global Atmospheric Watch (WMO-GAW) program (<https://gaw.kishou.go.jp/>), including measurements from other sites that are not operated as part of the four networks. The CH₄ in-situ monitoring network has grown significantly over the last decade due to the emergence of laser diode spectrometers which are robust and accurate enough to allow deployments with low maintenance enabling the development of denser networks in developed countries (Stanley et al., 2018; Yver Kwok et al., 2015), and new stations in remote environments (Bian et al., 2015; Nisbet et al., 2019).

The networks differ in their sampling strategies, including the frequency of observations, spatial distribution, and methods of calculating globally averaged CH₄ mole fractions. Details are given in the supplementary material of Kirschke et al. (2013). The global average values of CH₄ abundances at Earth's surface presented in Fig. 1 are computed using long-term measurements from background conditions with minimal influence from immediate emissions. All measurements are calibrated against gas standards either on the current WMO reference scale or on independent scales with well-estimate differences from the WMO scale. The current WMO reference scale, maintained by NOAA/ESRL, WMO-X2004A (Dlugokencky et al., 2005) was updated in July 2015. NOAA and CSIRO global means are on this scale. AGAGE uses an independent standard scale (based on work by Tohoku University (Aoki et al., 1992) and maintained at Scripps Institution

Supprimé: methane

Supprimé: 2017

Supprimé: methane

Supprimé: 2009-2017

Supprimé: ...)

Supprimé: the Supplementary Material

Mis en forme : Police :Gras, Couleur de police : Noir

Mis en forme : Normal, Espace Avant : 12 pt, Après : 12 pt, Paragraphes solidaires, Bordure : Haut: (Pas de bordure), Bas: (Pas de bordure), Gauche: (Pas de bordure), Droite: (Pas de bordure), Entre : (Pas de bordure)

Supprimé: ESRL, AGAGE, CSIRO and UCI). The data are archived at the World Data Centre for Greenhouse Gases (WDCGG) of the WMO Global Atmospheric Watch (WMO-GAW) program, including measurements from other sites that are not operated as part of the four networks. The CH₄ in-situ monitoring network has grown significantly over the last decade due to the emergence of laser diode spectrometers which are robust and accurate enough to allow deployments with minimal maintenance enabling the development of denser networks in developed countries (Stanley et al., 2018; Yver Kwok et al., 2015), and new stations in remote environment (Bian et al., 2015; Nisbet et al., 2019).

Mis en forme : Anglais (G.B.)

Supprimé: The networks differ in their sampling strategies, including the frequency of observations, spatial distribution, and methods of calculating globally averaged CH₄ mole fractions. Details are given in the supplementary material of Kirschke et al. (2013). The global average values of CH₄ concentrations presented in Fig. 1 are computed using long-time series measurements through gas chromatography with flame ionization detection (GC/FID), although chromatographic schemes vary among the labs. Because GC/FID is a relative measurement method, the instrument response must be calibrated against standards. The current WMO reference scale, maintained by NOAA/ESRL, WMO-X2004A (Dlugokencky et al., 2005) was updated in July 2015. NOAA and CSIRO global means are on this scale. AGAGE uses an independent standard scale maintained by Tohoku University (Aoki et al., 1992), but direct comparisons of standards and indirect comparisons of atmospheric measurements show that differences are below 5 ppb (Tans and Zwellberg, 2014; Vardag et al., 2014). UCI uses another independent scale that was established in 1978 and is traceable to NIST (Flores et al., 2015; Simpson et al., 2012), but has not been included in standard exchanges with other networks so differences with the other networks cannot be quantitatively defined. Additional experimental details are presented in the supplementary material from Kirschke et al. (2013) and references therein.

4084 of Oceanography (SIO)), but direct comparisons of standards and indirect comparisons of atmospheric measurements show
 4085 that differences are well below 5 ppb (Tans and Zwellberg, 2014; Vardag et al., 2014) and the TU-1987 scale used for
 4086 AGAGE measurements is only 0.5 ppb difference from WMO-X2004A at 1900 ppb level. UCI uses another independent
 4087 scale that was established in 1978 and is traceable to NIST (Flores et al., 2015; Simpson et al., 2012), but has not been
 4088 included in standard exchanges with other networks so differences with the other networks cannot be quantitatively defined.
 4089 Additional experimental details are presented in the supplementary material from Kirschke et al. (2013) and references
 4090 therein.

4091 In Fig. 1, (a) globally averaged CH₄ and (b) its growth rate (derivative of the deseasonalized trend curve) through to 2022
 4092 are plotted for the four measurement programs using a procedure of signal decomposition described in Thoning et al. (1989).
 4093 We define the annual G_{ATM} as the increase in the atmospheric concentrations from Jan. 1 in one year to Jan. 1 in the next
 4094 year. Agreement among the four networks is good for the global growth rate, especially since ~1990. The large differences
 4095 observed mainly before 1990 probably reflect the different spatial coverage of each network. The long-term behaviour of
 4096 globally averaged atmospheric CH₄ shows a positive growth rate (defined as the derivative of the deseasonalized mixing
 4097 ratio) that is slowing down from the early-1980s through 1998, a near-stabilisation of CH₄ concentrations from 1999 to
 4098 2006, and a renewed period with positive persistent overall accelerating growth rates since 2007, slightly larger after 2014.
 4099 When a constant atmospheric lifetime is assumed, the decreasing growth rate from 1983 through 2006 may imply that
 4100 atmospheric CH₄ was approaching steady state, leading to no trend in emissions. The NOAA global mean CH₄ concentration
 4101 was fitted with a function that describes the approach to a first-order steady state (ss index): $[CH_4](t) = [CH_4]_{ss} - ([CH_4]_{ss} - [CH_4]_0)e^{-t/\tau}$;
 4102 solving for the lifetime, τ , gives 9.3 years, which is very close to current literature values (e.g., Prather et al.
 4103 (2012), 9.1 ± 0.9 years). Such an approach includes uncertainties, especially due to the strong assumption of no trend in
 4104 lifetime. The result of constant emissions does not agree with some study explaining the stabilisation period by decreasing
 4105 emissions associated with increasing sink (e.g., Bousquet et al., 2006). However, this value seems consistent albeit higher
 4106 than the chemistry climate estimates (8.2 years, see Sect. 3.3.5)
 4107 From 1999 to 2006, the annual increase of atmospheric CH₄ was remarkably small at 0.6±0.1 ppb yr⁻¹. After 2006, the
 4108 atmospheric growth rate has increased to a level similar to that of the mid-1990s (~5 ppb yr⁻¹), and for 2014 and 2015 even
 4109 to that of the 1980s (>10 ppb yr⁻¹). In the two recent years 2020 and 2021, the highest growth rates of 15 ppb yr⁻¹ and 18
 4110 ppb yr⁻¹ (see Sect. 6) were unprecedented since the 1980s. On decadal timescales, the annual increase is on average 2.2±0.3
 4111 ppb yr⁻¹ for 2000-2009, 7.6±0.3 ppb yr⁻¹ for 2010-2019 and 15.2±0.4 ppb yr⁻¹ for the year 2020.

4.1.2 Satellite data of column average CH₄

4113 In this budget, we use satellite data from the JAXA satellite Greenhouse Gases Observing SATellite (GOSAT) launched in
 4114 January 2009 (Butz et al., 2011; Morino et al., 2011) containing the TANSO-FTS instrument, which observes in the
 4115 shortwave infrared (SWIR). Different retrievals of CH₄ based on TANSO-FTS/GOSAT products are made available to the

Supprimé : ,

Supprimé : 2017

Supprimé : Thoning et al. (1989).

Supprimé : probably

Supprimé : decreasing but

Supprimé : stabilization

Supprimé : with

Supprimé : . Prather et al. (2012), 9.1 ± 0.9 years).

Supprimé : and sinks, which

Supprimé : stabilization

Supprimé : to increasing sink (e.g. Bousquet et al., 2006).

Mis en forme : Anglais (G.B.)

Supprimé : recovered

Supprimé : or

Supprimé : for 2014 and 2015

Supprimé : 1

Supprimé : 6

Supprimé : 2008-2017

Supprimé : 6.1±1.

Supprimé : 2017

Mis en forme : Police :Gras, Couleur de police : Noir

Mis en forme : Normal, Espace Avant : 12 pt, Après : 12 pt, Paragraphes solidaires, Bordure : Haut: (Pas de bordure), Bas: (Pas de bordure), Gauche: (Pas de bordure), Droite: (Pas de bordure), Entre : (Pas de bordure)

Mis en forme : Couleur de police : Noir

Supprimé : In this budget, we use satellite data from the JAXA satellite Greenhouse Gases Observing SATellite (GOSAT) launched in January 2009 (Butz et al., 2011; Morino et al., 2011) containing the TANSO-FTS instrument, which observes in the shortwave infrared (SWIR). Different retrievals of methane based on TANSO-FTS/GOSAT products are made available to the community: from NIES (Yoshida et al., 2013), from SRON (Schepers et al., 2012) and from University of Leicester (Parker et al., 2011). The three retrievals are used by the top-down systems (Table 4 and S6). Although GOSAT retrievals still show significant unexplained biases and limited sampling in cloud covered regions and in the high latitude winter, it represents an important improvement compared to the first satellite measuring methane from space, SCIAMACHY (Scanning Imaging Absorption spectrometer for Atmospheric Cartography) both for random and systematic observation errors (see Table S2 of Buchwitz et al. (2016)).
 Atmospheric inversions based on SCIAMACHY and GOSAT CH₄ retrievals were reported in Saunio et al. (2016). Here, only inversions using GOSAT retrievals are used.

4154 community: from NIES (Yoshida et al., 2013), from SRON (Schepers et al., 2012) and from University of Leicester (Parker
4155 et al., 2020; Parker and Boesch, 2020). The three retrievals are used by the top-down systems (Table 4 and S6). Although
4156 GOSAT retrievals still show significant unexplained biases and limited sampling in cloud covered regions and in the high
4157 latitude winter, it represents an important improvement compared to the first satellite measuring CH₄ from space,
4158 SCIAMACHY (Scanning Imaging Absorption spectrometer for Atmospheric Cartography) both for random and systematic
4159 observation errors (see Table S2 of Buchwitz et al. (2016)).
4160 Here, as in Saunois et al. (2020), only inversions using GOSAT retrievals are used.

4.2 Top-down inversions used in the budget

4162 An atmospheric inversion is the optimal combination of atmospheric observations, of a model of atmospheric transport and
4163 chemistry, of a prior estimate of CH₄ sources and sinks, and of their uncertainties, to provide improved estimates of the
4164 sources and sinks, and their uncertainty. The theoretical principle of CH₄ inversions is detailed in the Supplementary
4165 Material and an overview of the different methods applied to CH₄ is presented in Houweling et al. (2017).

4166 We consider an ensemble of inversions gathering various chemistry transport models, differing in vertical and horizontal
4167 resolutions, meteorological forcing, advection and convection schemes, and boundary layer mixing. Including these
4168 different systems is a conservative approach that allows us to cover different potential uncertainties of the inversion, among
4169 them: model transport, set-up issues, and prior dependency. General characteristics of the inversion systems are provided in
4170 Table 4. Further details can be found in the referenced papers and in the Supplementary Material. Each group was asked to
4171 provide gridded flux estimates for the period 2000-2020, using either surface or satellite data, but no additional constraints
4172 were imposed so that each group could use their preferred inversion setup. Two sets of prior emission distributions were
4173 built from the most recent inventories or model-based estimates (see Supplementary Material), but its use was not mandatory
4174 (see Table S8 to S11 for the inversion characteristics). This approach corresponds to a flux assessment, but not to a model
4175 inter-comparison as the protocol was not too stringent. Estimating posterior uncertainty is time and computer resource
4176 consuming, especially for the 4D-var approaches and Monte Carlo methods. Posterior uncertainties have not been requested
4177 for this study, but they were found to be lower than the ensemble spread in Saunois et al. (2020). Indeed, chemistry transport
4178 models differ in inter-hemispheric transport, stratospheric CH₄ profiles, and OH distribution, limitations which are not fully
4179 considered in the individual posterior uncertainty. As a result, we report the minimum-maximum range among the different
4180 top-down approaches.

4181 Seven atmospheric inversion systems using global Eulerian transport models were used in this study: they contributed to the
4182 previous budgets that included eight atmospheric inversion systems in Saunois et al. (2016) and nine in Saunois et al. (2020).
4183 Each inversion system provided one or several simulations, including sensitivity tests varying the assimilated observations
4184 (surface or satellite), the OH inter-annual variability, or the prior fluxes ensemble. This represents a total of 24 inversion
4185 runs with different time coverage: generally, 2000-2020 for surface-based observations, and 2010-2020 for GOSAT-based

Mis en forme : Police :Gras, Couleur de police : Noir

Mis en forme : Police :Gras, Couleur de police : Noir

Mis en forme : Normal, Espace Avant : 12 pt, Après : 12 pt, Paragraphes solidaires, Bordure : Haut: (Pas de bordure), Bas: (Pas de bordure), Gauche: (Pas de bordure), Droite: (Pas de bordure), Entre : (Pas de bordure)

Supprimé : An atmospheric inversion is the optimal combination of atmospheric observations, of a model of atmospheric transport and chemistry, of a prior estimate of methane sources and sinks, and of their uncertainties, in order to provide improved estimates of the sources and sinks, and their uncertainty. The theoretical principle of methane inversions is detailed in the Supplementary Material (ST2) and an overview of the different methods applied to methane is presented in Houweling et al. (2017).[†]

Supprimé : here

Mis en forme : Anglais (G.B.)

Mis en forme : Anglais (G.B.)

Supprimé : 2017

Supprimé : A set

Supprimé : was

Supprimé : S6

Supprimé : provided by only two groups and are

Supprimé : .

Supprimé : methane

Supprimé : which

Supprimé : do not use the posterior uncertainties provided by these two groups but

Mis en forme : Anglais (G.B.)

Supprimé : Nine atmospheric inversion systems using global Eulerian transport models were used in this study compared to eight in Saunois et al. (2016). Each inversion system provided one or several simulations, including sensitivity tests varying the assimilated observations (surface or satellite) or the inversion setup. This represents a total of 22 inversion runs with different time coverage: generally, 2000-2017 for surface-based observations, and 2010-2017 for GOSAT-based inversions (Table 4 and Table S6). In poorly observed regions, top-down surface inversions may rely on the prior estimates and bring little or no additional information to constrain (often) spatially overlapping emissions (e.g. in India, China). Also, we recall that many top-down systems solve for the total fluxes at the surface only or for some categories that may differ from the GCP categories. When multiple sensitivity tests were performed the mean of this ensemble was used not to overweight one particular inverse system. It should also be noticed that some satellite-based inversions are in fact combined satellite and surface inversions as they use satellite retrievals and surface measurements simultaneously (Alexe et al., 2015; Bergamaschi et al., 2013; Houweling et al., 2014). Nevertheless, these inversions are still referred to as satellite-based inversions.[†]

Each group provided gridded monthly maps of emissions for both their prior and posterior total and for sources per category (see the†05)

4266 inversions (Table 4 and Table S7). In poorly observed regions, top-down surface inversions may rely on the prior estimates
4267 and bring little or no additional information to constrain (often) spatially overlapping emissions (e.g., in India, China). Also,
4268 we recall that many top-down systems solve for the total fluxes at the surface only or for some categories that may differ
4269 from the GCP categories. When multiple sensitivity tests were performed the mean of this ensemble was used not to
4270 overweight one particular inverse system. It should also be noticed that some satellite-based inversions are in fact combined
4271 satellite and surface inversions as they use surface-based inversions to correct the latitudinal bias of the satellite retrievals
4272 against the optimised atmosphere measurements to correct for errors in the transport model especially in the stratosphere
4273 (e.g., Segers et al., 2022; Maasackers et al., 2019). Nevertheless, these inversions are still referred to as satellite-based
4274 inversions. Most of the top-down models use the OH distribution from the TRANSCOM experiment (Patra et al., 2011)
4275 either as fixed over the period or with the inter-annual variability derived by Patra et al. (2021).
4276 Each group provided gridded monthly maps of emissions for both their prior and posterior total and for sources per category
4277 (see the categories Sect. 2.3). Results are reported in Sect. 5. Atmospheric sinks from the top-down approaches have been
4278 provided for this budget, and are compared with the values reported in Saunio et al. (2020). Not all inverse systems report
4279 their chemical sink; as a result, the global mass imbalance for the top-down budget is derived as the difference between total
4280 sources and total sinks for each model when both fluxes were reported.

4281 **5 Methane budget: top-down and bottom-up comparison**

4282 **5.1 Global methane budget**

4283 **5.1.1 Global total methane emissions-**

4284 **Top-down estimates.** At the global scale, the total annual emissions inferred by the ensemble of 24 inversions is 575 Tg
4285 $\text{CH}_4 \text{ yr}^{-1}$ [553-586] for the 2010-2019 decade (Table 3), with the highest ensemble mean emission of 608 Tg $\text{CH}_4 \text{ yr}^{-1}$ [581-
4286 627] for 2020. Global emissions for 2000-2009 (543 Tg $\text{CH}_4 \text{ yr}^{-1}$) are consistent with Saunio et al. (2016, 2020) and the
4287 range for global emissions, 526-558 Tg $\text{CH}_4 \text{ yr}^{-1}$ falls within the range in Saunio et al. (2016) (535-569) and Saunio et al.
4288 (2020) (524-560), although the ensemble of inverse systems contributing to this budget is different from Saunio et al. (2016,
4289 2020). Changes in ensemble members contributing to the different budgets are a feature of each new GMB release and,
4290 therefore, introduce a source of variation (Table S7). The range reported gives the minimum and maximum values among
4291 studies and does not reflect the individual full uncertainties. In addition, most of the top-down models use the same OH
4292 distribution from the TRANSCOM experiment (Patra et al., 2011), which introduces less variability to the global budget
4293 than is likely justified, and so contributes to the rather low range (10%) compared to bottom-up estimates (see below).

4294 **Bottom-up estimates.** The bottom-up estimates considered here differ substantially from the top-down results, with annual
4295 global emissions being about 15% larger at 669 Tg $\text{CH}_4 \text{ yr}^{-1}$ [512-849] for 2010-2019 (Table 3). Yet, thanks to the double
4296 counting corrections in this budget, bottom-up and top-down budgets are in better agreement compared to previous GMB

4297 releases. For the period 2000-2009, the discrepancy between bottom-up and top-down was about 30% of the top-down
 4298 estimates in Saunois et al. (2016, 2020) (167 and 156 Tg CH₄ yr⁻¹, respectively), a value that has been reduced significantly
 4299 in this budget (now 95 Tg CH₄ yr⁻¹ (<17%) for the same 2000-2009 period). This reduction is due to improvements from an
 4300 important decrease in the estimate of emissions from natural and indirect anthropogenic emissions from bottom-up
 4301 approaches, and more specifically inland freshwater emissions. From the previous budget, the estimate for inland freshwater
 4302 emissions (lakes, ponds, reservoirs, rivers, and streams) has decreased from 159 Tg CH₄ yr⁻¹ to 112 Tg CH₄ yr⁻¹ (47 Tg
 4303 decrease). Then, 23 Tg have been removed in the total freshwater ecosystem emissions due to double counting between
 4304 vegetated wetlands and mostly small ponds and lakes (Sect. 3.2.2). As a result the combined wetland and inland freshwater
 4305 emissions are estimated to be 242 Tg CH₄ yr⁻¹ for 2000-2009, compared with 306 Tg CH₄ yr⁻¹ in Saunois et al. (2020).
 4306 This budget is the first that reconciles bottom-up and top-down total emissions within the uncertainty ranges. However, the
 4307 uncertainty in the global budget remains high because of the large range reported for emissions from freshwater systems.
 4308 Still, the upper bound of global emissions from bottom-up approaches is not consistent with top-down estimates that rely
 4309 on OH burden constrained by methyl chloroform atmospheric observations and is still likely overestimated.

4310 5.1.2 Global methane emissions per source category

4311 The global CH₄ emissions from natural and anthropogenic sources (see Sect. 2.3) for 2010-2019 are presented in Fig. 6, Fig.
 4312 7, and Table 3. Top-down estimates attribute about 65% of total emissions to anthropogenic activities (range of 55-70%),
 4313 and 35% to natural emissions. Bottom-up estimates attribute 57% of emissions to direct anthropogenic and the rest to natural
 4314 plus indirect anthropogenic emissions. A current predominant role of direct anthropogenic sources of CH₄ emissions is
 4315 consistent with and strongly supported by available ice core and atmospheric CH₄ records. These data indicate that
 4316 atmospheric CH₄ varied around 700 ppb during the last millennium before increasing by a factor of 2.6 to ~1800 ppb since
 4317 pre-industrial times. Accounting for the decrease in mean-lifetime over the industrial period, Prather et al. (2012) estimated
 4318 from these data a total source of 554±56 Tg CH₄ in 2010 of which about 64% (352±45 Tg CH₄) was of direct anthropogenic
 4319 origin, consistent with the range in our stop-down estimates.

4320
 4321 **Natural and indirect anthropogenic emissions.** Although smaller than in previous Global Methane Budget releases, the
 4322 main remaining discrepancy between top-down and bottom-up budgets is found for the natural and indirect anthropogenic
 4323 emission total (105 Tg), with 311 [183-462] Tg CH₄ yr⁻¹ for bottom-up and only 206 [188-225] Tg CH₄ yr⁻¹ for top-down
 4324 over the 2010-2019 decade. In the bottom-up estimates, this discrepancy comes first from the estimates in both inland
 4325 freshwater sources (64 Tg) and second from other natural sources (20 Tg from geological sources, termites, oceans, and
 4326 permafrost). The top-down approaches may be biased due to missing fluxes (mainly inland freshwaters) in their prior
 4327 estimates.

Supprimé: 547 Tg CH₄ yr⁻¹ are consistent with Saunois et al. (2016) and the range for global emissions, 524-560 Tg CH₄ yr⁻¹ is in line with range in Saunois et al. (2016) (535-569), although the ensemble of inverse systems contributing to this budget is different than for Saunois et al. (2016). Indeed, only six inverse systems of the nine examined here (Table S7) contributed previously to the Saunois et al. (2016) budget. The range reported gives the minimum and maximum values among studies and do not reflect the individual full uncertainties. Also, most of the top-down models use the same OH distribution from the TRANSCOM experiment (Patra et al., 2011), leading to a global budget quite constrained, probably explaining the rather low range (10 %) compared to bottom-up estimates (see below).[†]

Déplacé vers le bas [2]: Bottom-up estimates.

Supprimé: The estimates made via the bottom-up approaches considered here are quite different from the top-down results, with global emissions almost 30% larger, at 737 Tg CH₄ yr⁻¹ [594-881] for 2008-2017 (Table 3). Moreover, the range estimated using bottom up approaches does not overlap with that of the top-down estimates. The bottom-up estimates are given by the sum of individual anthropogenic and natural processes, without any constraint on the total. For the period 2000-2009, the discrepancy between bottom-up and top-down was 30% of the top-down estimates in Saunois et al. (2016) (167 Tg CH₄ yr⁻¹); this has been reduced only slightly (now 156 Tg CH₄ yr⁻¹ for the same 2000-2009 period). This reduction is due to 1) a better agreement in the anthropogenic emissions (top-down and bottom-up difference reducing from 19 Tg CH₄ yr⁻¹ to 2 Tg CH₄ yr⁻¹), 2) a reduction in the estimates of some natural sources other than wetlands based on recent literature (by 7 Tg CH₄ yr⁻¹ from geological sources, by 8 Tg CH₄ yr⁻¹ from wild animals, and by 107

Mis en forme : Police :Gras, Couleur de police : Noir

Mis en forme ... [106]

Supprimé: methane

Supprimé: 2008-2017

Supprimé: 5

Supprimé: 6

Supprimé: 60

Supprimé:

Supprimé: 40

Supprimé: As natural

Supprimé: estimated from bottom-up approaches are much larger, the

Supprimé: versus natural emission ratio is nearly 1, not consistent with ice core data

Supprimé: methane

Supprimé: methane

Supprimé: methane

Supprimé: (2012)

Supprimé: Wetlands. For 2008-2017, the top-down and bottom-up derived estimates of 181 Tg CH₄ yr⁻¹ (range 159-200) and 149 Tg

4487 For 2010-2019, the top-down and bottom-up derived estimates for wetlands emissions of 165 [145-214] Tg CH₄ yr⁻¹ and
4488 159 [119-203] Tg CH₄ yr⁻¹, respectively, are comparable within their range. Based on diagnostic wetland area values (see
4489 notes in Table 3), bottom-up mean wetland emissions for the 2000-2009 period are smaller in this study than those of Sauniois
4490 et al. (2016) but larger than in Sauniois et al. (2020). The changes in wetland emissions from bottom-up models may be
4491 related to updates on the wetland extent data set (WAD2M), the use of two different meteorological forcings for this study
4492 and a different set of models (see Sect. 3.2.1). Conversely, the current 2000-2009 mean top-down wetland estimates are
4493 lower than those of Sauniois et al. (2016) and Sauniois et al. (2020) (Table 3). In the bottom-up estimates, the amplitude of
4494 the range of emissions of 116-189 is roughly similar to Sauniois et al. (2016) (151-222) and Sauniois et al. (2020) (102-179)
4495 for 2000-2009. Here, the larger range in bottom-up estimates of wetland emissions is due to the use of GSWP3-W5E5 and
4496 greater sensibilities of some models to the climate parameters, as discussed in Sect. 3.2.1. Bottom-up and top-down estimates
4497 for wetland emissions agree better in this study (~5 Tg yr⁻¹ for 2000-2009) than in Sauniois et al. (2016, 2020) (~17 Tg yr⁻¹
4498 and ~30 Tg yr⁻¹, respectively). Natural emissions from inland freshwater systems were not included in the prior fluxes used
4499 in the top-down approaches, due to unavailable or uncertain gridded products at the start of the modelling activity. However,
4500 emissions from these inland freshwater systems may be implicitly included in the posterior estimates of the top-down
4501 models, as these two sources are close and probably overlap at the rather coarse resolution of the top-down models. This is
4502 the reason why the ‘wetland emissions’ in the top-down budget in fact correspond to the sum of combined wetland and
4503 inland freshwaters emissions in the bottom-up budget. The double-counting of 23 Tg CH₄ reduces the bottom-up budget for
4504 combined wetland and inland freshwaters from 271 Tg CH₄ yr⁻¹ to 248 Tg CH₄ yr⁻¹ (Sect. 3.2.2). Comparing the 2000-2009
4505 decadal emissions from wetlands and inland freshwater ecosystems estimated by the bottom-up approaches across the last
4506 three Global Methane Budgets shows an upward and then a downward revision with 305 (183+122) Tg CH₄ yr⁻¹, 356
4507 (147+209) Tg CH₄ yr⁻¹ and 248 (159+112-23) Tg CH₄ yr⁻¹ (respectively from Sauniois et al. (2016, 2020) and this work; the
4508 sum in bracket corresponds to the sum of vegetated wetland emissions and inland water emissions estimated through the
4509 different budgets). The combined wetland and inland freshwater emissions discrepancy between bottom-up and top-down
4510 approaches amount to 105 Tg CH₄ yr⁻¹ for the 2010-2019 decade. From a top-down point of view, the sum of all the natural
4511 sources is more robust than the partitioning between wetlands, inland waters, and other natural sources. Including all known
4512 spatio-temporal distributions of natural emissions in top-down prior fluxes would be a step forward to consistently compare
4513 natural versus anthropogenic total emissions between top-down and bottom-up approaches.
4514 In the top-down budget, wetlands represent 28% on average of the total methane emissions but only 24% in the bottom-up
4515 budget (because of higher total emissions inferred). Given the large uncertainties, neither bottom-up nor top-down
4516 approaches included in this study point to significant changes in wetland emissions between the two decades 2000-2009 and
4517 2010-2019 at the global scale.
4518 For the 2010-2019 decade, top-down inversions infer “Other natural emissions” (Table 3) at 43 Tg CH₄ yr⁻¹ [40-46], whereas
4519 the sum of the individual bottom-up emissions is 63 Tg CH₄ yr⁻¹ [24-93], contributing to a 20 Tg discrepancy between

4520 bottom-up and top-down approaches. Atmospheric inversions infer the same amount over the decade 2000-2009 as over
 4521 2010-2019, which is almost half of the value reported in Saunois et al. (2016) (68 [21-130] Tg CH₄ yr⁻¹). This reduction in
 4522 magnitude and uncertainty is due to 1) a more consistent way of considering other natural emissions in the various inverse
 4523 systems (same prior estimate as in this budget) and 2) a difference in the ensemble of top-down inversions reported here
 4524 compared to previous releases. It is worth noting that, most of the top-down models include about the same ocean and
 4525 onshore geological emissions and termite emissions in their prior scenarios. However, none include freshwater or permafrost
 4526 emissions in their prior fluxes, and thus in their posterior estimates.

4527 Geological emissions are associated with relatively large uncertainties, and marine seepage emissions are still widely
 4528 debated (Thornton et al., 2020). However, summing up all bottom-up fossil-CH₄ related sources (including anthropogenic
 4529 emissions) leads to a total of 165 Tg CH₄ yr⁻¹ [135-190] in 2010-2019, which is about 29% of the top-down global
 4530 CH₄ emissions, and 25% of the bottom-up total global estimate. These results agree with the value inferred from ¹⁴C
 4531 atmospheric isotopic analyses of 30% contribution of fossil-CH₄ to global emissions (Etiopé et al., 2008; Lassey et al.,
 4532 2007b). This total fossil fuel emissions from bottom-up approaches agrees well with the ¹³C-based estimate of Schwietzke
 4533 et al. (2016) of 192 ± 32 Tg CH₄ yr⁻¹. In the bottom-up budget, the larger total emissions (due to uncertainties in bottom-up
 4534 estimates of natural emissions) leads to a lower fossil fuel contribution compared to Lassey et al. (2007b).

4535 **Anthropogenic direct emissions.** Total anthropogenic direct emissions for the period 2010-2019 were assessed to be
 4536 statistically consistent between top-down (369 Tg CH₄ yr⁻¹, range 350-391) and bottom-up approaches (358 Tg CH₄ yr⁻¹,
 4537 range 329-387), albeit top-down approaches infer direct anthropogenic emissions larger by 11 Tg CH₄ yr⁻¹ on average
 4538 compared to bottom-up approaches. The partitioning of anthropogenic direct emissions between agriculture and waste, fossil
 4539 fuels extraction and use, and biomass and biofuel burning, also shows good consistency between top-down and bottom-up
 4540 approaches, though top-down approaches still suggest less fossil fuel and more agriculture and waste emissions than bottom-
 4541 up estimates (Table 3 and Fig. 6 and 7). For 2010-2019, agriculture and waste contributed an estimated 228 Tg CH₄ yr⁻¹
 4542 [213-242] in the top-down budget and 211 Tg CH₄ yr⁻¹ [195-231] in the bottom-up budget. Fossil fuel emissions contributed
 4543 115 Tg CH₄ yr⁻¹ [100-124] in the top-down budget and 120 Tg CH₄ yr⁻¹ [117-125] in the bottom-up budget. Biomass and
 4544 biofuel burning contributed 27 Tg CH₄ yr⁻¹ [26-27] in the top-down budget and 28 Tg CH₄ yr⁻¹ [21-39] in the bottom-up
 4545 budget. Biofuel CH₄ emissions rely on very few estimates currently (Wuebbles and Hayhoe, 2002). Although biofuel is a
 4546 small source globally (~12 Tg CH₄ yr⁻¹), more estimates are needed to allow a proper uncertainty assessment. Overall for
 4547 top-down inversions the global fraction of total emissions for the different source categories is 40% for agriculture and
 4548 waste, 20% for fossil fuels, and 5% for biomass and biofuel burning. With the exception of biofuel emissions, the uncertainty
 4549 associated with global anthropogenic emissions appears to be smaller than that of natural sources but with an asymmetric
 4550 uncertainty distribution (mean significantly different than median). The relative agreement between top-down and bottom-
 4551 up approaches may indicate a limited capability of the inversion to separate emissions and a dependency to their prior fluxes;
 4552 this agreement should therefore be treated with caution. Indeed, in poorly observed regions, top-down inversions rely on the

- Supprimé: 2008-2017
- Supprimé: 359
- Supprimé: 336-376
- Supprimé: 366
- Supprimé: 349-393.
- Supprimé: 5
- Supprimé: 6
- Supprimé: 2008-2017
- Supprimé: 217
- Supprimé: 207-240] for
- Supprimé: 206
- Supprimé: 191-223] for
- Supprimé: 111
- Supprimé: 81-131] for
- Supprimé: 128
- Supprimé: 113-154] for
- Supprimé: 30
- Supprimé: 22-36] for
- Supprimé: 29
- Supprimé: 25
- Supprimé: for
- Supprimé: methane
- Supprimé: (Wuebbles and Hayhoe, 2002).
- Supprimé: 38
- Supprimé: 19
- Supprimé: the
- Supprimé: the

4580 prior estimates and bring little or no additional information to constrain (often) spatially overlapping emissions (e.g. in
4581 India, China). Also, as many top-down systems solve for the total fluxes at the surface or for some categories that may differ
4582 from the GCP categories, their posterior partitioning relies on the prior ratio between categories that are prescribed using
4583 bottom-up inventories.

4584 **5.1.3 Global budget of total methane sinks**

4585 **Top-down estimates.** The annual CH₄ chemical removal from the atmosphere is estimated to be 521 Tg CH₄ yr⁻¹ averaged
4586 over the period 2010-2019, with an uncertainty of about ±2% (range 485-532 Tg CH₄ yr⁻¹). All the inverse models account
4587 for CH₄ oxidation by OH and O(¹D), and some include stratospheric Cl oxidation (Table S8 to S11). Most of the top-down
4588 models use the OH distribution from the TRANSCOM experiment (Patra et al., 2011) either as fixed over the period or
4589 including inter annual variability from Patra et al. (2021). This study shows no trend in OH and IAV below ±4%, in
4590 agreement with Thompson et al. (2024) (no significant OH trend and IAV < 2%). As a result, the range of the top-down
4591 sink estimates is rather low compared to bottom-up estimates (see below). Differences between transport models affect the
4592 chemical removal of CH₄, leading to different chemical loss rates, even with the same OH distribution. However,
4593 uncertainties in the OH distribution and magnitude (around ±10% at the global scale, Zhao et al., 2019) are not considered
4594 in our study, while they could contribute to a significant change in the chemical sink, and then in the derived posterior
4595 emissions through the inverse process (Zhao et al., 2020), around ±17% at the global scale, much larger than the model
4596 spread derived here. The chemical sink represents more than 90% of the total sink, the rest being attributable to soil uptake
4597 (35 [35-36] Tg CH₄ yr⁻¹). The rather narrow range is due to the use of the same climatological soil sink provided within the
4598 modelling protocol which is based on Murgia-Flores et al. (2018). This sink estimate used as prior in the inversions is a bit
4599 higher than the mean estimate of the soil sink calculated by bottom-up models (30 Tg CH₄ yr⁻¹, Sec. 3.3.4).

4600 **Bottom-up estimates.** The total chemical loss for the 2010s reported here is 602 Tg CH₄ yr⁻¹ with an uncertainty of 21%
4601 (~125 Tg CH₄ yr⁻¹). Differences in chemistry schemes in the models (especially in the stratosphere) and in the volatile
4602 organic compound treatment probably explain most of the discrepancies among models (Zhao et al., 2019).

4603 **5.2 Latitudinal and regional methane budgets**

4604 The latitudinal and regional breakdown of the bottom-up budget is based on crude assumptions that we acknowledge here.
4605 Natural and indirect anthropogenic emissions are based on wetland gridded products from land surface models and the
4606 combination of the maps from lakes and ponds from Johnson et al. (2022), reservoirs from Johnson et al. (2022) and streams
4607 and rivers from Rocher-Ros et al. (2023), the sum of those three scaled to 89 Tg CH₄ yr⁻¹ (shown in Fig. 5) to artificially
4608 include the double counting (estimated only at the global scale) and match the global estimate. However, we acknowledge
4609 that this procedure distributes the double counting relatively to the final emission distribution and not according to the
4610 freshwater ecosystems where the double counting probably occurs. Wild animals and permafrost maps do not exist and are

Supprimé :

Mis en forme : Police :Gras, Couleur de police : Noir

Mis en forme : Normal, Espace Avant : 12 pt, Après : 12 pt, Paragraphes solidaires, Bordure : Haut: (Pas de bordure), Bas: (Pas de bordure), Gauche: (Pas de bordure), Droite: (Pas de bordure), Entre : (Pas de bordure)

Supprimé: The CH₄ chemical removal from the atmosphere is estimated to 518 Tg CH₄ yr⁻¹ over the period 2008-2017, with an uncertainty of about ±5% (range 474-532 Tg CH₄ yr⁻¹). All the inverse models account for CH₄ oxidation by OH and O(¹D), and some include stratospheric chlorine oxidation (Table S6). In addition, most of the top-down models use OH distribution from the TRANSCOM experiment (Patra et al., 2011), probably explaining the rather low range of estimates compared to bottom-up estimates (see below). Differences between transport models affect the chemical removal of CH₄, leading to different chemical loss rates, even with the same OH distribution. However, uncertainties in the OH distribution and magnitude (Zhao et al., 2019) are not considered in our study, while it could contribute to a significant change in the chemical sink, and then in the derived posterior emissions through the inverse process (Zhao et al., 2020). The chemical sink represents more than 90% of the total sink, the rest being attributable to soil uptake (38 [27-45] Tg CH₄ yr⁻¹). Half of the top-down models use the climatological soil uptake magnitude (37-38 Tg CH₄ yr⁻¹) and distribution from Ridgwell et al. (1999), while half of the models use an estimate from the biogeochemical model VISIT (Ito and Inatomi, 2012), which calculates varying uptake between 31 and 38 Tg CH₄ yr⁻¹ over the 2000-2017 period. These sink estimates used as prior in the inversions are generally

Déplacé (insertion) [2]

Supprimé: Bottom-up estimates. The total chemical loss for the 2000s reported here is 595 Tg CH₄ yr⁻¹ with an uncertainty of 22% (~130 Tg CH₄ yr⁻¹). Differences in chemical schemes (especially in the stratosphere) and in the volatile organic compound treatment probably explain most of the discrepancies among models (Zhao et al., 2019).

Mis en forme : Police :Gras, Couleur de police : Noir

Mis en forme : Police :Gras, Couleur de police : Noir

Mis en forme : Normal, Retrait : Première ligne : 0 cm

4641 missing from the calculation, leading to around 3 Tg CH₄ yr⁻¹ of discrepancy. Geological and ocean sources are based on
4642 Etiope et al. (2019) and Weber et al. (2019) gridded products scaled to 50 Tg CH₄ yr⁻¹ to be consistent to the reported global
4643 values. Finally, we use the termite emission map produced for this budget and used in the global budget. The latitudinal
4644 budget does not include the estimates from FAO and USEPA for the direct anthropogenic emissions as they are only
4645 provided at country scale.

4646 5.2.1 Latitudinal budget of total methane emissions

4647 The latitudinal breakdown of emissions inferred from atmospheric inversions reveals a dominance of tropical emissions of
4648 364 Tg CH₄ yr⁻¹ [337-390], representing 64% of the global total (Table 5 and 6). 32% of the emissions are from the mid-
4649 latitudes (187 Tg CH₄ yr⁻¹ [160-204]) and 4% from high latitudes (above 60°N). The ranges around the mean latitudinal
4650 emissions are larger than for the global CH₄ sources. While the top-down uncertainty is less than ±5% at the global scale, it
4651 increases to ±7% for the tropics, to ±12% the northern mid-latitudes and to more than ±20% in the northern high-latitudes
4652 (for 2010-2019, Table 5). Both top-down and bottom-up approaches consistently show that CH₄ decadal emissions have
4653 increased by ±21-27 Tg CH₄ yr⁻¹ in the tropics, and by ±5-16 Tg CH₄ yr⁻¹ in the northern mid-latitudes between 2000-2009
4654 and 2010-2019 using the mean ensemble estimate.

4655 Over 2010-2019, at the global scale, satellite-based inversions infer almost identical emissions to ground-based inversions
4656 (difference of +1 [-3-9] Tg CH₄ yr⁻¹, with GOSAT based inversion a bit higher than surface measurements-based inversions),
4657 when comparing consistently surface versus satellite-based inversions for each system, similar to Saunio et al. (2020). This
4658 difference is much lower than the range derived between the different systems (range of 20 Tg CH₄ yr⁻¹ using surface- or
4659 satellite-based inversions). This result reflects that differences in atmospheric transport among the systems probably have
4660 more impact on the estimated global emissions than the types of observations assimilated.

4661 As expected, considering the different coverage of observation datasets, regional distributions of inferred emissions differ
4662 depending on the nature of the observations used (satellite or surface). The largest differences (satellite-based minus surface-
4663 based inversions) are observed over the tropical region, between -10 and +43 Tg CH₄ yr⁻¹ (90°S to 30°N), and the northern
4664 mid-latitudes (between -36 and +2 Tg CH₄ yr⁻¹). Satellite data provide stronger constraints on fluxes in tropical regions than
4665 surface data, due to a much larger spatial coverage. It is therefore not surprising that differences between these two types of
4666 observations are found in the tropical band, and consequently in the northern mid-latitudes to balance total emissions, thus
4667 affecting the north-south gradient of emissions. However, the regional patterns of these differences are not consistent
4668 through the different inverse systems. Indeed, some systems found higher emissions in the tropics when using GOSAT
4669 instead of surface observations, while others found the opposite. This difference between inversion systems may depend on
4670 whether or not a bias correction is applied to the satellite data based on surface observations, and also on the modelled
4671 horizontal and vertical transports, in the troposphere and in the stratosphere.

Mis en forme : Police :Gras, Couleur de police : Noir

Mis en forme : Normal, Espace Avant : 12 pt, Après : 12 pt, Paragraphes solidaires, Bordure : Haut: (Pas de bordure), Bas: (Pas de bordure), Gauche: (Pas de bordure), Droite: (Pas de bordure), Entre : (Pas de bordure)

Supprimé: at 368

Supprimé: 399

Supprimé: 186

Supprimé: 166

Supprimé: methane

Supprimé: about ±

Supprimé: ±10

Supprimé: and

Supprimé: ±25

Supprimé: 2008-2017

Supprimé: methane

Supprimé: about 20

Supprimé: 7-18

Supprimé: 2008-2017, but not in

Supprimé: northern high latitudes

Supprimé: Over 2010-2017, at the global scale, satellite-based inversions infer almost identical emissions to ground-based inversions (difference of 3 [0-7] Tg CH₄ yr⁻¹), when comparing consistently surface versus satellite-based inversions for each system. This difference is much lower than the range derived between the different systems (range of 20 Tg CH₄ yr⁻¹ using surface- or satellite-based inversions). This result reflects that differences in atmospheric transport among the systems probably have more impact than the types of observations assimilated on the estimated global emissions. In Saunio et al. (2016), satellite-based inversions reported 12 Tg higher global methane emissions compared to surface-based inversions. Differences in the ensemble, the use of only GOSAT data and the treatment of satellite data within each system compared to Saunio et al. (2016) explain the contrasting results. As expected, the

Mis en forme : Anglais (G.B.)

Supprimé: 13

Supprimé: 26

Supprimé: 20

Supprimé: +15

Mis en forme : Anglais (G.B.)

Supprimé: the

Supprimé: model

4708 **5.2.2 Latitudinal methane emissions per source category**

4709 The analysis of the latitudinal CH_4 budget per source category (Fig. 8 and Table 6) can be performed both for bottom-up

4710 and top-down approaches but with limitations. Bottom-up estimates of natural and indirect anthropogenic emissions are

4711 based on assumptions as specified at the beginning of this section 5.2. For top-down estimates, as already noted, the

4712 partitioning of emissions per source category has to be considered with caution. Indeed, using only atmospheric

4713 CH_4 observations to constrain CH_4 emissions makes this partitioning largely dependent on prior emissions. However,

4714 differences in spatial patterns and seasonality of emissions can be utilised to constrain emissions from different categories

4715 by atmospheric methane observations (for those inversions solving for different sources categories, see Sect. 2.3).

4716 Agriculture and waste are the largest sources of CH_4 emissions in the tropics and southern hemisphere (140 [121-150] Tg

4717 $\text{CH}_4 \text{ yr}^{-1}$ in the bottom-up budget and 150 [135-168] Tg $\text{CH}_4 \text{ yr}^{-1}$ in the top-down budget, about 40% of total CH_4 emissions

4718 in this region). However, combined wetland and inland freshwater emissions are nearly as large with 151 [85-234] Tg CH_4

4719 yr^{-1} in the bottom-up budget and 128 [112-155] Tg $\text{CH}_4 \text{ yr}^{-1}$ in the top-down budget. Anthropogenic emissions dominate in

4720 the northern mid-latitudes, with the highest contribution from agriculture and waste emissions (40% of total emissions in

4721 the top-down budget), closely followed by fossil fuel emissions (32% of total emissions, top-down budget). Boreal regions

4722 are largely dominated by inland freshwater emissions (41% and 54% of total emissions, top-down and bottom-up budget,

4723 respectively).

4724 The largest discrepancies between the top-down and the bottom-up budgets are found in the mid-latitudes and boreal regions

4725 from the natural and indirect sources with bottom-up estimates twice as large as the top-down ones, especially in the inland

4726 freshwater category.

4727 The uncertainty for wetlands and inland freshwater emissions is larger in the bottom-up models than in the top-down models,

4728 (mostly wetlands), while uncertainty in anthropogenic emissions is larger in the top-down models than in the bottom-up

4729 inventories. The large uncertainty in tropical inland freshwater emissions (mostly wetlands) of $\pm 44\%$ results from large

4730 regional differences between the bottom-up land-surface models. Although they are using the same forcings, their responses

4731 in terms of flux density show different sensitivities to temperature, water vapour pressure, precipitation, and radiation.

4732 **5.2.3 Regional budget for total emissions**

4733 The regional breakdown of emissions is provided for 18 continental regions (see map in Fig. S3 and Table S1 with the

4734 country aggregation in the supplementary materials).

4735 At the regional scale and, for the 2010-2019 decade, total methane emissions are dominated by South East Asia with 63 [52-

4736 71] Tg $\text{CH}_4 \text{ yr}^{-1}$, China with 57 [37-72] Tg $\text{CH}_4 \text{ yr}^{-1}$, and South Asia with 52 [43-60] Tg $\text{CH}_4 \text{ yr}^{-1}$ (top-down budget). These

4737 top three emitters contribute 30% of total global CH_4 emissions. The following high emitting regions are Brazil 47 [41-58]

4738 Tg $\text{CH}_4 \text{ yr}^{-1}$, Equatorial Africa 47 [39-59] Tg $\text{CH}_4 \text{ yr}^{-1}$, USA 38 [32-46] Tg $\text{CH}_4 \text{ yr}^{-1}$, Southwest South America 38 [30-48]

- Mis en forme : Police :Gras, Couleur de police : Noir
- Mis en forme : Normal, Espace Avant : 12 pt, Après : 12 pt, Paragraphes solidaires, Bordure : Haut: (Pas de bordure), Bas: (Pas de bordure), Gauche: (Pas de bordure), Droite: (Pas de bordure), Entre : (Pas de bordure)
- Supprimé: methane
- Supprimé: 7
- Supprimé: On the bottom
- Supprimé: side, some
- Supprimé: not (yet) available
- Supprimé: regional scale (mainly inland waters). Therefore, for freshwater emissions, we applied the latitudinal distribution of Bastviken et al. (2011) to the global reported value. Further details...
- Supprimé: side
- Supprimé: methane
- Supprimé: methane
- Supprimé: utilized
- Supprimé: methane
- Supprimé: (130
- Supprimé: 137
- Supprimé: for
- Supprimé: 139 [127-157
- Supprimé: for
- Supprimé: 38
- Supprimé: methane
- Supprimé: 116 [71-146
- Supprimé: for
- Supprimé: 135 [116
- Supprimé: for
- Supprimé: One top-down model suggests lower emissions from...
- Supprimé: 42
- Supprimé: 31
- Supprimé: wetland
- Supprimé: 60
- Supprimé: wetland
- Supprimé: ,
- Supprimé: wetland
- Supprimé: 65%)
- Supprimé: wetland extent
- Supprimé: More regional discussions were developed in Supplementary...

4786 Tg CH₄ yr⁻¹, Russia 36 [27-45] Tg CH₄ yr⁻¹, Europe 31 [24-36] Tg CH₄ yr⁻¹, Middle East 31 [24-39] Tg CH₄ yr⁻¹, Northern
4787 Africa 25 [23-29] Tg CH₄ yr⁻¹, and Canada 20 [17-24] Tg CH₄ yr⁻¹. Other regions contribute less than 20 Tg CH₄ yr⁻¹.

4788 **5.2.4 Regional budget per source category**

4789 **Natural and indirect anthropogenic emissions versus direct anthropogenic emissions.** In agreement with Stavert et al.
4790 (2021), natural and indirect anthropogenic emissions are dominated by Brazil, Canada, Russia, Equatorial Africa and
4791 Southeast Asia, contributing 126 Tg CH₄ yr⁻¹ in the bottom-up and 105 Tg CH₄ yr⁻¹ in the top-down budget (Table 7), i.e.,
4792 47% and 50% of the global natural and indirect anthropogenic emissions in these budgets, respectively. At regional scale
4793 also, the range of uncertainty in natural and indirect anthropogenic emissions are much larger in the bottom-up budget than
4794 in the top-down budget (Fig. S5). Except for 4 regions (Canada, Brazil, Northern South America, Southwest South America),
4795 direct anthropogenic emissions contribute more than half of the total regional emissions. Due to the large uncertainty and
4796 discrepancies in natural and indirect emissions estimates, the regional direct anthropogenic fractions may differ between the
4797 bottom-up and top-down budgets. However, in absolute values, the highest direct anthropogenic emitters are the same in
4798 the two budgets with China and South Asia being the top two by far, contributing 56 [51-66] Tg CH₄ yr⁻¹ and 45 [44-47] Tg
4799 CH₄ yr⁻¹, respectively (bottom-up values, Fig. 9 and Table 7). These two regions contribute 28% (26%) of the global direct
4800 anthropogenic emissions in the bottom-up (top-down) budget. The ranks of direct anthropogenic emitters are similar to those
4801 presented in the last budget (Stavert et al., 2021). Southeast Asia, United States of America, Middle East, Europe, Equatorial
4802 Africa, and Russia emit between 32 Tg CH₄ yr⁻¹ and 23 Tg CH₄ yr⁻¹ as direct anthropogenic emissions (bottom-up values,
4803 Fig 8). Brazil, Northern Africa, and Southwest South America emit between 10 CH₄ yr⁻¹ and 20 CH₄ yr⁻¹, while the rest of
4804 the regions emit less than 10 CH₄ yr⁻¹ direct anthropogenic emissions.

4805
4806 **Sectoral emissions.** The sectoral partitioning at the regional scale has been derived from both bottom-up and top-down
4807 approaches. However, the top-down budget has more limitations, as the sectoral partitioning is usually based on the prior
4808 fluxes fractions at the pixel scale, and assimilating only total methane observations does not allow to disentangle the different
4809 source sectors overlapping in a pixel grid. However, differences in spatial patterns and seasonality of emissions can still be
4810 constrained by atmospheric CH₄ observations for those inversions solving for different sources categories (see Sect. 2.3).
4811 Bottom-up approaches allow deeper sectorial splitting, especially in terms of direct anthropogenic emissions (Fig. 9). Table
4812 7, Fig. 9 and Fig. 10 present the estimations of CH₄ emissions on average over 2010-2019. Fig. 10 presents the budgets for
4813 three main categories (Combined wetland and inland freshwaters, Fossil fuels and Agriculture & Waste), a more detailed
4814 figure and table including the five categories is available in the supplementary material (Fig. S6 and Table S13 to S18).
4815 Values for each individual data-set for the decades 2000-2009, 2010-2019, and the last year 2020 are made available in a
4816 spreadsheet (see Data Availability).

4817 For most regions, “Combined wetland and inland freshwater emissions” are the most uncertain in the bottom-up budget,
4818 and generally their range is larger than in the top-down budget. In the top-down budget, this category contributes the most
4819 to the regional emissions in Brazil 24 [20-33] Tg CH₄ yr⁻¹, Southeast Asia 24 [14-29] Tg CH₄ yr⁻¹ (though similar to their
4820 Agriculture and Waste emissions 24 [21-31] Tg CH₄ yr⁻¹, Equatorial Africa 22 [19-28] Tg CH₄ yr⁻¹, Southwest South
4821 America 22 [14-33] Tg CH₄ yr⁻¹, Canada 12 [9-18] Tg CH₄ yr⁻¹, Northern South America 8 [6-10] Tg CH₄ yr⁻¹, Southern
4822 Africa 7 [4-9] Tg CH₄ yr⁻¹. Agriculture and Waste emissions dominates in South Asia 39 [33-43] Tg CH₄ yr⁻¹, China 30 [13-
4823 37] Tg CH₄ yr⁻¹, Europe 19 [16-23] Tg CH₄ yr⁻¹, United States of America 13 [9-16] Tg CH₄ yr⁻¹, Northern Africa 13 [12-
4824 14] Tg CH₄ yr⁻¹, Central America 9 [8-10] Tg CH₄ yr⁻¹, and Korea and Japan 3 [3-4] Tg CH₄ yr⁻¹. Fossil fuel emissions
4825 dominate in the Middle East 18 [11-24] Tg CH₄ yr⁻¹ and Russia 14 [8-23] Tg CH₄ yr⁻¹ (close to their combined wetland and
4826 inland freshwater emissions of 11 [8-13] Tg CH₄ yr⁻¹).
4827 The four largest contributors to the Fossil Fuel sector remain China, the Middle East, Russia, and the United States of
4828 America. Altogether they contribute 67 (64) Tg CH₄ yr⁻¹ in the bottom-up (top-down) budget, around 55% of the global
4829 fossil fuel emissions. The bottom-up and top-down approaches generally agree in terms of ensemble mean, except for China
4830 for which the top-down estimates suggest lower emissions than the inventories. While Chinese fossil fuel emissions occur
4831 mainly through coal mining activity (88%), the Middle East, Russia and the USA extract mainly oil and gas (100%,
4832 80%,72%).
4833 The three largest contributors to the Agriculture and Waste sector remain South Asia, China, and Southeast Asia. Together
4834 they contribute 88 (92) Tg CH₄ yr⁻¹ in the bottom-up (top-down) budget, around 40% of the global agriculture and Waste
4835 sector. While the ensemble means tend to agree between bottom-up and top-down budgets, the uncertainty derived from the
4836 top-down approaches is larger, especially for these three regions. CH₄ emissions due to rice cultivation originate mostly
4837 from these same three regions (South East Asia, China and South Asia). Livestock management emissions occurs mainly in
4838 South Asia 20 [18-22] Tg CH₄ yr⁻¹, Brazil 12 [11-13] Tg CH₄ yr⁻¹, China 11 [8-16] Tg CH₄ yr⁻¹, and Europe 11 [10-12] Tg
4839 CH₄ yr⁻¹ (bottom-up estimates). The United States of America, Equatorial Africa, Northern Africa and Southwest South
4840 America emit between 7 Tg CH₄ yr⁻¹ and 10 Tg CH₄ yr⁻¹ in this sub-sector. Other regions emit less than 4 Tg CH₄ yr⁻¹ in the
4841 livestock management sector. The Waste sector emissions are dominated by three regions: China 11 [6-14] Tg CH₄ yr⁻¹,
4842 South Asia 9 [4-11] Tg CH₄ yr⁻¹, and Europe 8 [6-12] Tg CH₄ yr⁻¹ (bottom-up estimates). These three regions contribute
4843 around 40% of the global emissions of the Waste sector. It is worth noting that the uncertainty in the inventory estimates at
4844 the regional scale is around 40% (from the min-max range of the estimate, not including the uncertainty from each
4845 inventory).

4846 **6 Insights on the methane cycle from 2020-2022 during which there has been unprecedented high growth rates of**
4847 **methane emissions**

4848 The mean emissions estimate for the last year of the budget (2020) was 608 [581-627] Tg CH₄ yr⁻¹ (Top-down),) with 65%
4849 of the emissions from direct anthropogenic sources. This is 65 Tg CH₄ yr⁻¹ higher (11%) than the mean emissions of the
4850 2000-2009 decade and 6% higher than 2010-2019. 2020 was a second highest year in terms of atmospheric CH₄ growth rate
4851 (+15.2 ppb/yr) since systematic measurements began in the late 1980s, coming in just behind the highest in 2021 at 17.97
4852 ppb/yr. A few studies analysed the large growth rate increase between 2019 (+9.7 ppb/yr) and 2020 (+15.2 ppb/yr) of +5.4
4853 ppb/yr (corresponding to +14.4 ± 2.0 Tg CH₄ yr⁻¹) (Peng et al., 2022; Stevenson et al., 2022). Peng et al. (2022) estimated
4854 that the 2019-2020 growth rate change was almost equally due to an increase in wetland emissions (6.9 ± 2.1 Tg CH₄ yr⁻¹)
4855 and a decrease of the OH chemical loss (7.5 ± 0.8 Tg CH₄ yr⁻¹) due to reduced OH precursor emissions during the COVID
4856 lockdown (Laughner et al., 2021). The COVID19 lockdown resulted in decreased NO_x emissions and reduced fossil fuel
4857 related CH₄ emissions (Thorpe et al., 2023), leading to less OH production. At the global scale, Feng et al. (2023) calculated
4858 an emission increase of 27 Tg CH₄ yr⁻¹ between 2019 and 2020 considering constant OH, and a smaller increase of 21 Tg
4859 CH₄ yr⁻¹ when including a 1.4% decrease of OH. Increased emissions were mainly found in the northern tropics. Qu et al.
4860 (2022) also inferred a 31 Tg CH₄ yr⁻¹ increase of emissions, mostly in the tropics, half of it in Africa. Such a result is
4861 compatible with wetland driven abnormal emissions during a consecutive 3-year La Nina event spanning from 2020 to 2022
4862 (Zhang et al., 2023; Nisbet et al., 2023). The difference in terms of methodology and approaches between these three studies
4863 make it difficult to compare them quantitatively but provide a robust understanding on the possible causes. Importantly, all
4864 the studies indicate, in various proportions, increasing CH₄ emissions in the tropics and in the boreal region, potentially
4865 driven by microbial emission from wetlands due to wetter and warmer climate, and a significant contribution of reduced
4866 OH concentrations due to COVID lockdown.

4867 Based on our ensemble of data, we find that top-down approaches infer a much larger change in CH₄ emissions (median
4868 [Q1-Q3] at +23 [10-31] Tg CH₄ yr⁻¹) than bottom-up approaches (-1 [-5-3] Tg CH₄ yr⁻¹) between 2019 and 2020 (Fig. S7).
4869 Bottom-up approaches suggest a very small increase in wetland emissions (around +1 [0-3] Tg CH₄ yr⁻¹), while top-down
4870 approaches suggest on average a larger increase for wetlands of +8 [5-11] Tg CH₄ yr⁻¹, mainly in the tropics and mid-
4871 latitudes. It is worth noting that large uncertainties exist for a given year and that the inter annual variability is much lower
4872 than the ensemble spread. While bottom-up approaches suggest almost constant fossil fuel emissions and slight increase in
4873 agriculture and waste (+3 Tg CH₄ yr⁻¹), top-down approaches tend to derive higher emissions changes (+6 Tg CH₄ yr⁻¹
4874 from the fossil fuel sector and +11 Tg CH₄ yr⁻¹ from agriculture and waste as the median over the ensemble). Biomass
4875 burning emissions decreased using both approaches by about 5 Tg CH₄ yr⁻¹ in agreement with Peng et al. (2022). Some
4876 inversions were run with IAV of OH from Patra et al. (2021) and others with constant OH. However the inferred OH IAV
4877 in 2019 and 2020 are rather low (0.3% and 0.15% on yearly average) in Patra et al. (2021), leading to a small impact in

4878 [terms of emissions changes between 2019-2020, with +22 \[9-31\] \(median \[Q1-Q3\]\) based on the inversions with constant](#)
4879 [OH and 19 \[7-28\] based on the inversions with varying OH \(Fig S8\).](#)
4880 [This first analysis based on our ensemble shows how challenging it is to attribute CH₄ emissions changes to a specific sector](#)
4881 [or region between two years, because related uncertainties remain much larger than the targeted signal to explain. This calls](#)
4882 [again for further improvement of both approaches.](#)
4883 [NOAA estimates of 2021 and 2022 methane atmospheric growth rates 17.8.0±0.5 ppb/yr and 14.0±0.8 ppb/yr, respectively](#)
4884 [\(Lan et al., 2024\). They show a continuation of very high growth rates, challenging again our understanding of the methane](#)
4885 [budget. As of the time of submission of this manuscript, bottom-up estimates for anthropogenic emissions for 2021 and](#)
4886 [2022 are only available from the EDGARv8 data set \(\[https://edgar.jrc.ec.europa.eu/dataset_ghg80\]\(https://edgar.jrc.ec.europa.eu/dataset_ghg80\); EDGAR, 2023\). This](#)
4887 [research inventory suggests that anthropogenic emissions continued to increase from 2020 \(374 Tg CH₄ yr⁻¹\) to 2021 \(379](#)
4888 [Tg CH₄ yr⁻¹\) and 2022 \(386 Tg CH₄ yr⁻¹\) with around 62% of the increase due to the fossil fuel sources, 23 % from the](#)
4889 [Waste sector, and 14% from the agriculture sector \(Table S19\). The bottom-up estimate of wetland emissions for 2021-](#)
4890 [2023, derived from a single wetland model, indicates positive anomalies of 26 Tg CH₄ yr⁻¹ in 2020, 23 Tg CH₄ yr⁻¹ in](#)
4891 [2021, and 21 Tg CH₄ yr⁻¹ 2022 relative to the 2000-2006 baseline \(\[https://earth.gov/ghgcenter/data-catalog/lpjwsl-\]\(https://earth.gov/ghgcenter/data-catalog/lpjwsl-wetlandch4-grid-v1\)](#)
4892 [wetlandch4-grid-v1; Zhang et al., 2023\).](#)

4893 **7. Future developments, missing elements, and remaining uncertainties**

4894 [In this budget, robust features and uncertainties on sources and sinks estimated by bottom-up or top-down approaches have](#)
4895 [been highlighted as well as discrepancies between the two budgets. Limitations of the different approaches have also been](#)
4896 [highlighted. Four shortcomings of the CH₄ budget were already identified in Kirschke et al. \(2013\) and Sauniois et al. \(2016,](#)
4897 [2020\) and are revisited below pointing to key research areas. Although much progress has been made, they are still relevant,](#)
4898 [and actions are needed. However, these actions fall into different timescales and actors. Here, we revisit the four](#)
4899 [shortcomings of the contemporary methane budget and discuss how each weakness has been addressed since Sauniois et al.](#)
4900 [\(2020\). Each section ends by discussing remaining research needs with a list of suggestions, from higher to lower priority.](#)

- 4901
- 4902 1. [Shortcoming 1: Towards a decrease of the high uncertainty in the amount of methane emitted by wetland and inland](#)
4903 [water systems, and a weakened double counting issue.](#)

4904 [This first shortcoming has probably received the largest interest in the last few years with significant improvements. First a](#)
4905 [community effort has been made based on more studies, documenting, or modelling more inland freshwater systems and](#)
4906 [synthesising emissions from the complex and heterogeneous ensemble of emitting areas: wetlands, ponds, lakes, reservoirs,](#)
4907 [streams, rivers, estuaries, and marine systems. The range of wetland and inland water emissions has been narrowed down](#)
4908 [with improved wetland extent and refined estimates for inland freshwater systems. Double counting between inland](#)

Mis en forme : Police :Gras, Couleur de police : Noir

Mis en forme : Normal, Espace Avant : 24 pt, Après : 12 pt, Paragraphes solidaires, Bordure : Haut: (Pas de bordure), Bas: (Pas de bordure), Gauche: (Pas de bordure), Droite: (Pas de bordure), Entre : (Pas de bordure)

Supprimé : In this budget, uncertainties on sources and sinks estimated by bottom-up or top-down approaches have been highlighted as well as discrepancies between the two budgets. Limitations of the different approaches have also been highlighted. Four shortcomings of the methane budget were already identified in Kirschke et al. (2013) and Sauniois et al. (2016). Although progress has been made, they are still relevant, and actions are needed. However, these actions fall into different timescales and parties. In the following, we revisit the four shortcomings, or axis of research, of the current methane budget; how each weakness has been corrected since Sauniois et al. (2016), followed by a list of recommendations, from higher to lower priority, associated with the involved parties. ¶

Mis en forme : Normal, Hiérarchisation + Niveau : 1 + Style de numérotation : 1, 2, 3, ... + Commencer à : 1 + Alignement : Gauche + Alignement : 0 cm + Retrait : 0,63 cm, Bordure : Haut: (Pas de bordure), Bas: (Pas de bordure), Gauche: (Pas de bordure), Droite: (Pas de bordure), Entre : (Pas de bordure)

Mis en forme : Couleur de police : Noir

Supprimé : The remaining large uncertainties strongly suggest the need to develop more studies integrating the different systems (wetlands, ponds, lakes, reservoirs, streams, rivers, estuaries, and marine systems), to avoid double counting issues, to associate proper emission to each category, but also to account for lateral fluxes. Since Sauniois et al. (2016), several workshops (e.g. Turner et al., 2019) and publications (e.g. Knox et al., 2019; Thornton et al., 2016a) contributed to implement previous recommendations and strategies to reduce uncertainties of methane emissions due to wetlands and other freshwater systems. One achievement is the reduced estimate (by ~20%, i.e. 35 Tg CH₄ yr⁻¹) of the global wetland emissions, due to a refined wetland extent analysis and modifications of land surface model calibration. ¶ Methodology changes that could be integrated into the next methane budget releases include: ¶ Calibrating land surface models independently from top-down estimates; ¶ Evaluating land surface models against in-situ observations such as FLUXNET-CH₄ (Knox et al., 2019); and ¶ Using different wetland extent products to infer wetland emissions (e.g. WAD2M, GIEMS-2 (Prigent et al., 2020)). ¶

4943 freshwater systems has been estimated for the first time and accounted for in this budget. All these improvements decreased
 4944 the discrepancy between top-down and bottom-up estimate of combined wetland and inland freshwater emissions from
 4945 156 Tg CH₄ yr⁻¹ in Sauniois et al. (2020) down to 85 Tg CH₄ yr⁻¹ in this update for the 2000-2009 decade. Gridded maps
 4946 for lakes, ponds, reservoirs, and streams and rivers freshwater emissions have been produced over the past years (Johnson
 4947 et al., 2021, 2022; Rocher-Ros et al., 2023) making the spatial distribution of CH₄ sources almost complete for the first time
 4948 and allowing better description of prior emissions in future top-down inversions.

4949 Next steps include on the short term, from highest to lowest priority include:

4950 (i) integration of spatial distribution of inland waters in atmospheric inversion models to reach a full description of prior
 4951 methane sources and sinks.

4952 (ii) refinement of double counting estimation and its possible reduction with more precise spatial and temporal distributions
 4953 of the different systems contributing to inland freshwater emissions by using very high-resolution satellite data (down to
 4954 metre resolutions) to properly separate them. The development of a dynamical global high-resolution (typically few metres)
 4955 classification of saturated soils and inundated surfaces based on satellite data (visible and microwave), surface inventories,
 4956 and expert knowledge.

4957 (iii) continuation of ongoing efforts to calibrate and evaluate land surface models for wetland emissions against in-situ
 4958 observations such as FLUXNET-CH₄ (Knox et al., 2019; Delwiche et al., 2021) or BAWLD-CH₄ (Kuhn et al., 2021) for
 4959 boreal regions and avoid dependence on top-down estimates. It is still critical to increase the limited number of tropical
 4960 observations and to assimilate them in the inverse systems to help address the issue (e.g., Kallingal et al., 2023).

4961 (iv) continuation of ongoing efforts to develop a diversity of modelling approaches (among them process-based model or
 4962 machine learning approaches) to estimate wetland and inland freshwater CH₄ emissions, including lateral fluxes, and
 4963 reducing upscaling issues, as done by e.g. Zhuang et al. (2023) for lakes.

4964 (v) continuous integration of collected flux measurements such as in the FLUXNET-CH₄ activity (Knox et al., 2019;
 4965 Delwiche et al., 2021) or in BAWLD-CH₄ data set (Kuhn et al., 2021) to provide global flux maps based on machine
 4966 learning approaches or other approaches (Peltola et al., 2019, McNicol et al., 2023).

4967 Over the long run, developing measurement systems will help to improve estimates of the diversity of wetland and inland
 4968 freshwater sources, and further reduce uncertainties:

4969 - More systematic measurements of CH₄ fluxes and their isotopic signatures from sites reflecting the diversity of
 4970 environment of wetlands and inland waters, complemented with environmental meta-data (e.g., soil temperature
 4971 and moisture, vegetation types, water temperature, acidity, nutrient concentrations, NPP, soil carbon density for
 4972 wetlands, lake morphologies) will allow us to better understand and estimate the processes of production and
 4973 transport to the atmosphere (diffusive, ebullitive, plants mediated...) and to better constrain methane fluxes and
 4974 their isotopic signatures in the different modelling approaches (Glagolev et al., 2011; Turetsky et al., 2014).

4975

Supprimé: , in

Supprimé: , for modelling, can be addressed by the land biogeochemistry community:

Supprimé: Finalizing a

Mis en forme : Normal, Sans numérotation ni puces

Supprimé: tens of meters

Supprimé: This improved area distribution will prevent double counting between wetlands and other freshwater systems, when used by land surface models;

Supprimé: <#>Finalizing ongoing efforts to develop process-based modelling approaches to estimate freshwater methane emissions, including lateral fluxes, and avoiding upscaling issues, as recently done by e.g. Maavara et al. (2019) for N₂O; and <#>Using the collected flux measurements within the FLUXNET-CH₄ activity (Knox et al., 2019) to provide global flux maps based on machine learning approaches (Peltola et al., 2019).</#>

Supprimé: water

Supprimé: <#>More systematic measurements from sites reflecting the diverse lake morphologies will allow us to better understand the short-term biological control on ebullition variability, which remains poorly known (Wik et al., 2014, 2016a); and <#>Extending monitoring of methane fluxes year round from the different natural sources (wetlands, freshwaters) complemented with environmental meta-data (e.g., soil temperature and moisture, vegetation types, water temperature, acidity, nutrient concentrations, NPP, soil carbon density) will allow us to enrich the FLUXNET-CH₄ observation dataset, and to better constrain methane fluxes and their isotopic signatures in land-surface models (Glagolev et al., 2011; Turetsky et al., 2014).</#>

5006 2. Shortcoming 2: Towards a better assessment of uncertainties for global methane sinks in top-down and bottom-up
5007 budgets.

5008 The inverse systems used here have similar caveats than those described in Saunois et al. (2016, 2020) (same OH field, same
5009 kind of proxy method to optimise it) leading to quite constrained atmospheric sink and therefore total global CH₄ sources.
5010 Although we have used the latest release of CCMI-2022 (Plummer et al., 2021) and CMIP6 simulations (Collins et al.,
5011 2017), the uncertainty of derived CH₄ chemical loss from the chemistry climate models remains at the same (large) level
5012 compared to the previous intercomparison project ACCMIP (Lamarque et al., 2013). The causes of uncertainties on the
5013 CH₄ loss and the differences between the different OH fields derived from Chemistry Transport Models (CTM) and Climate
5014 Chemistry Models (CCM) have been widely discussed (Nicely et al., 2017; Zhao et al., 2019). These results emphasise the
5015 need to first assess, and then improve, atmospheric transport and chemistry models, especially vertically, and to integrate
5016 robust representation of OH fields in atmospheric models. For the latter, Zhao et al. (2023) have proposed a new approach
5017 based on OH precursor observations and a chemical box model to improve the 3D distributions of tropospheric OH radicals
5018 obtained from atmospheric chemistry models. Finally, soil uptake estimates rely on very few studies, and interannual
5019 variations remain underconstrained.

5020 Next steps, in the short term, could include developments by the modelling community in:

- 5021 - Estimating the soil uptake with different land surface models (creating an ensemble) and discussing its variations
5022 over the past decade.
- 5023 - Assessing the impact of using updated and varying soil uptake estimates, especially considering a warmer climate
5024 in the top-down approach. Indeed, for top-down models resolving for the net flux of CH₄ at the surface integrating
5025 a larger estimate of soil uptake would allow larger emissions, and then reduce the uncertainty with the bottom-up
5026 estimates of total CH₄ sources.
- 5027 - Further studying the reactivity of the air parcels in the chemistry climate models and defining new diagnostics to
5028 assess modelled CH₄ lifetimes.
- 5029 - Applying Zhao et al. (2023) recipe to several CTM used for top-down inversions in order to increase consistency
5030 between source and sink estimates in individual approaches.
- 5031 - Developing 3D inverse methods to optimise OH using CH₄ satellite data (Zhang et al., 2018) or halogenated
5032 compounds beyond methyl chloroform (MCF), such as done in box models (Thompson et al., 2024) to derive a 3D
5033 dynamical OH field or machine learning methods using satellite data to constrain OH (Anderson et al., 2023).
- 5034 - Integrating the aforementioned different potential OH chemical fields, including also inter-annual variability, to
5035 assess the impact on the methane budget following Zhao et al. (2020).

5036 Over the long run, other parameters should be (better) integrated into top-down approaches, among them:

- 5037 - The magnitude of the CH₄ loss through oxidation by tropospheric Cl, a process debated in the recent literature.
5038 More modelling (e.g., Thanwerdas et al., 2022b) and instrumental studies should be devoted to reducing the

Mis en forme : Couleur de police : Noir

Mis en forme : Normal, Hiérarchisation + Niveau : 1 + Style de numérotation : 1, 2, 3, ... + Commencer à : 1 + Alignement : Gauche + Alignement : 0 cm + Retrait : 0,63 cm, Bordure : Haut: (Pas de bordure), Bas: (Pas de bordure), Gauche: (Pas de bordure), Droite: (Pas de bordure), Entre : (Pas de bordure)

Supprimé : The inverse systems used here have the same caveats as described in Saunois et al. (2016) (same OH field, same kind of proxy method to optimize it) leading to quite constrained atmospheric sink and therefore total global methane sources. Although we have used a state-of-the-art ensemble of Chemistry Transport Models (CTM) and Climate Chemistry Models (CCM) simulations from the CCMI (Chemistry-Climate Model Initiative, Morgenstern et al. (2017)), the uncertainty of derived CH₄ chemical loss from the chemistry climate models remains at the same (large) level compared to the previous intercomparison project ACCMIP (Lamarque et al., 2013). Nicely et al. (2017) found that the main cause of the large differences in the CTM representation of CH₄ lifetime is variations in the chemical mechanisms implemented in the models. Using the ensemble of CTMs and CCMs from the CCMI experiment, Zhao et al. (2019) quantified the range of CH₄ loss induced by the ensemble of OH fields to be equivalent up to about half of the discrepancies between CH₄ observations and simulations as forced by the current anthropogenic inventories. These results emphasize the need to first assess, and then improve, atmospheric transport and chemistry models, especially vertically, and to integrate robust representation of OH fields in atmospheric models. Methodology changes that could be integrated into the next methane budget include: Integrating sensitivity tests on the prior fluxes (use of updated fluxes for natural sources, soil uptake); and Integrating sensitivity tests on chemical sinks (different OH fields, including interannual variability).

Supprimé : atmospheric

Mis en forme : Couleur de police : Noir

Mis en forme : Normal, Hiérarchisation + Niveau : 1 + Style de numérotation : Puce + Alignement : 0,63 cm + Retrait : 1,27 cm, Bordure : Haut: (Pas de bordure), Bas: (Pas de bordure), Gauche: (Pas de bordure), Droite: (Pas de bordure), Entre : (Pas de bordure)

Supprimé :

Mis en forme : Couleur de police : Noir

Supprimé :

Mis en forme : Couleur de police : Noir, Anglais (G.B.)

Supprimé :

Supprimé : <#>Developing robust representation of 3D OH fields to be used in the inverse models: based on chemistry climate models and using correction from measurements, on multi-
... [113]

Mis en forme : Couleur de police : Noir

Mis en forme ... [113]

Supprimé : chlorine, a process debated in the recent literature. More modeling (Thanwerdas et al., 2019) and instrumental studies

5087 uncertainty of this potential additional sink before integrating it in top-down models. This would be especially
5088 critical if inversions using ¹³C-CH₄ observations are included in GMB in the future.

5090 3. Shortcoming 3: Towards a better partitioning of methane sources and sinks by region and process using top-down
5091 models

5092 In this work, we report inversions assimilating satellite data from GOSAT, which bring more constraints than provided by
5093 surface stations alone, especially over tropical continents. However, we still found that satellite- and surface-based
5094 inversions, and the different inversion systems do not consistently infer the same regional flux distribution.

5095 The estimates contributing to the Global Methane budget are further used in more specific studies focusing on the
5096 comparison of the estimates from bottom-up and top-down approaches at national (Deng et al., 2022) and regional scales,
5097 including efforts from the GCP-REgional Carbon Cycle Assessment and Processes (RECCAP2) (Petrescu et al., 2021; 2023;
5098 Tibrewal et al., 2024; Lauerwald et al., 2023b; and other RECCAP-2 publications to come, see
5099 <https://www.globalcarbonproject.org/reccap/publications.htm>).

5100 Next steps, in the short term, could integrate developments to be made by the top-down community:

- 5101 - Including GOSAT 2 retrievals (Noël et al., 2022; Imasu et al., 2023) for the GOSAT-based inversions and
5102 considering TROPOMI-based inversions (as done in Tsuruta et al. (2023), Shen et al. (2023), Chen et al. (2022)
5103 and Qu et al. (2021)) in the next releases once at least 8 years of data are available to provide a decadal estimate
5104 and biases are reduced for global scale use (Lorente et al., 2023; Balasu et al., 2023). Indeed, recent satellite
5105 developments have provided higher temporal and spatial resolutions of CH₄ observations in regions with poor in-
5106 situ measurements (Figure S9, such as TROPOMI observations in North Africa).
- 5107 - Integrating the newly available updated gridded products for the different natural sources of CH₄ in their prior
5108 fluxes (e.g. inland freshwaters) to reach a full spatial description of sources and sinks, and to be able to better
5109 compare the top-down budget with the bottom-up budget.
- 5110 - Integration of the newly developed 4D variational inversion systems using isotopic species in the top-down budget
5111 (Basu et al., 2022; Thanwerdas et al., 2024; Drinkwater et al. 2023; Mannisenaho et al., 2023).
- 5112 - Improving the availability of in-situ data at high temporal resolution for the scientific community, especially ones
5113 covering poorly documented regions such as China (Liu et al., 2021b; Guo et al., 2020), India (Nomura et al., 2021;
5114 Lin et al., 2015; Tiwari and Kumar, 2012) and Siberia (Sasakawa et al., 2010, 2017; Fujita et al., 2020; Winderlich
5115 et al., 2010), which are not delivered so far to international databases, or only at poor temporal resolution.
- 5116 - Integrating the information from imagery satellites (e.g., TROPOMI, Carbon Mapper, Methane Sat, GHG Sat.) of
5117 high to super-emitters to improve prior fluxes of anthropogenic emissions in terms of quantity and locations for
5118 each covered sector.

Supprimé:

Mis en forme : Normal, Hiérarchisation + Niveau : 1 + Style de numérotation : 1, 2, 3, ... + Commencer à : 1 + Alignement : Gauche + Alignement : 0 cm + Retrait : 0,63 cm, Bordure : Haut: (Pas de bordure), Bas: (Pas de bordure), Gauche: (Pas de bordure), Droite: (Pas de bordure), Entre : (Pas de bordure)

Mis en forme : Couleur de police : Noir

Supprimé: inversions

Déplacé vers le bas [3]: Methodology changes that could be integrated into the next methane budget releases include:¶

Supprimé: Integrating GOSAT and GOSAT-2 (launched in October 2018, with expected improved precision and accuracy (JAXA, 2019)) for the satellite inversion; and ¶ Investigating the reasons for the regional differences derived by the inverse systems based on the model evaluation and more detailed questionnaire to the modelers on the treatment of satellite data (bias correction) and stratospheric profiles. ¶

Supprimé: <#>Evaluating the benefits of using new satellite missions with high spatial resolution and "imaging capabilities" (Crisp et al., 2018) at the global scale, such as the TROPOMI instrument on Sentinel 5P, launched in October 2017 (Hu et al., 2018).¶

Mis en forme : Couleur de police : Noir

Mis en forme : Normal, Hiérarchisation + Niveau : 1 + Style de numérotation : Puce + Alignement : 0,63 cm + Retrait : 1,27 cm, Bordure : Haut: (Pas de bordure), Bas: (Pas de bordure), Gauche: (Pas de bordure), Droite: (Pas de bordure), Entre : (Pas de bordure)

Mis en forme : Couleur de police : Noir

Supprimé: :

Supprimé: Releasing more regular updates and intercomparison

Supprimé: emission inventories in order to improve prior scenarios of inverse studies and reduce

Supprimé: need for extending them beyond their available coverage:¶
Developing

Supprimé: system

Mis en forme : Couleur de police : Noir

Supprimé: and/or co-emitted

Mis en forme : Couleur de police : Noir

Supprimé: . Indeed methane isotopes can provide additional constraints to partition the different CH₄ sources and sinks, if isotopic signatures can be better known spatially and temporally.¶5

Mis en forme : Couleur de police : Noir

Mis en forme : Couleur de police : Noir

Supprimé: <#>Improving the availability of in-situ data for the scientific community, especially ones covering poorly documented ¶6

5168 Over the long run, integrating more measurements and regional studies will help to improve the top-down systems, and
5169 further reduce the uncertainties:

- 5170 - Extending the CH₄ surface networks to poorly observed regions (e.g., Tropics, China, India, high latitudes) and to
5171 the vertical dimension: aircraft regular measurements (e.g., Filges et al., 2015; Brenninkmeijer et al., 2007; Paris
5172 et al., 2010; Sweeney et al., 2015); Aircore campaigns (e.g., Andersen et al., 2018; Membrive et al., 2017); TCCON
5173 observations (e.g., Wunch et al., 2011, 2019) remains critical to complement satellite data that do not observe well
5174 in cloudy regions and at high latitudes, and also to evaluate and eventually correct satellite biases (Buchwitz et al.,
5175 2016).
- 5176 - Extending and developing continuous isotopic measurements of CH₄ to help partitioning methane sources and to
5177 be integrated in 4D variational isotopic inversions (e.g., Yacovitch et al., 2021).
- 5178 - Integrating global data from future satellite instruments with intrinsic low-bias, such as active LIDAR techniques
5179 with MERLIN (Ehret et al., 2017), that are promising to overcome issues of systematic errors (Bousquet et al.,
5180 2018) and should provide measurements over the Arctic, contrary to the existing and planned passive missions.
- 5181 - Other co-emitted species such as radiocarbon for fossil/non-fossil emissions (Lassey et al., 2007a, 2007b; Petrenko
5182 et al., 2017), CO (e.g., Zheng et al., 2019) for biomass burning emissions, and ethane for fugitive emissions (e.g.,
5183 Ramsden et al., 2022) could bring additional information for partitioning emissions.

5184
5185 4. Shortcoming 4: Towards reducing uncertainties in the modelling of atmospheric transport in the models used in the
5186 top-down budget

5187 The TRANSCOM experiment synthesised in Patra et al. (2011) showed a large sensitivity of the representation of
5188 atmospheric transport on CH₄ abundances in the atmosphere. In particular, the modelled CH₄ budget appeared to depend
5189 strongly on the troposphere-stratosphere exchange rate and thus on the model vertical grid structure and circulation in the
5190 lower stratosphere. Also, regional changes in the CH₄ budget depend on the characteristics of the atmospheric transport
5191 models used in the inversion (Bruhwiler et al., 2017; Locatelli et al., 2015). This axis of research is demanding important
5192 development from the atmospheric modelling community. Waiting for future improvements (finer horizontal and vertical
5193 resolutions, more accurate physical parameterization, increase in computing resources...), assessing atmospheric transport
5194 error and the impact on the top-down budget remain crucial and mostly rely on the use of an ensemble of models.
5195 Methodology changes that could be integrated into the next methane budget releases include:

- 5196 - Evaluating more deeply the inversions provided against independent measurements such as aircraft regular
5197 campaigns available through for example the CH₄ GLOBALVIEWplus v6.0 ObsPack (Schuldt et al., 2023), the
5198 IAGOS data portal (<https://iagos.aeris-data.fr/download/>), the NIES portal
5199 (<https://db.cger.nies.go.jp/ged/en/datasetlist/index.html>) for CONTRAIL (e.g., Machida et al., 2008) and Siberian
5200 measurements (e.g., Sasakawa et al., 2017), the WDCG data portal (<https://gaw.kishou.go.jp/>) for additional

Supprimé: <#>Integrating global data from future satellite instruments with intrinsic low-bias, such as active LIDAR techniques with MERLIN (Ehret et al., 2017), that are promising to overcome issues of systematic errors (Bousquet et al., 2018) and should provide measurements over the Arctic, contrary to the existing and planned passive missions; <#>Extending the CH₄ surface networks to poorly observed regions (e.g. Tropics, China, India, high latitudes) and to the vertical dimension: aircraft regular campaigns (e.g. Paris et al., 2010; Sweeney et al., 2015); Aircore campaigns (e.g. Andersen et al., 2018; Membrive et al., 2017); TCCON observations (e.g. Wunch et al., 2011, 2019). These observations are still critical to complement satellite data that do not observe well in cloudy regions and at high latitudes, and also to evaluate and eventually correct satellite biases (Buchwitz et al., 2016); <#>

Mis en forme : Couleur de police : Noir

Supprimé: methane using laser-based instruments

Mis en forme : Couleur de police : Noir

Mis en forme : Normal, Hiérarchisation + Niveau : 1 + Style de numérotation : Puce + Alignement : 0,63 cm + Retrait : 1,27 cm, Bordure : Haut: (Pas de bordure), Bas: (Pas de bordure), Gauche: (Pas de bordure), Droite: (Pas de bordure), Entre : (Pas de bordure)

Supprimé :

Supprimé: <#>Developing regional components of the CH₄ budget to improve global totals by feeding them with regional top-down and bottom-up approaches; for example, regional inversions using regional measurements and high resolution models (such as the INGOS project (Bergamaschi et al., 2018b) or the VERIFY project (<https://verify.lsce.ipsl.fr>) with the European ICOS network (<https://www.icos-rf.eu/home>). The RECCAP-2 project should also provide a scientific framework to further refine GHG budgets, including methane, at regional scales (<https://www.reccap2-gotemba2019.org/>). <#>

Mis en forme : Normal, Hiérarchisation + Niveau : 1 + Style de numérotation : 1, 2, 3, ... + Commencer à : 1 + Alignement : Gauche + Alignement : 0 cm + Retrait : 0,63 cm, Bordure : Haut: (Pas de bordure), Bas: (Pas de bordure), Gauche: (Pas de bordure), Droite: (Pas de bordure), Entre : (Pas de bordure)

Mis en forme : Couleur de police : Noir

Déplacé (insertion) [4]

Mis en forme : Anglais (G.B.)

Déplacé (insertion) [3]

Supprimé: The TRANSCOM experiment synthesised in Patra et al. (2011) showed a large sensitivity of the representation of atmospheric transport on methane concentrations in the atmosphere. In particular, the modelled CH₄ budget appeared to depend strongly on the troposphere-stratosphere exchange rate and thus on the model vertical grid structure and circulation in the lower stratosphere. Also, regional changes in the methane budget depends on the characteristics of the atmospheric transport models

flights over three other Japanese airports and Orléans, France ; Aircore campaigns data set can be downloaded through the NOAA Global Monitoring Laboratory website (<https://gml.noaa.gov/ccgg/arc/?id=144>, Baier et al., 2021) and the French AirCore Program for atmospheric sampling (<https://aircore.aeris-data.fr>, Membrive et al., 2017); TCCON observations (<https://tcconda.org>; e.g., Wunch et al., 2011, 2019), and use this evaluation to weight the different models used in the CH₄ budget.

Next steps, in the short term, could include some development to be addressed by the top-down community to reduce atmospheric transport errors:

- Developing further methodologies to extract stratospheric partial column abundances from observations such as TCCON data (Saad et al., 2014; Wang et al., 2014), Aircore (e.g. Andersen et al., 2018; Membrive et al., 2017) or ACE-FTS (De Mazière et al., 2018) or MIPAS (Glatthor et al., 2023) satellite data.
- Combining SWIR and TIR measurements from space to better constrain the tropospheric column, from TROPOMI and IASI for example in the MethanePlus ESA project (<https://methaneplus.eu/#docs>, Buchwitz et al., 2023) or GOSAT (Kuze et al., 2020).
- Porting transport models codes to run on Graphics processing Units (GPU) to achieve sub-degrees resolution global inversions (Chevallier et al., 2023).

In the long run, developments within atmospheric transport models such as the implementation of hybrid vertical coordinates (Patra et al., 2018) or of hexagonal-icosahedric grid with finer resolution (Dubos et al., 2015; Niwa et al., 2017, 2022; Lloret et al., 2023), and improvements in the simulated boundary layer dynamics are promising to reduce atmospheric transport errors.

8 Conclusions

We have built an updated global methane budget by using and synthesizing a large ensemble of published methods and new results using a consistent, transparent, and traceable approach, including atmospheric observations and inversions (top-down models), process-based models for land surface emissions and atmospheric chemistry, and inventories of anthropogenic emissions (bottom-up models and inventories). For the 2010-2019 decade, global CH₄ emissions are 575 Tg CH₄ yr⁻¹ (range of 553-586 Tg CH₄ yr⁻¹), as estimated by top-down inversions. About 65% of global emissions are anthropogenic (range of 63-68%). Bottom-up models and inventories suggest larger global emissions (669 Tg CH₄ yr⁻¹ [512-849]) mostly because of larger and more uncertain natural emissions from inland freshwater systems, natural wetlands, and geological leaks, and likely some unresolved double counting of these sources. It is also likely that some of the individual bottom-up emission estimates are too high, leading to larger global emissions from the bottom-up approach than the atmospheric constraints suggest. However, the important progress in this update is that for the first time, the bottom-up and top-down budgets agree within their uncertainty ranges. This is substantial progress toward defining more accurate global methane emissions.

Déplacé vers le haut [4]: This axis of research is demanding important development from the atmospheric modelling community. Waiting for future improvements (finer horizontal and vertical resolutions, more accurate physical parameterization, increase in computing resources...), assessing atmospheric transport error and the impact on the top-down budget

Mis en forme : Anglais (G.B.)

Supprimé: remains crucial. Methodology changes that could be integrated into the next methane budget releases include: Evaluating the inversions provided against independent measurements such as aircraft regular campaigns (e.g. Paris et al., 2010; Sweeney et al., 2015); Aircore campaigns (e.g. Andersen et al., 2018; Membrive et al., 2017); TCCON observations (e.g. Wunch et al., 2011, 2019), and use this evaluation to weight the different models used in the methane budget

Mis en forme : Anglais (G.B.)

Mis en forme : Couleur de police : Noir, Anglais (G.B.)

Mis en forme : Normal, Hiérarchisation + Niveau : 1 + Style de numérotation : Puce + Alignement : 0,63 cm + Retrait : 1,27 cm, Bordure : Haut: (Pas de bordure), Bas: (Pas de bordure), Gauche: (Pas de bordure), Droite: (Pas de bordure), Entre : (Pas de bordure)

Supprimé: (Saad et al., 2014; Wang et al., 2014), Aircore or, even ACE-FTS or MIPAS satellite data, and use them to replace erroneous simulated stratospheric profiles

Mis en forme : Couleur de police : Noir

Supprimé: In the long run, developments within atmospheric transport models such as the implementation of hybrid vertical. [118]

Mis en forme ... [119]

Mis en forme : Police :Gras, Couleur de police : Noir

Supprimé: a

Supprimé: synthesizing

Supprimé: and

Supprimé: 2008-2017

Supprimé: 576

Supprimé: 550-594

Supprimé:

Supprimé: 60

Supprimé: 50-70

Supprimé: much

Supprimé: 737

Supprimé: 594-881

Supprimé: water

Supprimé: some

Supprimé: perspective

320 The latitudinal breakdown inferred from the top-down approach reveals a dominant role of tropical emissions (~64%)
 321 compared to mid (~32%) and high (~4%) northern latitudes (above 60°N) emissions.

322 Our results, including an extended set of atmospheric inversions, are compared with the previous budget syntheses of
 323 Kirschke et al. (2013) and Saunois et al. (2016; 2020). They show overall good consistency when comparing the same
 324 decade (2000-2009) at the global and latitudinal scales. The magnitude and uncertainty of most natural or indirect
 325 anthropogenic sources have been revised and updated. In particular, this new budget benefits from large efforts and
 326 collaborations from the research community to provide improved estimates of the magnitude and uncertainty of the different
 327 freshwater sources and helps reduce the potential double counting at the global scale. Of note, newly available gridded
 328 datasets for lakes, ponds, reservoirs, streams, and rivers allow building latitudinal and regional estimates for all these sources
 329 for the first time in these estimates. In the next review, we hope to be able to reduce uncertainties in emissions from inland
 330 freshwater systems by better quantifying the emission factors of each contributing sub-systems (streams, rivers, lakes,
 331 ponds) and estimating double counting at regional scale or avoiding double counting by better defining the surface areas of
 332 each ecosystem. Another important priority for improvements is the uncertainty on the chemical loss of CH₄ which still
 333 needs to be better assessed in both the top-down and the bottom-up budgets. Building on the improvement of the points
 334 detailed in Sect. 7, our aim is to update this budget synthesis as a living review paper regularly (~every three or four years).
 335 Each update will produce a more recent decadal CH₄ budget, highlight changes in emissions and trends, and incorporate
 336 newly available data and model improvements.

337 ▼

338 It is still under debate why exactly there are sustained increase of atmospheric CH₄ (more than +5 ppb yr⁻¹) since 2007
 339 (Nisbet et al., 2019; Turner et al., 2019). Some likely explanations, already introduced by Saunois et al. (2017) and further
 340 investigated by Jackson et al. (2020) and other studies, include, by decreasing order of certainty: 1) a positive contribution
 341 from microbial and fossil sources (e.g., Nisbet et al., 2019; Schwietzke et al., 2016; Jackson et al., 2020), a negative
 342 contribution from biomass burning emissions before 2014 (Giglio et al., 2013; Worden et al., 2017); 2) a negligible role of
 343 Arctic emission changes (e.g., Nisbet et al., 2019; Saunois et al., 2017); and 3) a tropical dominance of the increasing
 344 emissions (e.g., Saunois et al., 2017; Jackson et al., 2020; Wilson et al., 2021; Drinkwater et al., 2023). Although the
 345 accelerated atmospheric methane growth rate in 2020 (15.2 ppb/yr) has found some explanation with the impact of the world
 346 Pandemia in 2020, the sustained observed growth rates in 2021 (17.8 ppb/yr) and 2022 (14 ppb/yr) still challenge our
 347 understanding of the global methane cycle. While in Jackson et al. (2020), the increase in CH₄ emissions over the last two
 348 decades is attributed entirely to direct anthropogenic emissions, the uncertainty range from the GMB ensemble is large, and
 349 the contribution from natural emissions (wetlands) is still largely uncertain. Besides the decadal change in CH₄ emissions,
 350 large inter-annual variability can occur from these natural emissions. The recent high record of CH₄ growth rate highlights
 351 the potential of large variations from natural emissions from one year to another, in particular wetland emissions (e.g., Peng
 352 et al., 2022; Feng et al., 2023). These remain the challenges to be overcome in better quantifying global methane emissions.

Supprimé: approaches

Supprimé: (2013) and Saunois et al. (2016), and show overall good consistency when comparing the same decade (2000-2009) at the global and latitudinal scales, although estimation methods and reported studies have evolved between the three budgets. While, a comparison of top-down emissions estimates determined with and without satellite data agrees well globally they differ significantly at the latitudinal scale. Most worryingly, these differences were not even consistent in sign with some models showing notable increases in a given latitudinal flux and others decreases. This suggests that while the inclusion of satellite data may, in the future, significantly increase our ability to attribute fluxes regionally this is not currently the case due to their existing inherent biases along with the inconsistent application of methods to account for these biases, but also differences in model transport, especially in the stratosphere (see recommendations in Sect. 6).

Supprimé: Among the different uncertainties raised in Kirschke et al. (2013), Saunois et al. (2016) estimated that 30-40% of the large range associated with modelled wetland emissions in Kirschke et al. (2013) was due to the estimation of wetland extent. Here, wetland emissions are 35 Tg CH₄ yr⁻¹ smaller than previous estimates due to a refinement of wetland extent. The magnitude and uncertainty of all other natural sources have been revised and updated, leading to smaller emission estimates for oceans, geological sources, and wild animals, but higher emission estimates associated to larger range for non-wetland freshwater systems. This result places a number one priority on reducing uncertainties in emissions from inland water systems by better quantifying the emission factors of each contributing sub-systems (streams, rivers, lakes, ponds) and reducing both uncertain up-scaling and likely double counting with wetland emissions. As a second priority, the uncertainty on the chemical loss of methane need to be better assessed in both the top-down and the bottom-up budgets. Our work also suggests the need for more interactions among groups developing emission inventories in order to clarify the definition of the sectoral breakdown in inventories. Such an approach would allow easier comparisons at the sub-category scale. ¶

Building on the improvement of the points detailed in Sect. 6, our aim is to update this budget synthesis as a living review paper regularly (~every two/three years). Each update will produce a more recent decadal CH₄ budget, highlight changes in emissions and trends, and incorporate newly available data and model improvements. ¶

In addition to the decadal CH₄ budget presented in this paper, and following former studies (e.g. Bousquet et al., 2006), trends and year-to-year changes in the methane cycle continues to be thoroughly discussed in the recent literature (e.g. Nisbet et al., 2019; Turner et al., 2019). After almost a decade of stagnation in the late 1990s and early 2000s (Dlugokencky et al., 2011; Nisbet et al., 2016), a sustained atmospheric growth rate of more than +5 ppb yr⁻¹ has been observed since 2007, with a further acceleration after 2014 (Nisbet et al., 2019), and several years with a 2-digit atmospheric growth as in the 1980s. To date, no consensus has yet been reached in explaining the CH₄ trend since 2007. A likely explanatory scenario, already introduced in Saunois et al. (2017) and further investigated by some other studies since then, includes, by decreasing order of certainty, a positive contribution from microbial and fossil sources (e.g. Nisbet et al., 2019; Schwietzke et al., 2016), a negative contribution from biomass burning emissions before 2014 (Giglio et al., 2013; Worden et al., 2017), a downward revision of Chinese emissions, a negligible role of Arctic emission changes (e.g. Nisbet et al., 2019; Saunois et al., 2020).

5474 The GCP will continue to support and coordinate the development of improved flux estimates for all budget components
5475 and new underlying science to support improved modelling, acquisition of observations, and data integration. At regular
5476 intervals (3-4 years), we will continue to bring all flux components together to produce an improved and updated global
5477 CH₄ budget, and provide a global benchmark for other CH₄ products and assessments.

5478 **2 Data availability**

5479 The data presented here are made available in the belief that their dissemination will lead to greater understanding and new
5480 scientific insights on the methane budget and changes to it, and help to reduce its uncertainties. The free availability of the
5481 data does not constitute permission for publication of the data. For research projects, if the data used are essential to the
5482 work to be published, or if the conclusion or results largely depend on the data, co-authorship should be considered. Full
5483 contact details and information on how to cite the data are given in the accompanying database.

5484 The accompanying database includes a netcdf file defining the regions used, an archive with the maps of prior fluxes used
5485 in the top-down activity, an archive with data corresponding to Fig. 3 and 5, and one Excel file organised in the following
5486 spreadsheets.

5487 The file Global_Methane_Budget_2000-2020_v1.0.xlsx includes (1) a summary, (2) the methane observed mixing ratio and
5488 growth rate from the four global networks (NOAA, AGAGE, CSIRO and UCI), (3) the evolution of global anthropogenic
5489 methane emissions (including biomass burning emissions) used to produce Fig. 2, (4) the global and latitudinal budgets over
5490 2000–2009 based on bottom-up approaches, (5) the global and latitudinal budgets over 2000–2009 based on top-down
5491 approaches, (6) the global and latitudinal budgets over 2010–2019 based on bottom-up approaches, (7) the global and
5492 latitudinal budgets over 2010–2019 based on top-down approaches, (8) the global and latitudinal budgets for year 2020
5493 based on bottom-up approaches, (9) the global and latitudinal budgets for year 2020 based on top-down approaches, and
5494 (10) the list of contributors to contact for further information on specific data.

5495 This database is available from ICOS Carbon Portal (<https://doi.org/10.18160/GCP-CH4-2024/>, Martinez et al., 2024).

5497 **Author contributions.**

5498 MS, AM, and JT gathered the bottom-up and top-down data sets and performed the post processing and analysis.
5499 MS, BP, PB, PeC, and RJ coordinated the global budget. MS, BP, PB, PeC, RJ, PP and PCi contributed to the update of the
5500 full text and all coauthors appended comments. AM, ED, and XI produced the figures. DJB, NG, PH, AI, AJ, TK, TL, XI,
5501 KMcD, JMe, JMu, SP, CP, WR, HT, YY, WZ, ZZ, Qing Z, Qian Z and Qianlai Z performed surface land model simulations
5502 to compute wetland emissions. GA, DB, SC, BRD, GE, MAH, GH, MSJ, RL, SN, GRR, JAR, EHS, PRa, Pre, and TSW
5503 provided data sets useful for natural emission estimates and/or contributed to text on bottom-up natural emissions. LHI, SJS,
5504 TNF, GRvW, and MC provided anthropogenic data sets and contributed to the text for this section. AM, JT, PP, DBe, RJ,

Mis en forme : Normal, Espace Avant : 24 pt, Après : 12 pt, Paragraphes solidaires, Bordure : Haut: (Pas de bordure), Bas: (Pas de bordure), Gauche: (Pas de bordure), Droite: (Pas de bordure), Entre : (Pas de bordure)

Mis en forme : Police :Gras, Couleur de police : Noir

Supprimé : helping

Supprimé : organized

Supprimé : and two netcdf files defining the regions used to extend the anthropogenic inventories

Supprimé : 2017_v2

Supprimé : 2008–2017

Supprimé : 2008–2017

Supprimé : 2017

Supprimé : 2017

Supprimé : (<https://doi.org/10.18160/GCP-CH4-2019>, Saunois

Supprimé : 2019) and the Global Carbon Project (<http://www.globalcarbonproject.org>).

Supprimé : AS

Supprimé : BP

Supprimé : AS

Supprimé : AS

Supprimé : SH

Supprimé : MS

Supprimé : GP

Supprimé : VA

Supprimé : FJ

Supprimé : LL

Supprimé : PM,

Supprimé : SP,

Supprimé : HS,

Supprimé : MC, PC,

Supprimé : KC

Supprimé : KMJ, GL

Supprimé : CP

Supprimé : Pre, BT, NV, TW

Supprimé : usefull

Supprimé : contribute

Supprimé : GJM, FT, GvW, KMC,

Supprimé : contribute

Supprimé : BP, NC, MI, SM, JMcN

540 YN, AS, AT, and BZ performed atmospheric inversions to compute top-down methane emission estimates for sources and
 541 sinks. EJD, XL, DRB, PBK, JM, RJP, MR, MS, DWo, and YYo are PI of atmospheric observations used in top-down
 542 inversions and/or contributed the text describing atmospheric methane observations. FD, MS, and JT contributed to the
 543 bottom-up chemical sink section by providing data sets, processing data and/or contributing to the text. FMF provided data
 544 for the soil sink.

546 **Competing interests.** At least one of the (co-)authors is a member of the editorial board of Earth System Science Data.

548 Acknowledgements

549 This paper is the result of a collaborative international effort under the umbrella of the Global Carbon Project, a project of
 550 Future Earth and a research partner of the World Climate Research Programme (WCRP). We acknowledge all the people
 551 and institutions who provided the data used in the global methane budget as well as the institutions funding parts of this
 552 effort (see Table A3). We acknowledge the modelling groups for making their simulations available for this analysis, the
 553 joint WCRP Stratosphere-troposphere Processes And their Role in Climate/International Global Atmospheric Chemistry
 554 (SPARC/IGAC) Chemistry-Climate Model Initiative (CCMI) for organising and coordinating the model data analysis
 555 activity, and the British Atmospheric Data Centre (BADC) for collecting and archiving the CCMI model output. We
 556 acknowledge the long-term support provided by the Commonwealth Scientific and Industrial Research Organisation
 557 (CSIRO) and the National Environmental Science Program - Climate Systems Hub to coordinate and support activities of
 558 the Global Carbon Project. We are grateful to the Emissions Database for Global Atmospheric Research (EDGAR) team (M.
 559 Crippa, D. Guizzardi, F. Pagani, M. Banja, E. Schaaf, M. Muntean, W. Becker, F. Monforti-Ferrario) for the work needed
 560 to publish the EDGAR greenhouse gas emission datasets used in this work (<https://edgar.jrc.ec.europa.eu/>). We are
 561 particularly indebted to the dedicated station/instrumental operators/scientists that have gathered the data and ensured their
 562 high quality.

563 We acknowledge more specifically Katherine Jensen for her contribution to the Surface Water Microwave Product Series
 564 SWAMPS, Fortunat Joos for his contribution to simulations with the Land surface Processes and eXchanges model (LPX
 565 Bern), Ray Langenfeld for his contribution to CSIRO network, Paul Miller for his contribution to simulations with the
 566 Lund-Potsdam-Jena General Ecosystem Simulator (LPJ-GUESS), Peng Shushi for his contribution to simulations with the
 567 Organising Carbon and Hydrology In Dynamic Ecosystems (ORCHIDEE) model, Shamil Maksyutov for his contribution
 568 for simulations with the inverse model at the National Institute for Environmental Studies (NIES), Isobel Simpson for her
 569 contribution to the University of California Irvine (UCI) network, Paul Steele for his former contribution to CSIRO
 570 network, Ray Weiss for his contribution to the Advanced Global Atmospheric Gases Experiment (AGAGE) network,
 571 Christine Widenmeyer for her contribution with the Fire INventory from the National Center for Atmospheric Research
 572 (FINN) database, Xiaoming Xu for his contribution to simulations with with the The Integrated Science Assessment Model

- Supprimé: YY,
- Supprimé: .
- Supprimé: GB, CCr, CF, PK, RL, TM, IM, SO'D
- Supprimé: RP,
- Supprimé: IJS, PS, YT, RFW
- Supprimé: DWu,
- Supprimé: YZ, MvW, AV, VN, MIH
- Supprimé: set
- Supprimé: contribute
- Supprimé: and CCu
- Supprimé: and contributed to the text of this section
- Mis en forme : Anglais (G.B.)
- Supprimé: The
- Mis en forme : Anglais (G.B.)
- Supprimé: declare that they have no conflict of interest.
- Mis en forme : Police :Non Gras, Anglais (G.B.)
- Mis en forme : Anglais (E.U.)
- Supprimé: .
- Supprimé: A1
- Supprimé: We acknowledge Adrian Gustafson for his contribution to prepare the simulations of LPJ-GUESS. Paul A. Miller, Adrian Gustafson and Wenxin Zhang acknowledge this work as a contribution to the Strategic Research Area MERGE. FAOSTAT data collection, analysis

593 (ISAM), Yuanzhi Yao for his contribution to simulations with the Dynamic Land Ecosystem Model (DLEM), Diego
594 Guizzardi for his contribution to EDGAR, Maria Tenkanen for her contribution with the Carbon Tracker – Europe (CTE)
595 outputs, Giulia Conchedda for her contribution to the Food and Agriculture Organization (FAO) database. FAOSTAT data
596 collection, analysis, and dissemination is funded through FAO regular budget funds. The contribution of relevant experts in
597 member countries is gratefully acknowledged. We acknowledge Juha Hatakka from the Finnish Meteorological Institute
598 (FMI) for making methane measurements at the Pallas station and sharing the data with the community. We thank Ariana
599 Sutton-Grier and Lisamarie Windham-Myers for reviewing an earlier version of this manuscript. Any use of trade, firm, or
600 product names
601 is for descriptive purposes only and does not imply endorsement by the US Government.

604 References

- 605 [Abe, Y., Bignell, D. E. and Higashi, T., Eds.: Termites: Evolution, Sociality, Symbioses, Ecology, Springer Netherlands, Dordrecht, 2000.](#)
- 606 [Aho, K.S., J.H. Fair, J.D. Hosen, E.D. Kyzivat, L.A. Logozzo, G. Rocher-Ros, L.C. Weber, B. Yoon, and P.A. Raymond: Distinct concentration-discharge dynamics in temperate streams and rivers: CO₂ exhibits chemostasis while CH₄ exhibits source limitation due to temperature control, *Limnology and Oceanography*, 66\(10\): p. 3656-3668., 2021](#)
- 607 [Allan, W., Lowe, D. C., Gomez, A. J., Struthers, H. and Brailsford, G. W.: Interannual variation of ¹³C in tropospheric methane: Implications for a possible atomic chlorine sink in the marine boundary layer, *J. Geophys. Res.-Atmospheres*, 110\(D11\), doi:10.1029/2004JD005650, 2005.](#)
- 608 [Allan, W., Struthers, H. and Lowe, D. C.: Methane carbon isotope effects caused by atomic chlorine in the marine boundary layer: Global model results compared with Southern Hemisphere measurements, *J. Geophys. Res.-Atmospheres*, 112\(D4\), D04306, doi:10.1029/2006jd007369, 2007.](#)
- 609 [Allen, D. T., Torres, V. M., Thomas, J., Sullivan, D. W., Harrison, M., Hendler, A., Herndon, S. C., Kolb, C. E., Fraser, M. P., Hill, A. D., Lamb, B. K., Miskimins, J., Sawyer, R. F. and Seinfeld, J. H.: Measurements of methane emissions at natural gas production sites in the United States, *Proc Natl Acad Sci USA*, 110\(44\), 17,768-17,773, doi:10.1073/pnas.1304880110, 2013.](#)
- 610 [Allen, G. H., & Pavelsky, T. M.: Global extent of rivers and streams. *Science*, 361\(6402\), 585–588, https://doi.org/10.1126/science.aat0636, 2018](#)
- 611 [Alvarez, R. A., Zavala-Araiza, D., Lyon, D. R., Allen, D. T., Barkley, Z. R., Brandt, A. R., Davis, K. J., Herndon, S. C., Jacob, D. J., Karion, A., Kort, E. A., Lamb, B. K., Lauvaux, T., Maasackers, J. D., Marchese, A. J., Omara, M., Pacala, S. W., Peischl, J., Robinson, S. W., Peischl, J., Robinson, A. L., Shepson, P. B., Sweeney, C., Townsend-Small, A., Wofsy, S. C. and Hamburg, S. P.: Assessment of methane emissions from the U.S. oil and gas supply chain, *Science*, 361\(6398\), 186–188, doi:10.1126/science.aar7204, 2018.](#)
- 612 [Andersen, T., Scheeren, B., Peters, W. and Chen, H.: A UAV-based active AirCore system for measurements of greenhouse gases, *Atmospheric Meas. Tech.*, 11\(5\), 2683–2699, doi:10.5194/amt-11-2683-2018, 2018.](#)
- 613 [André, J.-C., Boucher, O., Bousquet, P., Chanin, M.-L., Chappellaz, J. and Tardieu, B.: Le méthane : d'où vient-il et quel est son impact sur le climat ?, *EDP Sciences, Académie des Sciences et Technologies, Paris*, 2014.](#)
- 614 [Aoki, S., Nakazawa, T., Murayama, S. and Kawaguchi, S.: Measurements of atmospheric methane at the Japanese Antarctic Station, *Syowa*, *Tellus*, 44B\(4\), 273–281, doi:10.1034/j.1600-0889.1992.t01.3-00005.x., 1992.](#)
- 615 [Arora, V. K., Melton, J. R. and Plummer, D.: An assessment of natural methane fluxes simulated by the CLASS-CTEM model, *Biogeosciences*, 15\(15\), 4683–4709, doi:10.5194/bg-15-4683-2018, 2018.](#)
- 616 [Bader, W., Bovy, B., Conway, S., Strong, K., Smale, D., Turner, A. J., Blumenstock, T., Boone, C., Collaud Coen, M., Coulon, A., Garcia, O., Griffith, D. W. T., Hase, F., Hausmann, P., Jones, N., Krummel, P., Murata, I., Morino, I., Nakajima, H., O'Doherty, S., Paton-Walsh, C., Robinson, J., Sandrin, R., Schneider, M., Servais, C., Sussmann, R. and Mahieu, E.: The recent increase of atmospheric methane from 10 years of ground-based NDACC FTIR observations since 2005, *Atmospheric Chem. Phys.*, 17\(3\), 2255–2277, doi:10.5194/acp-17-2255-2017, 2017.](#)
- 617 [Bačič, P.: The Birds and Rice Connection, *Bird Watch Dig.*, \[121\]](#)

Mis en forme : Anglais (G.B.)

Supprimé: Abe, Y., Bignell, D. E. and Higashi, T., Eds.: Termites: Evolution, Sociality, Symbioses, Ecology, Springer Netherlands, Dordrecht, 2000.
Alexe, M., Bergamaschi, P., Segers, A., Detmers, R., Butz, A., Hasekamp, O., Guerlet, S., Parker, R., Boesch, H., Frankenberg, C., Scheepmaker, R. A., Dlugokenky, E., Sweeney, C., Wofsy, S. C. and Kort, E. A.: Inverse modelling of CH₄ emissions for 2010–2011 using different satellite retrieval products from GOSAT and SCIAMACHY, *Atmos Chem Phys*, 15(1), 113–133, doi:10.5194/acp-15-113-2015, 2015.
Allan, W., Lowe, D. C., Gomez, A. J., Struthers, H. and Brailsford, G. W.: Interannual variation of ¹³C in tropospheric methane: Implications for a possible atomic chlorine sink in the marine boundary layer, *J. Geophys. Res.-Atmospheres*, 110(D11), doi:10.1029/2004JD005650, 2005.
Allan, W., Struthers, H. and Lowe, D. C.: Methane carbon isotope effects caused by atomic chlorine in the marine boundary layer: Global model results compared with Southern Hemisphere measurements, *J. Geophys. Res.-Atmospheres*, 112(D4), D04306, doi:10.1029/2006jd007369, 2007.
Allen, D. T., Torres, V. M., Thomas, J., Sullivan, D. W., Harrison, M., Hendler, A., Herndon, S. C., Kolb, C. E., Fraser, M. P., Hill, A. D., Lamb, B. K., Miskimins, J., Sawyer, R. F. and Seinfeld, J. H.: Measurements of methane emissions at natural gas production sites in the United States, *Proc Natl Acad Sci USA*, 110(44), 17,768-17,773, doi:10.1073/pnas.1304880110, 2013.
Alvarez, R. A., Zavala-Araiza, D., Lyon, D. R., Allen, D. T., Barkley, Z. R., Brandt, A. R., Davis, K. J., Herndon, S. C., Jacob, D. J., Karion, A., Kort, E. A., Lamb, B. K., Lauvaux, T., Maasackers, J. D., Marchese, A. J., Omara, M., Pacala, S. W., Peischl, J., Robinson, A. L., Shepson, P. B., Sweeney, C., Townsend-Small, A., Wofsy, S. C. and Hamburg, S. P.: Assessment of methane emissions from the U.S. oil and gas supply chain, *Science*, 361(6398), 186–188, doi:10.1126/science.aar7204, 2018.
Andersen, T., Scheeren, B., Peters, W. and Chen, H.: A UAV-based active AirCore system for measurements of greenhouse gases, *Atmospheric Meas. Tech.*, 11(5), 2683–2699, doi:10.5194/amt-11-2683-2018, 2018.
André, J.-C., Boucher, O., Bousquet, P., Chanin, M.-L., Chappellaz, J. and Tardieu, B.: Le méthane : d'où vient-il et quel est son impact sur le climat ?, *EDP Sciences, Académie des Sciences et Technologies, Paris*, 2014.
Aoki, S., Nakazawa, T., Murayama, S. and Kawaguchi, S.: Measurements of atmospheric methane at the Japanese Antarctic Station, *Syowa*, *Tellus*, 44B(4), 273–281, doi:10.1034/j.1600-0889.1992.t01.3-00005.x., 1992.
Arora, V. K., Melton, J. R. and Plummer, D.: An assessment of natural methane fluxes simulated by the CLASS-CTEM model, *Biogeosciences*, 15(15), 4683–4709, doi:10.5194/bg-15-4683-2018, 2018.
Bader, W., Bovy, B., Conway, S., Strong, K., Smale, D., Turner, A. J., Blumenstock, T., Boone, C., Collaud Coen, M., Coulon, A., Garcia, O., Griffith, D. W. T., Hase, F., Hausmann, P., Jones, N., Krummel, P., Murata, I., Morino, I., Nakajima, H., O'Doherty, S., Paton-Walsh, C., Robinson, J., Sandrin, R., Schneider, M., Servais, C., Sussmann, R. and Mahieu, E.: The recent increase of atmospheric methane from 10 years of ground-based NDACC FTIR observations since 2005, *Atmospheric Chem. Phys.*, 17(3), 2255–2277, doi:10.5194/acp-17-2255-2017, 2017.
Bačič, P.: The Birds and Rice Connection, *Bird Watch Dig.*, [121]

759 [doi:10.1126/science.aar7204](https://doi.org/10.1126/science.aar7204), 2018.

760 Andersen, T., Scheeren, B., Peters, W. and Chen, H.: A UAV-based active AirCore system for measurements of
761 greenhouse gases, *Atmospheric Meas. Tech.*, 11(5), 2683–2699, doi:10.5194/amt-11-2683-2018, 2018.

762 Anderson, D. C., Duncan, B. N., Nicely, J. M., Liu, J., Strode, S. A., and Follette-Cook, M. B.: Technical note:
763 Constraining the hydroxyl (OH) radical in the tropics with satellite observations of its drivers – first steps toward
764 assessing the feasibility of a global observation strategy, *Atmos. Chem. Phys.*, 23, 6319–6338,
765 <https://doi.org/10.5194/acp-23-6319-2023>, 2023.

766 André, J.-C., Boucher, O., Bousquet, P., Chanin, M.-L., Chappellaz, J. and Tardieu, B.: Le méthane : d'où vient-il et quel
767 est son impact sur le climat ?, EDP Sciences, Académie des Sciences et Technologies, Paris., 2014.

768 Aoki, S., Nakazawa, T., Murayama, S. and Kawaguchi, S.: Measurements of atmospheric methane at the Japanese
769 Antarctic Station, Syowa., *Tellus*, 44B(4), 273–281, doi:10.1034/j.1600-0889.1992.t01-3-00005.x., 1992.

770 Arora, V. K., Melton, J. R. and Plummer, D.: An assessment of natural methane fluxes simulated by the CLASS-CTEM
771 model, *Biogeosciences*, 15(15), 4683–4709, doi:10.5194/bg-15-4683-2018, 2018.

772 Bader, W., Bovy, B., Conway, S., Strong, K., Smale, D., Turner, A. J., Blumenstock, T., Boone, C., Collaud Coen, M.,
773 Coulon, A., Garcia, O., Griffith, D. W. T., Hase, F., Hausmann, P., Jones, N., Krummel, P., Murata, I., Morino, I.,
774 Nakajima, H., O'Doherty, S., Paton-Walsh, C., Robinson, J., Sandrin, R., Schneider, M., Servais, C., Sussmann, R.
775 and Mahieu, E.: The recent increase of atmospheric methane from 10 years of ground-based NDACC FTIR
776 observations since 2005, *Atmospheric Chem. Phys.*, 17(3), 2255–2277, doi:10.5194/acp-17-2255-2017, 2017.

777 Baicich, P.: The Birds and Rice Connection, *Bird Watch. Dig.* [online] Available from:
778 http://www.greatbirdingprojects.com/images/BWD_J-A_13_BIRDS_N_RICE.pdf, 2013.

779 Baier, B., Sweeney, C., Newberger, T., Higgs, J., Wolter, S., & NOAA Global Monitoring Laboratory : NOAA AirCore
780 atmospheric sampling system profiles (Version 20230831) [Data set]. NOAA GML. [https://doi.org/10.15138/6AV0-](https://doi.org/10.15138/6AV0-MY81)
781 [MY81](https://doi.org/10.15138/6AV0-MY81), 2021

782 Balasus, N., Jacob, D. J., Lorente, A., Maasackers, J. D., Parker, R. J., Boesch, H., Chen, Z., Kelp, M. M., Nesser, H., and
783 Varon, D. J.: A blended TROPOMI+GOSAT satellite data product for atmospheric methane using machine learning
784 to correct retrieval biases, *Atmos. Meas. Tech.*, 16, 3787–3807, <https://doi.org/10.5194/amt-16-3787-2023>, 2023.

785 Bansal, S., Van Der Berg, M.P., Fern, R.R., Jones, J.W., Lo, R., McKenna, O.P., Tangen, B.A., Zhang, Z., and Gleason,
786 R.A.: Large increases in methane emissions expected from North America's largest wetland complex, *Sci. Adv.*, 9,
787 eade1112, doi:10.1126/sciadv.ade1112, 2023.

788 Barba, J., Bradford, M. A., Brewer, P. E., Bruhn, D., Covey, K., van Haren, J., Magonigal, J. P., Mikkelsen, T. N., Pangala,
789 S. R., Pihlatie, M., Poulter, B., Rivas-Ubach, A., Schadt, C. W., Terazawa, K., Warner, D. L., Zhang, Z. and Vargas,
790 R.: Methane emissions from tree stems: a new frontier in the global carbon cycle, *New Phytol.*, 222(1), 18–28,
791 doi:10.1111/nph.15582, 2019.

8792 [Bastviken, D., Tranvik, L. J., Downing, J. A., Crill, P. M. and Enrich-Prast, A.: Freshwater Methane Emissions Offset the](#)
8793 [Continental Carbon Sink, *Science*, 331\(6013\), 50–50, doi:10.1126/science.1196808, 2011.](#)

8794 [Bastviken, D., C.C. Treat, S.R. Pangala, V. Gauci, A. Enrich-Prast, M. Karlson, M. Gålfalk, M.B. Romano, and H.O.](#)
8795 [Sawakuchi, The importance of plants for methane emission at the ecosystem scale. *Aquatic Botany*, 184: p. 103596,](#)
8796 [2023.](#)

8797 [Basu, S., Lan, X., Dlugokencky, E., Michel, S., Schwietzke, S., Miller, J. B., Bruhwiler, L., Oh, Y., Tans, P. P., Apadula,](#)
8798 [F., Gatti, L. V., Jordan, A., Necki, J., Sasakawa, M., Morimoto, S., Di Iorio, T., Lee, H., Arduini, J., and Manca, G.:](#)
8799 [Estimating emissions of methane consistent with atmospheric measurements of methane and \$\delta^{13}\text{C}\$ of methane. *Atmos.*
8800 \[Chem. Phys.\]\(#\), 22, 15351–15377, <https://doi.org/10.5194/acp-22-15351-2022>, 2022.](#)

8801 [Beaulieu, J.J., DelSontro, T. & Downing, J.A.: Eutrophication will increase methane emissions from lakes and](#)
8802 [impoundments during the 21st century. *Nat Commun* 10, 1375 , <https://doi.org/10.1038/s41467-019-09100-5>, 2019](#)

8803 [Beck, H., Zimmermann, N., McVicar, T. *et al.* Present and future Köppen-Geiger climate classification maps at 1-km](#)
8804 [resolution. *Sci Data* 5, 180214, doi.org/10.1038/sdata.2018.214, 2018](#)

8805 [Beerling, D.J., Woodward, F.I., *Vegetation and the Terrestrial Carbon Cycle: Modelling the First 400 Million Years.*](#)
8806 [Cambridge University Press, Cambridge, 2001](#)

8807 [Begum, M.S., M.J. Bogard, D.E. Butman, E. Chea, S. Kumar, X. Lu, O.K. Nayna, L. Ran, J.E. Richey, S.M. Tareq, D.T.](#)
8808 [Xuan, R. Yu, and J.-H. Park, Localized Pollution Impacts on Greenhouse Gas Dynamics in Three Anthropogenically](#)
8809 [Modified Asian River Systems. *Journal of Geophysical Research: Biogeosciences*, 126\(5\): p. e2020JG006124, 2021](#)

8810 [Bergamaschi, P., Houweling, S., Segers, A., Krol, M., Frankenberg, C., Scheepmaker, R. A., Dlugokencky, E., Wofsy, S.](#)
8811 [C., Kort, E. A., Sweeney, C., Schuck, T., Brenninkmeijer, C., Chen, H., Beck, V. and Gerbig, C.: Atmospheric CH₄ in](#)
8812 [the first decade of the 21st century: Inverse modeling analysis using SCIAMACHY satellite retrievals and NOAA](#)
8813 [surface measurements. *J. Geophys. Res. Atmospheres*, 118\(13\), 7350–7369, doi:10.1002/jgrd.50480, 2013.](#)

8814 [Bergamaschi, P., DANILA, A. M., Weiss, R., Thompson, R. L., Brunner, D., Levin, I., meijer, Y., Chevallier, F., Janssens-](#)
8815 [Maenhout, G., Bovensmann, H., Crisp, D., Basu, S., Dlugokencky, E. J., Engelen, R., Gerbig, C., Günther, D.,](#)
8816 [Hammer, S., Henne, S., Houweling, S., Karstens, U., Kort, E. A., Maione, M., Manning, A. J., Miller, J., Montzka, S.,](#)
8817 [Pandey, S., Peters, W., Peylin, P., Pinty, B., Ramonet, M., Reimann, S., Röckmann, T., Schmidt, M., Strogies, M.,](#)
8818 [Sussams, J., Tarasova, O., Van Aardenne, J., Vermeulen, A. and Vogel, F.: Atmospheric monitoring and inverse](#)
8819 [modelling for verification of greenhouse gas inventories, EUR - Scientific and Technical Research Reports,](#)
8820 [Publications Office of the European Union. \[online\] Available from: \[https://ec.europa.eu/jrc/en/publication/eurscientific-and-technical-research-reports/atmospheric-monitoring-and-inverse-modelling-verification-greenhouse-\]\(https://ec.europa.eu/jrc/en/publication/eurscientific-and-technical-research-reports/atmospheric-monitoring-and-inverse-modelling-verification-greenhouse-gas-inventories\)](#)
8821 [gas-inventories \(Accessed 17 March 2020a\), 2018.](#)

8822 [Best, A. I., Richardson, M. D., Boudreau, B. P., Judd, A. G., Leifer, I., Lyons, A. P., et al.: Shallow Seabed Methane Gas](#)
8823 [Could Pose Coastal hazard. *Eos Trans. AGU* 87 \(22\), 213–217. doi:10.1029/2006EO220001, 2006](#)
8824

825 [Bian, L., Gao, Z., Sun, Y., Ding, M., Tang, J. and Schnell, R. C.: CH4 Monitoring and Background Concentration at](#)
826 [Zhongshan Station, Antarctica, Atmospheric Clim. Sci., 6\(1\), 135–144, doi:10.4236/acs.2016.61012, 2015.](#)

827 [Bignell, D.E., Eggleton, P. Termites in ecosystems. In: Abe, T., Higashi, M. and Bignell, D.E. \(Eds\), Termites: Evolution,](#)
828 [Sociality, Symbioses, Ecology. Kluwer, Dordrecht, Netherlands, 363–387, 2000.](#)

829 [Biskaborn, B.K., Smith, S.L., Noetzi, J. et al. Permafrost is warming at a global scale. Nat Commun 10, 264, https://doi-](#)
830 [org.insu.bib.cnrs.fr/10.1038/s41467-018-08240-4, 2019](#)

831 [Blake, D. R. and Rowland, F. S.: World-wide increase in tropospheric methane, 1978–1983, J. Atmospheric Chem., 4,](#)
832 [43–62, 1986.](#)

833 [Blake, D. R., Mayer, E. W., Tyler, S. C., Makide, Y., Montague, D. C. and Rowland, F. S.: Global Increase in Atmospheric](#)
834 [Methane Concentrations between 1978 and 1980, Geophys. Res. Lett., 9\(4\), 477–480, 1982.](#)

835 [Bloom, A. A., Lee-Taylor, J., Madronich, S., Messenger, D. J., Palmer, P. I., Reay, D. S. and McLeod, A. R.: Global](#)
836 [methane emission estimates from ultraviolet irradiation of terrestrial plant foliage, New Phytol., doi:10.1111/j.1469-](#)
837 [8137.2010.03259.x, 2010.](#)

838 [Bohn, T. J., Melton, J. R., Ito, A., Kleinen, T., Spahni, R., Stocker, B. D., Zhang, B., Zhu, X., Schroeder, R., Glagolev, M.](#)
839 [V., Maksyutov, S., Brovkin, V., Chen, G., Denisov, S. N., Eliseev, A. V., Gallego-Sala, A., McDonald, K. C., Rawlins,](#)
840 [M. A., Riley, W. J., Subin, Z. M., Tian, H., Zhuang, Q. and Kaplan, J. O.: WETCHIMP-WSL: Intercomparison of](#)
841 [wetland methane emissions models over West Siberia, Biogeosciences, 12\(11\), 3321–3349, doi:10.5194/bg-12-3321-](#)
842 [2015, 2015.](#)

843 [Bodmer, P., Vroom, R. J. E., Stepina, T., del Giorgio, P. A., Kosten, S.: Methane dynamics in vegetated habitats in inland](#)
844 [waters: quantification, regulation, and global significance, Frontiers in Water, 5, DOI=10.3389/frwa.2023.1332968,](#)
845 [2024](#)

846 [Borges, A. V. and Abril, G.: Carbon Dioxide and Methane Dynamics in Estuaries, in Treatise on Estuarine and Coastal](#)
847 [Science, vol. 5, pp. 119–161, Academic Press, Waltham. \[online\] Available from: doi:10.1016/B978-0-12-374711-](#)
848 [2.00504-0, 2011.](#)

849 [Borges, A., G. Abril, and S. Bouillon: Carbon dynamics and CO2 and CH4 outgassing in the Mekong delta,](#)
850 [Biogeosciences, 15: p. 1093-1114., 2018](#)

851 [Borges, A.V., F. Darchambeau, T. Lambert, C. Morana, G.H. Allen, E. Tambwe, A. Toengaho Sembaito, T. Mambo, J.](#)
852 [Nlandu Wabakhangazi, J.P. Descy, C.R. Teodoru, and S. Bouillon: Variations in dissolved greenhouse gases \(CO2,](#)
853 [CH4, N2O\) in the Congo River network overwhelmingly driven by fluvial-wetland connectivity, Biogeosciences,](#)
854 [16\(19\): p. 3801-3834, 2019](#)

855 [Borges, A. V., Deirmendjian, L., Bouillon, S., Okello, W., Lambert, T., Roland, F.A. E., Razanamahandry, V. F.,](#)
856 [Voarintsoa, N.R. G., Darchambeau, F., Kimirei, I. A., Descy, J-P., Allen, G. H. and Morana, C.: Greenhouse gas](#)
857 [emissions from African lakes are no longer a blind spot. Sci. Adv. 8, eabi8716, DOI:10.1126/sciadv.abi8716, 2022](#)

§858 [Bousquet, P., Ciais, P., Miller, J. B., Dlugokencky, E. J., Hauglustaine, D. A., Prigent, C., Van der Werf, G. R., Peylin, P.,](#)
§859 [Brunke, E. G., Carouge, C., Langenfelds, R. L., Lathiere, J., Papa, F., Ramonet, M., Schmidt, M., Steele, L. P., Tyler,](#)
§860 [S. C. and White, J.: Contribution of anthropogenic and natural sources to atmospheric methane variability, *Nature*,](#)
§861 [443\(7110\), 439–443, 2006.](#)

§862 [Bousquet, P., Pierangelo, C., Bacour, C., Marshall, J., Peylin, P., Ayar, P. V., Ehret, G., Bréon, F.-M., Chevallier, F.,](#)
§863 [Crevoisier, C., Gibert, F., Rairoux, P., Kiemle, C., Armante, R., Bès, C., Cassé, V., Chinaud, J., Chomette, O.,](#)
§864 [Delahaye, T., Edouard, D., Estève, F., Fix, A., Friker, A., Klonecki, A., Wirth, M., Alpers, M. and Millet, B.: Error](#)
§865 [Budget of the MEthane Remote LIdar mission and Its Impact on the Uncertainties of the Global Methane Budget, *J.*](#)
§866 [Geophys. Res. Atmospheres](#), 123(20), 11,766–11,785, doi:10.1029/2018JD028907, 2018.

§867 [Brandt, A. R., Heath, G. A., Kort, E. A., O’Sullivan, F., Pétron, G., Jordaán, S. M., Tans, P., Wilcox, J., Gopstein, A. M.,](#)
§868 [Arent, D., Wofsy, S., Brown, N. J., Bradley, R., Stucky, G. D., Eardley, D. and Harriss, R.: Methane Leaks from North](#)
§869 [American Natural Gas Systems, *Science*](#), 343(6172), 733–735, doi:10.1126/science.1247045, 2014.

§870 [Brasseur, G. P. and Solomon, S.: Aeronomy of the Middle Atmosphere: Chemistry and Physics of the Stratosphere and](#)
§871 [Mesosphere](#), 3rd ed., Springer Netherlands, 2005.

§872 [Brenninkmeijer C. A. M., Crutzen, P., Boumard, F., Dauer, T., Dix, B., Ebinghaus, R., Filippi, D., Fischer, H., Franke, H.,](#)
§873 [Fries, U., Heintzenberg, J., Helleis, F., Hermann, M., Kock, H. H., Koeppel, C., Lelieveld, J., Leuenberger, M.,](#)
§874 [Martinsson, B. G., Miemczyk, S., Moret, H. P., Nguyen, H. N., Nyfeler, P., Oram, D., O’Sullivan, D., Penkett, S., Platt,](#)
§875 [U., Pucek, M., Ramonet, M., Randa, B., Reichelt, M., Rhee, T. S., Rohwer, J., Rosenfeld, K., Scharffe, D., Schlager,](#)
§876 [H., Schumann, U., Slemr, F., Sprung, D., Stock, P., Thaler, R., Valentino, F., van Velthoven, P., Waibel, A., Wandel,](#)
§877 [A., Waschitschek, K., Wiedensohler, A., Xueref- Remy, I., Zahn, A., Zech, U., and Ziereis, H.: Civil Aircraft for the](#)
§878 [regular investigation of the atmosphere based on an instrumented container: The new CARIBIC system, *Atmos. Chem.*](#)
§879 [Phys.](#), 7, 4953–4976, doi:10.5194/acp-7-4953-2007, 2007.

§880 [Bruhwiler, L. M., Basu, S., Bergamaschi, P., Bousquet, P., Dlugokencky, E., Houweling, S., Ishizawa, M., Kim, H.-S.,](#)
§881 [Locatelli, R., Maksyutov, S., Montzka, S., Pandey, S., Patra, P. K., Petron, G., Saunio, M., Sweeney, C., Schwietzke,](#)
§882 [S., Tans, P. and Weatherhead, E. C.: U.S. CH₄ emissions from oil and gas production: Have recent large increases](#)
§883 [been detected?, *J. Geophys. Res. Atmospheres*](#), 122(7), 4070–4083, doi:10.1002/2016JD026157, 2017.

§884 [Brune, A.: Symbiotic digestion of lignocellulose in termite guts, *Nat Rev Microbiol*](#) 12, 168–180,
§885 [doi.org/10.1038/nrmicro3182, 2014](#)

§886 [Buchwitz, M., de Beek, R., Burrows, J. P., Bovensmann, H., Warneke, T., Notholt, J., Meirink, J. F., Goede, A. P. H.,](#)
§887 [Bergamaschi, P., Korner, S., Heimann, M. and Schulz, A.: Atmospheric methane and carbon dioxide from](#)
§888 [SCIAMACHY satellite data: initial comparison with chemistry and transport models, *Atmospheric Chem. Phys.*](#), 5,
§889 [941–962, 2005a.](#)

§890 [Buchwitz, M., de Beek, R., Noel, S., Burrows, J. P., Bovensmann, H., Bremer, H., Bergamaschi, P., Korner, S. and](#)

891 [Heimann, M.: Carbon monoxide, methane and carbon dioxide columns retrieved from SCIAMACHY by WFM-](#)
892 [DOAS: year 2003 initial data set, Atmospheric Chem. Phys., 5, 3313–3329, 2005b.](#)

893 [Buchwitz, M., Dils, B., Boesch, H., Crevoisier, C., Detmers, R., Frankenberg, C., Hasekamp, O., Hewson, W., Laeng, A.,](#)
894 [Noel, S., Nothold, J., Parker, R., Reuter, M. and Schneising, O.: Product Validation and Intercomparison Report](#)
895 [\(PVIR\) for the Essential Climate Variable \(ECV\) Greenhouse Gases \(GHG\), ESA Climate Change Initiative \(CCI\),](#)
896 [report version 4, Feb 2016, \[http://www.esa-ghg-cci.org/?q=webfm_send/300\]\(http://www.esa-ghg-cci.org/?q=webfm_send/300\), 2016.](#)

897 [Buchwitz, M., Schneising, O., Vanselow, S., Houweling, S., van Peet, J., Siddans, R., Kerridge, B., Ventress, L., Knappett,](#)
898 [D., Crevoisier, C., Meilhac, N., Borsdorf, T., Lorente, A. and Aben, I.: Final Report of the Methane Plus ESA project,](#)
899 [TN-D15/16-CH4PLUS, <https://methaneplus.eu/#docs>, Accessed on February 13 2024, 202](#)

900 [Butz, A., Guerlet, S., Hasekamp, O., Schepers, D., Galli, A., Aben, I., Frankenberg, C., Hartmann, J. M., Tran, H., Kuze,](#)
901 [A., Keppel-Aleks, G., Toon, G., Wunch, D., Wennberg, P., Deutscher, N., Griffith, D., Macatangay, R.,](#)
902 [Messerschmidt, J., Notholt, J. and Warneke, T.: Toward accurate CO₂ and CH₄ observations from GOSAT, Geophys.](#)
903 [Res. Lett., 38\(14\), L14812, doi:10.1029/2011gl047888, 2011.](#)

904 [Cai, Z. C., Xing, G., Yan, X., Xu, H., Tsuruta, H., Yagi, K. and Minami, K.: Methane and nitrous oxide emissions from](#)
905 [rice paddy fields as affected by nitrous fertilizers and water management, Plant Soil, 196, 7–14, 1997.](#)

906 [Cael, B.B., J. Biggs, and D.A. Seekell, The size-distribution of earth’s lakes and ponds: Limits to power-law behavior,](#)
907 [Frontiers in Environmental Science, 10.-, 2022](#)

908 [Call, M., D. T. Maher, I. R. Santos, and others.: Spatial and temporal variability of carbon dioxide and methane fluxes](#)
909 [over semi-diurnal and spring–neap–spring timescales in a mangrove creek. Geochim. Cosmochim. Acta **150**: 211–225,](#)
910 [doi:10.1016/j.gca.2014.11.023, 2015](#)

911 [Canadell, J.G., P.M.S. Monteiro, M.H. Costa, L. Cotrim da Cunha, P.M. Cox, A.V. Eliseev, S. Henson, M. Ishii, S. Jaccard,](#)
912 [C. Koven, A. Lohila, P.K. Patra, S. Piao, J. Rogelj, S. Syampungani, S. Zaehle, and K. Zickfeld: Global Carbon and](#)
913 [other Biogeochemical Cycles and Feedbacks. In *Climate Change 2021: The Physical Science Basis. Contribution of*](#)
914 [Working Group I to the Sixth Assessment Report of the Intergovernmental Panel on Climate Change \[Masson-](#)
915 [Delmotte, V., P. Zhai, A. Pirani, S.L. Connors, C. Péan, S. Berger, N. Caud, Y. Chen, L. Goldfarb, M.I. Gomis, M.](#)
916 [Huang, K. Leitzell, E. Lonnoy, J.B.R. Matthews, T.K. Maycock, T. Waterfield, O. Yelekçi, R. Yu, and B. Zhou \(eds.\)\],](#)
917 [Cambridge University Press, Cambridge, United Kingdom and New York, NY, USA, pp. 673–816, doi:](#)
918 [10.1017/9781009157896.007, 2021](#)

919 [Carlson, K. M., Gerber, J. S., Mueller, N. D., Herrero, M., MacDonald, G. K., Brauman, K. A., Havlik, P., O’Connell, C.](#)
920 [S., Johnson, J. A., Saatchi, S. and West, P. C.: Greenhouse gas emissions intensity of global croplands, Nat. Clim.](#)
921 [Change, 7\(1\), 63–68, doi:10.1038/nclimate3158, 2017.](#)

922 [Castelán-Ortega, O. A., Carlos Ku-Vera, J. and Estrada-Flores, J. G.: Modeling methane emissions and methane](#)
923 [inventories for cattle production systems in Mexico, *Atmósfera*, 27\(2\), 185–191, doi:10.1016/S0187-6236\(14\)71109-](#)

924 [9, 2014.](#)

925 [Cathles, L., Brown, L., Taam, M. and Hunter, A.: A commentary on “The greenhouse-gas footprint of natural gas in shale](#)

926 [formations” by R.W. Howarth, R. Santoro, and Anthony Ingraffea, *Clim. Change*, 113\(2\), 525–535,](#)

927 [doi:10.1007/s10584-011-0333-0, 2012.](#)

928 [Caulton, D., Shepson, P. B., Santoro, R. L., Sparks, J. P., Howarth, R. W., Anthony R. Ingraffea, A. R., Cambaliza, M. O.](#)

929 [L., Sweeney, C., Karion, A., Davis, K. J., Stirm, B. H., Montzka, S. A. and Miller, B. R.: Toward a better understanding](#)

930 [and quantification of methane emissions from shale gas development, *Proc. Natl. Acad. Sci. USA*, 111\(17\), 6237–](#)

931 [6242, doi:10.1073/pnas.1316546111, 2014.](#)

932 [Chandra, N., P. K. Patra, J. S. H. Bisht, A. Ito, T. Umezawa, S. Morimoto, S. Aoki, G. Janssens-Maenhout, R. Fujita, M.](#)

933 [Takigawa, S. Watanabe, N. Saitoh, J.G. Canadell, Emissions from the oil and gas sectors, coal mining and ruminant](#)

934 [farming drive methane growth over the past three decades, *J. Meteorol. Soc. Jpn.*, 99\(2\), doi:10.2151/jmsj.2021-015,](#)

935 [2021.](#)

936 [Chang, J., Peng, S., Ciais, P., Saunois, M., Dangal, S. R. S., Herrero, M., Havlik, P., Tian, H. and Bousquet, P.: Revisiting](#)

937 [enteric methane emissions from domestic ruminants and their \$\delta^{13}\text{C}\$ CH₄ source signature, *Nat. Commun.*, 10\(1\), 1–](#)

938 [14, doi:10.1038/s41467-019-11066-3, 2019.](#)

939 [Chang, J., Peng, S., Yin, Y., Ciais, P., Havlik, P., & Herrero, M.: The key role of production efficiency changes in](#)

940 [livestock methane emission mitigation. *AGU Advances*, 2, e2021AV000391, <https://doi.org/10.1029/2021AV000391>,](#)

941 [2021](#)

942 [Chappellaz, J., Blunier, T., Raynaud, D., Barnola, J. M., Schwander, J. and Stauffert, B.: Synchronous changes in](#)

943 [atmospheric CH₄ and Greenland climate between 40 and 8 kyr BP, *Nature*, 366\(6454\), 443–445,](#)

944 [doi:10.1038/366443a0, 1993.](#)

945 [Chen, H., Zhu, Q., Peng, C., Wu, N., Wang, Y., Fang, X., Jiang, H., Xiang, W., Chang, J., Deng, X. and Yu, G.: Methane](#)

946 [emissions from rice paddies natural wetlands, lakes in China: Synthesis new estimate, *Glob. Change Biol.*, 19\(1\), 19–](#)

947 [32, doi:10.1111/gcb.12034, 2013.](#)

948 [Chen, Y. H. and Prinn, R. G.: Estimation of atmospheric methane emissions between 1996 and 2001 using a three-](#)

949 [dimensional global chemical transport model, *J. Geophys. Res.-Atmospheres*, 111\(D10307\),](#)

950 [doi:10.1029/2005JD006058, 2006.](#)

951 [Chen, Z., Jacob, D. J., Nesser, H., Sulprizio, M. P., Lorente, A., Varon, D. J., Lu, X., Shen, L., Qu, Z., Penn, E., and Yu,](#)

952 [X.: Methane emissions from China: a high-resolution inversion of TROPOMI satellite observations, *Atmos. Chem.*](#)

953 [Phys.](#), 22, 10809–10826, <https://doi.org/10.5194/acp-22-10809-2022>, 2022.

954 [Chen, Y., Hall, J., van Wees, D., Andela, N., Hantson, S., Giglio, L., van der Werf, G. R., Morton, D. C., and Randerson,](#)

955 [J. T.: Multi-decadal trends and variability in burned area from the fifth version of the Global Fire Emissions Database](#)

956 [\(GFED5\), *Earth Syst. Sci. Data*, 15, 5227–5259, <https://doi.org/10.5194/essd-15-5227-2023>, 2023.](#)

957 [Chevallier, F., Lloret, Z., Cozic, A., Takache, S., and Remaud, M.: Toward high-resolution global atmospheric inverse](#)
958 [modeling using graphics accelerators. *Geophysical Research Letters*, 50\(5\), 1–9.](#)
959 <https://doi.org/10.1029/2022GL102135>, 2023

960 [Ciais, P., Sabine, C., Bala, G., Bopp, L., Brovkin, V., Canadell, J., Chhabra, A., DeFries, R., Galloway, J., Heimann, M.,](#)
961 [Jones, C., Le Quééré, C., Myneni, R. B., Piao, S. and Thornton, P.: Carbon and Other Biogeochemical Cycles, in *In*](#)
962 [Climate Change 2013: The Physical Science Basis. Contribution of Working Group I to the Fifth Assessment Report](#)
963 [of IPCC, edited by T. F. Stocker, D. Qin, G.-K. Plattner, M. Tignor, S. K. Allen, J. Boschung, A. Nauels, Y. Xia, V.](#)
964 [Bex, and P. M. Midgley, Cambridge University Press, Cambridge., 2013.](#)

965 [Cicerone, R. J. and Oremland, R. S.: Biogeochemical aspects of atmospheric methane. *Glob. Biogeochem. Cycles*, 2, 299–](#)
966 [327, 1988.](#)

967 [Cicerone, R. J. and Shetter, J. D.: Sources of atmospheric methane: Measurements in rice paddies and a discussion. *J.*](#)
968 [Geophys. Res.](#), 86, 7203–7209, 1981.

969 [Collins, W. J., Lamarque, J. F., Schulz, M., Boucher, O., Eyring, V., Hegglin, M. I., Maycock, A., Myhre, G., Prather, M.,](#)
970 [Shindell, D. and Smith, S.J.: AerChemMIP: quantifying the effects of chemistry and aerosols in CMIP6. *Geoscientific*](#)
971 [Model Development](#) 10, 585–607. doi:10.5194/gmd-10-585-2017, 2017.

972 [Comer-Warner, S.A., P. Romeijn, D.C. Gooddy, S. Ullah, N. Kettridge, B. Marchant, D.M. Hannah, and S.](#)
973 [Krause:Thermal sensitivity of CO2 and CH4 emissions varies with streambed sediment properties. *Nature*](#)
974 [Communications](#), 9(1): p. 2803, 2018

975 [Conley, S., Franco, G., Faloona, I., Blake, D. R., Peischl, J. and Ryerson, T. B.: Methane emissions from the 2015 Aliso](#)
976 [Canyon blowout in Los Angeles, CA. *Science*, 351\(6279\), 1317–1320, doi:10.1126/science.aaf2348, 2016.](#)

977 [Conrad, R., Klose, M. and Claus, P.: Phosphate Inhibits Acetotrophic Methanogenesis on Rice Roots. *Appl. Environ.*](#)
978 [Microbiol.](#), 66(2), 828–831, 2000.

979 [Covey, K. R. and Magonigal, J. P.: Methane production and emissions in trees and forests, *New Phytol.*, 222\(1\), 35–51,](#)
980 <doi:10.1111/nph.15624>, 2019.

981 [Covey, K. R., Wood, S. A., Warren, R. J., Lee, X. and Bradford, M. A.: Elevated methane concentrations in trees of an](#)
982 [upland forest. *Geophys. Res. Lett.*, 39\(15\), doi:10.1029/2012gl052361, 2012.](#)

983 [Covey, K. R., de Mesquita, C. P. B., Oberle, B., Maynard, D. S., Bettigole, C., Crowther, T. W., Duguid, M. C., Steven,](#)
984 [B., Zanne, A. E., Lapin, M., Ashton, M. S., Oliver, C. D., Lee, X. and Bradford, M. A.: Greenhouse trace gases in](#)
985 [deadwood, *Biogeochemistry*, 130\(3\), 215–226, doi:10.1007/s10533-016-0253-1, 2016.](#)

986 [Crawford, J.T. and E.H. Stanley: Controls on methane concentrations and fluxes in streams draining human-dominated](#)
987 [landscapes. *Ecological Applications*, 26\(5\): p. 1581-1591, 2016](#)

988 [Crevoisier, C., Nobileau, D., Fiore, A. M., Armante, R., Chedin, A. and Scott, N. A.: Tropospheric methane in the tropics](#)
989 [- first year from IASI hyperspectral infrared observations, *Atmospheric Chem. Phys.*, 9\(17\), 6337–6350, 2009.](#)

0990 [Crippa, M., Guizzardi, D., Solazzo, E., Muntean, M., Schaaf, E., Monforti-Ferrario, F., Banja, M., Olivier, J.G.J., Grassi,](#)
0991 [G., Rossi, S., Vignati, E., GHG emissions of all world countries - 2021 Report, EUR 30831 EN, Publications Office of](#)
0992 [the European Union, Luxembourg, 2021, ISBN 978-92-76-41547-3, doi:10.2760/173513, JRC126363, 2021](#)

0993 [Crippa, M., Guizzardi, D., Pagani, F., Banja, M., Muntean, M., Schaaf E., Becker, W., Monforti-Ferrario, F., Quadrelli,](#)
0994 [R., Riskey Martin, A., Taghavi-Moharamli, P., Köykkä, J., Grassi, G., Rossi, S., Brandao De Melo, J., Oom, D.,](#)
0995 [Branco, A., San-Miguel, J., Vignati, E., GHG emissions of all world countries, Publications Office of the European](#)
0996 [Union, Luxembourg, 2023, doi:10.2760/953322, JRC134504, 2023](#)

0997 [Crutzen, P. J., Aselmann, I. and Seiler, W.: Methane production by domestic animals, wild ruminants, other herbivorous](#)
0998 [fauna, and humans, Tellus B, 38B\(3–4\), 271–284, doi:10.1111/j.1600-0889.1986.tb00193.x, 1986.](#)

0999 [Cucchi, M., Weedon, G. P., Amici, A., Bellouin, N., Lange, S., Müller Schmied, H., Hersbach, H. and Buontempo, C.:](#)
0000 [WFDE5: bias-adjusted ERA5 reanalysis data for impact studies. Earth System Science Data, 12, 2097–2120, 2020](#)

0001 [Cunnold, D. M., Steele, L. P., Fraser, P. J., Simmonds, P. G., Prinn, R. G., Weiss, R. F., Porter, L. W., O’Doherty, S.,](#)
0002 [Langenfelds, R. L., Krummel, P. B., Wang, H. J., Emmons, L., Tie, X. X. and Dlugokencky, E. J.: In situ measurements](#)
0003 [of atmospheric methane at GAGE/AGAGE sites during 1985-2000 and resulting source inferences, J. Geophys. Res.](#)
0004 [- Atmospheres, 107\(D14\), doi:10.1029/2001jd001226, 2002.](#)

0005 [Curry, C. L.: Modeling the soil consumption of atmospheric methane at the global scale, Glob. Biogeochem. Cycles, 21\(4\),](#)
0006 [GB4012, doi:10.1029/2006gb002818, 2007.](#)

0007 [Dalsøren, S. B., Isaksen, I. S. A., Li, L. and Richter, A.: Effect of emission changes in Southeast Asia on global hydroxyl](#)
0008 [and methane lifetime, Tellus B, 61\(4\), 588–601, doi:10.1111/j.1600-0889.2009.00429.x, 2009.](#)

0009 [Darmenov, A. and da Silva, A.: The quick fire emissions dataset \(QFED\) - Documentation of versions 2.1, 2.2 and](#)
0010 [2.4, Technical Report Series on Global Modeling and Data Assimilation, NASA Global Modeling and Assimilation](#)
0011 [Office., \[online\] Available from: <https://gmao.gsfc.nasa.gov/pubs/docs/Darmenov796.pdf> \(Accessed 11 March 2020\),](#)
0012 [2015.](#)

0013 [De Mazière, M., Vigouroux, C., Bernath, P. F., Baron, P., Blumenstock, T., Boone, C., Brogniez, C., Catoire, V., Coffey,](#)
0014 [M., Duchatelet, P., Griffith, D., Hannigan, J., Kasai, Y., Kramer, I., Jones, N., Mahieu, E., Manney, G. L., Piccolo, C.,](#)
0015 [Randall, C., Robert, C., Senten, C., Strong, K., Taylor, J., Tétard, C., Walker, K. A., and Wood, S.: Validation of ACE-](#)
0016 [FTS v2.2 methane profiles from the upper troposphere to the lower mesosphere, Atmos. Chem. Phys., 8, 2421–2435,](#)
0017 <https://doi.org/10.5194/acp-8-2421-2008>, 2008.

0018 [Deemer, B. R., Harrison, J. A., Li, S., Beaulieu, J. J., DelSontro, T., Barros, N., Bezerra-Neto, J. F., Powers, S. M., dos](#)
0019 [Santos, M. A. and Vonk, J. A.: Greenhouse Gas Emissions from Reservoir Water Surfaces: A New Global Synthesis,](#)
0020 [BioScience, 66\(11\), 949–964, doi:10.1093/biosci/biw117, 2016.](#)

0021 [Deemer, B.R. and M.A. Holgerson, Drivers of Methane Flux Differ Between Lakes and Reservoirs, Complicating Global](#)
0022 [Upscaling Efforts. Journal of Geophysical Research: Biogeosciences 126\(4\): p. e2019JG005600., 2021.](#)

0023 [Defratyka, S. M., Paris, J.-D., Yver-Kwok, C., Fernandez, J. M., Korben, P., and Bousquet, P.: Mapping Urban Methane](#)
0024 [Sources in Paris, France, Environmental Science & Technology, 55, 8583-8591, 10.1021/acs.est.1c00859, 2021.](#)

0025 [DeISontro, T., Beaulieu, J. J. and Downing, J. A.: Greenhouse gas emissions from lakes and impoundments: Upscaling in](#)
0026 [the face of global change, Limnol. Oceanogr. Lett., 3\(3\), 64–75, doi:10.1002/lol2.10073, 2018.](#)

0027 [Delwiche, K. B., Knox, S. H., Malhotra, A., Fluet-Chouinard, E., McNicol, G., Feron, S., Ouyang, Z., Papale, D., Trotta,](#)
0028 [C., Canfora, E., Cheah, Y.-W., Christianson, D., Alberto, Ma. C. R., Alekseychik, P., Aurela, M., Baldocchi, D.,](#)
0029 [Bansal, S., Billesbach, D. P., Bohrer, G., Bracho, R., Buchmann, N., Campbell, D. I., Celis, G., Chen, J., Chen, W.,](#)
0030 [Chu, H., Dalmagro, H. J., Dengel, S., Desai, A. R., Detto, M., Dolman, H., Eichelmann, E., Euskirchen, E., Famulari,](#)
0031 [D., Fuchs, K., Goeckede, M., Gogo, S., Gondwe, M. J., Goodrich, J. P., Gottschalk, P., Graham, S. L., Heimann, M.,](#)
0032 [Helbig, M., Helfter, C., Hemes, K. S., Hirano, T., Hollinger, D., Hörtnagl, L., Iwata, H., Jacotot, A., Jurasinski, G.,](#)
0033 [Kang, M., Kasak, K., King, J., Klatt, J., Koebisch, F., Krauss, K. W., Lai, D. Y. F., Lohila, A., Mammarella, I., Belelli](#)
0034 [Marchesini, L., Manca, G., Matthes, J. H., Maximov, T., Merbold, L., Mitra, B., Morin, T. H., Nemitz, E., Nilsson, M.](#)
0035 [B., Niu, S., Oechel, W. C., Oikawa, P. Y., Ono, K., Peichl, M., Peltola, O., Reba, M. L., Richardson, A. D., Riley, W.,](#)
0036 [Runkle, B. R. K., Ryu, Y., Sachs, T., Sakabe, A., Sanchez, C. R., Schuur, E. A., Schäfer, K. V. R., Sonnentag, O.,](#)
0037 [Sparks, J. P., Stuart-Haëntjens, E., Sturtevant, C., Sullivan, R. C., Szutu, D. J., Thom, J. E., Torn, M. S., Tuittila, E.-](#)
0038 [S., Turner, J., Ueyama, M., Valach, A. C., Vargas, R., Varlagin, A., Vazquez-Lule, A., Verfaillie, J. G., Vesala, T.,](#)
0039 [Vourlitis, G. L., Ward, E. J., Wille, C., Wohlfahrt, G., Wong, G. X., Zhang, Z., Zona, D., Windham-Myers, L., Poulter,](#)
0040 [B., and Jackson, R. B.: FLUXNET-CH4: a global, multi-ecosystem dataset and analysis of methane seasonality from](#)
0041 [freshwater wetlands, Earth Syst. Sci. Data, 13, 3607–3689, <https://doi.org/10.5194/essd-13-3607-2021>, 2021.](#)

0042 [Deng, Z., Ciais, P., Tzompa-Sosa, Z. A., Saunio, M., Qiu, C., Tan, C., Sun, T., Ke, P., Cui, Y., Tanaka, K., Lin, X.,](#)
0043 [Thompson, R. L., Tian, H., Yao, Y., Huang, Y., Lauerwald, R., Jain, A. K., Xu, X., Bastos, A., Sitch, S., Palmer, P. I.,](#)
0044 [Lauvaux, T., d'Aspremont, A., Giron, C., Benoit, A., Poulter, B., Chang, J., Petrescu, A. M. R., Davis, S. J., Liu, Z.,](#)
0045 [Grassi, G., Albergel, C., Tubiello, F. N., Perugini, L., Peters, W., and Chevallier, F.: Comparing national greenhouse](#)
0046 [gas budgets reported in UNFCCC inventories against atmospheric inversions, Earth Syst. Sci. Data, 14, 1639–1675,](#)
0047 <https://doi.org/10.5194/essd-14-1639-2022>, 2022.

0048 [Denman, K. L., G. Brasseur, A. Chidthaisong, P. Ciais, P. M. Cox, R. E. Dickinson, D. Hauglustaine, C. Heinze, E.](#)
0049 [Holland, D. Jacob, U. Lohmann, S Ramachandran, P. L. da Silva Dias, S. C. Wofsy and X. Zhang: Couplings Between](#)
0050 [Changes in the Climate System and Biogeochemistry, Cambridge University Press, Cambridge, United Kingdom and](#)
0051 [New York, NY, USA., 2007.](#)

0052 [Dirmeyer, P. A., Gao, X., Zhao, M., Guo, Z., Oki, T., and Hanasaki, N. GSWP-2: Multimodel analysis and impli- cations](#)
0053 [for our perception of the land surface. Bulletin of the American Meteorological Society, 87\(10\):1381–1398, 2006.](#)

0054 [Dlugokencky, E. J., Dutton, E. G., Novelli, P. C., Tans, P. P., Masarie, K. A., Lantz, K. O. and Madronich, S.: Changes in](#)
0055 [CH₄ and CO growth rates after the eruption of Mt Pinatubo and their link with changes in tropical tropospheric UV](#)

0056 [flux, *Geophys. Res. Lett.*, 23\(20\), 2761–2764, 1996.](#)

0057 [Dlugokencky, E. J., Myers, R. C., Lang, P. M., Masarie, K. A., Crotwell, A. M., Thoning, K. W., Hall, B. D., Elkins, J.](#)

0058 [W. and Steele, L. P.: Conversion of NOAA atmospheric dry air CH₄ mole fractions to a gravimetrically prepared](#)

0059 [standard scale, *J Geophys Res.*, 110\(D18306\), doi:10.1029/2005JD006035., 2005.](#)

0060 [Dlugokencky, E. J., Bruhwiler, L., White, J. W. C., Emmons, L. K., Novelli, P. C., Montzka, S. A., Masarie, K. A., Lang,](#)

0061 [P. M., Crotwell, A. M., Miller, J. B. and Gatti, L. V.: Observational constraints on recent increases in the atmospheric](#)

0062 [CH₄ burden, *Geophys. Res. Lett.*, 36, 5 PP., doi:200910.1029/2009GL039780, 2009.](#)

0063 [Dlugokencky, E. J., Nisbet, E. G., Fisher, R. and Lowry, D.: Global atmospheric methane: budget, changes and dangers,](#)

0064 [Philos. Trans. R. Soc. - Math. Phys. Eng. Sci., 369\(1943\), 2058–2072, 2011.](#)

0065 [Dong, B., Xi, Y., Cui, Y., and Peng, S.: Quantifying Methane Emissions from Aquaculture Ponds in China, *Environ. Sci.*](#)

0066 [Technol., 57, 1576–1583, <https://doi.org/10.1021/acs.est.2c05218>, 2023.](#)

0067 [Downing, J.: Emerging global role of small lakes and ponds: Little things mean a lot. *Limnetica*, 29: p. 9-24, 2010](#)

0068 [Drinkwater, A., Palmer, P. I., Feng, L., Arnold, T., Lan, X., Michel, S. E., Parker, R., and Boesch, H.: Atmospheric data](#)

0069 [support a multi-decadal shift in the global methane budget towards natural tropical emissions, *Atmos. Chem. Phys.*,](#)

0070 [23, 8429–8452, <https://doi.org/10.5194/acp-23-8429-2023>, 2023.](#)

0071 [Dubos, T., Dubey, S., Tort, M., Mittal, R., Meurdesoif, Y. and Hourdin, F.: DYNAMICO-1.0, an icosahedral hydrostatic](#)

0072 [dynamical core designed for consistency and versatility, *Geosci. Model Dev.*, 8\(10\), 3131–3150, doi:10.5194/gmd-8-](#)

0073 [3131-2015, 2015.](#)

0074 [Dueck, T. A., de Visser, R., Poorter, H., Persijn, S., A. Gorissen, A., W. de Visser, W., Schapendonk, A., Verhagen, J.,](#)

0075 [Snel, J., Harren, F. J. M., Ngai, A. K. Y., Verstappen, F., Bouwmeester, H., Voosenek, L. A. C. J. and van der Werf,](#)

0076 [A.: No evidence for substantial aerobic methane emission by terrestrial plants: a ¹³C-labelling approach, *New Phytol.*,](#)

0077 [doi:10.1111/j.1469-8137.2007.02103.x, 2007.](#)

0078 [Dutaur, L. and Verchot, L. V.: A global inventory of the soil CH₄ sink, *Glob. Biogeochem Cycles*, 21, GB4012,](#)

0079 [doi:10.1029/2006GB002734, 2007.](#)

0080 [EDGAR \(Emissions Database for Global Atmospheric Research\) Community GHG Database, a collaboration between the](#)

0081 [European Commission, Joint Research Centre \(JRC\), the International Energy Agency \(IEA\), and comprising IEA-](#)

0082 [EDGAR CO₂, EDGAR CH₄, EDGAR N₂O, EDGAR F-GASES version 8.0, European Commission, JRC \(Datasets\),](#)

0083 [available at \[https://edgar.jrc.ec.europa.eu/dataset_ghg80\]\(https://edgar.jrc.ec.europa.eu/dataset_ghg80\), 2023](#)

0084 [Eggleton, P., Homathevi, R., Jones, D., MacDonald, J., Jeeva, D., Bignell, D., Davies, R., and Maryati, M.: Termite](#)

0085 [assemblages, forest disturbance and greenhouse gas fluxes in Sabah, East Malaysia, *Philos. T. Roy. Soc. B*, 354, 1791–](#)

0086 [1802, doi: 10.1098/rstb.1999.0521, 1999](#)

0087 [Ehhalt, D., Prather, M., Dentener, F., Derwent, R., Dlugokencky, E., Holland, E., Isaksen, I., Katima, J., Kirchhoff, V.,](#)

0088 [Matson, P., Midgley, P. and Wang, M.: Atmospheric chemistry and greenhouse gases. In: *Climate Change 2001: The*](#)

6089 [Scientific Basis. Contribution of Working Group I to the Third Assessment Report of the Intergovernmental Panel on](#)
6090 [Climate Change. \[Houghton, J.T., et al. \(eds.\)\]. Cambridge University Press, Cambridge, United Kingdom and New](#)
6091 [York, NY, USA, pp. 239-287, 2001.](#)

6092 [Ehhalt, D. H.: The atmospheric cycle of methane. *Tellus*, 26\(1–2\), 58–70. doi:10.1111/j.2153-3490.1974.tb01952.x, 1974.](#)
6093 [Ehret, G., Bousquet, P., Pierangelo, C., Alpers, M., Millet, B., Abshire, J. B., Bovensmann, H., Burrows, J. P., Chevallier,](#)
6094 [F., Ciais, P., Crevoisier, C., Fix, A., Flamant, P., Frankenberg, C., Gibert, F., Heim, B., Heimann, M., Houweling, S.,](#)
6095 [Hubberten, H. W., Jockel, P., Law, K., Low, A., Marshall, J., Agusti-Panareda, A., Payan, S., Prigent, C., Rairoux, P.,](#)
6096 [Sachs, T., Scholze, M. and Wirth, M.: MERLIN: A French-German Space Lidar Mission Dedicated to Atmospheric](#)
6097 [Methane. *Remote Sens.*, 9\(10\), 2017.](#)

6098 [Etiopie, G.: Natural Gas Seepage. *The Earth's Hydrocarbon Degassing*, Springer International Publishing., 2015.](#)
6099 [Etiopie, G.: Natural emissions of methane from geological seepage in Europe. *Atmosph. Environment*, 43, 1430-1443,](#)
6100 [doi:10.1016/j.atmosenv.2008.03.014., 2009](#)

6101 [Etiopie, G. and Schwietzke, S.: Global geological methane emissions: an update of top-down and bottom-up estimates,](#)
6102 [*Elem Sci Anth*, 7\(1\), 47. doi:10.1525/elementa.383, 2019.](#)

6103 [Etiopie, G., Lassey, K. R., Klusman, R. W. and Boschi, E.: Reappraisal of the fossil methane budget and related emission](#)
6104 [from geologic sources. *Geophys. Res. Lett.*, 35\(9\), L09307. doi:10.1029/2008gl033623, 2008.](#)

6105 [Etiopie, G., Nakada, R., Tanaka, K. and Yoshida, N.: Gas seepage from Tokamachi mud volcanoes, onshore Niigata](#)
6106 [Basin \(Japan\): origin, post-genetic alterations and CH₄-CO₂ fluxes. *App. Geochem.*, 26, 348-359, 2011.](#)

6107 [Etiopie, G., Ciotoli, G., Schwietzke, S. and Schoell, M.: Gridded maps of geological methane emissions and their isotopic](#)
6108 [signature, *Earth Syst Sci Data*, 11\(1\), 1–22. doi:10.5194/essd-11-1-2019, 2019.](#)

6109 [EU-Landfill-Directive: <https://eur-lex.europa.eu/legal-content/EN/TXT/?uri=CELEX:31999L0031>, 1999.](#)

6110 [FAO: FAOSTAT Emissions Land Use database. Food and Agriculture Organization of the United Nations. Statistical](#)
6111 [Division., \[online\] Available from: <http://www.fao.org/faostat/en/#data/GL> \(Accessed December 2022\), 2022.](#)

6112 [Federici, S., Tubiello, F. N., Salvatore, M., Jacobs, H. and Schmidhuber, J.: New estimates of CO₂ forest emissions and](#)
6113 [removals: 1990–2015. *For. Ecol. Manag.*, 352, 89–98. doi:10.1016/j.foreco.2015.04.022, 2015.](#)

6114 [Feng, L., Braun, C., Arnold, S. R. and Gidden, M.: *iiasa/emissions_downscaling: Supplemental Data*,](#)
6115 [doi:10.5281/zenodo.2538194, 2019.](#)

6116 [Feng, L., Palmer, P. I., Parker, R. J., Lunt, M. F., and Bösch, H.: Methane emissions are predominantly responsible for](#)
6117 [record-breaking atmospheric methane growth rates in 2020 and 2021. *Atmos. Chem. Phys.*, 23, 4863–4880,](#)
6118 [https://doi.org/10.5194/acp-23-4863-2023, 2023.](#)

6119 [Filges, A., Gerbig, C., Chen, H., Franke, H., Klaus, C., and Jordan, A.: The IAGOS-core greenhouse gas package: a](#)
6120 [measurement system for continuous airborne observations of CO₂, CH₄, H₂O and CO, *Tellus B*, 68, 27989,](#)
6121 [https://doi.org/10.3402/tellusb.v67.27989, 2015.](#)

6122 [Fleischer, P., Orsi, T. H., Richardson, M. D., and Anderson, A. L. \(2001\). Distribution of free gas in marine sediments: a](#)
6123 [global overview. *Geo-Marine Lett.*, 21, 103–122, 2001.](#)

6124 [Flores, E., Rhoderick, G. C., Viallon, J., Moussay, P., Choteau, T., Gameson, L., Guenther, F. R. and Wielgosz, R. I.:](#)
6125 [Methane standards made in whole and synthetic air compared by cavity ring down spectroscopy and gas](#)
6126 [chromatography with flame ionization detection for atmospheric monitoring applications. *Anal. Chem.*, 87\(6\), 3272–](#)
6127 [3279, doi:10.1021/ac5043076, 2015.](#)

6128 [Fluet-Chouinard, E., Stocker, BD, Zhang, Z., Malhotra, A., Melton, JR, Poulter, B., Kaplan, JO, Goldewijk, KK, Siebert, S,](#)
6129 [Minayeva, T, Hugelius, G, Joosten, H, Barthelmes, A, Prigent, C, Aires, F, Hoyt, AM, Davidson, N, Finlayson, CM,](#)
6130 [Lehner, B, Jackson, RB, McIntyre, PB: Extensive global wetland loss over the past three centuries. *Nature*, 614\(7947\)](#)
6131 [281-286, doi:10.1038/s41586-022-05572-6, 2023](#)

6132 [Forster, P., T. Storelvmo, K. Armour, W. Collins, J.-L. Dufresne, D. Frame, D.J. Lunt, T. Mauritsen, M.D. Palmer, M.](#)
6133 [Watanabe, M. Wild, and H. Zhang: The Earth’s Energy Budget, Climate Feedbacks, and Climate Sensitivity. In](#)
6134 [Climate Change 2021: The Physical Science Basis. Contribution of Working Group I to the Sixth Assessment Report](#)
6135 [of the Intergovernmental Panel on Climate Change \[Masson-Delmotte, V., P. Zhai, A. Pirani, S.L. Connors, C. Péan,](#)
6136 [S. Berger, N. Caud, Y. Chen, L. Goldfarb, M.I. Gomis, M. Huang, K. Leitzell, E. Lonnoy, J.B.R. Matthews, T.K.](#)
6137 [Maycock, T. Waterfield, O. Yelekçi, R. Yu, and B. Zhou \(eds.\)\]. Cambridge University Press, Cambridge, United](#)
6138 [Kingdom and New York, NY, USA, pp. 923–1054, doi: 10.1017/9781009157896.009, 2021](#)

6139 [Foschi M., Etiopie G., Cartwright J.A.: Seismic evidence of extensive microbial gas migration and trapping in submarine](#)
6140 [marine hydrates \(Rakhine Basin, Bay of Bengal\). *Mar. Petrol. Geol.*, 149, 106100,](#)
6141 [https://doi.org/10.1016/j.marpetgeo.2023.106100., 2023](#)

6142 [Francey, R. J., Steele, L. P., Langenfelds, R. L. and Pak, B. C.: High precision long-term monitoring of radiatively active](#)
6143 [and related trace gases at surface sites and from aircraft in the southern hemisphere atmosphere. *J. Atmospheric Sci.*,](#)
6144 [56\(2\), 279–285, 1999.](#)

6145 [Frankenberg, C., Meirink, J. F., van Weele, M., Platt, U. and Wagner, T.: Assessing methane emissions from global space-](#)
6146 [borne observations. *Science*, 308\(5724\), 1010–1014, 2005.](#)

6147 [Fraser, P. J., Rasmussen, R. A., Creffield, J. W., French, J. R. and Khalil, M. A. K.: Termites and global methane – Another](#)
6148 [assessment. *J. Atmospheric Chem.*, 4, 295–310, 1986.](#)

6149 [Fraser, W. T., Blei, E., Fry, S. C., Newman, M. F., Reay, D. S., Smith, K. A. and McLeod, A. R.: Emission of methane,](#)
6150 [carbon monoxide, carbon dioxide and short-chain hydrocarbons from vegetation foliage under ultraviolet irradiation,](#)
6151 [Plant Cell Environ., 38\(5\), 980–989, doi:10.1111/pce.12489, 2015.](#)

6152 [Fujita, R., Morimoto, S., Maksyutov, S., Kim, H.-S., Arshinov, M., Brailsford, G., Aoki, S. and Nakazawa, T.: Global and](#)
6153 [Regional CH4 Emissions for 1995–2013 Derived From Atmospheric CH4, δ13C-CH4, and δD-CH4 Observations and](#)
6154 [a 715 Chemical Transport Model. *J. Geophys. Res. Atmos.*, 125: e2020JD032903,](#)

6155 <https://doi.org/10.1029/2020JD032903>, 2020

6156 [Gauci, V., Figueiredo, V., Gedney, N., Pangala, S. R., Stauffer, T., Weedon, G., P. and Enrich-Prast A. Non-flooded](#)

6157 [riparian Amazon trees are a regionally significant methane source. *Phil. Trans. R. Soc. A*.3802020044620200446](#)

6158 <http://doi.org/10.1098/rsta.2020.0446>, 2021.

6159 [Gedney, N., Huntinford, C., Comyn Platt, E. and Wiltshire, A. Significant feedbacks of wetland methane release on climate](#)

6160 [change and the causes of their uncertainty. *Env. Res. Letts.* 14, 084027 doi:10.1088/1748-9326/ab2726](#), 2019.

6161 [Gidden, M. J., Riahi, K., Smith, S. J., Fujimori, S., Luderer, G., Kriegler, E., Vuuren, D. P. van, Berg, M. van den, Feng,](#)

6162 [L., Klein, D., Calvin, K., Doelman, J. C., Frank, S., Fricko, O., Harmsen, M., Hasegawa, T., Havlik, P., Hilaire, J.,](#)

6163 [Hoesly, R., Horing, J., Popp, A., Stehfest, E. and Takahashi, K.: Global emissions pathways under different](#)

6164 [socioeconomic scenarios for use in CMIP6: a dataset of harmonized emissions trajectories through the end of the](#)

6165 [century. *Geosci. Model Dev.*, 12\(4\), 1443–1475, doi:10.5194/gmd-12-1443-2019](#), 2019.

6166 [Giglio, L., Randerson, J. T. and van der Werf, G. R.: Analysis of daily, monthly, and annual burned area using the fourth-](#)

6167 [generation global fire emissions database \(GFED4\). *J. Geophys. Res. - Biogeosciences*, 118\(1\), 317–328,](#)

6168 [doi:10.1002/jgrg.20042](#), 2013.

6169 [Glagolev, M., Kleptsova, I., Filippov, I., Maksyutov, S. and Machida, T.: Regional methane emission from West Siberia](#)

6170 [mire landscapes. *Environ. Res. Lett.*, 6\(4\), 045214, doi:doi:10.1088/1748-9326/6/4/045214](#), 2011.

6171 [Glatthor, N., von Clarmann, T., Funke, B., Garcia-Comas, M., Grabowski, U., Höpfner, M., Kellmann, S., Kiefer, M.,](#)

6172 [Laeng, A., Linden, A., Lopez-Puertas, M., and Stiller, G. P.: IMK/IAA MIPAS retrievals version 8: CH4 and N2O,](#)

6173 [EGUsphere \[preprint\], <https://doi.org/10.5194/egusphere-2023-919>](#), 2023.

6174 [Global Methane Pledge, Global Methane Pledge website: Pledges, 1 September. \[https://www.\]\(https://www.globalmethanepledge.org/#pledges\)](#)

6175 [globalmethanepledge.org/#pledges](#). Accessed 28 September 2023, 2023.

6176 [Griffiths, K., A. Jeziorski, D. Antoniadis, M. Beaulieu, J.P. Smol, and I. Gregory-Eaves, Pervasive changes in algal](#)

6177 [indicators since pre-industrial times: A paleolimnological study of changes in primary production and diatom](#)

6178 [assemblages from ~200 Canadian lakes. *Science of The Total Environment*, 838: p. 155938.](#), 2022.

6179 [Grinham, A., M. Dunbabin, D. Gale, and J. Udy, Quantification of ebullitive and diffusive methane release to atmosphere](#)

6180 [from a water storage. *Atmospheric Environment*, 45\(39\): p. 7166-7173.](#), 2011.

6181 [Gromov, S., Brenninkmeijer, C. A. M. and Jöckel, P.: A very limited role of tropospheric chlorine as a sink of the](#)

6182 [greenhouse gas methane. *Atmospheric Chem. Phys.*, 18\(13\), 9831–9843, doi:10.5194/acp-18-9831-2018](#), 2018.

6183 [Guo, M., Fang, S., Liu, S., Liang, M., Wu, H., Yang, L., Li, Z., Liu, P., Zhang, F.: Comparison of atmospheric CO2, CH4,](#)

6184 [and CO at two stations in the Tibetan Plateau of China, *Earth Space Sci.* 7, e2019EA001051](#), 2020

6185 [Gurney, K. R., Law, R. M., Denning, A. S., Rayner, P. J., Pak, B. C., Baker, D., Bousquet, P., Bruhwiler, L., Chen, Y. H.,](#)

6186 [Ciais, P., Fung, I. Y., Heimann, M., John, J., Maki, T., Maksyutov, S., Peylin, P., Prather, M. and Taguchi, S.: Transcom](#)

6187 [3 inversion intercomparison: Model mean results for the estimation of seasonal carbon sources and sinks, *Glob.*](#)

188 [Biogeochem. Cycles](#), 18(1), GB2010, doi:10.1029/2003gb002111, 2004.

189 [Harris, S. A., French, H. M., Heginbottom, J. A., Johnston, G. H., Ladanyi, B., Sego, D. C. and van Everdingen, R. O.:](#)

190 [Glossary of permafrost and related ground-ice terms, National Research Council of Canada. Associate Committee on](#)

191 [Geotechnical Research. Permafrost Subcommittee., 1988.](#)

192 [Harris, I., Jones, P.D., Osborn, T.J. and Lister, D.H.:](#) Updated high-resolution grids of monthly climatic observations – the

193 [CRU TS3.10 Dataset, *Int. J. Climatol.*, 34: 623-642, <https://doi.org/10.1002/joc.3711>, 2014](#)

194 [Harrison, J.A., Y.T. Prairie, S. Mercier-Blais, and C. Soued:](#) Year-2020 Global Distribution and Pathways of Reservoir

195 [Methane and Carbon Dioxide Emissions According to the Greenhouse Gas From Reservoirs \(G-res\) Model. *Global*](#)

196 [Biogeochemical Cycles 35\(6\): p. e2020GB006888, 2021.](#)

197 [Heathcote, A. J., C. T. Filstrup, and J. A. Downing \(2013\):](#) Watershed sediment losses to lakes accelerating despite

198 [agricultural soil conservation efforts, *PLoS One*, 8\(1\), e53554, doi:10.1371/journal.pone.0053554, 2013](#)

199 [Heděnc, P., Jiménez, J.J., Moradi, J. et al.:](#) Global distribution of soil fauna functional groups and their estimated litter

200 [consumption across biomes. *Sci Rep* 12, 17362, <https://doi.org/10.1038/s41598-022-21563-z>, 2022](#)

201 [Hmiel, B., Petrenko, V. V., Dyonisius, M. N., Buizert, C., Smith, A. M., Place, P. F., Harth, C., Beaudette, R., Hua, Q.,](#)

202 [Yang, B., Vimont, I., Michel, S. E., Severinghaus, J. P., Etheridge, D., Bromley, T., Schmitt, J., Faïn, X., Weiss, R. F.](#)

203 [and Dlugokencky, E.:](#) Preindustrial 14 CH 4 indicates greater anthropogenic fossil CH 4 emissions, *Nature*, 578(7795),

204 [409–412, doi:10.1038/s41586-020-1991-8, 2020.](#)

205 [Ho, J.C., A.M. Michalak, and N. Pahlevan:](#) Widespread global increase in intense lake phytoplankton blooms since the

206 [1980s. *Nature*, 574\(7780\): p. 667-670, 2019](#)

207 [Hoesly, R. M., Smith, S. J., Feng, L., Klimont, Z., Janssens-Maenhout, G., Pitkanen, T., Seibert, J. J., Vu, L., Andres, R.](#)

208 [J., Bolt, R. M., Bond, T. C., Dawidowski, L., Kholod, N., Kurokawa, J. I., Li, M., Liu, L., Lu, Z., Moura, M. C. P.,](#)

209 [O'Rourke, P. R. and Zhang, Q.:](#) Historical (1750–2014) anthropogenic emissions of reactive gases and aerosols from

210 [the Community Emissions Data System \(CEDS\), *Geosci Model Dev*, 11\(1\), 369–408, doi:10.5194/gmd-11-369-2018,](#)

211 [2018.](#)

212 [Höglund-Isaksson, L.:](#) Bottom-up simulations of methane and ethane emissions from global oil and gas systems 1980 to

213 [2012, *Environ. Res. Lett.*, 12\(2\), 024007, doi:10.1088/1748-9326/aa583e, 2017.](#)

214 [Höglund-Isaksson, L., Thomson, A., Kupiainen, K., Rao, S. and Janssens-Maenhout, G.:](#) Anthropogenic methane sources,

215 [emissions and future projections, Chapter 5 in AMAP Assessment 2015: Methane as an Arctic Climate Forcer, p. 39-](#)

216 [59, available at \[http://www.amap.no/documents/doc/AMAP-Assessment-2015-Methane-as-an-Arctic-climate-\]\(http://www.amap.no/documents/doc/AMAP-Assessment-2015-Methane-as-an-Arctic-climate-forcer/1285\)](#)

217 [forcer/1285](#), 2015.

218 [Höglund-Isaksson, L., Gómez-Sanabria, A., Klimont, Z., Rafaj, P., Schöpp, W.:](#) Technical potentials and costs for

219 [reducing global anthropogenic methane emissions in the 2050 timeframe -results from the GAINS model, *Environ.*](#)

220 [Res. Comm.](#) 2(2), <https://iopscience.iop.org/article/10.1088/2515-7620/ab7457> , 2020

6221 [Holgerson, M. A. and Raymond, P. A.: Large contribution to inland water CO₂ and CH₄ emissions from very small](#)
6222 [ponds, *Nat. Geosci.*, 9\(3\), 222–226, doi:10.1038/ngeo2654, 2016.](#)

6223 [Holmes, C. D., Prather, M. J., Søvde, O. A. and Myhre, G.: Future methane, hydroxyl, and their uncertainties: key climate](#)
6224 [and emission parameters for future predictions, *Atmospheric Chem. Phys.*, 13\(1\), 285–302, doi:10.5194/acp-13-285-](#)
6225 [2013, 2013.](#)

6226 [Hopcroft, P.O., P.J. Valdes & D.J. Beerling, \(2011\). Simulating idealised Dansgaard-Oeschger events and their potential](#)
6227 [influence on the global methane cycle, *Quaternary Science Reviews*, 30, 3258-3268,](#)
6228 [doi: 10.1016/j.quascirev.2011.08.01., 2011](#)

6229 [Hossaini, R., Chipperfield, M. P., Saiz-Lopez, A., Fernandez, R., Monks, S., Feng, W., Brauer, P. and Glasow, R. von: A](#)
6230 [global model of tropospheric chlorine chemistry: Organic versus inorganic sources and impact on methane oxidation,](#)
6231 [*J. Geophys. Res. Atmospheres*, 121\(23\), 14,271-14,297, doi:10.1002/2016JD025756, 2016.](#)

6232 [Houweling, S., Bergamaschi, P., Chevallier, F., Heimann, M., Kaminski, T., Krol, M., Michalak, A. M. and Patra, P.:](#)
6233 [Global inverse modeling of CH₄ sources and sinks: an overview of methods, *Atmospheric Chem. Phys.*, 17\(1\), 235–](#)
6234 [256, doi:10.5194/acp-17-235-2017, 2017.](#)

6235 [M. Hovland, A.G. Judd, R.A. Burke: The global flux of methane from shallow submarine sediments, *Chemosphere*,](#)
6236 [Volume 26, Issues 1–4, Pages 559-578, doi:10.1016/0045-6535\(93\)90442-8., 1993](#)

6237 [Howarth, R. W.: Ideas and perspectives: is shale gas a major driver of recent increase in global atmospheric methane?](#)
6238 [*Biogeosciences*, 16\(15\), 3033–3046, doi:10.5194/bg-16-3033-2019, 2019.](#)

6239 [Hu, H., Landgraf, J., Detmers, R., Borsdorff, T., Brugh, J. A. de, Aben, I., Butz, A. and Hasekamp, O.: Toward Global](#)
6240 [Mapping of Methane With TROPOMI: First Results and Intersatellite Comparison to GOSAT, *Geophys. Res. Lett.*,](#)
6241 [45\(8\), 3682–3689, doi:10.1002/2018GL077259, 2018.](#)

6242 [Hugelius, G., Tarnocai, C., Broll, G., Canadell, J. G., Kuhry, P., & Swanson, D. K.. The Northern Circumpolar Soil Carbon](#)
6243 [Database: spatially distributed datasets of soil coverage and soil carbon storage in the northern permafrost regions,](#)
6244 [*Earth System Science Data*, 5\(1\), 3–13, https://doi.org/10.5194/essd-5-3-2013, 2013](#)

6245 [Hugelius, G., Strauss, J., Zubrzycki, S., Harden, J. W., Schuur, E. A. G., Ping, C. L., Schirmermeister, L., Grosse, G.,](#)
6246 [Michaelson, G. J., Koven, C. D., O'Donnell, J. A., Elberling, B., Mishra, U., Camill, P., Yu, Z., Palmtag, J. and Kuhry,](#)
6247 [P.: Estimated stocks of circumpolar permafrost carbon with quantified uncertainty ranges and identified data gaps,](#)
6248 [*Biogeosciences*, 11\(23\), 6573–6593, doi:10.5194/bg-11-6573-2014, 2014.](#)

6249 [Hugelius, Gustaf, Loisel, J., Chadburn, S., Jackson, R. B., Jones, M., MacDonald, G., et al. : Large stocks of peatland](#)
6250 [carbon and nitrogen are vulnerable to permafrost thaw. *Proceedings of the National Academy of Sciences*, 117\(34\),](#)
6251 [20438–20446. https://doi.org/10.1073/pnas.1916387117, 2020](#)

6252 [Hugelius, G., Ramage, J.L., Burke, E.J., Chatterjee, A., Smallman, T.L., Aalto, T., Bastos, A., Biasi, C., Canadell, J.G.,](#)
6253 [Chandra, N. and Chevallier, F., et al. Two decades of permafrost region CO₂, CH₄, and N₂O budgets suggest a small](#)

net greenhouse gas source to the atmosphere. Preprint in ESS Open Archive. September 11, 2023. DOI: 10.22541/essoar.169444320.01914726/v1, 2023

IEA, *Coal Information: Overview*, IEA, Paris <https://www.iea.org/reports/coal-information-overview>, License: CC BY 4.0, Accessed 17 January 2024, 2021

IEA (2023), *Energy Statistics Data Browser*, IEA, Paris <https://www.iea.org/data-and-statistics/data-tools/energy-statistics-data-browser>, Accessed 17 January 2024, 2023a

IEA, *US natural gas production by source, 2013-2023*, IEA, Paris <https://www.iea.org/data-and-statistics/charts/us-natural-gas-production-by-source-2013-2023>, IEA. Licence: CC BY 4.0, Accessed 17 January 2024, 2023b

Imasu, R.; Matsunaga, T.; Nakajima, M.; Yoshida, Y.; Shiomi, K.; Morino, I.; Saitoh, N.; Niwa, Y.; Someya, Y.; Oishi, Y.; et al. Greenhouse Gases Observing SATellite 2 (GOSAT-2): Mission Overview. *Prog. Earth Planet. Sci.*, *10*, 33, 2023.

Inoue, M., Morino, I., Uchino, O., Nakatsuru, T., Yoshida, Y., Yokota, T., Wunch, D., Wennberg, P. O., Roehl, C. M., Griffith, D. W. T., Velasco, V. A., Deutscher, N. M., Warneke, T., Notholt, J., Robinson, J., Sherlock, V., Hase, F., Blumenstock, T., Rettinger, M., Sussmann, R., Kyrö, E., Kivi, R., Shiomi, K., Kawakami, S., Mazière, M. D., Arnold, S. G., Feist, D. G., Barrow, E. A., Barney, J., Dubey, M., Schneider, M., Iraci, L. T., Podolske, J. R., Hillyard, P. W., Machida, T., Sawa, Y., Tsuboi, K., Matsueda, H., Sweeney, C., Tans, P. P., Andrews, A. E., Biraud, S. C., Fukuyama, Y., Pittman, J. V., Kort, E. A. and Tanaka, T.: Bias corrections of GOSAT SWIR XCO₂ and XCH₄ with TCCON data and their evaluation using aircraft measurement data, *Atmospheric Meas. Tech.*, 9(8), 3491–3512, doi:10.5194/amt-9-3491-2016, 2016.

IPCC: *Good Practice Guidance and Uncertainty Management in National Greenhouse Gas Inventories*. Intergovernmental Panel on Climate Change, National Greenhouse Gas Inventories Programme. Montreal, IPCC-XVI/Doc.10(1.IV.2000), May 2000., 2000.

IPCC: *Climate change 2001: The scientific basis. Contribution of working group I to the third assessment report of the Intergovernmental Panel on Climate Change*. Cambridge University Press, Cambridge, United Kingdom and New York, NY, USA., 2001.

IPCC: *IPCC Guidelines for National Greenhouse Gas Inventories*. The National Greenhouse Gas Inventories Programme, Eggleston H.S., Buendia L., Miwa K., Ngara T. and Tanabe K. (eds). The Intergovernmental Panel on Climate Change, IPCC TSU NGGIP, IGES, Institute for Global Environmental Strategy, Hayama, Kanagawa, Japan. Available online at: http://www.ipcc-nggip.iges.or.jp/support/Primer_2006GLs.pdf, 2006.

IPCC: *2019 Refinement to the 2006 IPCC Guidelines for National Greenhouse Gas Inventories — IPCC*. [online] Available from: <https://www.ipcc.ch/report/2019-refinement-to-the-2006-ipcc-guidelines-for-national-greenhouse-gas-inventories/> (Accessed 17 March 2020), 2019.

Ito, A. and Inatomi, M.: Use of a process-based model for assessing the methane budgets of global terrestrial ecosystems

6287 [and evaluation of uncertainty, *Biogeosciences*, 9\(2\), 759–773, doi:10.5194/bg-9-759-2012, 2012.](#)

6288 [Jacob, D. J., Varon, D. J., Cusworth, D. H., Dennison, P. E., Frankenberg, C., Gautam, R., Guanter, L., Kelley, J.,](#)

6289 [McKeever, J., Ott, L. E., Poulter, B., Qu, Z., Thorpe, A. K., Worden, J. R., and Duren, R. M.: Quantifying methane](#)

6290 [emissions from the global scale down to point sources using satellite observations of atmospheric methane, *Atmos.*](#)

6291 [Chem. Phys.](#), 22, 9617–9646, <https://doi.org/10.5194/acp-22-9617-2022>, 2022.

6292 [Jackson, R. B., Down, A., Phillips, N. G., Ackley, R. C., Cook, C. W., Plata, D. L. and Zhao, K.: Natural gas pipeline](#)

6293 [leaks across Washington, D.C, *Environ. Sci. Technol.*, 48\(3\), 2051–2058, doi:10.1021/es404474x, 2014a.](#)

6294 [Jackson, R. B., Vengosh, A., Carey, J. W., Davies, R. J., Darrah, T. H., O’Sullivan, F. and Pétron, G.: The Environmental](#)

6295 [Costs and Benefits of Fracking, *Annu. Rev. Environ. Resour.*, 39, 327–362, doi:10.1146/annurev-environ-031113-](#)

6296 [144051, 2014b.](#)

6297 [Jackson, R. B., Saunois, M., Bousquet, P., Canadell, J. G., Poulter, B., Stavert, A. R., Poulter, B., Bergamaschi, P., Niwa,](#)

6298 [Y., Segers, A., Tsuruta, A.: Increasing anthropogenic methane emissions arise equally from agricultural and fossil fuel](#)

6299 [sources, *Environmental Research Letters*, 15, 7, <https://doi.org/10.1088/1748-9326/ab9ed2>, 2020](#)

6300 [Jamali, H., Livesley, S.J., Dawes, T.Z. *et al.* Termite mound emissions of CH₄ and CO₂ are primarily determined by](#)

6301 [seasonal changes in termite biomass and behaviour, *Oecologia* 167, 525–534, doi.org/10.1007/s00442-011-1991-3,](#)

6302 [2011](#)

6303 [Janssens-Maenhout, G., Crippa, M., Guizzardi, D., Muntean, M., Schaaf, E., Dentener, F., Bergamaschi, P., Pagliari, V.,](#)

6304 [Olivier, J., Peters, J., van Aardenne, J., Monni, S., Doering, U., Petrescu, R., Solazzo, E. and Oreggioni, G.: EDGAR](#)

6305 [v4.3.2 Global Atlas of the three major Greenhouse Gas Emissions for the period 1970–2012, *Earth Syst Sci Data*](#)

6306 [Discuss](#), 2019, 1–52, doi:10.5194/essd-2018-164, 2019.

6307 [JAXA: GOSAT-2: Greenhouse gases Observing SATellite-2@ibuki2_JAXA"IBUKI-2". \[online\] Available from:](#)

6308 <https://global.jaxa.jp/projects/sat/gosat2/index.html> (Accessed 25 March 2020), 2019.

6309 [Jensen, K. and Mcdonald, K.: Surface Water Microwave Product Series Version 3: A Near-Real Time and 25-Year](#)

6310 [Historical Global Inundated Area Fraction Time Series From Active and Passive Microwave Remote Sensing, *IEEE*](#)

6311 [Geosci. Remote Sens. Lett.](#), 16(9), 1402–1406, doi:10.1109/LGRS.2019.2898779, 2019.

6312 [Jiang, Y., Groenigen, K. J. van, Huang, S., Hungate, B. A., Kessel, C. van, Hu, S., Zhang, J., Wu, L., Yan, X., Wang, L.,](#)

6313 [Chen, J., Hang, X., Zhang, Y., Horwath, W. R., Ye, R., Linquist, B. A., Song, Z., Zheng, C., Deng, A. and Zhang, W.:](#)

6314 [Higher yields and lower methane emissions with new rice cultivars, *Glob. Change Biol.*, 23\(11\), 4728–4738,](#)

6315 [doi:10.1111/gcb.13737](https://doi.org/10.1111/gcb.13737), 2017.

6316 [Johnson, D. E., Phetteplace, H. W. and Seidl, A. F.: Methane, nitrous oxide and carbon dioxide emissions from ruminant](#)

6317 [livestock production systems, edited by J. Takahashi and B. A. Young, pp. 77–85, Elsevier, Amsterdam, The](#)

6318 [Netherlands, 2002.](#)

6319 [Johnson, M.S., E. Matthews, J. Du, V. Genovese, and D. Bastviken, Methane Emission From Global Lakes: New](#)

6320 [Spatiotemporal Data and Observation-Driven Modeling of Methane Dynamics Indicates Lower Emissions, *Journal of*](#)
6321 [Geophysical Research: Biogeosciences](#), 127(7): p. e2022JG006793, 2022

6322 [Johnson, M. S., E. Matthews, D. Bastviken, B. Deemer, J. Du, and V. Genovese, Spatiotemporal methane emission from](#)
6323 [global reservoirs, *Journal of Geophysical Research: Biogeosciences*, 126, e2021JG006305,](#)
6324 <https://doi.org/10.1029/2021JG006305>, 2021

6325 [Judd, A.G. \(2004\). Natural seabed seeps as sources of atmospheric methane, *Environ. Geol.*, 46, 988–996, 2004.](#)

6326 [Jung, M., Reichstein, M., Margolis, H. A., Cescatti, A., Richardson, A. D., Arain, M. A., Armeth, A., Bernhofer, C., Bonal,](#)
6327 [D., Chen, J., Gianelle, D., Gobron, N., Kiely, G., Kutsch, W., Lasslop, G., Law, B. E., Lindroth, A., Merbold, L.,](#)
6328 [Montagnani, L., Moors, E. J., Papale, D., Sottocornola, M., Vaccari, F., and Williams, C.: Global patterns of land-](#)
6329 [atmosphere fluxes of carbon dioxide, latent heat, and sensible heat derived from eddy covariance, satellite, and](#)
6330 [meteorological observations, *J. Geophys. Res.*, 116, G00J07,https://doi.org/10.1029/2010jg001566, 2011.](#)

6331 [Kai, F. M., Tyler, S. C., Randerson, J. T. and Blake, D. R.: Reduced methane growth rate explained by decreased Northern](#)
6332 [Hemisphere microbial sources, *Nature*, 476\(7359\), 194–197, 2011.](#)

6333 [Kaiser, J. W., Heil, A., Andreae, M. O., Benedetti, A., Chubarova, N., Jones, L., Morcrette, J. J., Razinger, M., Schultz,](#)
6334 [M. G., Suttie, M. and van der Werf, G. R.: Biomass burning emissions estimated with a global fire assimilation system](#)
6335 [based on observed fire radiative power, *Biogeosciences*, 9\(1\), 527–554, doi:10.5194/bg-9-527-2012, 2012.](#)

6336 [Kallingal, J. T., Lindström, J., Miller, P. A., Rinne, J., Raivonen, M., and Scholze, M.: Optimising CH₄ simulations from](#)
6337 [the LPJ-GUESS model v4.1 using an adaptive MCMC algorithm, *Geosci. Model Dev. Discuss.* \[preprint\],](#)
6338 <https://doi.org/10.5194/gmd-2022-302>, in review, 2023.

6339 [Karion, A., Sweeney, C., Pétron, G., Frost, G., Michael Hardesty, R., Kofler, J., Miller, B. R., Newberger, T., Wolter, S.,](#)
6340 [Banta, R., Brewer, A., Dlugokencky, E., Lang, P., Montzka, S. A., Schnell, R., Tans, P., Trainer, M., Zamora, R. and](#)
6341 [Conley, S.: Methane emissions estimate from airborne measurements over a western United States natural gas field,](#)
6342 [Geophys. Res. Lett.](#), 40(16), 4393–4397, doi:10.1002/grl.50811, 2013.

6343 [Karl, D., Beversdorf, L., Björkman, K. *et al.* Aerobic production of methane in the sea. *Nature Geosci* 1, 473–478 .](#)
6344 <https://doi.org/10.1038/ngeo234>, 2008

6345 [Karlson, M., and Bastviken, D.: Multi-Source Mapping of Peatland Types Using Sentinel-1, Sentinel-2, and Terrain](#)
6346 [Derivatives—A Comparison Between Five High-Latitude Landscapes. *Journal of Geophysical Research:*](#)
6347 [Biogeosciences](#) 128, e2022JG007195. <https://doi.org/10.1029/2022JG007195>, 2023

6348 [Keppler, F., Hamilton, J. T. G., Brass, M. and Rockmann, T.: Methane emissions from terrestrial plants under aerobic](#)
6349 [conditions, *Nature*, 439, 187–191, doi:10.1038/nature04420, 2006.](#)

6350 [Kholod, N., Evans, M., Pilcher, R. C., Roshchanka, V., Ruiz, F., Coté, M. and Collings, R.: Global methane emissions](#)
6351 [from coal mining to continue growing even with declining coal production, *J. Clean. Prod.*, 256, 120489,](#)
6352 [doi:10.1016/j.jclepro.2020.120489](https://doi.org/10.1016/j.jclepro.2020.120489), 2020.

6353 [Kim H., Global Soil Wetness Project Phase 3 Atmospheric Boundary Conditions \(Experiment 1\) \[Data set\]. Data](#)
6354 [Integration and Analysis System \(DIAS\). https://doi.org/10.20783/DIAS.501, 2017](#)

6355 [King, J.R., Warren, R.J., Bradford, M.A. Correction: Social Insects Dominate Eastern US Temperate Hardwood Forest](#)
6356 [Macroinvertebrate Communities in Warmer Regions. PLOS ONE 8\(10\): 10.1371/annotation/87285c86-f1df-4f8b-](#)
6357 [bc08-d64643d351f4, 2013.](#)

6358 [Kirk, L. and MJ Cohen: River Corridor Sources Dominate CO₂ Emissions From a Lowland River Network. Journal of](#)
6359 [Geophysical Research, Biogeosciences, 128\(1\), e2022JG006954, 2023.](#)

6360 [Kirschke, S., Bousquet, P., Ciais, P., Saunois, M., Canadell, J. G., Dlugokencky, E. J., Bergamaschi, P., Bergmann, D.,](#)
6361 [Blake, D. R., Bruhwiler, L., Cameron-Smith, P., Castaldi, S., Chevallier, F., Feng, L., Fraser, A., Heimann, M.,](#)
6362 [Hodson, E. L., Houweling, S., Josse, B., Fraser, P. J., Krummel, P. B., Lamarque, J. F., Langenfelds, R. L., Le Quere,](#)
6363 [C., Naik, V., O'Doherty, S., Palmer, P. I., Pison, I., Plummer, D., Poulter, B., Prinn, R. G., Rigby, M., Ringeval, B.,](#)
6364 [Santini, M., Schmidt, M., Shindell, D. T., Simpson, I. J., Spahn, R., Steele, L. P., Strode, S. A., Sudo, K., Szopa, S.,](#)
6365 [van der Werf, G. R., Voulgarakis, A., van Weele, M., Weiss, R. F., Williams, J. E. and Zeng, G.: Three decades of](#)
6366 [global methane sources and sinks. Nat. Geosci., 6\(10\), 813–823, doi:10.1038/ngeo1955, 2013.](#)

6367 [Klauda, J. B. and Sandler, S. I.: Global distribution of methane hydrate in ocean sediment. Energy Fuels, 19\(2\), 459–470,](#)
6368 [2005.](#)

6369 [Kleinen, T., Brovkin, V. and Schuldt, R. J.: A dynamic model of wetland extent and peat accumulation: results for the](#)
6370 [Holocene. Biogeosciences, 9\(1\), 235–248, doi:10.5194/bg-9-235-2012, 2012.](#)

6371 [Kleinen, T., Mikolajewicz, U., and Brovkin, V.: Terrestrial methane emissions from the Last Glacial Maximum to the](#)
6372 [preindustrial period. Clim. Past, 16, 575–595, doi:10.5194/cp-16-575-2020, 2020.](#)

6373 [Kleinen, T., Gromov, S., Steil, B., and Brovkin, V.: Atmospheric methane underestimated in future climate projections.](#)
6374 [Environ. Res. Lett., 16, 094006, doi:10.1088/1748-9326/ac1814, 2021.](#)

6375 [Kleinen, T., Gromov, S., Steil, B., and Brovkin, V.: Atmospheric methane since the last glacial maximum was driven by](#)
6376 [wetland sources. Clim. Past, 19, 1081–1099, doi:10.5194/cp-19-1081-2023, 2023](#)

6377 [Knittel K and Boetius A : Anaerobic oxidation of methane: progress with an unknown process methane. Annu Rev](#)
6378 [Microbiol 63:311–334, 2009](#)

6379 [Knox, S. H., Jackson, R. B., Poulter, B., McNicol, G., Fluet-Chouinard, E., Zhang, Z., Hugelius, G., Bousquet, P.,](#)
6380 [Canadell, J. G., Saunois, M., Papale, D., Chu, H., Keenan, T. F., Baldocchi, D., Torn, M. S., Mammarella, I., Trotta,](#)
6381 [C., Aurela, M., Bohrer, G., Campbell, D. I., Cescatti, A., Chamberlain, S., Chen, J., Chen, W., Dengel, S., Desai, A.](#)
6382 [R., Euskirchen, E., Friborg, T., Gasbarra, D., Goded, I., Goeckede, M., Heimann, M., Helbig, M., Hirano, T., Hollinger,](#)
6383 [D. Y., Iwata, H., Kang, M., Klatt, J., Krauss, K. W., Kutzbach, L., Lohila, A., Mitra, B., Morin, T. H., Nilsson, M. B.,](#)
6384 [Niu, S., Noormets, A., Oechel, W. C., Peichl, M., Peltola, O., Reba, M. L., Richardson, A. D., Runkle, B. R. K., Ryu,](#)
6385 [Y., Sachs, T., Schäfer, K. V. R., Schmid, H. P., Shurpali, N., Sonnentag, O., Tang, A. C. I., Ueyama, M., Vargas, R.,](#)

6386 [Vesala, T., Ward, E. J., Windham-Myers, L., Wohlfahrt, G. and Zona, D.: FLUXNET-CH4 Synthesis Activity:](#)
6387 [Objectives, Observations, and Future Directions, *Bull. Am. Meteorol. Soc.*, 100\(12\), 2607–2632, doi:10.1175/BAMS-](#)
6388 [D-18-0268.1, 2019.](#)

6389 [Knox, S. H., Bansal, S., McNicol, G., Schafer, K., Sturtevant, C., Ueyama, M., et al.: Identifying dominant environmental](#)
6390 [predictors of freshwater wetland methane fluxes across diurnal to seasonal time scales. *Global Change Biology*,](#)
6391 [27\(15\), 3582–3604. <https://doi.org/10.1111/gcb.15661>, 2021](#)

6392 [Kretschmer, K., Biastoch, A., Rüpke, L. and Burwicz, E.: Modeling the fate of methane hydrates under global warming,](#)
6393 [Gloab. Biogeochem Cycles, 29\(5\), 610–625, doi:1002/2014GB005011, 2015.](#)

6394 [Kuhn, M.A., Varner, R.K., Bastviken, D., Crill, P., MacIntyre, S., Turetsky, M., Walter Anthony, K., McGuire, A.D., and](#)
6395 [Olefeldt, D. \(2021\). BAWLD-CH4: a comprehensive dataset of methane fluxes from boreal and arctic ecosystems.](#)
6396 [Earth Syst. Sci. Data 13, 5151-5189. \[10.5194/essd-13-5151-2021\]\(https://doi.org/10.5194/essd-13-5151-2021\).](#)

6397 [Kuze A, Kikuchi N, Kataoka F, Suto H, Shiomi K, Kondo Y. Detection of Methane Emission from a Local Source Using](#)
6398 [GOSAT Target Observations. *Remote Sensing*, 12\(2\):267. <https://doi.org/10.3390/rs12020267>, 2020](#)

6399 [Kyzivat, E.D., L.C. Smith, F. Garcia-Tigueros, C. Huang, C. Wang, T. Langhorst, J.V. Fayne, M.E. Harlan, Y. Ishitsuka,](#)
6400 [D. Feng, W. Dolan, L.H. Pitcher, K.P. Wickland, M.M. Domblaser, R.G. Striegl, T.M. Pavelsky, D.E. Butman, and](#)
6401 [C.J. Gleason, The Importance of Lake Emergent Aquatic Vegetation for Estimating Arctic-Boreal Methane Emissions,](#)
6402 [Journal of Geophysical Research: Biogeosciences 127\(6\): p. e2021JG006635, 2022.](#)

6403 [Lamarque, J. F., Shindell, D. T., Josse, B., Young, P. J., Cionni, I., Eyring, V., Bergmann, D., Cameron-Smith, P., Collins,](#)
6404 [W. J., Doherty, R., Dalsoren, S., Faluvegi, G., Folberth, G., Ghan, S. J., Horowitz, L. W., Lee, Y. H., MacKenzie, I.](#)
6405 [A., Nagashima, T., Naik, V., Plummer, D., Righi, M., Rumbold, S. T., Schulz, M., Skeie, R. B., Stevenson, D. S.,](#)
6406 [Strode, S., Sudo, K., Szopa, S., Voulgarakis, A. and Zeng, G.: The Atmospheric Chemistry and Climate Model](#)
6407 [Intercomparison Project \(ACCMIP\): overview and description of models, simulations and climate diagnostics, *Geosci.*](#)
6408 [Model Dev.](#), 6(1), 179–206, doi:10.5194/gmd-6-179-2013, 2013.

6409 [Lamb, B. K., Edburg, S. L., Ferrara, T. W., Howard, T., Harrison, M. R., Kolb, C. E., Townsend-Small, A., Dyck, W.,](#)
6410 [Possolo, A. and Whetstone, J. R.: Direct Measurements Show Decreasing Methane Emissions from Natural Gas Local](#)
6411 [Distribution Systems in the United States, *Environ. Sci. Technol.*, 49\(8\), 5161–5169, doi:10.1021/es505116p, 2015.](#)

6412 [Lan, X., K.W. Thoning, and E.J. Dlugokencky: Trends in globally-averaged CH4, N2O, and SF6 determined from NOAA](#)
6413 [Global Monitoring Laboratory measurements. Version 2024-02, <https://doi.org/10.15138/P8XG-AA10>, 2024](#)

6414 [Lange S., WFDE5 over land merged with ERA5 over the ocean \(WSE5\). V. 1.0. 2019. doi:10.5880/pik.2019.023, 2019](#)

6415 [Laruelle, G. G., Dürr, H. H., Lauerwald, R., Hartmann, J., Slomp, C. P., Goossens, N. and Regnier, P. A. G.: Global multi-](#)
6416 [scale segmentation of continental and coastal waters from the watersheds to the continental margins, *Hydrol. Earth*](#)
6417 [Syst. Sci.](#), 17(5), 2029–2051, doi:10.5194/hess-17-2029-2013, 2013.

6418 [Laruelle, G. G., Rosentreter, J. A. & Regnier P.: Extrapolation based regionalized re-evaluation of the global estuarine](#)
6419 [surface area. Preprint at Earth ArXiv <https://doi.org/10.31223/X5X664>, 2023.](#)

6420 [Lassez, K. R., Etheridge, D. M., Lowe, D. C., Smith, A. M. and Ferretti, D. F.: Centennial evolution of the atmospheric](#)
6421 [methane budget: what do the carbon isotopes tell us?, *Atmospheric Chem. Phys.*, 7\(8\), 2119–2139, 2007a.](#)

6422 [Lassez, K. R., Lowe, D. C. and Smith, A. M.: The atmospheric cycling of radiomethane and the “fossil fraction” of the](#)
6423 [methane source, *Atmospheric Chem. Phys.*, 7\(8\), 2141–2149, 2007b.](#)

6424 [Lauerwald, R., Allen, G.H., Deemer, B.R., Liu, S., Maavara, T., Raymond, P., Alcott, L., Bastviken, D., Hastie, A.,](#)
6425 [Holgerson, M.A., Johnson, M.S., Lehner, B., Lin, P., Marzadri, A., Ran, L., Tian, H., Yang, X., Yao, Y. and Regnier,](#)
6426 [P. Inland water greenhouse gas budgets for RECCAP2: 1. State-of- the-art of global scale assessments. *Global*](#)
6427 [Biogeochemical Cycles](#), 37, e2022GB007657. <https://doi.org/10.1029/2022GB007657>, 2023a.

6428 [Lauerwald, R., Allen, G.H., Deemer, B.R., Liu, S., Maavara, T., Raymond, P., Alcott, L., Bastviken, D., Hastie, A.,](#)
6429 [Holgerson, M.A., Johnson, M.S., Lehner, B., Lin, P., Marzadri, A., Ran, L., Tian, H., Yang, X., Yao, Y. and Regnier,](#)
6430 [P. Inland water greenhouse gas budgets for RECCAP2: 2 Regionalization and homogenization of estimates following](#)
6431 [the RECCAP2 framework, *Global Biogeochemical Cycles*, 37, e2022GB007658. \[https://doi.\]\(https://doi.org/10.1029/2022GB007658\)](#)
6432 [org/10.1029/2022GB007658](#), 2023b.

6433 [Laughner, J. L., Neu, J. L., Schimel, D., Wennberg, P. O., Barsanti, K., Bowman, K. W., Chatterjee, A., Croes, B. E.,](#)
6434 [Fitzmaurice, H. L., Henze, D. K., Kim, J., Kort, E. A., Liu, Z., Miyazaki, K., Turner, A. J., Anenberg, S., Avise, J.,](#)
6435 [Cao, H., Crisp, D., de Gouw, J., Eldering, A., Fyfe, J. C., Goldberg, D. L., Gurney, K. R., Hasheminassab, S., Hopkins,](#)
6436 [F., Ivey, C. E., Jones, D. B. A., Liu, J., Lovenduski, N. S., Martin, R. V., McKinley, G. A., Ott, L., Poulter, B., Ru, M.,](#)
6437 [Sander, S. P., Swart, N., Yung, Y. L., and Zeng, Z.-C.: Societal shifts due to COVID-19 reveal large-scale complexities](#)
6438 [and feedbacks between atmospheric chemistry and climate change, *P. Natl. Acad. Sci. USA*, 118, e2109481118,](#)
6439 [https://doi.org/10.1073/pnas.2109481118](#), 2021.

6440 [Lauvaux, T., Giron, C., Mazzolini, M., d’Aspremont, A., Duren, R., Cusworth, D., Shindell, D., and Ciais, P.: Global](#)
6441 [assessment of oil and gas methane ultra-emitters, *Science*, 375, 557–561, <https://doi.org/10.1126/science.abj4351>,](#)
6442 [2022.](#)

6443 [Lelieveld, J., Crutzen, P. J. and Dentener, F. J.: Changing concentration, lifetime and climate forcing of atmospheric](#)
6444 [methane, *Tellus Ser. B-Chem. Phys. Meteorol.*, 50\(2\), 128–150, doi:10.1034/j.1600-0889.1998.t01-1-00002.x](#), 1998.

6445 [Lelieveld, J., Lechtenbohmer, S., Assonov, S. S., Brenninkmeijer, C. A. M., Dienst, C., Fishedick, M. and Hanke, T.:](#)
6446 [Greenhouse gases: Low methane leakage from gas pipelines, *Nature*, 434\(7035\), 841–842, doi:10.1038/434841a](#), 2005.

6447 [Lenhart, K., Klintzsch, T., Langer, G., Nehrke, G., Bunge, M., Schnell, S. and Keppler, F.: Evidence for methane](#)
6448 [production by the marine algae *Emiliania huxlevi*, *Biogeosciences*, 13\(10\), 3163–3174, doi:10.5194/bg-13-3163-2016,](#)
6449 [2016.](#)

6450 [Lewan, M. D.: Comment on Ideas and perspectives: is shale gas a major driver of recent increase in global atmospheric](#)

methane? by Robert W. Howarth (2019). *Biogeosciences Discuss.*, 1–10, doi:10.5194/bg-2019-419, 2020.

Li, C., Frolking, S., Xiao, X., Moore, B., Boles, S., Qiu, J., Huang, Y., Salas, W. and Sass, R.: Modeling impacts of farming management alternatives on CO₂, CH₄, and N₂O emissions: A case study for water management of rice agriculture of China. *Glob. Biogeochem. Cycles*, 19(3), doi:10.1029/2004gb002341, 2005.

Li T, Huang Y, Zhang W, Song C: CH4MODwetland: A biogeophysical model for simulating methane emissions from natural wetlands. *Ecological Modelling* 221: 666–680, 2010.

Li, Y., J. Shang, C. Zhang, W. Zhang, L. Niu, L. Wang, and H. Zhang. The role of freshwater eutrophication in greenhouse gas emissions: A review. *Science of The Total Environment*, 768: p. 144582., 2021

Lin, X., Indira, N. K., Ramonet, M., Delmotte, M., Ciais, P., Bhatt, B. C., Reddy, M. V., Angchuk, D., Balakrishnan, S., Jorphaik, S., Dorjai, T., Mahey, T. T., Patnaik, S., Begum, M., Brenninkmeijer, C., Durairaj, S., Kirubakaran, R., Schmidt, M., Swathi, P. S., Vinithkumar, N. V., Yver Kwok, C. and Gaur, V. K.: Long-lived atmospheric trace gases measurements in flask samples from three stations in India. *Atmospheric Chem. Phys.*, 15(17), 9819–9849, doi:10.5194/acp-15-9819-2015, 2015.

Lin, P., Pan, M., Beck, H. E., Yang, Y., Yamazaki, D., Frasson, R., et al.: Global reconstruction of naturalized river flows at 2.94 million reaches. *Water Resources Research*, 55, 6499–6516. <https://doi.org/10.1029/2019WR025287>, 2019

Liu, Z., Guan, D., Wei, W., Davis, S. J., Ciais, P., Bai, J., Peng, S., Zhang, Q., Hubacek, K., Marland, G., Andres, R. J., Crawford-Brown, D., Lin, J., Zhao, H., Hong, C., Boden, T. A., Feng, K., Peters, G. P., Xi, F., Liu, J., Li, Y., Zhao, Y., Zeng, N. and He, K.: Reduced carbon emission estimates from fossil fuel combustion and cement production in China. *Nature*, 524(7565), 335–338, doi:10.1038/nature14677, 2015.

Liu, G., Peng, S., Lin, X., Ciais, P., Li, X., Xi, Y., Lu, Z., Chang, J., Saunois, M., Wu, Y., Patra, P., Chandra, N., Zeng, H., and Piao, S.: Recent Slowdown of Anthropogenic Methane Emissions in China Driven by Stabilized Coal Production. *Environ. Sci. Technol. Lett.*, 8, 739–746, <https://doi.org/10.1021/acs.estlett.1c00463>, 2021a.

Liu, S., Fang, S., Liu, P., Liang, M., Guo, M., and Feng, Z.: Measurement report: Changing characteristics of atmospheric CH₄ in the Tibetan Plateau: records from 1994 to 2019 at the Mount Waliguan station. *Atmos. Chem. Phys.*, 21, 393–413, <https://doi.org/10.5194/acp-21-393-2021>, 2021b

Liu, S., C. Kuhn, G. Amatulli, K. Aho, D.E. Butman, G.H. Allen, P. Lin, M. Pan, D. Yamazaki, C. Brinkerhoff, C. Gleason, X. Xia, and P.A. Raymond: The importance of hydrology in routing terrestrial carbon to the atmosphere via global streams and rivers. *Proceedings of the National Academy of Sciences*, 119(11): p. e2106322119, 2022.

Loret, Z., Chevallier, F., Cozic, A., Remaud, M., and Meurdesoif, Y.: Simulating the variations of carbon dioxide in the global atmosphere on the hexagonal grid of DYNAMICO coupled with the LMDZ6 model. *Geosci. Model Dev. Discuss.* [preprint], <https://doi.org/10.5194/gmd-2023-140>, in review, 2023.

Locatelli, R., Bousquet, P., Saunois, M., Chevallier, F. and Cressot, C.: Sensitivity of the recent methane budget to LMDz

6484 [sub-grid-scale physical parameterizations, *Atmospheric Chem. Phys.*, 15\(17\), 9765–9780, doi:10.5194/acp-15-9765-](#)
6485 [2015, 2015.](#)

6486 [Lohila, A., Aalto, T., Aurela, M., Hatakka, J., Tuovinen, J.-P., Kilkki, J., Penttilä, T., Vuorenmaa, J., Hänninen, P., Sutinen,](#)
6487 [R., Viisanen, Y. and Laurila, T.: Large contribution of boreal upland forest soils to a catchment-scale CH₄ balance in](#)
6488 [a wet year, *Geophys. Res. Lett.*, 43\(6\), 2946–2953, doi:10.1002/2016gl067718, 2016.](#)

6489 [Lorente, A., Borsdorff, T., Martinez-Velarte, M. C., and Landgraf, J.: Accounting for surface reflectance spectral features](#)
6490 [in TROPOMI methane retrievals, *Atmos. Meas. Tech.*, 16, 1597–1608, https://doi.org/10.5194/amt-16-1597-2023,](#)
6491 [2023.](#)

6492 [Lu, X., Jacob, D. J., Zhang, Y., Maasakkers, J. D., Sulprizio, M. P., Shen, L., Qu, Z., Scarpelli, T. R., Nesser, H., Yantosca,](#)
6493 [R. M., Sheng, J., Andrews, A., Parker, R. J., Boesch, H., Bloom, A. A., and Ma, S.: Global methane budget and trend,](#)
6494 [2010–2017: complementarity of inverse analyses using in situ \(GLOBALVIEWplus CH₄ ObsPack\) and satellite](#)
6495 [\(GOSAT\) observations, *Atmos. Chem. Phys.*, 21, 4637–4657, https://doi.org/10.5194/acp-21-4637-2021, 2021](#)

6496 [Lu, X., Jacob, D. J., Zhang, Y., Maasakkers, J. D., Zhang, Y., Qu, Z., Chen, Z., Sulprizio, M. P., Varon, D., Hmiel, H.,](#)
6497 [Parker, R. J., Boesch, H., and Fan, S.: Observation-derived 2010–2019 trends in methane emissions and intensities from](#)
6498 [US oil and gas fields tied to activity metrics, *P. Natl. Acad. Sci. USA*, 120, e2217900120,](#)
6499 [https://doi.org/10.1073/pnas.2217900120, 2023.](#)

6500 [Maasakkers, J. D., Jacob, D. J., Sulprizio, M. P., Scarpelli, T. R., Nesser, H., Sheng, J.-X., Zhang, Y., Hersher, M., Bloom,](#)
6501 [A. A., Bowman, K. W., Worden, J. R., Janssens-Maenhout, G., and Parker, R. J.: Global distribution of methane](#)
6502 [emissions, emission trends, and OH concentrations and trends inferred from an inversion of GOSAT satellite data for](#)
6503 [2010–2015, *Atmos. Chem. Phys.*, 19, 7859–7881, https://doi.org/10.5194/acp-19-7859-2019, 2019.](#)

6504 [Maasakkers, J. D., Jacob, D. J., Sulprizio, M. P., Scarpelli, T. R., Nesser, H., Sheng, J., Zhang, Y., Lu, X., Bloom, A. A.,](#)
6505 [Bowman, K. W., Worden, J. R., and Parker, R. J.: 2010–2015 North American methane emissions, sectoral](#)
6506 [contributions, and trends: a high-resolution inversion of GOSAT observations of atmospheric methane, *Atmos. Chem.*](#)
6507 [Phys., 21, 4339–4356, https://doi.org/10.5194/acp-21-4339-2021, 2021.](#)

6508 [Maavara, T., Lauerwald, R., Regnier, P. and Van Capellen P.: Global perturbation of organic carbon cycling by river](#)
6509 [damming, *Nat Commun* 8, 153, https://doi.org/10.1038/ncomms15347, 2017.](#)

6510 [Machida, T., H. Matsueda, Y. Sawa, Y. Nakagawa, K. Hirotsu, N. Kondo, K. Goto, N. Nakazawa, K. Ishikawa and T.](#)
6511 [Ogawa: Worldwide measurements of atmospheric CO₂ and other trace gas species using commercial airlines, *J. Atmos.*](#)
6512 [Oceanic Technol., 25\(10\), 1744–1754, doi:10.1175/2008JTECHA1082.1, 2008](#)

6513 [Maksytov, S., Oda, T., Saito, M., Janardanan, R., Belikov, D., Kaiser, J. W., Zhuravlev, R., Ganshin, A., Valsala, V. K.,](#)
6514 [Andrews, A., Chmura, L., Dlugokencky, E., Haszpra, L., Langenfelds, R. L., Machida, T., Nakazawa, T., Ramonet,](#)
6515 [M., Sweeney, C. and Worthy, D.: Technical note: A high-resolution inverse modelling technique for estimating surface](#)
6516 [CO₂ fluxes based on the NIES-TM & FLEXPART coupled transport model and its adjoint, *Atmospheric Chem.*](#)

517 [Phys. Discuss., 1–33, doi:10.5194/acp-2020-251, 2020.](#)

518 [Malerba, M.E., T. de Kluyver, N. Wright, L. Schuster, and P.I. Macreadie: Methane emissions from agricultural ponds are](#)

519 [underestimated in national greenhouse gas inventories. *Communications Earth & Environment*, 3\(1\): p. 306, 2022](#)

520 [Maltby, J., L. Steinle, C. R. Löscher, H. W. Bange, M. A. Fischer, M. Schmidt, and T. Treude: Microbial methanogenesis](#)

521 [in the sulfate-reducing zone of sediments in the Eckernförde Bay, SW Baltic Sea. *Biogeosciences* **15**: 137–157,](#)

522 [doi:10.5194/bg-15-137-2018, 2018](#)

523 [Manning, F. C., Kho, L. K., Hill, T. C., Cornulier, T., and Teh, Y A: Carbon Emissions From Oil Palm Plantations on](#)

524 [Peat Soil. *Front. For. Glob. Change, Sec. Tropical Forests, Volume 2*, <https://doi.org/10.3389/ffgc.2019.0003>, 2019](#)

525 [Mannisenaho V, Tsuruta A, Backman L, Houweling S, Segers A, Krol M, Saunois M, Poulter B, Zhang Z, Lan X, et al.](#)

526 [Global Atmospheric \$\delta^{13}\text{C}_{\text{CH}_4}\$ and \$\text{CH}_4\$ Trends for 2000–2020 from the Atmospheric Transport Model TM5 Using \$\text{CH}_4\$](#)

527 [from Carbon Tracker Europe– \$\text{CH}_4\$ Inversions. *Atmosphere*, 14\(7\):1121. <https://doi.org/10.3390/atmos14071121>, 2023](#)

528 [van Marle, M. J. E., Kloster, S., Magi, B. I., Marlon, J. R., Daniau, A.-L., Field, R. D., Armeth, A., Forrest, M., Hantson,](#)

529 [S., Kehrwald, N. M., Knorr, W., Lasslop, G., Li, F., Mangeon, S., Yue, C., Kaiser, J. W. and Werf, G. R. van der:](#)

530 [Historic global biomass burning emissions for CMIP6 \(BB4CMIP\) based on merging satellite observations with](#)

531 [proxies and fire models \(1750–2015\). *Geosci. Model Dev.*, 10\(9\), 3329–3357, doi:10.5194/gmd-10-3329-2017, 2017.](#)

532 [Martinez, A., Saunois, M., Poulter, B., Zhen, Z., Raymond, P., Regnier, P. Canadell, J. G., Jackson, R. B., Patra, P. K.,](#)

533 [Bousquet, P., Ciais, P., Dlugokencky, E.J., Lan, X., Allen, G., Bastviken, D., Beerling, D. J., Belikov, D., Blake, D.,](#)

534 [Castaldi, S., Crippa, M., Deemer, B.R., Dennison, F., Etiope, G., Gedney, N., Höglund-Isaksson, L., Holgerson, M.A.,](#)

535 [Hopcroft, P. O., Hugelius, G., Ito, A., Jain, A. K., Janardanan, R., Johnson, M. S., Kleinen, T., Krummel, P. B.,](#)

536 [Lauerwald, R., Li, T., Liu, X., McDonald, K. C., Melton, J. R., Mühle, J., Müller, J., Murguía-Flores, F., Niwa, Y.,](#)

537 [Noce, S., Pan, S., Parker, R. J., Peng, C., Ramonet, M., Riley, W. J., Rocher-Ros, G., Rosentreter, J. A., Sasakawa,](#)

538 [M., Segers A., Smith, S. J., Stanley, E. H., Thanwerdas, J., Tian, H., Tsuruta, A., Tubiello, F. N., Weber, T. S., van](#)

539 [der Werf, G. R., Worthy, D. E. J., Xi, Y., Yoshida Y., Zhang, W., Zheng, B., Zhu, Qing, Zhu, Qian, and Zhuang,](#)

540 [Q.: *Supplemental data of the Global Carbon Project Methane Budget 2024 v1*. \[Data set\],](#)

541 <https://doi.org/10.18160/GCP-CH4-2024/>, 2024

542 [Matthews, E. and Fung, I.: Methane emission from natural wetlands: Global distribution, area, and environmental](#)

543 [characteristics of sources, *Glob. Biogeochem. Cycles*, 1\(1\), 61–86, doi:d10.1029/GB001i001p00061, 1987.](#)

544 [Mazzini A., Etiope G. \(2017\). Mud volcanism: an updated review. *Earth Sci. Rev.*, 168, 81-112.](#)

545 <http://dx.doi.org/10.1016/j.earscirev.2017.03.001>, 2017

546 [McCalley, C. K., Woodcroft, B. J., Hodgkins, S. B., Wehr, R. A., Kim, E.-H., Mondav, R., Crill, P. M., Chanton, J. P.,](#)

547 [Rich, V. I., Tyson, G. W. and Saleska, S. R.: Methane dynamics regulated by microbial community response to](#)

548 [permafrost thaw, *Nature*, 514\(7523\), 478–481, doi:10.1038/nature13798, 2014.](#)

549 [McCarthy, M. C., Boering, K. A., Rice, A. L., Tyler, S. C., Connell, P. and Atlas, E.: Carbon and hydrogen isotopic](#)

6550 [compositions of stratospheric methane: 2. Two-dimensional model results and implications for kinetic isotope effects](#),
6551 [J. Geophys. Res. Atmospheres](#), 108(D15), doi:10.1029/2002JD003183, 2003.

6552 [McGinnis, D. F., J. Greinert, Y. Artemov, S. E. Beaubien, and A. Wüest: Fate of rising methane bubbles in stratified](#)
6553 [waters: How much methane reaches the atmosphere?](#), *J. Geophys. Res.*, 111, C09007, doi:10.1029/2005JC003183,
6554 2006

6555 [McGuire, A. D., Christensen, T. R., Heroult, A., Miller, P. A., Hayes, D., Euskirchen, E., Kimball, J. S., Yi, Y., Koven,](#)
6556 [C., Lafleur, P., Oechel, W., Peylin, P. and Williams, M.: An assessment of the carbon balance of Arctic tundra](#), *Comp.*
6557 [Obs. Process Models Atmospheric Inversions](#), 9(Article), 3185–3204, doi:10.5194/bg-9-3185-2012, 2012.

6558 [McKain, K., Down, A., Raciti, S. M., Budney, J., Hutyra, L. R., Floerchinger, C., Herndon, S. C., Nehrkorn, T., Zahniser,](#)
6559 [M. S., Jackson, R. B., Phillips, N. and Wofsy, S. C.: Methane emissions from natural gas infrastructure and use in the](#)
6560 [urban region of Boston, Massachusetts](#), *Proc. Natl. Acad. Sci.*, 112(7), 1941–1946, doi:10.1073/pnas.1416261112,
6561 2015.

6562 [McNicol, G., Fluet-Chouinard, E., Ouyang, Z., Knox, S., Zhang, Z., Aalto, T., et al.: Upscaling wetland methane](#)
6563 [emissions from the FLUXNET-CH4 eddy covariance network \(UpCH4 v1.0\): Model development, network](#)
6564 [assessment, and budget comparison](#), *AGU Advances*, 4, e2023AV000956, <https://doi.org/10.1029/2023AV000956>,
6565 2023

6566 [Meinshausen, M., Smith, S., Calvin, K., Daniel, J., Kainuma, M., Lamarque, J. F., Matsumoto, K., Montzka, S., Raper,](#)
6567 [S., Riahi, K., Thomson, A., Velders, G. and van Vuuren, D. P.: The RCP greenhouse gas concentrations and their](#)
6568 [extensions from 1765 to 2300](#), *Clim. Change*, 109(1), 213–241, doi:10.1007/s10584-011-0156-z, 2011.

6569 [Meinshausen, M., Vogel, E., Nauels, A., Lorbacher, K., Meinshausen, N., Etheridge, D. M., Fraser, P. J., Montzka, S. A.,](#)
6570 [Rayner, P. J., Trudinger, C. M., Krummel, P. B., Beyerle, U., Canadell, J. G., Daniel, J. S., Enting, I. G., Law, R. M.,](#)
6571 [Lunder, C. R., O'Doherty, S., Prinn, R. G., Reimann, S., Rubino, M., Velders, G. J. M., Vollmer, M. K., Wang, R. H.](#)
6572 [J., and Weiss, R.: Historical greenhouse gas concentrations for climate modelling \(CMIP6\)](#), *Geosci. Model Dev.*, 10,
6573 2057–2116, <https://doi.org/10.5194/gmd-10-2057-2017>, 2017.

6574 [Meinshausen, M., Nicholls, Z. R. J., Lewis, J., Gidden, M. J., Vogel, E., Freund, M., Beyerle, U., Gessner, C., Nauels, A.,](#)
6575 [Bauer, N., Canadell, J. G., Daniel, J. S., John, A., Krummel, P. B., Luderer, G., Meinshausen, N., Montzka, S. A.,](#)
6576 [Rayner, P. J., Reimann, S., Smith, S. J., van den Berg, M., Velders, G. J. M., Vollmer, M. K., and Wang, R. H. J.: The](#)
6577 [shared socio-economic pathway \(SSP\) greenhouse gas concentrations and their extensions to 2500](#), *Geosci. Model*
6578 [Dev., 13, 3571–3605, <https://doi.org/10.5194/gmd-13-3571-2020>, 2020.](#)

6579 [Melton, J. R. and Arora, V. K.: Competition between plant functional types in the Canadian Terrestrial Ecosystem Model](#)
6580 [\(CTEM\) v. 2.0](#), *Geosci. Model Dev.*, 9(1), 323–361, doi:10.5194/gmd-9-323-2016, 2016.

6581 [Melton, J. R., Wania, R., Hodson, E. L., Poulter, B., Ringeval, B., Spahni, R., Bohn, T., Avis, C. A., Beerling, D. J., Chen,](#)
6582 [G., Eliseev, A. V., Denisov, S. N., Hopcroft, P. O., Lettenmaier, D. P., Riley, W. J., Singarayer, J. S., Subin, Z. M.,](#)

6583 [Tian, H., Zürcher, S., Brovkin, V., van Bodegom, P. M., Kleinen, T., Yu, Z. C. and Kaplan, J. O.: Present state of](#)
6584 [global wetland extent and wetland methane modelling: conclusions from a model intercomparison project](#)
6585 [\(WETCHIMP\), Biogeosciences, 10\(2\), 753–788, doi:10.5194/bg-10-753-2013, 2013.](#)

6586 [Membrive, O., Crevoisier, C., Sweeney, C., Danis, F., Hertzog, A., Engel, A., Bönisch, H. and Picon, L.: AirCore-HR: a](#)
6587 [high-resolution column sampling to enhance the vertical description of CH₄ and CO₂, Atmospheric Meas. Tech., 10\(6\),](#)
6588 [2163–2181, doi:10.5194/amt-10-2163-2017, 2017.](#)

6589 [Messenger, M. L., Lehner, B., Grill, G., Nedeva, I. and Schmitt, O.: Estimating the volume and age of water stored in global](#)
6590 [lakes using a geo-statistical approach, Nat. Commun., 7\(1\), 1–11, doi:10.1038/ncomms13603, 2016.](#)

6591 [Mijling, B., van der A, R. J. and Zhang, Q.: Regional nitrogen oxides emission trends in East Asia observed from space,](#)
6592 [Atmospheric Chem. Phys., 13\(23\), 12003–12012, doi:10.5194/acp-13-12003-2013, 2013.](#)

6593 [Milkov, A. V.: Molecular and stable isotope compositions of natural gas hydrates: A revised global dataset and basic](#)
6594 [interpretations in the context of geological settings, Org. Geochem., 36\(5\), 681–702, 2005.](#)

6595 [Minkinen, K. and Laine, J.: Vegetation heterogeneity and ditches create spatial variability in methane fluxes from](#)
6596 [peatlands drained for forestry, Plant Soil, 285\(1\), 289–304, doi:10.1007/s11104-006-9016-4, 2006.](#)

6597 [Monforti Ferrario, Fabio; Crippa, Monica; Guizzardi, Diego; Muntean, Marilena; Schaaf, Edwin; Lo Vullo, Eleonora;](#)
6598 [Solazzo, Efsio; Olivier, Jos; Vignati, Elisabetta: EDGAR v6.0 Greenhouse Gas Emissions, European Commission,](#)
6599 [Joint Research Centre \(JRC\) \[Dataset\] PID: http://data.europa.eu/89h/97a67d67-c62e-4826-b873-9d972c4f670b, 2021](#)

6600 [Montzka, S. A., Krol, M., Dlugokencky, E., Hall, B., Jockel, P. and Lelieveld, J.: Small Interannual Variability of Global](#)
6601 [Atmospheric Hydroxyl, Science, 331\(6013\), 67–69, 2011.](#)

6602 [Moore, C. W., Zielinska, B., Pétron, G. and Jackson, R. B.: Air impacts of increased natural gas acquisition, processing,](#)
6603 [and use: a critical review, Environ. Sci. Technol., 48, 8349–8359, doi:10.1021/es4053472, 2014.](#)

6604 [Morgenstern, O., Hegglin, M. I., Rozanov, E., O'Connor, F. M., Abraham, N. L., Akiyoshi, H., Archibald, A. T., Bekki,](#)
6605 [S., Butchart, N., Chipperfield, M. P., Deushi, M., Dhomse, S. S., Garcia, R. R., Hardiman, S. C., Horowitz, L. W.,](#)
6606 [Jöckel, P., Josse, B., Kinnison, D., Lin, M., Mancini, E., Manyin, M. E., Marchand, M., Maréchal, V., Michou, M.,](#)
6607 [Oman, L. D., Pitari, G., Plummer, D. A., Revell, L. E., Saint-Martin, D., Schofield, R., Stenke, A., Stone, K., Sudo,](#)
6608 [K., Tanaka, T. Y., Tilmes, S., Yamashita, Y., Yoshida, K., and Zeng, G.: Review of the global models used within](#)
6609 [phase 1 of the Chemistry–Climate Model Initiative \(CCMI\), Geosci. Model Dev., 10, 639–671,](#)
6610 [https://doi.org/10.5194/gmd-10-639-2017, 2017.](#)

6611 [Morino, I., Uchino, O., Inoue, M., Yoshida, Y., Yokota, T., Wennberg, P. O., Toon, G. C., Wunch, D., Roehl, C. M.,](#)
6612 [Notholt, J., Warneke, T., Messerschmidt, J., Griffith, D. W. T., Deutscher, N. M., Sherlock, V., Connor, B., Robinson,](#)
6613 [J., Sussmann, R. and Rettinger, M.: Preliminary validation of column-averaged volume mixing ratios of carbon dioxide](#)
6614 [and methane retrieved from GOSAT short-wavelength infrared spectra, Atmospheric Meas. Tech., 4\(6\), 1061–1076,](#)
6615 [2011.](#)

616 [Murguía-Flores, F., Arndt, S., Ganesan, A. L., Murray-Tortarolo, G. and Hornibrook, E. R. C.: Soil Methanotrophy Model](#)
617 [\(MeMo v1.0\): a process-based model to quantify global uptake of atmospheric methane by soil, *Geosci. Model Dev.*,](#)
618 [11\(6\), 2009–2032, doi:10.5194/gmd-11-2009-2018, 2018.](#)

619 [Myer, A., Myer, M.H., Trettin, C.C. and Forschler, B.T.: The fate of carbon utilized by the subterranean termite](#)
620 [Reticulitermes flavipes. *Ecosphere* 12 \(12\):e03872,doi:10.1002/ecs2.3872, 2021](#)

621 [Myhre, G., Shindell, D., Bréon, F.-M., Collins, W., Fuglestedt, J., Huang, J., Koch, D., Lamarque, J.-F., Lee, D.,](#)
622 [Mendoza, B., Nakajima, T., Robock, A., Stephens, G., Takemura, T. and Zhang, H.: Anthropogenic and Natural](#)
623 [Radiative Forcing., in *In Climate Change 2013: The Physical Science Basis. Contribution of Working Group I to the*](#)
624 [Fifth Assessment Report of the Intergovernmental Panel on Climate Change., edited by T. F. Stocker, D. D. Qin, G.-](#)
625 [K. Plattner, M. Tignor, S. K. Allen, J. Boschung, A. Nauels, Y. Xia, V. Bex, and P. M. Midgley, Cambridge University](#)
626 [Press, Cambridge, United Kingdom and New York, NY, USA., 2013.](#)

627 [Naik, V., Voulgarakis, A., Fiore, A. M., Horowitz, L. W., Lamarque, J. F., Lin, M., Prather, M. J., Young, P. J., Bergmann,](#)
628 [D., Cameron-Smith, P. J., Cionni, I., Collins, W. J., Dalsoren, S. B., Doherty, R., Eyring, V., Faluvegi, G., Folberth,](#)
629 [G. A., Josse, B., Lee, Y. H., MacKenzie, I. A., Nagashima, T., van Noije, T. P. C., Plummer, D. A., Righi, M., Rumbold,](#)
630 [S. T., Skeie, R., Shindell, D. T., Stevenson, D. S., Strode, S., Sudo, K., Szopa, S. and Zeng, G.: Preindustrial to present](#)
631 [day changes in tropospheric hydroxyl radical and methane lifetime from the Atmospheric Chemistry and Climate](#)
632 [Model Intercomparison Project \(ACCMIP\). *Atmospheric Chem. Phys.*, 13\(10\), 5277–5298, doi:10.5194/acp-13-5277-](#)
633 [2013, 2013.](#)

634 [Nakazawa, T., Machida, T., Tanaka, M., Fujii, Y., Aoki, S. and Watanabe, O.: Differences of the atmospheric CH₄](#)
635 [concentration between the Arctic and Antarctic regions in pre-industrial/pre-agricultural era, *Geophys. Res. Lett.*,](#)
636 [20\(10\), 943–946, doi:10.1029/93GL00776, 1993.](#)

637 [Natchimuthu, S., I. Sundgren, M. Gålfalk, L. Klemetsson, P. Crill, Å. Danielsson, and D. Bastviken, Spatio-temporal](#)
638 [variability of lake CH₄ fluxes and its influence on annual whole lake emission estimates. *Limnology and*](#)
639 [Oceanography, 61\(S1\): p. S13-S26, 2016.](#)

640 [Nauer, P. A., Hutley, L. B., and Arndt, S. K.: Termite mounds mitigate half of termite methane emissions, *P. Natl. Acad.*](#)
641 [Sci. USA, 115, 13306–13311, 2018.](#)

642 [Nicely, J. M., Salawitch, R. J., Canty, T., Anderson, D. C., Arnold, S. R., Chipperfield, M. P., Emmons, L. K., Flemming,](#)
643 [J., Huijnen, V., Kinnison, D. E., Lamarque, J.-F., Mao, J., Monks, S. A., Steenrod, S. D., Tilmes, S. and Turquety, S.:](#)
644 [Quantifying the causes of differences in tropospheric OH within global models, *J. Geophys. Res. Atmospheres*, 122\(3\),](#)
645 [1983–2007, doi:10.1002/2016JD026239, 2017.](#)

646 [Nirmal Rajkumar, A., J. Barnes, R. Ramesh, R. Purvaja, and R.C. Upstill-Goddard, Methane and nitrous oxide fluxes in](#)
647 [the polluted Adyar River and estuary, SE India. *Marine Pollution Bulletin*, 56\(12\): p. 2043-2051, 2008](#)

648 [Nisbet, E. G., Manning, M. R., Dlugokencky, E. J., Fisher, R. E., Lowry, D., Michel, S. E., Myhre, C. L., Platt, S. M.,](#)

6649 [Allen, G., Bousquet, P., Brownlow, R., Cain, M., France, J. L., Hermansen, O., Hossaini, R., Jones, A. E., Levin, I.,](#)
6650 [Manning, A. C., Myhre, G., Pyle, J. A., Vaughn, B., Warwick, N. J. and White, J. W. C.: Very strong atmospheric](#)
6651 [methane growth in the four years 2014-2017: Implications for the Paris Agreement, *Glob. Biogeochem. Cycles*, 0\(ja\),](#)
6652 [doi:10.1029/2018GB006009, 2019.](#)

6653 [Nisbet, E. G., Manning, M. R., Dlugokencky, E. J., Michel, S. E., Lan, X., Röckmann, T., van der Denier Gon, H. A.,](#)
6654 [Schmitt, J., Palmer, P. I., Dyonisius, M. N., Oh, Y., Fisher, R. E., Lowry, D., France, J. L., White, J. W. C., Brailsford,](#)
6655 [G., and Bromley, T.: Atmospheric methane: Comparison between methane's record in 2006–2022 and during glacial](#)
6656 [terminations, *Global Biogeochem. Cy.*, 37, e2023GB007875, <https://doi.org/10.1029/2023GB007875>, 2023.](#)

6657 [Nisbet, R. E. R., Fisher, R., Nimmo, R. H., Bendall, D. S., Crill, P. M., Gallego-Sala, A. V., Hornibrook, E. R. C., Lopez-](#)
6658 [Juez, E., Lowry, D., Nisbet, P. B. R., Shuckburgh, E. F., Sriskantharajah, S., Howe, C. J. and Nisbet, E. G.: Emission](#)
6659 [of methane from plants, *Proc. R. Soc. B-Biol. Sci.*, 276\(1660\), 1347–1354, 2009.](#)

6660 [Niwa, Y., Fujii, Y., Sawa, Y., Iida, Y., Ito, A., Satoh, M., Imasu, R., Tsuboi, K., Matsueda, H. and Saigusa, N.: A 4D-Var](#)
6661 [inversion system based on the icosahedral grid model \(NICAM-TM 4D-Var v1.0\) – Part 2: Optimization scheme and](#)
6662 [identical twin experiment of atmospheric CO₂ inversion, *Geosci. Model Dev.*, 10\(6\), 2201–2219, doi:10.5194/gmd-](#)
6663 [10-2201-2017, 2017.](#)

6664 [Niwa, Y., Ishijima, K., Ito, A. and Iida, Y.: Toward a long-term atmospheric CO₂ inversion for elucidating natural carbon](#)
6665 [fluxes: technical notes of NISMON-CO₂ v2021.1, *Prog. Earth Planet Sci.*, 9, 42, doi:10.1186/s40645-022-00502-6,](#)
6666 [2022](#)

6667 [Noël, S., Reuter, M., Buchwitz, M., Borchardt, J., Hilker, M., Schneising, O., Bovensmann, H., Burrows, J. P., Di Noia,](#)
6668 [A., Parker, R. J., Suto, H., Yoshida, Y., Buschmann, M., Deutscher, N. M., Feist, D. G., Griffith, D. W. T., Hase, F.,](#)
6669 [Kivi, R., Liu, C., Morino, I., Notholt, J., Oh, Y.-S., Ohyama, H., Petri, C., Pollard, D. F., Rettinger, M., Roehl, C.,](#)
6670 [Rousogonous, C., Sha, M. K., Shiomi, K., Strong, K., Sussmann, R., Té, Y., Velazco, V. A., Vrekoussis, M., and](#)
6671 [Warneke, T.: Retrieval of greenhouse gases from GOSAT and GOSAT-2 using the FOCAL algorithm, *Atmos. Meas.*](#)
6672 [Tech.](#), 15, 3401–3437, <https://doi.org/10.5194/amt-15-3401-2022>, 2022.

6673 [Nomura, S., Naja, M., Ahmed, M. K., Mukai, H., Terao, Y., Machida, T., Sasakawa, M., and Patra, P. K.: Measurement](#)
6674 [report: Regional characteristics of seasonal and long-term variations in greenhouse gases at Nainital, India, and](#)
6675 [Comilla, Bangladesh, *Atmos. Chem. Phys.*, 21, 16427–16452, <https://doi.org/10.5194/acp-21-16427-2021>, 2021](#)

6676 [Obu, J., Westermann, S., Bartsch, A., Berdnikov, N., Christiansen, H. H., Dashtseren, A., Delaloye, R., Elberling, B.,](#)
6677 [Etzelmüller, B., Kholodov, A., Khomutov, A., Kääb, A., Leibman, M. O., Lewkowitz, A. G., Panda, S. K.,](#)
6678 [Romanovsky, V., Way, R. G., Westergaard-Nielsen, A., Wu, T., Yamkhin, J. and Zou, D.: Northern Hemisphere](#)
6679 [permafrost map based on TTOP modelling for 2000–2016 at 1 km² scale, *Earth-Sci. Rev.*, 193, 299–316,](#)
6680 [doi:10.1016/j.earscirev.2019.04.023, 2019.](#)

6681 [Ocko, I. B., Sun, T., Shindell, D., Oppenheimer, M., Hristov, A. N., Pacala, S. W., Mauzerall, D. L., Xu, Y. and Hamburg,](#)
6682 [S. P.: Acting rapidly to deploy readily available methane mitigation measures by sector can immediately slow global](#)
6683 [warming, *Environ. Res. Lett.*, 16, 054042, doi :10.1088/1748-9326/abf9c8, 2021](#)

6684 [Odelson, D.A. and Breznak, J. A. Volatile fatty acid production by the hindgut microbiota of xilophagus termites. *Applied*](#)
6685 [and *Environmental Microbiology*, 45, 1602-1613, 1983. doi: 10.1128/aem.45.5.1602-1613.1983.](#)

6686 [Olivier, J. G. J. and Janssens-Maenhout, G.: Part III: Total Greenhouse Gas Emissions, of CO₂ Emissions from Fuel](#)
6687 [Combustion \(2014 ed.\), International Energy Agency, Paris, ISBN-978-92-64-21709-6., 2014.](#)

6688 [Ollivier, Q. R., Maher, D. T., Pitfield, C. and Macreadie, P. I.: Punching above their weight: Large release of greenhouse](#)
6689 [gases from small agricultural dams. *Glob. Change Biol.*, 25\(2\), 721–732, doi:10.1111/gcb.14477, 2019.](#)

6690 [O’Neill, B. C., Tebaldi, C., Vuuren, D. P. van, Eyring, V., Friedlingstein, P., Hurtt, G., Knutti, R., Kriegler, E., Lamarque,](#)
6691 [J.-F., Lowe, J., Meehl, G. A., Moss, R., Riahi, K. and Sanderson, B. M.: The Scenario Model Intercomparison Project](#)
6692 [\(ScenarioMIP\) for CMIP6. *Geosci. Model Dev.*, 9\(9\), 3461–3482. doi:https://doi.org/10.5194/gmd-9-3461-2016,](#)
6693 [2016.](#)

6694 [Oreggioni, G. D., F. Monforti Ferrario, M. Crippa, M. Muntean, E. Schaaf, D. Guizzardi, E. Solazzo, M. Duerr, M. Perry](#)
6695 [and E. Vignati: Climate change in a changing world: Socio-economic and technological transitions, regulatory](#)
6696 [frameworks and trends on global greenhouse gas emissions from EDGAR v.5.0. *Global Environmental Change*,](#)
6697 [doi:10.1016/j.gloenvcha.2021.10235, 2021](#)

6698 [Oremland, R. S. Methanogenic activity in plankton samples and fish intestines: a mechanism for *in situ* methanogenesis](#)
6699 [in oceanic surface waters. *Limnol. Oceanogr.* 24, 1136–1141, 1979.](#)

6700 [O’Rourke, P. R., Smith, S. J., Mott, A., Ahsan, H., McDuffie, E. E., Crippa, M., Klimont, S., McDonald, B., Z., Wang,](#)
6701 [Nicholson, M. B., Feng, L., and Hoesly, R. M., CEDS v-2021-02-05 Emission Data 1975-2019 \(Version Feb-05-2021\).](#)
6702 [Zenodo. <http://doi.org/10.5281/zenodo.4509372>, 2021](#)

6703 [Ovalle, A. R. C., C. E. Rezende, L. D. Lacerda, and C. A. R. Silva: Factors affecting the hydrochemistry of a mangrove](#)
6704 [tidal creek, Sepetiba Bay, Brazil. *Estuar. Coast. Shelf Sci.* 31: 639–650. doi:10.1016/0272-7714\(90\)90017-L, 1990](#)

6705 [Pacala, S. W.: Verifying greenhouse gas emissions: Methods to support international climate agreements. National](#)
6706 [Academies Press., 2010](#)

6707 [Pandey, S., Gautam, R., Houweling, S., Gon, H. D. van der, Sadavarte, P., Borsdorff, T., Hasekamp, O., Landgraf, J., Tol,](#)
6708 [P., Kempen, T. van, Hoogeveen, R., Hees, R. van, Hamburg, S. P., Maasackers, J. D. and Aben, I.: Satellite](#)
6709 [observations reveal extreme methane leakage from a natural gas well blowout. *Proc. Natl. Acad. Sci.*, 116\(52\), 26376–](#)
6710 [26381, doi:10.1073/pnas.1908712116, 2019.](#)

6711 [Pangala, S. R., Moore, S., Hornibrook, E. R. C. and Gauci, V.: Trees are major conduits for methane egress from tropical](#)
6712 [forested wetlands, *New Phytol.*, 197\(2\), 524–531, doi:10.1111/nph.12031, 2013.](#)

6713 [Pangala, S. R., Hornibrook, E. R. C., Gowing, D. J. and Gauci, V.: The contribution of trees to ecosystem methane](#)

6714 [emissions in a temperate forested wetland, *Glob. Change Biol.*, 21\(7\), 2642–2654, doi:10.1111/gcb.12891, 2015.](#)

6715 [Pangala, S. R., Enrich-Prast, A., Basso, L. S., Peixoto, R. B., Bastviken, D., Hornibrook, E. R. C., Gatti, L. V., Marotta,](#)

6716 [H., Calazans, L. S. B., Sakuragui, C. M., Bastos, W. R., Malm, O., Gloor, E., Miller, J. B. and Gauci, V.: Large](#)

6717 [emissions from floodplain trees close the Amazon methane budget, *Nature*, 552\(7684\), 230–234,](#)

6718 [doi:10.1038/nature24639, 2017.](#)

6719 [Paris, J.-D., Ciais, P., Nédélec, P., Stohl, A., Belan, B. D., Arshinov, M. Y., Carouge, C., Golitsyn, G. S. and Granberg, I.](#)

6720 [G.: New insights on the chemical composition of the Siberian air shed from the YAK AEROSIB aircraft campaigns,](#)

6721 [Bull. Am. Meteorol. Soc., 91\(5\), 625–641, doi:10.1175/2009BAMS2663.1., 2010.](#)

6722 [Parker, R. J., Webb, A., Boesch, H., Somkuti, P., Barrio Guillo, R., Di Noia, A., Kalaitzi, N., Anand, J. S., Bergamaschi,](#)

6723 [P., Chevallier, F., Palmer, P. I., Feng, L., Deutscher, N. M., Feist, D. G., Griffith, D. W. T., Hase, F., Kivi, R., Morino,](#)

6724 [L., Notholt, J., Oh, Y.-S., Ohyama, H., Petri, C., Pollard, D. F., Roehl, C., Sha, M. K., Shiomi, K., Strong, K., Sussmann,](#)

6725 [R., Té, Y., Velasco, V. A., Warneke, T., Wennberg, P. O., and Wunch, D.: A decade of GOSAT Proxy satellite CH4](#)

6726 [observations, *Earth Syst. Sci. Data*, 12, 3383–3412, <https://doi.org/10.5194/essd-12-3383-2020>, 2020.](#)

6727 [Parker, R. and Boesch, H. \(2020\): University of Leicester GOSAT Proxy XCH4 v9.0. Centre for Environmental Data](#)

6728 [Analysis, 07 May 2020. <https://dx.doi.org/10.5285/18ef8247f52a4cb6a14013f8235cc1eb>, 2020.](#)

6729 [Parker, R. J., Wilson, C., Comyn-Platt, E., Hayman, G., Marthews, T. R., Bloom, A. A., Lunt, M. F., Gedney, N., Dadson,](#)

6730 [S. J., McNorton, J., Humpage, N., Boesch, H., Chipperfield, M. P., Palmer, P. I., and Yamazaki, D.: Evaluation of](#)

6731 [wetland CH4 in the Joint UK Land Environment Simulator \(JULES\) land surface model using satellite observations,](#)

6732 [Biogeosciences, 19, 5779–5805, <https://doi.org/10.5194/bg-19-5779-2022>, 2022.](#)

6733 [Pathak, H., Li, C. and Wassmann, R.: Greenhouse gas emissions from Indian rice fields: calibration and upscaling using](#)

6734 [the DNDC model, *Biogeosciences*, 1\(1\), 1–11, 2005.](#)

6735 [Patra, P. K., Houweling, S., Krol, M., Bousquet, P., Belikov, D., Bergmann, D., Bian, H., Cameron-Smith, P., Chipperfield,](#)

6736 [M. P., Corbin, K., Fortems-Cheiney, A., Fraser, A., Gloor, E., Hess, P., Ito, A., Kawa, S. R., Law, R. M., Loh, Z.,](#)

6737 [Maksyutov, S., Meng, L., Palmer, P. I., Prinn, R. G., Rigby, M., Saito, R. and Wilson, C.: TransCom model simulations](#)

6738 [of CH4 and related species: linking transport, surface flux and chemical loss with CH4 variability in the troposphere](#)

6739 [and lower stratosphere, *Atmospheric Chem. Phys.*, 11\(24\), 12,813-12,837, doi:10.5194/acp-11-12813-2011, 2011.](#)

6740 [Patra, P. K., Krol, M. C., Montzka, S. A., Arnold, T., Atlas, E. L., Lintner, B. R., Stephens, B. B., Xiang, B., Elkins, J. W.,](#)

6741 [Fraser, P. J., Ghosh, A., Hints, E. J., Hurst, D. F., Ishijima, K., Krummel, P. B., Miller, B. R., Miyazaki, K., Moore,](#)

6742 [F. L., Mühle, J., O'Doherty, S., Prinn, R. G., Steele, L. P., Takigawa, M., Wang, H. J., Weiss, R. F., Wofsy, S. C. and](#)

6743 [Young, D.: Observational evidence for interhemispheric hydroxyl-radical parity, *Nature*, 513\(7517\), 219–223,](#)

6744 [doi:10.1038/nature13721, 2014.](#)

6745 [Patra, P. K., Takigawa, M., Watanabe, S., Chandra, N., Ishijima, K. and Yamashita, Y.: Improved Chemical Tracer](#)

6746 [Simulation by MIROC4.0-based Atmospheric Chemistry-Transport Model \(MIROC4-ACTM\), *SOLA*, 14\(0\), 91–96,](#)

6747 [doi:10.2151/sola.2018-016](https://doi.org/10.2151/sola.2018-016), 2018.

6748 [Patra, P. K., Krol, M. C., Prinn, R. G., Takigawa, M., Mühle, J., Montzka, S. A., Lal, S., Yamashita, Y., Naus, S., Chandra,](#)

6749 [N., Weiss, R. F., Krummel, P. B., Fraser, P. J., O'Doherty, S., and Elkins, J. W.: Methyl Chloroform Continues to](#)

6750 [Constrain the Hydroxyl \(OH\) Variability in the Troposphere, *J. Geophys. Res.-Atmos.*, 126, e2020JD033862,](#)

6751 <https://doi.org/10.1029/2020JD033862>, 2021.

6752 [Paull, C. K., Brewer, P. G., Ussler, W., Peltzer, E. T., Rehder, G. and Clague, D.: An experiment demonstrating that marine](#)

6753 [slumping is a mechanism to transfer methane from seafloor gas-hydrate deposits into the upper ocean and atmosphere,](#)

6754 [Geo-Mar. Lett., 22\(4\), 198–203, doi:10.1007/s00367-002-0113-y, 2002.](#)

6755 [Peacock, M., J. Audet, D. Bastviken, M.N. Futter, V. Gauci, A. Grinham, J.A. Harrison, M.S. Kent, S. Kosten, C.E.](#)

6756 [Lovelock, A.J. Veraart, and C.D. Evans, Global importance of methane emissions from drainage ditches and canals,](#)

6757 [Environmental Research Letters, 16\(4\): p. 044010., 2021](#)

6758 [Peischl, J., Ryerson, T. B., Aikin, K. C., de Gouw, J. A., Gilman, J. B., Holloway, J. S., Lerner, B. M., Nadkarni, R.,](#)

6759 [Neuman, J. A., Nowak, J. B., Trainer, M., Warneke, C. and Parrish, D. D.: Quantifying atmospheric methane emissions](#)

6760 [from the Haynesville, Fayetteville, and northeastern Marcellus shale gas production regions, *J. Geophys. Res.*](#)

6761 [Atmospheres, 120\(5\), 2119–2139, doi:10.1002/2014jd022697, 2015.](#)

6762 [Pekel, J.-F., Cottam, A., Gorelick, N. and Belward, A. S.: High-resolution mapping of global surface water and its long-](#)

6763 [term changes, *Nature*, 540\(7633\), 418–422, doi:10.1038/nature20584, 2016.](#)

6764 [Peltola, O., Vesala, T., Gao, Y., Rätty, O., Alekseychik, P., Aurela, M., Chojnicki, B., Desai, A. R., Dolman, A. J.,](#)

6765 [Euskirchen, E. S., Friborg, T., Göckede, M., Helbig, M., Humphreys, E., Jackson, R. B., Jocher, G., Joos, F., Klatt, J.,](#)

6766 [Knox, S. H., Kowalska, N., Kutzbach, L., Lienert, S., Lohila, A., Mammarella, I., Nadeau, D. F., Nilsson, M. B.,](#)

6767 [Oechel, W. C., Peichl, M., Pypker, T., Quinton, W., Rinne, J., Sachs, T., Samson, M., Schmid, H. P., Sonnentag, O.,](#)

6768 [Wille, C., Zona, D. and Aalto, T.: Monthly gridded data product of northern wetland methane emissions based on](#)

6769 [upscaling eddy covariance observations, *Earth Syst. Sci. Data*, 11\(3\), 1263–1289, doi:10.5194/essd-11-1263-2019,](#)

6770 [2019.](#)

6771 [Peng, S. S., Piao, S. L., Bousquet, P., Ciais, P., Li, B. G., Lin, X., Tao, S., Wang, Z. P., Zhang, Y. and Zhou, F.: Inventory](#)

6772 [of anthropogenic methane emissions in Mainland China from 1980 to 2010, *Atmospheric Chem. Phys. Discuss.*, 2016,](#)

6773 [1–29, doi:10.5194/acp-2016-139, 2016.](#)

6774 [Peng, S., Lin, X., Thompson, R. L., Xi, Y., Liu, G., Hauglustaine, D., Lan, X., Poulter, B., Ramonet, M., Saunio, M.,](#)

6775 [Yin, Y., Zhang, Z., Zheng, B., and Ciais, P.: Wetland emission and atmospheric sink changes explain methane growth](#)

6776 [in 2020, *Nature*, 612, 477–482, https://doi.org/10.1038/s41586-022-05447-w, 2022.](#)

6777 [Pérez-Barbería, F. J.: Scaling methane emissions in ruminants and global estimates in wild populations, *Sci. Total*](#)

6778 [Environ., 579, 1572–1580, doi:10.1016/j.scitotenv.2016.11.175, 2017.](#)

6779 [Petersen, H. and Luxton, M. A comparative analysis of soil fauna populations and their role in decomposition processes.](#)

6780 [Oikos 39: 287–388,doi.org/10.2307/3544689](https://doi.org/10.2307/3544689), 1982

6781 [Petrenko, V. V., Smith, A. M., Schaefer, H., Riedel, K., Brook, E., Baggenstos, D., Harth, C., Hua, Q., Buizert, C., Schilt,](#)

6782 [A., Fain, X., Mitchell, L., Bauska, T., Orsi, A., Weiss, R. F. and Severinghaus, J. P.: Minimal geological methane](#)

6783 [emissions during the Younger Dryas–Preboreal abrupt warming event, *Nature*, 548, 443, doi:10.1038/nature23316](#)

6784 <https://www.nature.com/articles/nature23316#supplementary-information>, 2017.

6785 [Petrescu, A. M. R., Qiu, C., Ciais, P., Thompson, R. L., Peylin, P., McGrath, M. M., Solazzo, E., Janssens-Maenhout, G.,](#)

6786 [Tubiello, F. N., Bergamaschi, P., Brunner, D., Peters, G. P., Höglund- Isaksson, L., Regnier, P., Lauerwald, R.,](#)

6787 [Bastviken, D., Tsuruta, A., Winiwarter, W., Patra, P. P., Kuhnert, M., Oreggioni, G. D., Crippa, M., Saunio, M.,](#)

6788 [Perugini, L., Markkanen, T., Aalto, T., Groot Zwaafink, C. C., Yao, Y., Wilson, C. C., Conchedda, G., Günther, D.,](#)

6789 [Leip, A., Smith, P., Haussaire, J. M., Leppänen, A., Manning, A. J., McNorton, J., Brockmann, P., & Dolman, A. J. H.](#)

6790 [A. The consolidated European synthesis of CH₄ and N₂O emissions for the European Union and United Kingdom:](#)

6791 [1990–2017. *Earth System Science Data*, 13\(5\), 2307–2362, doi:10.5194/essd-13-2307-2021](#), 2021.

6792 [Petrescu, A. M. R., Qiu, C., McGrath, M. J., Peylin, P., Peters, G. P., Ciais, P., Thompson, R. L., Tsuruta, A., Brunner,](#)

6793 [D., Kuhnert, M., Matthews, B., Palmer, P. I., Tarasova, O., Regnier, P., Lauerwald, R., Bastviken, D., Höglund-](#)

6794 [Isaksson, L., Winiwarter, W., Etiopie, G., Aalto, T., Balsamo, G., Bastrikov, V., Berchet, A., Brockmann, P., Ciotoli,](#)

6795 [G., Conchedda, G., Crippa, M., Dentener, F., Groot Zwaafink, C. D., Guizzardi, D., Günther, D., Haussaire, J.-M.,](#)

6796 [Houweling, S., Janssens-Maenhout, G., Kouyate, M., Leip, A., Leppänen, A., Lugato, E., Maisonnier, M., Manning,](#)

6797 [A. J., Markkanen, T., McNorton, J., Muntean, M., Oreggioni, G. D., Patra, P. K., Perugini, L., Pison, I., Raivonen, M.](#)

6798 [T., Saunio, M., Segers, A. J., Smith, P., Solazzo, E., Tian, H., Tubiello, F. N., Vesala, T., van der Werf, G. R., Wilson,](#)

6799 [C., and Zaehle, S.: The consolidated European synthesis of CH₄ and N₂O emissions for the European Union and United](#)

6800 [Kingdom: 1990–2019. *Earth Syst. Sci. Data*, 15, 1197–1268, https://doi.org/10.5194/essd-15-1197-2023](#), 2023.

6801 [Pétron, G., Karion, A., Sweeney, C., Miller, B. R., Montzka, S. A., Frost, G. J., Trainer, M., Tans, P., Andrews, A., Kofler,](#)

6802 [J., Helmig, D., Guenther, D., Dlugokencky, E., Lang, P., Newberger, T., Wolter, S., Hall, B., Novelli, P., Brewer, A.,](#)

6803 [Conley, S., Hardesty, M., Banta, R., White, A., Noone, D., Wolfe, D. and Schnell, R.: A new look at methane and](#)

6804 [nonmethane hydrocarbon emissions from oil and natural gas operations in the Colorado Denver-Julesburg Basin, *J.*](#)

6805 [Geophys. Res. Atmospheres](#), 119(11), 6836–6852, doi:10.1002/2013jd021272, 2014.

6806 [Phillips, N. G., Ackley, R., Crosson, E. R., Down, A., Hutyra, L. R., Brondfield, M., Karr, J. D., Zhao, K. and Jackson, R.](#)

6807 [B.: Mapping urban pipeline leaks: Methane leaks across Boston, *Environ. Pollut.*, 173, 1–4,](#)

6808 [doi:10.1016/j.envpol.2012.11.003](https://doi.org/10.1016/j.envpol.2012.11.003), 2013.

6809 [Pison, I., Ringeval, B., Bousquet, P., Prigent, C. and Papa, F.: Stable atmospheric methane in the 2000s: key-role of](#)

6810 [emissions from natural wetlands, *Atmospheric Chem. Phys. Discuss.*, 13\(4\), 9017–9049, doi:10.5194/acpd-13-9017-](#)

6811 [2013](#), 2013.

6812 [Pitz, S. and Magonigal, J. P.: Temperate forest methane sink diminished by tree emissions, *New Phytol.*, 214\(4\), 1432–](#)

1439, doi:10.1111/nph.14559, 2017.

Platt, U., Allan, W. and Lowe, D.: Hemispheric average Cl atom concentration from $^{13}\text{C}/^{12}\text{C}$ ratios in atmospheric methane, *Atmos Chem Phys*, 4, 2393–2399, 2004.

Plummer, D., Nagashima, T., Tilmes, S., Archibald, A., Chiodo, G., Fadnavis, S., Garny, H., Josse, B., Kim, J., Lamarque, J.-F., Morgenstern, O., Murray, L., Orbe, C., Tai, A., Chipperfield, M., Funke, B., Jukes, M., Kinnison, D., Kunze, M., Luo, B., Matthes, K., Newman, P. A., Pascoe, C. and Peter, T.: CCMI- 2022: a new set of Chemistry–Climate Model Initiative (CCMI) community simulations to update the assessment of models and support upcoming ozone assessment activities. *SPARC Newsletter* 57, 22–30, 2021.

Pollard, D. F., Sherlock, V., Robinson, J., Deutscher, N. M., Connor, B. and Shiona, H.: The Total Carbon Column Observing Network site description for Lauder, New Zealand, *Earth Syst. Sci. Data*, 9(2), 977–992, doi:10.5194/essd-9-977-2017, 2017.

Portmann, F. T., Siebert, S. & Döll, P. : MIRCA2000 – Global monthly irrigated and rainfed crop areas around the year 2000: A new high-resolution data set for agricultural and hydrological modeling, *Global Biogeochemical Cycles*, 24, GB 1011, doi:10.1029/2008GB003435, 2010

Portmann, R. W., Daniel, J. S. and Ravishankara, A. R.: Stratospheric ozone depletion due to nitrous oxide: influences of other gases, *Philos. Trans. R. Soc. Lond. B Biol. Sci.*, 367(1593), 1256–1264, doi:10.1098/rstb.2011.0377, 2012.

Poulter, B., Bousquet, P., Canadell, J. G., Ciais, P., Peregón, A., Saunois, M., Arora, V. K., Beerling, D. J., Brovkin, V., Jones, C. D., Joos, F., Gedney, N., Ito, A., Kleinen, T., Koven, C. D., McDonald, K., Melton, J. R., Peng, C. H., Peng, S. S., Prigent, C., Schroeder, R., Riley, W. J., Saito, M., Spahni, R., Tian, H. Q., Taylor, L., Viovy, N., Wilton, D., Wiltshire, A., Xu, X. Y., Zhang, B. W., Zhang, Z. and Zhu, Q. A.: Global wetland contribution to 2000–2012 atmospheric methane growth rate dynamics, *Environ. Res. Lett.*, 12(9), doi:10.1088/1748-9326/aa8391, 2017.

Prairie, Y. T., J. Alm, J. Beaulieu, N. Barros, T. Battin, J. Cole, P. del Giorgio, T. DelSontro, F. Guérin, A. Harby, J. Harrison, S. Mercier-Blais, D. Serça, S. Sobek, and D. Vachon, *Greenhouse Gas Emissions from Freshwater Reservoirs: What Does the Atmosphere See? Ecosystems*, 21(5): p. 1058-1071, 2018

Prather, M. J., Holmes, C. D. and Hsu, J.: Reactive greenhouse gas scenarios: Systematic exploration of uncertainties and the role of atmospheric chemistry, *Geophys. Res. Lett.*, 39(9), L09803, doi:10.1029/2012gl051440, 2012.

Prinn, R. G., Weiss, R. F., Arduini, J., Arnold, T., DeWitt, H. L., Fraser, P. J., Ganesan, A. L., Gasore, J., Harth, C. M., Hermansen, O., Kim, J., Krummel, P. B., Li, S., Loh, Z. M., Lunder, C. R., Maione, M., Manning, A. J., Miller, B. R., Mitrevski, B., Mühle, J., O'Doherty, S., Park, S., Reimann, S., Rigby, M., Saito, T., Salameh, P. K., Schmidt, R., Simmonds, P. G., Steele, L. P., Vollmer, M. K., Wang, R. H., Yao, B., Yokouchi, Y., Young, D., and Zhou, L.: History of chemically and radiatively important atmospheric gases from the Advanced Global Atmospheric Gases Experiment (AGAGE), *Earth Syst. Sci. Data*, 10, 985–1018, <https://doi.org/10.5194/essd-10-985-2018>, 2018.

Prosperi, P., Bloise, M., Tubiello, F.N. *et al.* New estimates of greenhouse gas emissions from biomass burning and peat

fires using MODIS Collection 6 burned areas. *Climatic Change* **161**, 415–432. <https://doi.org/10.1007/s10584-020-02654-0>, 2020

Purvaja, R., Ramesh, R., & Frenzel, P.: Plant-mediated methane emission from an Indian mangrove. *Global Change Biology*, **10**, 1825–1834, 2004

Qin, B., Zhou, J., Elser, J.J., Gardner, W.S., Deng, J., and J.D. Brookes: Water depth underpins the relative roles and fates of nitrogen and phosphorus in lakes. *Environmental Science & Technology* **2020**, *54* (6), 3191-3198, DOI: [10.1021/acs.est.9b05858](https://doi.org/10.1021/acs.est.9b05858), 2020.

Qu, Z., Jacob, D. J., Shen, L., Lu, X., Zhang, Y., Scarpelli, T. R., Nesser, H., Sulprizio, M. P., Maasakkers, J. D., Bloom, A. A., Worden, J. R., Parker, R. J., and Delgado, A. L.: Global distribution of methane emissions: a comparative inverse analysis of observations from the TROPOMI and GOSAT satellite instruments. *Atmos. Chem. Phys.*, **21**, 14159–14175. <https://doi.org/10.5194/acp-21-14159-2021>, 2021.

Qu, Z., Jacob, D. J., Zhang, Y., Shen, L., Varon, D. J., Lu, X., Scarpelli, T., Bloom, A., Worden, J., and Parker, R. J.: Attribution of the 2020 surge in atmospheric methane by inverse analysis of GOSAT observations. *Environ. Res. Lett.*, **17**, 094003. <https://doi.org/10.1088/1748-9326/ac8754>, 2022.

Randerson, J. T., Chen, Y., van der Werf, G. R., Rogers, B. M. and Morton, D. C.: Global burned area and biomass burning emissions from small fires. *J. Geophys. Res. Biogeosciences*, **117**, G4. doi:10.1029/2012jg002128, 2012.

Ramage, J.L., Kuhn, M., Virkkala, A.M., Voigt, C., Marushchak, M.E., Bastos, A., Biasi, C., Canadell, J.G., Ciais, P., López-Blanco, E., Natali, S.M., et al.: The net GHG balance and budget of the permafrost region (2000-2020) from ecosystem flux upscaling. Preprint in ESS Open Archive. September 11, 2023. DOI: [10.22541/essoar.169447408.86275712/v1](https://doi.org/10.22541/essoar.169447408.86275712/v1), 2023

Ramsden, A. E., Ganesan, A. L., Western, L. M., Rigby, M., Manning, A. J., Foulds, A., France, J. L., Barker, P., Levy, P., Say, D., Wisher, A., Arnold, T., Rennick, C., Stanley, K. M., Young, D., and O'Doherty, S.: Quantifying fossil fuel methane emissions using observations of atmospheric ethane and an uncertain emission ratio. *Atmos. Chem. Phys.*, **22**, 3911–3929. <https://doi.org/10.5194/acp-22-3911-2022>, 2022.

Ray, N.E., Holgerson, M.A., Andersen, M.R., Bikše, J., Bortolotti, L.E., Futter, M., Kokorite, I., Law, A., McDonald, C., Mesman, J.P., Peacock, M., Richardson, D.C., Arsenaault, J., Bansal, S., Cawley, K., Kuhn, M., Shahabinia, A.R. and Smufer, F.: Spatial and temporal variability in summertime dissolved carbon dioxide and methane in temperate ponds and shallow lakes. *Limnol Oceanogr.*, **68**: 1530-1545. <https://doi.org/10.1002/lno.12362>, 2023

Regnier P., Arndt, S., Dale, A.W., LaRowe, D.E., Mogollon, J. and Van Cappellen, P. Advances in the biogeochemical modeling of anaerobic oxidation of methane (AOM). *Earth Science Reviews*, **106**, 105-130, 2011;

Ren, W. E. I., Tian, H., Xu, X., Liu, M., Lu, C., Chen, G., Melillo, J., Reilly, J. and Liu, J.: Spatial and temporal patterns of CO₂ and CH₄ fluxes in China's croplands in response to multifactor environmental changes. *Tellus B*, **63**(2), 222–240. doi:10.1111/j.1600-0889.2010.00522.x, 2011.

6879 [Repeta, D. J., Ferrón, S., Sosa, O. A., Johnson, C. G., Repeta, L. D., Acker, M., DeLong, E. F. and Karl, D. M.: Marine](#)
6880 [methane paradox explained by bacterial degradation of dissolved organic matter, *Nat. Geosci.*, 9\(12\), 884–887,](#)
6881 [doi:10.1038/ngeo2837, 2016.](#)

6882 [Riahi, K., van Vuuren, D. P., Kriegler, E., Edmonds, J., O'Neill, B. C., Fujimori, S., Bauer, N., Calvin, K., Dellink, R.,](#)
6883 [Fricko, O., Lutz, W., Popp, A., Cuaresma, J. C., Kc, S., Leimbach, M., Jiang, L., Kram, T., Rao, S., Emmerling, J.,](#)
6884 [Ebi, K., Hasegawa, T., Havlik, P., Humpenöder, F., Da Silva, L. A., Smith, S., Stehfest, E., Bosetti, V., Eom, J.,](#)
6885 [Gernaat, D., Masui, T., Rogelj, J., Strefler, J., Drouet, L., Krey, V., Luderer, G., Harmsen, M., Takahashi, K.,](#)
6886 [Baumstark, L., Doelman, J. C., Kainuma, M., Klimont, Z., Marangoni, G., Lotze-Campen, H., Obersteiner, M., Tabeau,](#)
6887 [A. and Tavoni, M.: The Shared Socioeconomic Pathways and their energy, land use, and greenhouse gas emissions](#)
6888 [implications: An overview, *Glob. Environ. Change*, 42, 153–168, doi:10.1016/j.gloenvcha.2016.05.009, 2017.](#)

6889 [Rice, A. L., Butenhoff, C. L., Shearer, M. J., Teama, D., Rosenstiel, T. N. and Khalil, M. A. K.: Emissions of anaerobically](#)
6890 [produced methane by trees, *Geophys. Res. Lett.*, 37, L03807, doi:10.1029/2009GL041565, 2010.](#)

6891 [Ridgwell, A. J., Marshall, S. J. and Gregson, K.: Consumption of atmospheric methane by soils: A process-based model,](#)
6892 [*Glob. Biogeochem. Cycles*, 13\(1\), 59–70, doi:10.1029/1998gb900004, 1999.](#)

6893 [Riedel, T. P., Wolfe, G. M., Danas, K. T., Gilman, J. B., Kuster, W. C., Bon, D. M., Vlasenko, A., Li, S. M., Williams, E.](#)
6894 [J., Lerner, B. M., Veres, P. R., Roberts, J. M., Holloway, J. S., Lefer, B., Brown, S. S. and Thornton, J. A.: An MCM](#)
6895 [modeling study of nitryl chloride \(ClNO₂\) impacts on oxidation, ozone production and nitrogen oxide partitioning in](#)
6896 [polluted continental outflow, *Atmospheric Chem. Phys.*, 14\(8\), 3789–3800, doi:10.5194/acp-14-3789-2014, 2014.](#)

6897 [Rigby, M., Montzka, S. A., Prinn, R. G., White, J. W. C., Young, D., O'Doherty, S., Lunt, M. F., Ganesan, A. L., Manning,](#)
6898 [A. J., Simmonds, P. G., Salameh, P. K., Harth, C. M., Mühle, J., Weiss, R. F., Fraser, P. J., Steele, L. P., Krummel, P.](#)
6899 [B., McCulloch, A. and Park, S.: Role of atmospheric oxidation in recent methane growth, *Proc. Natl. Acad. Sci.*,](#)
6900 [114\(21\), 5373, 2017.](#)

6901 [Riley, W. J., Subin, Z. M., Lawrence, D. M., Swenson, S. C., Tom, M. S., Meng, L., Mahowald, N. M. and Hess, P.:](#)
6902 [Barriers to predicting changes in global terrestrial methane fluxes: analyses using CLM4Me, a methane](#)
6903 [biogeochemistry model integrated in CESM, *Biogeosciences*, 8\(7\), 1925–1953, doi:10.5194/bg-8-1925-2011, 2011.](#)

6904 [Ringeval, B., Friedlingstein, P., Koven, C., Ciais, P., de Noblet-Ducoudre, N., Decharme, B. and Cadule, P.: Climate-CH₄](#)
6905 [feedback from wetlands and its interaction with the climate-CO₂ feedback, *Biogeosciences*, 8\(8\), 2137–2157,](#)
6906 [doi:10.5194/bg-8-2137-2011, 2011.](#)

6907 [Robison, A.L., W.M. Wollheim, B. Turek, C. Bova, C. Snay, and R.K. Varner, Spatial and temporal heterogeneity of](#)
6908 [methane ebullition in lowland headwater streams and the impact on sampling design, *Limnology and Oceanography*,](#)
6909 [66\(12\): p. 4063-4076, 2021](#)

6910 [Rocher-Ros, G., Stanley, E.H., Loken, L.C., Casson, N.J., Raymond, P.A., Liu, S., Amatulli, G. and Sponseller, R.A.,](#)
6911 [Global methane emissions from rivers and streams. *Nature*, pp.1-6, 621, 530–535, https://doi.org/10.1038/s41586-023-](#)

06344-6, 2023

Rosentreter, J. A., Maher, D. T., Erler, D. V., Murray, R. H. and Eyre, B. D.: Methane emissions partially offset “blue carbon” burial in mangroves, *Sci. Adv.*, 4(6), eaao4985, doi:10.1126/sciadv.aao4985, 2018.

Rosentreter, J. A., A. V Borges, B. R. Deemer, and others : Half of global methane emissions come from highly variable aquatic ecosystem sources. *Nat. Geosci.* 14: 225–230. doi:10.1038/s41561-021-00715-2, 2021

Rosentreter, J.A., Laruelle, G.G., Bange, H.W., Bianchi, T.S., Busecke, J.J.M., Cai, W-J, Eyre, B.D., Forbrich, I., Kwon, E.Y., Mavara, T., Moosdorf, N., Van Dam, B. and Regnier, P. Coastal vegetation and estuaries are collectively a greenhouse gas sink. *Nature Climate Change*, 13, 579–587, doi: 10.1038/s41558-023-01682-9, 2023.

Rosentreter, J.A., Alcott, L., Maavara, T., Sun, X., Zhou, Y., Planavsky, N., & Raymond, P. Revisiting the Global Methane Cycle Through Expert Opinion (submitted to *Earth Future*).

Ruppel, C. D., and J. D. Kessler (2017). The interaction of climate change and methane hydrates. *Rev. Geophys.*, 55, 126-168. doi:10.1002/2016RG000534, 2017

Saad, K. M., Wunch, D., Toon, G. C., Bernath, P., Boone, C., Connor, B., Deutscher, N. M., Griffith, D. W. T., Kivi, R., Notholt, J., Roehl, C., Schneider, M., Sherlock, V. and Wennberg, P. O.: Derivation of tropospheric methane from TCCON CH₄ and HF total column observations. *Atmospheric Meas. Technol.*, 7(9), 2907–2918, doi:10.5194/amt-7-2907-2014, 2014.

Sanderson, M. G.: Biomass of termites and their emissions of methane and carbon dioxide: A global database. *Glob. Biogeochem. Cycles*, 10(4), 543–557, doi:10.1029/96gb01893, 1996.

Sasakawa, M., Shimoyama, K., Machida, T., Tsuda, N., Suto, H., Arshinov, M., Davydov, D., Fofonov, A., Krasnov, O., Saeki, T., Koyama, Y. and Maksyutov, S.: Continuous measurements of methane from a tower network over Siberia. *Tellus B*, 62(5), 403–416, doi:10.1111/j.1600-0889.2010.00494.x, 2010.

Sasakawa, M., Machida, T., Ishijima, K., Arshinov, M., Patra, P. K., Ito, A., Aoki, S., and Petrov, V.: Temporal characteristics of CH₄ vertical profiles observed in the West Siberian Lowland over Surgut from 1993 to 2015 and Novosibirsk from 1997 to 2015. *Journal of Geophysical Research: Atmospheres*, 122, 11,261– 11,273. <https://doi.org/10.1002/2017JD026836>, 2017.

Saunio, M., Bousquet, P., Poulter, B., Pregon, A., Ciais, P., Canadell, J. G., Dlugokencky, E. J., Etiope, G., Bastviken, D., Houweling, S., Janssens-Maenhout, G., Tubiello, F. N., Castaldi, S., Jackson, R. B., Alexe, M., Arora, V. K., Beerling, D. J., Bergamaschi, P., Blake, D. R., Brailsford, G., Brovkin, V., Bruhwiler, L., Crevoisier, C., Crill, P., Covey, K., Curry, C., Frankenberg, C., Gedney, N., Höglund-Isaksson, L., Ishizawa, M., Ito, A., Joos, F., Kim, H. S., Kleinen, T., Krummel, P., Lamarque, J. F., Langenfelds, R., Locatelli, R., Machida, T., Maksyutov, S., McDonald, K. C., Marshall, J., Melton, J. R., Morino, I., Naik, V., O’Doherty, S., Parmentier, F. J. W., Patra, P. K., Peng, C., Peng, S., Peters, G. P., Pison, I., Prigent, C., Prinn, R., Ramonet, M., Riley, W. J., Saito, M., Santini, M., Schroeder, R., Simpson, I. J., Spahni, R., Steele, P., Takizawa, A., Thornton, B. F., Tian, H., Tohjima, Y., Viovy, N., Voulgarakis,

0945 [A., van Weele, M., van der Werf, G. R., Weiss, R., Wiedinmyer, C., Wilton, D. J., Wiltshire, A., Worthy, D., Wunch,](#)
 0946 [D., Xu, X., Yoshida, Y., Zhang, B., Zhang, Z. and Zhu, Q.: The global methane budget 2000–2012, *Earth Syst Sci*](#)
 0947 [Data, 8\(2\), 697–751, doi:10.5194/essd-8-697-2016, 2016.](#)
 0948 [Saunio, M., Bousquet, P., Poulter, B., Peregón, A., Ciais, P., Canadell, J. G., Dlugokencky, E. J., Etiope, G., Bastviken,](#)
 0949 [D., Houweling, S., Janssens-Maenhout, G., Tubiello, F. N., Castaldi, S., Jackson, R. B., Alexe, M., Arora, V. K.,](#)
 0950 [Beerling, D. J., Bergamaschi, P., Blake, D. R., Brailsford, G., Bruhwiler, L., Crevoisier, C., Crill, P., Covey, K.,](#)
 0951 [Frankenberg, C., Gedney, N., Höglund-Isaksson, L., Ishizawa, M., Ito, A., Joos, F., Kim, H. S., Kleinen, T., Krummel,](#)
 0952 [P., Lamarque, J. F., Langenfelds, R., Locatelli, R., Machida, T., Maksyutov, S., Melton, J. R., Morino, I., Naik, V.,](#)
 0953 [O’Doherty, S., Parmentier, F. J. W., Patra, P. K., Peng, C., Peng, S., Peters, G. P., Pison, I., Prinn, R., Ramonet, M.,](#)
 0954 [Riley, W. J., Saito, M., Santini, M., Schroeder, R., Simpson, I. J., Spahni, R., Takizawa, A., Thornton, B. F., Tian, H.,](#)
 0955 [Tohjima, Y., Viovy, N., Voulgarakis, A., Weiss, R., Wilton, D. J., Wiltshire, A., Worthy, D., Wunch, D., Xu, X.,](#)
 0956 [Yoshida, Y., Zhang, B., Zhang, Z. and Zhu, Q.: Variability and quasi-decadal changes in the methane budget over the](#)
 0957 [period 2000–2012, *Atmospheric Chem. Phys.*, 17\(18\), 11135–11161, doi:10.5194/acp-17-11135-2017, 2017.](#)
 0958 [Saunio, M., Stavert, A. R., Poulter, B., Bousquet, P., Canadell, J. G., Jackson, R. B., Raymond, P. A., Dlugokencky, E.](#)
 0959 [J., Houweling, S., Patra, P. K., Ciais, P., Arora, V. K., Bastviken, D., Bergamaschi, P., Blake, D. R., Brailsford, G.,](#)
 0960 [Bruhwiler, L., Carlson, K. M., Carrol, M., Castaldi, S., Chandra, N., Crevoisier, C., Crill, P. M., Covey, K., Curry, C.](#)
 0961 [L., Etiope, G., Frankenberg, C., Gedney, N., Hegglin, M. I., Höglund-Isaksson, L., Hugelius, G., Ishizawa, M., Ito, A.,](#)
 0962 [Janssens-Maenhout, G., Jensen, K. M., Joos, F., Kleinen, T., Krummel, P. B., Langenfelds, R. L., Laruelle, G. G., Liu,](#)
 0963 [L., Machida, T., Maksyutov, S., McDonald, K. C., McNorton, J., Miller, P. A., Melton, J. R., Morino, I., Müller, J.,](#)
 0964 [Murguía-Flores, F., Naik, V., Niwa, Y., Noce, S., O’Doherty, S., Parker, R. J., Peng, C., Peng, S., Peters, G. P., Prigent,](#)
 0965 [C., Prinn, R., Ramonet, M., Regnier, P., Riley, W. J., Rosentretter, J. A., Segers, A., Simpson, I. J., Shi, H., Smith, S.](#)
 0966 [J., Steele, L. P., Thornton, B. F., Tian, H., Tohjima, Y., Tubiello, F. N., Tsuruta, A., Viovy, N., Voulgarakis, A., Weber,](#)
 0967 [T. S., van Weele, M., van der Werf, G. R., Weiss, R. F., Worthy, D., Wunch, D., Yin, Y., Yoshida, Y., Zhang, W.,](#)
 0968 [Zhang, Z., Zhao, Y., Zheng, B., Zhu, Q., Zhu, Q., and Zhuang, Q.: The Global Methane Budget 2000–2017, *Earth*](#)
 0969 [Syst. Sci. Data](#), 12, 1561–1623, <https://doi.org/10.5194/essd-12-1561-2020>, 2020.
 0970 [Sayers, M.J., Grimm, A.G., Shuchman, R.A., Deines, A.M., Bunnell, D.B., Raymer, Z.B., Rogers, M.W., Woelmer, W.,](#)
 0971 [Bennion, D.H., Brooks, C.N., Whitley, M.A.A., Warner, D.M., and J. Mychek-Londer: A new method to generate a](#)
 0972 [high-resolution global distribution map of lake chlorophyll, *International Journal of Remote Sensing*, 36:7, 1942–1964,](#)
 0973 [DOI: 10.1080/01431161.2015.1029099, 2015](#)
 0974 [Schepers, D., Guerlet, S., Butz, A., Landgraf, J., Frankenberg, C., Hasekamp, O., Blavier, J. F., Deutscher, N. M., Griffith,](#)
 0975 [D. W. T., Hase, F., Kyro, E., Morino, I., Sherlock, V., Sussmann, R. and Aben, I.: Methane retrievals from Greenhouse](#)
 0976 [Gases Observing Satellite \(GOSAT\) shortwave infrared measurements: Performance comparison of proxy and physics](#)
 0977 [retrieval algorithms, *J. Geophys. Res. Atmospheres*, 117, D10, doi:10.1029/2012jd017549, 2012.](#)

6978 [Schmale O, Greinert J, Rehder G \(2005\) Methane emission from high-intensity marine gas seeps in the Black Sea into the](#)
6979 [atmosphere. *Geophys Res Lett* 32:L07609. doi:10.1029/2004GL021138, 2005](#)

6980 [Schmid, M., Batist, M.D., Granin, N.G., Kapitanov, V.A., McGinnis, D.F., Mizandrontsev, I.B., Obzhirov, A.I., and](#)
6981 [Wüest, A.. Sources and sinks of methane in Lake Baikal: A synthesis of measurements and modelling. *Limnol.*](#)
6982 [Oceanogr., 52\(5\), 1824–1837. doi: 10.4319/lo.2007.52.5.1824, 2007](#)

6983 [Schneising, O., Burrows, J. P., Dickerson, R. R., Buchwitz, M., Reuter, M. and Bovensmann, H.: Remote sensing of](#)
6984 [fugitive methane emissions from oil and gas production in North American tight geologic formations, *Earths Future*,](#)
6985 [2, 548–558. doi:10.1002/2014EF000265, 2014.](#)

6986 [Schorn, S., S. Ahmerkamp, E. Bullock, and others. : Diverse methylophilic methanogenic archaea cause high methane](#)
6987 [emissions from seagrass meadows. *Proc. Natl. Acad. Sci.* 119: 1–12. doi:10.1073/pnas.2106628119, 2022](#)

6988 [Schuldt, K. N., Mund, J., Aalto, T., Arlyn Andrews, Apadula, F., Jgor Arduini, Arnold, S., Baier, B., Bäni, L., Bartyzel,](#)
6989 [J., Bergamaschi, P., Biermann, T., Biraud, S. C., Pierre-Eric Blanc, Boenisch, H., Brailsford, G., Brand, W. A.,](#)
6990 [Brunner, D., Bui, T. P. V., ... Mirosław Zimnoch. : *Multi-laboratory compilation of atmospheric carbon dioxide data*](#)
6991 [for the period 1983-2022: obspack ch4 1 GLOBALVIEWplus v6.0 2023-12-01 \[Data set\]. NOAA Global](#)
6992 [Monitoring Laboratory. <https://doi.org/10.25925/20231001>, 2023](#)

6993 [Schoor, E.A., Abbott, B.W., Commane, R., Ermakovich, J., Euskirchen, E., Hugelius, G., Grosse, G., Jones, M., Koven,](#)
6994 [C., Leshyk, V. and Lawrence, D. \(2022\) Permafrost and climate change: carbon cycle feedbacks from the warming](#)
6995 [Arctic. *Annual Review of Environment and Resources*, 47, pp.343-371. \[https://doi.org/10.1146/annurev-environ-\]\(https://doi.org/10.1146/annurev-environ-012220-011847\)](#)
6996 [012220-011847, 2022](#)

6997 [Schwietzke, S., Sherwood, O. A., Bruhwiler, L. M. P., Miller, J. B., Etiope, G., Dlugokencky, E. J., Michel, S. E., Arling,](#)
6998 [V. A., Vaughn, B. H., White, J. W. C. and Tans, P. P.: Upward revision of global fossil fuel methane emissions based](#)
6999 [on isotope database. *Nature*, 538\(7623\), 88–91, doi:10.1038/nature19797, 2016.](#)

7000 [Segers, A., Steinke, T., and Houweling, S.: Description of the CH4 Inversion Production Chain, CAMS \(Copernicus](#)
7001 [Atmospheric Monitoring Service\) Report. \[online\] Available from:](#)
7002 [https://atmosphere.copernicus.eu/sites/default/files/2022-10/CAMS255_2021SC1_D55.5.2.1-](https://atmosphere.copernicus.eu/sites/default/files/2022-10/CAMS255_2021SC1_D55.5.2.1-2021CH4_202206_production_chain_CH4_v1.pdf)
7003 [2021CH4_202206_production_chain_CH4_v1.pdf](https://atmosphere.copernicus.eu/sites/default/files/2022-10/CAMS255_2021SC1_D55.5.2.1-2021CH4_202206_production_chain_CH4_v1.pdf) (Accessed 1 février 2024), 2022.

7004 [Shen, L., Gautam, R., Omara, M., Zavala-Araiza, D., Maasakkers, J. D., Scarpelli, T. R., Lorente, A., Lyon, D., Sheng, J.,](#)
7005 [Varon, D. J., Nesser, H., Qu, Z., Lu, X., Sulprizio, M. P., Hamburg, S. P., and Jacob, D. J.: Satellite quantification of](#)
7006 [oil and natural gas methane emissions in the US and Canada including contributions from individual basins, *Atmos.*](#)
7007 [Chem. Phys.](#), 22, 11203–11215, <https://doi.org/10.5194/acp-22-11203-2022>, 2022.

7008 [Shen, L., Jacob, D.J., Gautam, R. et al. National quantifications of methane emissions from fuel exploitation using high](#)
7009 [resolution inversions of satellite observations. *Nat Commun* 14, 4948 , <https://doi.org/10.1038/s41467-023-40671-6>,](#)
7010 [2023](#)

1011 [Sherwen, T., Schmidt, J. A., Evans, M. J., Carpenter, L. J., Großmann, K., Eastham, S. D., Jacob, D. J., Dix, B., Koenig,](#)
1012 [T. K., Sinreich, R., Ortega, I., Volkamer, R., Saiz-Lopez, A., Prados-Roman, C., Mahajan, A. S., and Ordóñez, C.:](#)
1013 [Global impacts of tropospheric halogens \(Cl, Br, I\) on oxidants and composition in GEOS-Chem, *Atmos. Chem. Phys.*,](#)
1014 [16, 12239–12271, <https://doi.org/10.5194/acp-16-12239-2016>, 2016.](#)

1015 [Shindell, D., Kuylentstierna, J. C. I., Vignati, E., van Dingenen, R., Amann, M., Klimont, Z., Anenberg, S. C., Muller, N.,](#)
1016 [Janssens-Maenhout, G., Raes, F., Schwartz, J., Faluvegi, G., Pozzoli, L., Kupiainen, K., Höglund-Isaksson, L.,](#)
1017 [Emberson, L., Streets, D., Ramanathan, V., Hicks, K., Oanh, N. T. K., Milly, G., Williams, M., Demkine, V. and](#)
1018 [Fowler, D.: Simultaneously Mitigating Near-Term Climate Change and Improving Human Health and Food Security,](#)
1019 [*Science*, 335\(6065\), 183–189, doi:10.1126/science.1210026, 2012.](#)

1020 [Shorter, J. H., Mcmanus, J. B., Kolb, C. E., Allwine, E. J., Lamb, B. K., Mosher, B. W., Harriss, R. C., Partchatka, U.,](#)
1021 [Fischer, H., Harris, G. W., Crutzen, P. J. and Karbach, H.-J.: Methane emission measurements in urban areas in Eastern](#)
1022 [Germany, *J. Atmospheric Chem.*, 124\(2\), 121–140, 1996.](#)

1023 [Shu, S., Jain, A.K. and Khesghi, H.S.: Investigating Wetland and Nonwetland Soil Methane Emissions and Sinks Across](#)
1024 [the Contiguous United States Using a Land Surface Model. *Global Biogeochem. Cycles*, 34: e2019GB006251,](#)
1025 <https://doi-org.insu.bib.cnrs.fr/10.1029/2019GB006251>, 2020

1026 [Simpson, I. J., Thurtell, G. W., Kidd, G. E., Lin, M., Demetriades-Shah, T. H., Flitcroft, I. D., Kanemasu, E. T., Nie, D.,](#)
1027 [Bronson, K. F. and Neue, H. U.: Tunable diode laser measurements of methane fluxes from an irrigated rice paddy](#)
1028 [field in the Philippines, *J. Geophys. Res. Atmospheres*, 100\(D4\), 7283–7290, doi:10.1029/94jd03326, 1995.](#)

1029 [Simpson, I. J., Sulbaek Andersen, M. P., Meinardi, S., Bruhwiler, L., Blake, N. J., Helmig, D., Rowland, F. S. and Blake,](#)
1030 [D. R.: Long-term decline of global atmospheric ethane concentrations and implications for methane, *Nature*,](#)
1031 [488\(7412\), 490–494, doi:10.1038/nature11342, 2012.](#)

1032 [Smith I.R., Grasby S.E., Lane L.S.: An investigation of gas seeps and aquatic chemistry in Fisherman Lake, southwest](#)
1033 [Northwest Territories. Geological Survey of Canada, Current Research 2005-A3, 8 p., 2005](#)

1034 [Solomon EA, Kastner M, MacDonald IR, Leifer I: Considerable methane fluxes to the atmosphere from hydrocarbon](#)
1035 [seeps in the Gulf of Mexico. *Nat Geosci* 2:561–565, 2009](#)

1036 [Spahni, R., Wania, R., Neef, L., van Weele, M., Pison, I., Bousquet, P., Frankenberg, C., Foster, P. N., Joos, F., Prentice,](#)
1037 [I. C. and van Velthoven, P.: Constraining global methane emissions and uptake by ecosystems, *Biogeosciences*, 8\(6\),](#)
1038 [1643–1665, doi:10.5194/bg-8-1643-2011, 2011.](#)

1039 [Stanley, E. H., Casson, N. J., Christel, S. T., Crawford, J. T., Loken, L. C. and Oliver, S. K.: The ecology of methane in](#)
1040 [streams and rivers: patterns, controls, and global significance, *Ecol. Monogr.*, doi:10.1890/15-1027, 2016.](#)

1041 [Stanley, K. M., Grant, A., O’Doherty, S., Young, D., Manning, A. J., Stavert, A. R., Spain, T. G., Salameh, P. K., Harth,](#)
1042 [C. M., Simmonds, P. G., Sturges, W. T., Oram, D. E. and Derwent, R. G.: Greenhouse gas measurements from a UK](#)
1043 [network of tall towers: technical description and first results, *Atmospheric Meas. Tech.*, 11\(3\), 1437–1458,](#)

1044 [doi:10.5194/amt-11-1437-2018](https://doi.org/10.5194/amt-11-1437-2018), 2018.

1045 [Stanley, E. H., Loken, L. C., Casson, N. J., Oliver, S. K., Sponseller, R. A., Wallin, M. B., Zhang, L., and Rocher-Ros,](#)

1046 [G.: GRiMeDB: the Global River Methane Database of concentrations and fluxes, *Earth Syst. Sci. Data*, 15, 2879–](#)

1047 [2926, <https://doi.org/10.5194/essd-15-2879-2023>, 2023.](#)

1048 [Stavert, A. R., Saunois, M., Canadell, J. G., Poulter, B., Jackson, R. B., Regnier, P., Lauerwald, R., Raymond, P. A.,](#)

1049 [Allen, G. H., Patra, P. K., Bergamaschi, P., Bousquet, P., Chandra, N., Ciais, P., Gustafson, A., Ishizawa, M., Ito,](#)

1050 [A., Kleinen, T., Maksyutov, S., Joe McNorton, Joe R. Melton, Jurek Müller, Yosuke Niwa, Shushi Peng, William](#)

1051 [J. Riley, Arjo Segers, Hanqin Tian, Aki Tsuruta, Yi Yin, Zhen Zhang, Bo Zheng, Zhuang, Q. Regional trends](#)

1052 [and drivers of the global methane budget. *Global Change Biology*, 28, 182–200. <https://doi.org/10.1111/gcb.15901>,](#)

1053 [2021](#)

1054 [Steele, L. P., Fraser, P. J., Rasmussen, R. A., Khalil, M. A. K., Conway, T. J., Crawford, A. J., Gammon, R. H., Masarie,](#)

1055 [K. A. and Thoning, K. W.: The global distribution of methane in the troposphere, *J. Atmospheric Chem.*, 5, 125–171,](#)

1056 [1987.](#)

1057 [Stevenson, D. S., Derwent, R. G., Wild, O., and Collins, W. J.: COVID-19 lockdown emission reductions have the](#)

1058 [potential to explain over half of the coincident increase in global atmospheric methane, *Atmos. Chem. Phys.*, 22,](#)

1059 [14243–14252. <https://doi.org/10.5194/acp-22-14243-2022>, 2022.](#)

1060 [Stocker, B. D., Spahni, R. and Joos, F.: DYPTOP: a cost-efficient TOPMODEL implementation to simulate sub-grid](#)

1061 [spatio-temporal dynamics of global wetlands and peatlands, *Geosci. Model Dev.*, 7\(6\), 3089–3110. doi:10.5194/gmd-](#)

1062 [7-3089-2014, 2014.](#)

1063 [Strauss, J., Abbott, B.W., Hugelius, G., Schuur, E., Treat, C., Fuchs, M., Schädel, C., Ulrich, M., Turetsky, M., Keuschig,](#)

1064 [M. and Biasi, C. \(2021\) Chapter 9. Permafrost. In *FAO Recarbonizing global soils—A technical manual of*](#)

1065 [recommended management practices: Volume 2—Hot spots and bright spots of soil organic carbon](#), p.130, 2021

1066 [Strode, S. A., Wang, J. S., Manyin, M., Duncan, B., Hossaini, R., Keller, C. A., Michel, S. E., and White, J. W. C.: Strong](#)

1067 [sensitivity of the isotopic composition of methane to the plausible range of tropospheric chlorine, *Atmos. Chem. Phys.*,](#)

1068 [20, 8405–8419. <https://doi.org/10.5194/acp-20-8405-2020>, 2020.](#)

1069 [Sugimoto, A., Inoue, T., Kitibutr, N., Abe, T: Methane oxidation by termite mounds estimate by the carbon isotope](#)

1070 [composition of methane. *Glob. Biogeochem. Cy.* 12, 595-605. 1998.](#)

1071 [Sweeney, C., Karion, A., Wolter, S., Newberger, T., Guenther, D., Higgs, J. A., Andrews, A. E., Lang, P. M., Neff, D.,](#)

1072 [Dlugokencky, E., Miller, J. B., Montzka, S. A., Miller, B. R., Masarie, K. A., Biraud, S. C., Novelli, P. C., Crotwell,](#)

1073 [M., Crotwell, A. M., Thoning, K. and Tans, P. P.: Seasonal climatology of CO₂ across North America from aircraft](#)

1074 [measurements in the NOAA/ESRL Global Greenhouse Gas Reference Network, *J. Geophys. Res. Atmospheres*,](#)

1075 [120\(10\), 5155–5190, doi:10.1002/2014jd022591, 2015.](#)

1076 [Tan, Z. and Zhuang, Q.: Methane emissions from pan-Arctic lakes during the 21st century: An analysis with process-](#)

7077 [based models of lake evolution and biogeochemistry, *J. Geophys. Res. Biogeosciences*, 120\(12\), 2641–2653,](#)
7078 [doi:10.1002/2015JG003184, 2015.](#)

7079 [Tans, P. and Zwellberg, C.: 17th WMO/IAEA Meeting on Carbon Dioxide, Other Greenhouse Gases and Related Tracers](#)
7080 [Measurement Techniques \(GGMT-2013\). GAW Report, WMO, Geneva. \[online\] Available from:](#)
7081 https://library.wmo.int/index.php?lvl=notice_display&id=16373#.XnpBPW7jIq8, 2014.

7082 [Taranu, Z.E., I. Gregory-Eaves, P.R. Leavitt, L. Bunting, T. Buchaca, J. Catalan, I. Domaizon, P. Guilizzoni, A. Lami, S.](#)
7083 [McGowan, H. Moorhouse, G. Morabito, F.R. Pick, M.A. Stevenson, P.L. Thompson, and R.D. Vinebrooke:](#)
7084 [Acceleration of cyanobacterial dominance in north temperate-subarctic lakes during the Anthropocene. *Ecology*](#)
7085 [Letters](#), 18(4): p. 375-384., 2015

7086 [Taylor, P. G., Bilinski, T. M., Fancher, H. R. F., Cleveland, C. C., Nemergut, D. R., Weintraub, S. R., Wieder, W. R. and](#)
7087 [Townsend, A. R.: Palm oil wastewater methane emissions and bioenergy potential, *Nat. Clim. Change*, 4\(3\), 151–152,](#)
7088 [doi:10.1038/nclimate2154, 2014.](#)

7089 [le Texier, H., Solomon, S. and Garcia, R. R.: The role of molecular hydrogen and methane oxidation in the water vapour](#)
7090 [budget of the stratosphere, *Q. J. R. Meteorol. Soc.*, 114\(480\), 281–295, doi:10.1002/qj.49711448002, 1988.](#)

7091 [Thanwerdas, J., Saunois, M., Berchet, A., Pison, I., Vaughn, B. H., Michel, S. E., and Bousquet, P.: Variational inverse](#)
7092 [modeling within the Community Inversion Framework v1.1 to assimilate \$\delta^{13}\text{C}\(\text{CH}_4\)\$ and \$\text{CH}_4\$: a case study with](#)
7093 [model LMDz-SACS, *Geosci. Model Dev.*, 15, 4831–4851, <https://doi.org/10.5194/gmd-15-4831-2022>, 2022a.](#)

7094 [Thanwerdas, J., Saunois, M., Pison, I., Hauglustaine, D., Berchet, A., Baier, B., Sweeney, C., and Bousquet, P.: How do](#)
7095 [Cl concentrations matter for the simulation of \$\text{CH}_4\$ and \$\delta^{13}\text{C}\(\text{CH}_4\)\$ and estimation of the \$\text{CH}_4\$ budget through](#)
7096 [atmospheric inversions?, *Atmos. Chem. Phys.*, 22, 15489–15508, <https://doi.org/10.5194/acp-22-15489-2022>, 2022b.](#)

7097 [Thanwerdas, J., Saunois, M., Berchet, A., Pison, I., and Bousquet, P.: Investigation of the renewed methane growth post-](#)
7098 [2007 with high-resolution 3-D variational inverse modeling and isotopic constraints, *Atmos. Chem. Phys.*, 24, 2129–](#)
7099 [2167, <https://doi.org/10.5194/acp-24-2129-2024>, 2024.](#)

7100 [Thompson, R. L., Montzka, S. A., Vollmer, M. K., Arduini, J., Crotwell, M., Krummel, P. B., Lunder, C., Mühle, J.,](#)
7101 [O'Doherty, S., Prinn, R. G., Reimann, S., Vimont, I., Wang, H., Weiss, R. F., and Young, D.: Estimation of the](#)
7102 [atmospheric hydroxyl radical oxidative capacity using multiple hydrofluorocarbons \(HFCs\), *Atmos. Chem. Phys.*, 24,](#)
7103 [1415–1427, <https://doi.org/10.5194/acp-24-1415-2024>, 2024.](#)

7104 [Thoning, K. W., Tans, P. P. and Komhyr, W. D.: Atmospheric carbon dioxide at Mauna Loa Observatory. 2. Analysis of](#)
7105 [the NOAA GMCC data, 1974,1985, *J. Geophys. Res.*, 94\(D6\), 8549–8565, 1989.](#)

7106 [Thorneloe, S. A., Barlaz, M. A., Peer, R., Huff, L. C., Davis, L. and Mangino, J.: Waste management, in *Atmospheric*](#)
7107 [Methane: Its Role in the Global Environment](#), edited by M. Khalil, pp. 234–262, Springer-Verlag, New York., 2000.

7108 [Thornton, B. F., Prytherch, J., Andersson, K., Brooks, I. M., Salisbury, D., Tjernström, M. and Crill, P. M.: Shipborne](#)
7109 [eddy covariance observations of methane fluxes constrain Arctic sea emissions, *Sci. Adv.*, 6\(5\), eaay7934,](#)

1110 [doi:10.1126/sciadv.aay7934](https://doi.org/10.1126/sciadv.aay7934), 2020.

1111 [Thornton B.F., Etiope G., Schwietzke S., Milkov A.V., Klusman R.W., Judd A., Oehler D.Z.: Conflicting estimates of](#)
1112 [natural geologic methane emissions. *Elem. Sci. Anth.*, 9, 1, doi:https://doi.org/10.1525/elementa.2021.00031, 2021](#)

1113 [Thornton, J. A., Kercher, J. P., Riedel, T. P., Wagner, N. L., Cozic, J., Holloway, J. S., Dubé, W. P., Wolfe, G. M., Quinn,](#)
1114 [P. K., Middlebrook, A. M., Alexander, B. and Brown, S. S.: A large atomic chlorine source inferred from mid-](#)
1115 [continental reactive nitrogen chemistry, *Nature*, 464\(7286\), 271–274, doi:10.1038/nature08905, 2010.](#)

1116 [Thorpe, A. K., Kort, E. A., Cusworth, D. H., Avasse, A. K., Bue, B. D., Yadav, V., Thompson, D. R., Frankenberg, C.](#)
1117 [, Hermer, J., Falk, M., Green, R. O., Miller, C. E., and Duren, R. M.: Methane emissions decline from reduced oil,](#)
1118 [natural gas, and refinery production during COVID-19. *Environmental Research Communications*, 5, 021006, 2023](#)

1119 [Tian, H., Xu, X., Liu, M., Ren, W., Zhang, C., Chen, G. and Lu, C.: Spatial and temporal patterns of CH₄ and N₂O fluxes](#)
1120 [in terrestrial ecosystems of North America during 1979–2008: application of a global biogeochemistry model,](#)
1121 [Biogeosciences, 7\(9\), 2673–2694, doi:10.5194/bg-7-2673-2010, 2010.](#)

1122 [Tian, H., Xu, X., Lu, C., Liu, M., Ren, W., Chen, G., Melillo, J. and Liu, J.: Net exchanges of CO₂, CH₄, and N₂O between](#)
1123 [China's terrestrial ecosystems and the atmosphere and their contributions to global climate warming. *J. Geophys. Res.*](#)
1124 [Biogeosciences, 116, G2, doi:10.1029/2010jg001393, 2011.](#)

1125 [Tian, H., Chen, G., Lu, C., Xu, X., Ren, W., Zhang, B., Banger, K., Tao, B., Pan, S., Liu, M., Zhang, C., Bruhwiler, L.](#)
1126 [and Wofsy, S.: Global methane and nitrous oxide emissions from terrestrial ecosystems due to multiple environmental](#)
1127 [changes. *Ecosyst. Health Sustain.*, 1\(1\), 1–20, doi:doi:10.1890/ehs14-0015.1, 2015.](#)

1128 [Tian, H., Lu, C., Ciais, P., Michalak, A. M., Canadell, J. G., Saikawa, E., Huntzinger, D. N., Gurney, K. R., Sitch, S.,](#)
1129 [Zhang, B., Yang, J., Bousquet, P., Bruhwiler, L., Chen, G., Dlugokencky, E., Friedlingstein, P., Melillo, J., Pan, S.,](#)
1130 [Poulter, B., Prinn, R., Saunio, M., Schwalm, C. R. and Wofsy, S. C.: The terrestrial biosphere as a net source of](#)
1131 [greenhouse gases to the atmosphere. *Nature*, 531\(7593\), 225–228, doi:10.1038/nature16946, 2016.](#)

1132 [Tian, H., Xu, R., Canadell, J. G., Thompson, R. L., Winiwarter, W., Suntharalingam, P., Davidson, E. A., Ciais, P.,](#)
1133 [Jackson, R. B., Janssens-Maenhout, G., Prather, M. J., Regnier, P., Pan, N., Pan, S., Peters, G. P., Shi, H., Tubiello, F.](#)
1134 [N., Zaehle, S., Zhou, F., Arneeth, A., Battaglia, G., Berthet, S., Bopp, L., Bouwman, A. F., Buitenhuis, E. T., Chang,](#)
1135 [J., Chipperfield, M. P., Dangal, S. R. S., Dlugokencky, E., Elkins, J. W., Eyre, B. D., Fu, B., Hall, B., Ito, A., Joos, F.,](#)
1136 [Krummel, P. B., Landolfi, A., Laruelle, G. G., Lauerwald, R., Li, W., Lienert, S., Maavara, T., MacLeod, M., Millet,](#)
1137 [D. B., Olin, S., Patra, P. K., Prinn, R. G., Raymond, P. A., Ruiz, D. J., van der Werf, G. R., Vuichard, N., Wang, J.,](#)
1138 [Weiss, R. F., Wells, K. C., Wilson, C., Yang, J., and Yao, Y.: A comprehensive quantification of global nitrous oxide](#)
1139 [sources and sinks, *Nature*, 586, 248–256, https://doi.org/10.1038/s41586-020-2780-0, 2020.](#)

1140 [Tian, H., Yao, Y., Li, Y., Shi, H., Pan, S., Najjar, R. G., et al. \(2023\). Increased terrestrial carbon export and CO₂ evasion](#)
1141 [from global inland waters since the preindustrial era. *Global Biogeochemical Cycles*, 37, e2023GB007776.](#)
1142 <https://doi.org/10.1029/2023GB007776>, 2023

143 [Tibrewal, K., Ciais, P., Saunio, M., Martinez, A., Lin, X., Thanwerdas, J., Deng, Z., Chevallier, F., Giron, C., Albergel,](#)
144 [C., Tanaka, K., Patra, P., Tsuruta, A., Zheng, B., Belikov, D., Niwa, Y., Janardanan, R., Maksyutov, S., Segers, A.,](#)
145 [Tzompa-Sosa, Z. A., Bousquet, P., and Sciare, J.: Assessment of methane emissions from oil, gas and coal sectors](#)
146 [across inventories and atmospheric inversions. *Commun Earth Environ* 5, 26. \[https://doi.org/10.1038/s43247-023-\]\(https://doi.org/10.1038/s43247-023-01190-w\)](#)
147 [01190-w, 2024](#)

148 [Tiwari, Y. K. and Kumar, K. R.: GHG observation programs in India. *Asian GAWgreenhouse Gases 3 Korea Meteorol.*](#)
149 [Adm. Chungnam South Korea, 2012.](#)

150 [Tsuruta, A., Aalto, T., Backman, L., Hakkarainen, J., Laan-Luijckx, I. T. van der, Krol, M. C., Spahni, R., Houweling, S.,](#)
151 [Laine, M., Dlugokencky, E., Gomez-Pelaez, A. J., Schoot, M. van der, Langenfelds, R., Ellul, R., Arduini, J., Apadula,](#)
152 [E., Gerbig, C., Feist, D. G., Kivi, R., Yoshida, Y. and Peters, W.: Global methane emission estimates for 2000–2012](#)
153 [from CarbonTracker Europe-CH₄ v1.0. *Geosci. Model Dev.*, 10\(3\), 1261–1289, doi:10.5194/gmd-10-1261-2017,](#)
154 [2017.](#)

155 [Tsuruta, A.; Kivimäki, E.; Lindqvist, H.; Karppinen, T.; Backman, L.; Hakkarainen, J.; Schneising, O.; Buchwitz, M.;](#)
156 [Lan, X.; Kivi, R.; et al. CH₄ Fluxes Derived from Assimilation of TROPOMI XCH₄ in CarbonTracker Europe-CH₄:](#)
157 [Evaluation of Seasonality and Spatial Distribution in the Northern High Latitudes. *Remote Sens.* 2023, 15, 1620.](#)
158 [https://doi.org/10.3390/rs15061620, 2023](#)

159 [Tubiello, F. N.: Greenhouse Gas Emissions Due to Agriculture, in *Elsevier Encyclopedia of Food Systems.*, 2019.](#)

160 [Tubiello, F. N., Salvatore, M., Rossi, S., Ferrara, A., Fitton, N. and Smith, P.: The FAOSTAT database of greenhouse gas](#)
161 [emissions from agriculture, *Environ. Res. Lett.*, 8\(1\), 015009, doi:10.1088/1748-9326/8/1/015009, 2013.](#)

162 [Tubiello, F. N., Karl, K., Flammini, A., Gütschow, J., Obli-Laryea, G., Conchedda, G., Pan, X., Qi, S. Y., Halldórudóttir](#)
163 [Heiðarsdóttir, H., Wanner, N., Quadrelli, R., Rocha Souza, L., Benoit, P., Hayek, M., Sandalow, D., Mencos Contreras,](#)
164 [E., Rosenzweig, C., Rosero Moncayo, J., Conforti, P., and Torero, M.: Pre- and post-production processes increasingly](#)
165 [dominate greenhouse gas emissions from agri-food systems, *Earth Syst. Sci. Data*, 14, 1795–1809,](#)
166 [https://doi.org/10.5194/essd-14-1795-2022, 2022.](#)

167 [Turetsky, M. R., Kotowska, A., Bubier, J., Dise, N. B., Crill, P., Hornibrook, E. R. C., Minkinen, K., Moore, T. R.,](#)
168 [Myers-Smith, I. H., Nykänen, H., Olefeldt, D., Rinne, J., Saarnio, S., Shurpali, N., Tuittila, E.-S., Waddington, J. M.,](#)
169 [White, J. R., Wickland, K. P. and Wilkening, M.: A synthesis of methane emissions from 71 northern, temperate, and](#)
170 [subtropical wetlands, *Glob. Change Biol.*, 20\(7\), 2183–2197, doi:10.1111/gcb.12580, 2014.](#)

171 [Turetsky, M. R., Abbott, B. W., Jones, M. C., Anthony, K. W., Olefeldt, D., Schuur, E. A. G., et al.: Carbon release](#)
172 [through abrupt permafrost thaw. *Nature Geoscience*, 13\(2\), 138–143. <https://doi.org/10.1038/s41561-019-0526-0>,](#)
173 [2020](#)

174 [Turner, A. J., Fung, I., Naik, V., Horowitz, L. W. and Cohen, R. C.: Modulation of hydroxyl variability by ENSO in the](#)
175 [absence of external forcing, *Proc. Natl. Acad. Sci.*, 115\(36\), 8931–8936, doi:10.1073/pnas.1807532115, 2018.](#)

176 [Turner, A. J., Frankenberg, C. and Kort, E. A.: Interpreting contemporary trends in atmospheric methane. Proc. Natl. Acad.](#)
177 [Sci., 116\(8\), 2805, doi:10.1073/pnas.1814297116, 2019.](#)

178 [UNEP, United Nations Environment Programme and Climate and Clean Air Coalition. Global Methane Assessment:](#)
179 [Benefits and Costs of Mitigating Methane Emissions. Nairobi: United Nations Environment Programme., 2021](#)

180 [UNEP, United Nations Environment Programme/Climate and Clean Air Coalition. Global Methane Assessment: 2030](#)
181 [Baseline Report. Nairobi, 2022](#)

182

183 [USEPA: Greenhouse Gas Emissions Estimation Methodologies for Biogenic Emissions from Selected Source Categories:](#)
184 [Solid Waste Disposal Wastewater Treatment Ethanol Fermentation. Measurement Policy Group, US EPA. \[online\]](#)
185 [Available from: \[https://www3.epa.gov/ttnchie1/efpac/ghg/GHG_Biogenic_Report_draft_Dec1410.pdf\]\(https://www3.epa.gov/ttnchie1/efpac/ghg/GHG_Biogenic_Report_draft_Dec1410.pdf\) \(Accessed 11](#)
186 [March 2020a\), 2010a.](#)

187 [USEPA: Office of Atmospheric Programs \(6207J\), Methane and Nitrous Oxide Emissions From Natural Sources, U.S.](#)
188 [Environmental Protection Agency, EPA 430-R-10-001. Available online at <http://nepis.epa.gov/>, Washington, DC](#)
189 [20460., 2010b.](#)

190 [USEPA: Draft: Global Anthropogenic Non-CO₂ Greenhouse Gas Emissions: 1990-2030. EPA 430-R-03-002, United](#)
191 [States Environmental Protection Agency, Washington D.C., 2011.](#)

192 [USEPA: Global Anthropogenic Non-CO₂ Greenhouse Gas Emissions 1990-2030, EPA 430-R-12-006, US Environmental](#)
193 [Protection Agency, Washington DC., 2012.](#)

194 [USEPA: Draft Inventory of U.S. Greenhouse gas Emissions and Sinks: 1990-2014. EPA 430-R-16-002. February 2016.](#)
195 [U.S. Environmental protection Agency, Washington, DC, USA., 2016.](#)

196 [USEPA: Global Non-CO₂ Greenhouse Gas Emission Projections & Mitigation Potential: 2015-2050, EPA-430-R-19-010,](#)
197 [U.S. Environmental protection Agency, Washington, DC, USA., 2019](#)

198 [Valentine, D. W., Holland, E. A. and Schimel, D. S.: Ecosystem and physiological controls over methane production in](#)
199 [northern wetlands. J. Geophys. Res., 99\(D1\), 1563–1571, 1994.](#)

200 [Vardag, S. N., Hammer, S., O’Doherty, S., Spain, T. G., Wastine, B., Jordan, A. and Levin, I.: Comparisons of continuous](#)
201 [atmospheric CH₄, CO₂ and N₂O measurements – results from a travelling instrument campaign at Mace Head,](#)
202 [Atmospheric Chem. Phys., 14\(16\), 8403–8418, doi:10.5194/acp-14-8403-2014, 2014.](#)

203 [VODCA2GPP – a new, global, long-term \(1988–2020\) gross primary production dataset from microwave remote sensing,](#)
204 [Earth Syst. Sci. Data, 14, 1063–1085, <https://doi.org/10.5194/essd-14-1063-2022>, 2022.](#)

205 [Voulgarakis, A., Naik, V., Lamarque, J. F., Shindell, D. T., Young, P. J., Prather, M. J., Wild, O., Field, R. D., Bergmann,](#)
206 [D., Cameron-Smith, P., Cionni, I., Collins, W. J., Dalsøren, S. B., Doherty, R. M., Eyring, V., Faluvegi, G., Folberth,](#)
207 [G. A., Horowitz, L. W., Josse, B., MacKenzie, I. A., Nagashima, T., Plummer, D. A., Righi, M., Rumbold, S. T.,](#)
208 [Stevenson, D. S., Strode, S. A., Sudo, K., Szopa, S. and Zeng, G.: Analysis of present day and future OH and methane](#)

lifetime in the ACCMIP simulations. *Atmospheric Chem. Phys.*, 13(5), 2563–2587, doi:10.5194/acp-13-2563-2013, 2013.

Voulgarakis, A., Marlier, M. E., Faluvegi, G., Shindell, D. T., Tsigaridis, K. and Mangeon, S.: Interannual variability of tropospheric trace gases and aerosols: The role of biomass burning emissions, *J. Geophys. Res. Atmospheres*, 120(14), 7157–7173, doi:10.1002/2014jd022926, 2015.

Wallmann, K., Pinero, E., Burwicz, E., Haeckel, M., Hensen, C., Dale, A. and Ruepke, L.: The Global Inventory of Methane Hydrate in Marine Sediments: A Theoretical Approach, *Energies*, 5(7), 2449, 2012.

Walter Anthony, K.M., Anthony, P., Grosse, G. and Chanton, J.: Geologic methane seeps along boundaries of Arctic permafrost thaw and melting glaciers. *Nature Geoscience*, 5(6), pp.419-426., DOI: 10.1038/ngeo1480, 2012

Wang, F., Maksyutov, S., Tsuruta, A., Janardanan, R., Ito, A., Sasakawa, M., Machida, T., Morino, I., Yoshida, Y., Kaiser, J. W., Janssens-Maenhout, G., Dlugokencky, E. J., Mammarella, I., Lavric, J. V. and Matsunaga, T.: Methane Emission Estimates by the Global High-Resolution Inverse Model Using National Inventories, *Remote Sens.*, 11(21), 2489, doi:10.3390/rs11212489, 2019a.

Wang, G., X. Xia, S. Liu, L. Zhang, S. Zhang, J. Wang, N. Xi, and Q. Zhang. Intense methane ebullition from urban inland waters and its significant contribution to greenhouse gas emissions. *Water Research*, 189: p. 116654, 2021a

Wang, X., Jacob, D. J., Eastham, S. D., Sulprizio, M. P., Zhu, L., Chen, Q., Alexander, B., Sherwen, T., Evans, M. J., Lee, B. H., Haskins, J. D., Lopez-Hilfiker, F. D., Thornton, J. A., Huey, G. L. and Liao, H.: The role of chlorine in global tropospheric chemistry, *Atmospheric Chem. Phys.*, 19(6), 3981–4003, doi:10.5194/acp-19-3981-2019, 2019b.

Wang, X., Jacob, D. J., Downs, W., Zhai, S., Zhu, L., Shah, V., Holmes, C. D., Sherwen, T., Alexander, B., Evans, M. J., Eastham, S. D., Neuman, J. A., Veres, P. R., Koenig, T. K., Volkamer, R., Huey, L. G., Bannan, T. J., Percival, C. J., Lee, B. H., and Thornton, J. A.: Global tropospheric halogen (Cl, Br, I) chemistry and its impact on oxidants, *Atmos. Chem. Phys.*, 21, 13973–13996, <https://doi.org/10.5194/acp-21-13973-2021>, 2021b.

Wang, Z., Deutscher, N. M., Warneke, T., Notholt, J., Dils, B., Griffith, D. W. T., Schmidt, M., Ramonet, M. and Gerbig, C.: Retrieval of tropospheric column-averaged CH₄ mole fraction by solar absorption FTIR-spectrometry using N₂O as a proxy, *Atmospheric Meas. Tech.*, 7(10), 3295–3305, doi:10.5194/amt-7-3295-2014, 2014.

Wang, Z.-P., Gu, Q., Deng, F.-D., Huang, J.-H., Megonigal, J. P., Yu, Q., Lü, X.-T., Li, L.-H., Chang, S., Zhang, Y.-H., Feng, J.-C. and Han, X.-G.: Methane emissions from the trunks of living trees on upland soils, *New Phytol.*, 211(2), 429–439, doi:10.1111/nph.13909, 2016.

Wania, R., I. Ross and I. C. Prentice: Implementation and evaluation of a new methane model within a dynamic global vegetation model: LPJ-WHyMe v1.3, *Geosci. Model Dev. Discuss.*, 3, 1–59, 2010.

Wania, R., Melton, J. R., Hodson, E. L., Poulter, B., Ringeval, B., Spahni, R., Bohn, T., Avis, C. A., Chen, G., Eliseev, A. V., Hopcroft, P. O., Riley, W. J., Subin, Z. M., Tian, H., van Bodegom, P. M., Kleinen, T., Yu, Z. C., Singarayer, J. S., Zurcher, S., Lettenmaier, D. P., Beerling, D. J., Denisov, S. N., Prigent, C., Papa, F. and Kaplan, J. O.: Present state

2242 [of global wetland extent and wetland methane modelling: Methodology of a model inter-comparison project](#)
2243 [\(WETCHIMP\), *Geosci. Model Dev.*, 6\(3\), 617–641, 2013.](#)

2244 [Wassmann, R., Lantin, R. S., Neue, H. U., Buendia, L. V., Corton, T. M. and Lu, Y.: Characterization of methane emissions](#)
2245 [in Asia III: Mitigation options and future research needs, *Nutr. Cycl. Agroecosystems*, 58, 23–36, 2000.](#)

2246 [Weber, T., Wiseman, N. A. and Kock, A.: Global ocean methane emissions dominated by shallow coastal waters, *Nat.*](#)
2247 [Comm., 10\(1\), 1–10, doi:10.1038/s41467-019-12541-7, 2019.](#)

2248 [Wells, N. S., J. J. Chen, D. T. Maher, P. Huang, D. V. Erler, M. Hipsey, and B. D. Eyre: Changing sediment and surface](#)
2249 [water processes increase CH₄ emissions from human-impacted estuaries, *Geochim. Cosmochim. Acta* **280**: 130–147,](#)
2250 [doi:10.1016/j.gca.2020.04.020, 2020](#)

2251 [van der Werf, G. R., Randerson, J. T., Giglio, L., Collatz, G. J., Mu, M., Kasibhatla, P. S., Morton, D. C., DeFries, R. S.,](#)
2252 [Jin, Y. and van Leeuwen, T. T.: Global fire emissions and the contribution of deforestation, savanna, forest,](#)
2253 [agricultural, and peat fires \(1997–2009\), *Atmospheric Chem. Phys.*, 10\(23\), 11,707–11,735, 2010.](#)

2254 [van der Werf, G. R., Randerson, J. T., Giglio, L., Leeuwen, T. T. van, Chen, Y., Rogers, B. M., Mu, M., Marle, M. J. E.](#)
2255 [van, Morton, D. C., Collatz, G. J., Yokelson, R. J. and Kasibhatla, P. S.: Global fire emissions estimates during 1997–](#)
2256 [2016, *Earth Syst. Sci. Data*, 9\(2\), 697–720, doi:10.5194/essd-9-697-2017, 2017.](#)

2257 [Whalen, S. C.: Biogeochemistry of Methane Exchange between Natural Wetlands and the Atmosphere, *Environ. Eng.*](#)
2258 [Sci., 22\(1\), 73–94, doi:10.1089/ees.2005.22.73, 2005.](#)

2259 [Wiedinmyer, C., Kimura, Y., McDonald-Buller, E. C., Emmons, L. K., Buchholz, R. R., Tang, W., Seto, K., Joseph, M.](#)
2260 [B., Barsanti, K. C., Carlton, A. G., and Yokelson, R.: The Fire Inventory from NCAR version 2.5: an updated global](#)
2261 [fire emissions model for climate and chemistry applications, *EGUsphere* \[preprint\], \[https://doi.org/10.5194/egusphere-\]\(https://doi.org/10.5194/egusphere-2023-124\)](#)
2262 [2023-124, 2023.](#)

2263 [Wik, M., Thornton, B. F., Bastviken, D., Uhlbäck, J. and Crill, P. M.: Biased sampling of methane release from northern](#)
2264 [lakes: A problem for extrapolation, *Geophys. Res. Lett.*, 43\(3\), 1256–1262, doi:10.1002/2015gl066501, 2016a.](#)

2265 [Wik, M., Varner, R. K., Anthony, K. W., MacIntyre, S. and Bastviken, D.: Climate-sensitive northern lakes and ponds are](#)
2266 [critical components of methane release, *Nat. Geosci.*, 9\(2\), 99–105, doi:10.1038/ngeo2578, 2016b.](#)

2267 [Wild, B., Teubner, I., Moesinger, L., Zotta, R.-M., Forkel, M., van der Schalie, R., Sitch, S., and Dorigo, W.:](#)
2268 [VODCA2GPP – a new, global, long-term \(1988–2020\) gross primary production dataset from microwave remote](#)
2269 [sensing, *Earth Syst. Sci. Data*, 14, 1063–1085, <https://doi.org/10.5194/essd-14-1063-2022>, 2022.](#)

2270 [Winderlich, J., Chen, H., Gerbig, C., Seifert, T., Kolle, O., Lavrič, J. V., Kaiser, C., Höfer, A. and Heimann, M.:](#)
2271 [Continuous low-maintenance CO₂/CH₄/H₂O measurements at the Zotino Tall Tower Observatory \(ZOTTO\) in Central](#)
2272 [Siberia, *Atmospheric Meas. Tech.*, 3\(4\), 1113–1128, doi:10.5194/amt-3-1113-2010, 2010.](#)

2273 [Wilson, C., Chipperfield, M. P., Gloor, M., Parker, R. J., Boesch, H., McNorton, J., Gatti, L. V., Miller, J. B., Basso, L.](#)
2274 [S., and Monks, S. A.: Large and increasing methane emissions from eastern Amazonia derived from satellite data,](#)

275 [2010–2018, Atmos. Chem. Phys., 21, 10643–10669, https://doi.org/10.5194/acp-21-10643-2021, 2021.](https://doi.org/10.5194/acp-21-10643-2021)

276 [Wood, T.G. and Sands, W.A. The role of termites in ecosystems. In: Brian, M.V. \(Ed.\), Production Ecology of Ants and](#)

277 [Termites. Cambridge University Press, Cambridge, UK, 245–292, 1978.](#)

278 [Woodward G, Perkins D.M., and Brown L. E.: Climate change and freshwater ecosystems: impacts across multiple levels](#)

279 [of organization, Philos Trans R Soc Lond B Biol Sci. 365\(1549\), 2093-106, doi: 10.1098/rstb.2010.0055, 2010](#)

280 [Woodward, G., Gessner, M. O., Giller, P. S., Gulis, V., Hladyz, S., Lecerf, A., Malmqvist, B., McKie, B. G., Tiegs, S. D.,](#)

281 [Cariss, H., Dobson, M., Elozegi, A., Ferreira, V., Graça, M. A. S., Fleituch, T., Lacoursière, J. O., Nistorescu, M.,](#)

282 [Poza, J., Risnoveanu, G., Schindler, M., Vadineanu, A., Vought, L. B.-M. and Chauvet, E.: Continental-Scale Effects](#)

283 [of Nutrient Pollution on Stream Ecosystem Functioning. Science, 336\(6087\), 1438–1440,](#)

284 [doi:10.1126/science.1219534, 2012.](#)

285 [Woolway RI, Jones ID, Maberly SC, French JR, Livingstone DM, Monteith DT, et al.: Diel Surface Temperature Range](#)

286 [Scales with Lake Size, PLoS ONE 11\(3\): e0152466, doi:10.1371/journal.pone.0152466, 2016](#)

287 [Worden, J. R., Bloom, A. A., Pandey, S., Jiang, Z., Worden, H. M., Walker, T. W., Houweling, S. and Röckmann, T.:](#)

288 [Reduced biomass burning emissions reconcile conflicting estimates of the post-2006 atmospheric methane budget,](#)

289 [Nat. Commun., 8\(1\), 2227, doi:10.1038/s41467-017-02246-0, 2017.](#)

290 [Wu, Z., Li, J., Sun, Y. et al. : Imbalance of global nutrient cycles exacerbated by the greater retention of phosphorus over](#)

291 [nitrogen in lakes. Nat. Geosci. 15, 464–468, https://doi.org/10.1038/s41561-022-00958-7, 2022](#)

292 [Wuebbles, D. J. and Hayhoe, K.: Atmospheric methane and global change, Earth-Sci. Rev., 57\(3–4\), 177–210, 2002.](#)

293 [Wunch, D., Toon, G. C., Blavier, J.-F. L., Washenfelder, R. A., Notholt, J., Connor, B. J., Griffith, D. W. T., Sherlock, V.,](#)

294 [and Wennberg, P. O.: The Total Carbon Column Observing Network, Philos. Trans. R. Soc. A, 369\(1943\),](#)

295 [doi:10.1098/rsta.2010.0240, 2011.](#)

296 [Wunch, D., Toon, G. C., Hedelius, J. K., Vizenor, N., Roehl, C. M., Saad, K. M., Blavier, J.-F. L., Blake, D. R. and](#)

297 [Wennberg, P. O.: Quantifying the loss of processed natural gas within California’s South Coast Air Basin using long-](#)

298 [term measurements of ethane and methane, Atmospheric Chem. Phys., 16\(22\), 14091–14105, doi:10.5194/acp-16-](#)

299 [14091-2016, 2016.](#)

300 [Wunch, D., Jones, D. B. A., Toon, G. C., Deutscher, N. M., Hase, F., Notholt, J., Sussmann, R., Warneke, T., Kuenen, J.,](#)

301 [Denier van der Gon, H., Fisher, J. A. and Maasakkers, J. D.: Emissions of methane in Europe inferred by total column](#)

302 [measurements, Atmos Chem Phys, 19\(6\), 3963–3980, doi:10.5194/acp-19-3963-2019, 2019.](#)

303 [Xiao, K., F. Beulig, H. Røy, B. B. Jørgensen, and N. Risgaard-Petersen: Methylophilic methanogenesis fuels cryptic](#)

304 [methane cycling in marine surface sediment. Limnol. Oceanogr. 63: 1519–1527. doi:10.1002/lno.10788, 2018](#)

305 [Xu, X. F., Tian, H. Q., Zhang, C., Liu, M. L., Ren, W., Chen, G. S., Lu, C. Q. and Bruhwiler, L.: Attribution of spatial and](#)

306 [temporal variations in terrestrial methane flux over North America, Biogeosciences, 7\(11\), 3637–3655,](#)

307 [doi:10.5194/bg-7-3637-2010, 2010.](#)

308 [Xu, X., P Sharma, S Shu, TZ Lin, P Ciaï, F Tubiello, P Smith, N Campbell and AK Jain \(2021\), Global Greenhouse Gas](#)
309 [Emissions from Plant- and Animal-Based Food, Nature Food, <https://doi.org/10.1038/s43016-021-00358-x>, 2021](#)

310 [Yacovitch, T. I., C. Daube, S. C. Herndon, and J. B. McManus: Isotopes on a Boat: Real-Time Spectroscopic Measurement](#)
311 [of Methane Isotopologues from Offshore Oil and Gas Emissions, OSA Optical Sensors and Sensing Congress 2021](#)
312 [\(AIS, FTS, HISE, SENSORS, ES\), S. Buckley, F. Vanier, S. Shi, K. Walker, I. Coddington, S. Paine, K. Lok Chan,](#)
313 [W. Moses, S. Qian, P. Pellegrino, F. Vollmer, G. , J. Jágerská, R. Menzies, L. Emmenegger, and J. Westberg, eds.,](#)
314 [OSA Technical Digest \(Optica Publishing Group, 2021\), paper EW5D.3, 2021](#)

315 [Yan, X., Akiyama, H., Yagi, K. and Akimoto, H.: Global estimations of the inventory and mitigation potential of methane](#)
316 [emissions from rice cultivation conducted using the 2006 Intergovernmental Panel on Climate Change Guidelines,](#)
317 [Glob. Biogeochem. Cycles, 23\(2\), doi:10.1029/2008gb003299, 2009.](#)

318 [Yang, P., D. Y. F. Lai, H. Yang, and others: Large increase in CH4 emission following conversion of coastal marsh to](#)
319 [aquaculture ponds caused by changing gas transport pathways. Water Res. 222: 118882,](#)
320 [doi:10.1016/j.watres.2022.118882, 2022](#)

321 [Yin, Y., Chevallier, F., Ciaï, P., Broquet, G., Fortems-Cheiney, A., Pison, I. and Saunois, M.: Decadal trends in global](#)
322 [CO emissions as seen by MOPITT, Atmospheric Chem. Phys., 15\(23\), 13433–13451, doi:10.5194/acp-15-13433-](#)
323 [2015, 2015.](#)

324 [Yoshida, Y., Kikuchi, N., Morino, I., Uchino, O., Oshchepkov, S., Bril, A., Saeki, T., Schutgens, N., Toon, G. C., Wunch,](#)
325 [D., Roehl, C. M., Wennberg, P. O., Griffith, D. W. T., Deutscher, N. M., Warneke, T., Notholt, J., Robinson, J.,](#)
326 [Sherlock, V., Connor, B., Rettinger, M., Sussmann, R., Ahonen, P., Heikkinen, P., Kyrö, E., Mendonca, J., Strong, K.,](#)
327 [Hase, F., Dohe, S. and Yokota, T.: Improvement of the retrieval algorithm for GOSAT SWIR XCO₂ and XCH₄ and](#)
328 [their validation using TCCON data, Atmospheric Meas. Tech., 6\(6\), 1533–1547, doi:10.5194/amt-6-1533-2013, 2013.](#)

329 [Yuan, J., J. Xiang, D. Liu, and others: Rapid growth in greenhouse gas emissions from the adoption of industrial-scale](#)
330 [aquaculture. Nat. Clim. Chang. 9: 318–322, doi:10.1038/s41558-019-0425-9, 2019](#)

331 [Yver Kwok, C. E., Müller, D., Caldow, C., Lebégue, B., Mønster, J. G., Rella, C. W., Scheutz, C., Schmidt, M., Ramonet,](#)
332 [M., Warneke, T., Broquet, G. and Ciaï, P.: Methane emission estimates using chamber and tracer release experiments](#)
333 [for a municipal waste water treatment plant, Atmospheric Meas. Tech., 8\(7\), 2853–2867, doi:10.5194/amt-8-2853-](#)
334 [2015, 2015.](#)

335 [Zavala-Araiza, D., Lyon, D. R., Alvarez, R. A., Davis, K. J., Harriss, R., Herndon, S. C., Karion, A., Kort, E. A., Lamb,](#)
336 [B. K., Lan, X., Marchese, A. J., Pacala, S. W., Robinson, A. L., Shepson, P. B., Sweeney, C., Talbot, R., Townsend-](#)
337 [Small, A., Yacovitch, T. I., Zimmerle, D. J. and Hamburg, S. P.: Reconciling divergent estimates of oil and gas methane](#)
338 [emissions, Proc. Natl. Acad. Sci. USA, 112, 15597–15602, doi:10.1073/pnas.1522126112, 2015.](#)

339 [Zhang: Magnitude, spatio-temporal variability and environmental controls of methane emissions from global rice fields:](#)
340 [Implications for water management and climate mitigation, Glob. Change Biol., 2016.](#)

341 [Zhang, B. and Chen, G. Q.: China's CH₄ and CO₂ Emissions: Bottom-Up Estimation and Comparative Analysis, *Ecol*](#)
342 [Indic., 47, 112–122, doi:10.1016/j.ecolind.2014.01.022, 2014.](#)

343 [Zhang, L., X. Xia, S. Liu, S. Zhang, S. Li, J. Wang, G. Wang, H. Gao, Z. Zhang, Q. Wang, W. Wen, R. Liu, Z. Yang, E.H.](#)
344 [Stanley, and P.A. Raymond: Significant methane ebullition from alpine permafrost rivers on the East Qinghai–Tibet](#)
345 [Plateau. *Nature Geoscience*, 13\(5\): p. 349-354, 2020](#)

346 [Zhang, L., H. Tian, H. Shi, S. Pan, J. Chang, S. R. S. Dangal, X. Qin, S. Wang, F. N. Tubiello, J. G. Canadell, R. B.](#)
347 [Jackson: A 130-year global inventory of methane emissions from livestock: Trends, patterns, and drivers, *Global*](#)
348 [Change Biology, 28 \(17\), 5142-5158. <https://doi.org/10.1111/gcb.16280>, 2022](#)

349 [Zhang, Y., Xiao, X., Wu, X., Zhou, S., Zhang, G., Qin, Y., and Dong, J.: A global moderate resolution dataset of gross](#)
350 [primary production of vegetation for 2000–2016, *Sci. Data*, 4, 1–13, <https://doi.org/10.1038/sdata.2017.165>, 2017.](#)

351 [Zhang, Y., Jacob, D. J., Maasakkers, J. D., Sulprizio, M. P., Sheng, J.-X., Gautam, R., and Worden, J.: Monitoring global](#)
352 [tropospheric OH concentrations using satellite observations of atmospheric methane, *Atmos. Chem. Phys.*, 18, 15959–](#)
353 [15973, <https://doi.org/10.5194/acp-18-15959-2018>, 2018.](#)

354 [Zhang, Z., Zimmermann, N. E., Kaplan, J. O. and Poulter, B.: Modeling spatiotemporal dynamics of global wetlands:](#)
355 [comprehensive evaluation of a new sub-grid TOPMODEL parameterization and uncertainties, *Biogeosciences*, 13\(5\),](#)
356 [1387–1408, doi:10.5194/bg-13-1387-2016, 2016.](#)

357 [Zhang, Z., Fluet-Chouinard, E., Jensen, K., McDonald, K., Hugelius, G., Gumbrecht, T., et al. Development of the global](#)
358 [dataset of Wetland Area and Dynamics for Methane Modeling \(WAD2M\), *Earth System Science Data*, 13\(5\), 2001–](#)
359 [2023. <https://doi.org/10.5194/essd-13-2001-2021>, 2021.](#)

360 [Zhang, Z., Poulter, B., Feldman, A.F., Ying, Q. Ciais, P., Peng, S. and Li, X.: Recent intensification of wetland methane](#)
361 [feedback, *Nat. Clim. Chang*, 13, 430–433, <https://doi.org/10.1038/s41558-023-01629-0>, 2023](#)

362 [Zhang, Z., Poulter, B., Melton, J., Riley, W., Allen, G., Beerling D., Bousquet P., Canadell, J., Fluet-Chouinard E., Ciais,](#)
363 [P., Gedney, N., Hopcroft, P., Ito, A., Jackson, R., Jain, A., Jensen, K., Joos, F., Kleinen, T., Knox, S., Li, T., Li, X.,](#)
364 [Liu, X., McDonald, K., McNicol, G., Miller, P., Müller, J., Patra, P., Prigent, C., Peng, C., Peng, S., Qin, Z., Riggs,](#)
365 [R., Saunois, M., Sun Q., Tian, H., Xu, X., Yao Y., Yi, X., Zhang, W., Zhu, Q., Zhu, Q., and Zhuang, Q.: Ensemble](#)
366 [estimates of global wetland methane emissions over 2000-2020. *Global Change Biology*, in review.](#)

367 [Zhao, J., M. Zhang, W. Xiao, L. Jia, X. Zhang, J. Wang, Z. Zhang, Y. Xie, Y. Pu, S. Liu, Z. Feng, and X. Lee: Large](#)
368 [methane emission from freshwater aquaculture ponds revealed by long-term eddy covariance observation. *Agricultural*](#)
369 [and Forest Meteorology, 308-309: p. 108600, 2021](#)

370 [Zhao, Y., Saunois, M., Bousquet, P., Lin, X., Berchet, A., Hegglin, M. I., Canadell, J. G., Jackson, R. B., Hauglustaine,](#)
371 [D. A., Szopa, S., Stavert, A. R., Abraham, N. L., Archibald, A. T., Bekki, S., Deushi, M., Jöckel, P., Josse, B., Kinnison,](#)
372 [D., Kirner, O., Maréchal, V., O'Connor, F. M., Plummer, D. A., Revell, L. E., Rozanov, E., Stenke, A., Strode, S.,](#)
373 [Tilmes, S., Dlugokencky, E. J. and Zheng, B.: Inter-model comparison of global hydroxyl radical \(OH\) distributions](#)

374 [and their impact on atmospheric methane over the 2000–2016 period, *Atmospheric Chem. Phys.*, 19\(21\), 13701–](#)
375 [13723, doi:10.5194/acp-19-13701-2019, 2019.](#)

376 [Zhao, Y., Saunio, M., Bousquet, P., Lin, X., Berchet, A., Hegglin, M. I., Canadell, J. G., Jackson, R. B., Dlugokencky,](#)
377 [E. J., Langenfelds, R. L., Ramonet, M., Worthy, D. and Zheng, B.: Influences of hydroxyl radicals \(OH\) on top-down](#)
378 [estimates of the global and regional methane budgets, *Atmospheric Chem. Phys. Discuss.*, 1–45, doi:10.5194/acp-](#)
379 [2019-1208, 2020.](#)

380 [Zhao, Y., Saunio, M., Bousquet, P., Lin, X., Hegglin, M. I., Canadell, J. G., Jackson, R. B., and Zheng, B.: Reconciling](#)
381 [the bottom-up and top-down estimates of the methane chemical sink using multiple observations, *Atmos. Chem. Phys.*,](#)
382 [23, 789–807, <https://doi.org/10.5194/acp-23-789-2023>, 2023.](#)

383 [Zheng, B., Chevallier, F., Ciais, P., Yin, Y. and Wang, Y.: On the Role of the Flaming to Smoldering Transition in the](#)
384 [Seasonal Cycle of African Fire Emissions, *Geophys. Res. Lett.*, 45\(21\), 11,998-12,007, doi:10.1029/2018GL079092,](#)
385 [2018a.](#)

386 [Zheng, B., Chevallier, F., Ciais, P., Yin, Y., Deeter, M. N., Worden, H. M., Wang, Y., Zhang, Q. and He, K.: Rapid decline](#)
387 [in carbon monoxide emissions and export from East Asia between years 2005 and 2016, *Environ. Res. Lett.*, 13\(4\),](#)
388 [044007, doi:10.1088/1748-9326/aab2b3, 2018b.](#)

389 [Zheng, B., Chevallier, F., Yin, Y., Ciais, P., Fortems-Cheiney, A., Deeter, M. N., Parker, R. J., Wang, Y., Worden, H. M.,](#)
390 [and Zhao, Y.: Global atmospheric carbon monoxide budget 2000–2017 inferred from multi-species atmospheric](#)
391 [inversions, *Earth Syst. Sci. Data*, 11, 1411–1436, doi: 10.5194/essd-11-1411-2019, 2019.](#)

392 [Zheng, B., Ciais, P., Chevallier, F., Yang, H., Canadell, J. G., Chen, Y., van der Velde, I. R., Aben, I., Chuvieco, E., Davis,](#)
393 [S. J., Deeter, M., Hong, C., Kong, Y., Li, H., Li, H., Lin, X., He, K., and Zhang, Q.: Record-high CO₂ emissions from](#)
394 [boreal fires in 2021, *Science*, 379, 912-917,doi: 10.1126/science.ade0805, 2023.](#)

395 [Zhu, Q., Liu, J., Peng, C., Chen, H., Fang, X., Jiang, H., Yang, G., Zhu, D., Wang, W. and Zhou, X.: Modelling methane](#)
396 [emissions from natural wetlands by development and application of the TRIPLEX-GHG model, *Geosci. Model Dev.*,](#)
397 [7\(3\), 981–999, doi:10.5194/gmd-7-981-2014, 2014.](#)

398 [Zhu, Q., Peng, C., Chen, H., Fang, X., Liu, J., Jiang, H., Yang, Y. and Yang, G.: Estimating global natural wetland methane](#)
399 [emissions using process modelling: spatio-temporal patterns and contributions to atmospheric methane fluctuations,](#)
400 [Gloab. Ecol. Biogeogr., 24, 959–972, 2015.](#)

401 [Zhu, Y., K.J. Purdy, Ö. Eyice, L. Shen, S.F. Harpenslager, G. Yvon-Durocher, A.J. Dumbrell, and M. Trimmer:](#)
402 [Disproportionate increase in freshwater methane emissions induced by experimental warming. *Nature Climate Change*,](#)
403 [10\(7\): p. 685-690., 2020](#)

404 [Zhuang, Q., Melillo, J. M., Kicklighter, D. W., Prinn, R. G., McGuire, A. D., Steudler, P. A., Felzer, B. S. and Hu, S.:](#)
405 [Methane fluxes between terrestrial ecosystems and the atmosphere at northern high latitudes during the past century:](#)
406 [A retrospective analysis with a process-based biogeochemistry model, *Glob. Biogeochem Cycles*, 18\(3\), GB3010,](#)

7407 [doi:10.1029/2004gb002239](https://doi.org/10.1029/2004gb002239), 2004.

7408 [Zhuang, Q., Chen, M., Xu, K., Tang, J., Saikawa, E., Lu, Y., Melillo, J. M., Prinn, R. G. and McGuire, A. D.: Response](#)

7409 [of global soil consumption of atmospheric methane to changes in atmospheric climate and nitrogen deposition, *Glob.*](#)

7410 [Biogeochem. Cycles, 27\(3\), 650–663, doi:10.1002/gbc.20057, 2013.](#)

7411 [Zhuang, Q., M. Guo, J.M. Melack, X. Lan, Z. Tan, Y. Oh, and L.R. Leung: Current and Future Global Lake Methane](#)

7412 [Emissions: A Process-Based Modeling Analysis. *Journal of Geophysical Research: Biogeosciences*, 128\(3\): p.](#)

7413 [e2022JG007137, 2023](#)

Table 1: Bottom-up (BU) models and inventories for anthropogenic and biomass burning used in this study. *Due to its limited sectoral breakdown this dataset was not used in Table 3.

B-U models and inventories	Contribution	Time period (resolution)	Gridded	References
CEDS (country based)	Fossil fuels, Agriculture and waste, Biofuel	1970-2019 (yearly)	no	Hoesly et al. (2018)
CEDS (gridded)*	Fossil fuels, Agriculture and waste, Biofuel	1970-2020 (monthly)	0.5x0.5°	Hoesly et al. (2018) O'Rourke et al. (2021)
EDGARv6	Fossil fuels, Agriculture and waste, Biofuel	1990-2018^ (yearly, monthly for some sectors)	0.1x0.1°	Oreggioni et al. (2021), Crippa et al. (2021)
EDGARv7	Fossil fuels, Agriculture and waste, Biofuel	1990-2021 (yearly)	0.1x0.1°	Crippa et al. (2023)
IIASA GAINS v4.0	Fossil fuels, Agriculture and waste, Biofuel	1990-2020 (yearly)	0.5x0.5°	Höglund-Isaksson et al. (2020)
USEPA	Fossil fuels, Agriculture and waste, Biofuel, Biomass Burning	1990-2030 (10-yr interval, interpolated to yearly)	no	USEPA (2019)
FAO-CH4	Agriculture, Biomass Burning	1961-2020 (Yearly)	no	Federici et al. (2015); Tubiello et al. (2013); Tubiello (2019)
FINNv2.5	Biomass burning	2002-2020 (daily)	1km resolution	Wiedinmyer et al. (2023)
GFASv1.3	Biomass burning	2003-2020 (daily)	0.1x0.1°	Kaiser et al. (2012)
GFEDv4.1s	Biomass burning	1997-2020 (monthly)	0.25x0.25°	Giglio et al. (2013); van der Werf et al. (2017)
QFEDv2.5	Biomass burning	2000-2020 (daily)	0.1x0.1°	Darmenov and da Silva (2015)

- Mis en forme : Anglais (G.B.)
- Supprimé: inventories
- Mis en forme : Forcer une largeur de colonne identique
- Supprimé: B-U
- Mis en forme : Anglais (G.B.)
- Mis en forme : Anglais (G.B.)
- Supprimé: sectorial
- Supprimé: ^Extended to 2017 for this study as described in Section 3.1.1.
- Tableau mis en forme
- Supprimé: 2015^
- Supprimé: Hoesly et al. (2018)*
- Supprimé: Hoesly et al. (2018)* ... [122]
- Supprimé: 2014
- Mis en forme : Français
- Supprimé: 2012
- Supprimé: Janssens-Maenhout et al. (2019)
- Supprimé: EDGARv4.2.3
- Mis en forme : Français
- Supprimé: 2015^
- Supprimé: Höglund-Isaksson (2012)
- Tableau mis en forme
- Supprimé: ECLIPSEv6
- Supprimé: (1990-2015 yearly, >2015 5-yr interval interpolated) [123]
- Supprimé: USEPA (2012)
- Supprimé: Federici et al. (2015); Tubiello et al. (2013); Tubiello (2019) [124]
- Supprimé: 2016^
- Supprimé: 2016
- Mis en forme : Français
- Supprimé: 2018
- Supprimé: FINNv1
- Supprimé: Wiedinmyer et al. (2011)
- Supprimé: 2016
- Supprimé: Kaiser et al. (2012)
- Supprimé: 2017
- Supprimé: Giglio et al. (2013)
- Mis en forme : Français
- Supprimé: 2017
- Supprimé: Darmenov and da Silva (2015)

Table 2: Biogeochemical models that computed wetland emissions used in this study. Model runs were performed with two climate inputs, CRU and GSWP3-W5E5. Models were run with prognostic (using their own calculation of wetland areas) and/or diagnostic (using WAD2M, (Zhang et al., 2021b)) wetland surface areas (see Sect 3.2.1).

Model	Institution	Prognostic		Diagnostic		References
		CRU	GSWP3-W5E5	CRU	GSWP3-W5E5	
CH4MOD_{wetland}	Institute of Atmospheric Physics, CAS	n	n	y	y	Li et al. (2010)
CLASSIC	Environment and Climate Change Canada	y	y*	y	y*	Arora et al. (2018); Melton and Arora (2016)
DLEM	Boston College	y	y	y	y	Tian et al. (2015, 2023)
ELM-ECA	Lawrence Berkeley National Laboratory	y	y	y	y	Riley et al. (2011)
ISAM	University of Illinois, Urbana-Champaign	y	y	y	y	Shu et al. (2020) Xu et al. (2021)
JSBACH	MPI	y	y	y	y	Kleinen et al. (2020, 2021, 2023)
JULES	UKMO	y	y	y	y	Gedney et al. (2019)
LPI-GUESS	Lund University	n	n	y	y	McGuire et al. (2012)
LPI-MPI	MPI	y	y	y	y	Kleinen et al. (2012)
LPI-WSL	NASA GSFC	y	y	y	y	Zhang et al. (2016)
LPX-Bern	University of Bern	y	y	y	y	Spahni et al. (2011), Stocker et al. (2014)
ORCHIDEE	LSCE	y	y	y	y	Ringeval et al. (2011)

- Supprimé: Runs
- Supprimé: for the whole period 2000-2017. Models
- Supprimé:)
- Tableau mis en forme
- Mis en forme : Bordure : Haut: (Pas de bordure), Bas: (Pas de bordure), Gauche: (Pas de bordure), Droite: (Pas de bordure), Entre : (Pas de bordure)
- Supprimé: Arora et al. (2018); Melton and Arora (2016)
- Supprimé: CLASS-CTEM
- Cellules insérées
- Cellules insérées
- Tableau mis en forme
- Mis en forme : Anglais (G.B.)
- Supprimé: Auburn University
- Supprimé: n
- Supprimé: Tian et al. (2010, 2015)
- Supprimé: ... [125]
- Supprimé: Kleinen et al. (2019)
- Tableau mis en forme
- Supprimé: n
- Cellules insérées
- Cellules insérées
- Supprimé: Hayman et al. (2014)
- Supprimé: y
- Supprimé: McGuire et al. (2012)
- Mis en forme : Anglais (G.B.)
- Mis en forme : Anglais (G.B.)
- Supprimé:
- Mis en forme : Anglais (G.B.)
- Supprimé: n
- Mis en forme : Anglais (G.B.)
- Supprimé: Kleinen et al. (2012)
- Mis en forme : Anglais (G.B.)
- Mis en forme : Anglais (G.B.)
- Supprimé: Zhang et al. (2016)
- Supprimé: Spahni et al. (2011)
- Supprimé: Ringeval et al. (2011)

SDGVM	University of Birmingham/University of Sheffield	y	y	y	y	Beerling & Woodward (2001), Hopcroft et al. (2011, 2020)
TEM-MDM	Purdue University	n	y	y	y	Zhuang et al. (2004)
TRIPLEX _{GHG}	UQAM	n	y	y	y	Zhu et al. (2014, 2015)
VISIT	NIES	y	y	y	y	Ito and Inatomi (2012)

***CLASSIC uses GSWP3-W5E version 2 that covers the time period till 2016. All other models use GSWP-W5E5 version 3.**

- Supprimé: y
- Tableau mis en forme
- Cellules insérées
- Supprimé: Zhuang et al. (2004)
- Cellules insérées
- Supprimé: _
- Supprimé: y
- Supprimé: Zhu et al. (2014, 2015)
- Supprimé: Ito and Inatomi (2012)

Table 3: Global methane emissions by source type in Tg CH₄ yr⁻¹ from Saunois et al. (2020) (left column pair) and from this work using bottom-up and top-down approaches. Because top-down models cannot fully separate individual processes, only five categories of emissions are provided (see text). Uncertainties are reported as [min-max] range of reported studies. The mean, minimum and maximum values are calculated while discarding outliers, for each category of source and sink. As a result, discrepancies may occur when comparing the sum of categories and their corresponding total due to differences in outlier detections. Differences of 1 Tg CH₄ yr⁻¹ in the totals can also occur due to rounding errors. Compared to Saunois et al. (2020), emissions are split between “direct anthropogenic” emissions and “natural and indirect anthropogenic” sources. We also propose an estimate of the double-counting between bottom-up wetland and inland freshwater ecosystems emissions.

Period of time	Saunois et al. (2020)		2000-2009		This work			
	2000-2009		2000-2009		2010-2019		2020	
Approaches	bottom-up	top-down	bottom-up	top-down	bottom-up	top-down	bottom-up	top-down
NATURAL & indirect anthropogenic SOURCES								
Combined wetlands and inland freshwaters	306 [229-391]	180 [153-196]	242 [156-355]	158 [145-172]	248 [159-369]	165 [145-214]	251 [171-364]	175 [151-229]
Wetlands	147 [102-179]	180 [153-196]	153 [116-189]	158 [145-172]	159 [119-203]	165 [145-214]	161 [131-198]	175 [151-229]
Inland freshwaters ^a	159 [117-212]	▲	112 [49-202]	▲	112 [49-202]	▲	112 [49-202]	▲
Double counting ^b	NA	▲	-23 [-9-36]	▲	-23 [-9-36]	▲	-23 [-9-36]	▲
Other natural sources	63 [26-94]	35 [21-47]	63 [24-93]	44 [40-46]	63 [24-93]	43 [40-46]	63 [24-93]	44 [40-47]
Land sources	50 [17-72]	▲	51 [18-73]	▲	▲	▲	▲	▲
Geological (onshore)	38 [13-53]	▲	38 [13-53]	▲	▲	▲	▲	▲
Wild animals	2 [1-3]	▲	2 [1-3]	▲	▲	▲	▲	▲
Termites	9 [3-15]	▲	10 [4-16]	▲	▲	▲	▲	▲
Wildfires	(**)	▲	(**)	▲	▲	▲	▲	▲
Permafrost soils (direct)	1 [0-1]	▲	1 [0-1]	▲	▲	▲	▲	▲
Vegetation	(*)	▲	(*)	▲	▲	▲	▲	▲
Oceanic sources ^c	13 [9-22]	▲	12 [6-20]	▲	▲	▲	▲	▲
Biogenic	6 [4-10]	▲	5 [3-10]	▲	▲	▲	▲	▲
Geological (offshore)	7 [5-12]	▲	7 [5-12]	▲	▲	▲	▲	▲
TOTAL NATURAL & INDIRECT SOURCES	369 [245-485]	215 [176-243]	305 [180-448]	204 [189-223]	311 [183-462]	206 [188-225]	314 [195-457]	216 [193-241]
DIRECT ANTHROPOGENIC SOURCES								
Agriculture and waste	192 [178-206]	202 [198-219]	194 [181-208]	210 [197-223]	211 [195-231]	228 [213-242]	211 [204-216]	245 [232-259]
Agriculture	132 [INA]	▲	134 [125-142]	▲	143 [132-155]	▲	147 [143-149]	▲
Enteric ferm. & manure	104 [93-109]	▲	104 [100-110]	▲	112 [107-118]	▲	117 [114-124]	▲
Rice cultivation	28 [23-34]	▲	30 [24-34]	▲	32 [25-37]	▲	32 [29-37]	▲
Landfills and waste	60 [55-63]	▲	61 [52-71]	▲	69 [56-80]	▲	71 [60-84]	▲
Fossil fuels	110 [94-129]	101 [71-151]	105 [97-123]	105 [88-115]	120 [117-125]	115 [100-124]	128 [120-133]	122 [101-133]
Coal mining	32 [24-42]	▲	(****)	▲	(****)	▲	(****)	▲

- Supprimé: 2016...020) (left column pair) and for...rom this [126]
- Supprimé: 2016
- Tableau mis en forme ... [127]
- Supprimé: 2008-2017
- Supprimé: 2017
- Mis en forme ... [128]
- Tableau mis en forme ... [129]
- Déplacé (insertion) [5]
- Supprimé: 183%
- Supprimé: 147%
- Supprimé: 181%
- Supprimé: 145%
- Supprimé: 194%
- Supprimé: 166%
- Déplacé (insertion) [6]
- Mis en forme ... [135]
- Mis en forme ... [136]
- Mis en forme ... [141]
- Déplacé vers le haut [5]: 180%
- Mis en forme ... [139]
- Mis en forme ... [140]
- Supprimé: 149%
- Mis en forme ... [146]
- Mis en forme ... [147]
- Mis en forme ... [152]
- Mis en forme ... [153]
- Mis en forme ... [133]
- Mis en forme ... [130]
- Mis en forme ... [132]
- Mis en forme ... [143]
- Mis en forme ... [149]
- Mis en forme ... [138]
- Mis en forme ... [144]
- Mis en forme ... [150]
- Mis en forme ... [154]
- Supprimé: 199%
- Supprimé: 68%
- Supprimé: 222%
- Supprimé: 35%
- Supprimé: 222%
- Supprimé: 37%
- Supprimé: 222%
- Supprimé: 39%
- Mis en forme ... [157]
- Mis en forme ... [156]
- Mis en forme ... [158]
- Supprimé: 130
- Mis en forme ... [160]
- Mis en forme ... [162]
- Mis en forme ... [164]
- Mis en forme ... [166]
- Mis en forme ... [168]
- Mis en forme ... [170]
- Supprimé: Other land sources ... [171]

Oil & Gas Industry Transport	23 [60-85] 2 [0-6] 4 [1-11]		30 [26-32] 65 [63-71] 4 [1-8] 3 [1-8]		40 [37-44] 67 [57-74] 5 [1-9] 2 [1-3]		41 [38-43] 74 [67-80] 5 [1-8] 2 [1-3]	
Biomass & biof. burn.	31 [26-36]	29 [23-35]	30 [22-44]	26 [22-29]	28 [21-39]	27 [26-27]	27 [20-41]	26 [22-27]
Biomass burning	19 [15-22]		19 [14-29]		17 [12-24]		17 [13-27]	
TOTAL DIRECT ANTHROGENIC SOURCES	334 ^d [321-358]	332 [312-347]	333 ^d [305-365]	341 [319-355]	358 ^d [329-387]	369 [350-391]	372 ^d [345-409]	392 [368-409]
SINKS								
Total chemical loss	595 [489-749]	505 [459-516]	585 [481-716]	504 ^e [496-511]	602 [496-747]	521 ^e [485-532]	602 [496-747]	538 ^e [503-554]
Tropospheric OH	553 [476-677]		546 [446-663]		563 [462-663]		563 [462-663]	
Stratospheric loss	31 [12-37]		34 [10-51]		35 [10-51]		35 [10-51]	
Tropospheric Cl	11 [1-35]		6 [1-13]		6 [1-13]		6 [1-13]	
Soil uptake	30 [11-49]	34 [27-41]	30 [11-49]	34 [24-34]	31 [11-49]	35 [35-35]	31 [11-49]	36 [35-36]
TOTAL SINKS	625 [500-798]	540 [486-556]	615 [492-765]	538 [530-545]	633 [507-796]	554 [520-567]	633 [507-796]	575 [566-589]
SOURCES – SINKS IMBALANCE								
TOTAL SOURCES	703 [566-842]	547 ^e [524-560]	638 [485-813]	543 [526-558]	669 [512-849]	575 [553-586]	685 [540-865]	608 [581-627]
TOTAL SINKS	625 [500-798]	540 [486-556]	615 [492-765]	538 [530-545]	633 [507-796]	554 [520-567]	633 [507-796]	575 [566-589]
IMBALANCE	78	3 [-10-38]	23	5 [-4-13] ^e	36	21 [19-33] ^e	52	32 [15-38] ^e
ATMOSPHERIC GROWTH		5.8 [4.9-6.6] ^f		6.1 [5.2-6.9] ^f		20.9 [20.1-21.7] ^f		41.8 [40.7-42.9] ^f

(*) uncertain but likely small for upland forest and aerobic emissions, potentially large for forested wetland, but likely included elsewhere

(**) We stop reporting this value to avoid potential double counting with satellite-based products of biomass burning (see Sect. 3.1.5)

(***) Here the numbers are from prognostic runs. To ensure a fair comparison with previous budgets (Saunois et al., 2020), the numbers are 163 [117-195] for 2000-2009 from diagnostic runs with CRU/CRU-JRA-55 climate inputs (see Sect. 3.2.1).

(****) Up to 8 Tg of additional emissions could account for ultra emitters (Lauvaux et al., 2022), as in Tibrewal et al. (2024), that are fully or partly missed in regular anthropogenic inventories

a: Freshwater includes lakes, ponds, reservoirs, streams and rivers, part of it is due to anthropogenic disturbances estimated in Sect.3.2.2

b: The double counting estimate is discussed in Sect. 3.2.2

c: includes flux from hydrates considered at 0 for this study, includes estuaries

d: Total anthropogenic emissions are based on estimates of full anthropogenic inventory and not on the sum of "Agriculture and Waste", "Fossil fuels" and "Biofuel and biomass burning" categories (see Sect. 3.1.2)

e: Some inversions did not provide the chemical sink. These values are derived from a subset of the inversion ensemble.

f: Atmospheric growth rates are given in the same unit Tg CH₄ yr⁻¹, based on the conversion factor of 2.75 Tg CH₄ ppb⁻¹ given by Prather et al. (2012) and the atmospheric growth rates provided in the text in ppb yr⁻¹.

Supprimé: 76 [64...3 [60-85] ^d	... [243]
Déplacé vers le haut [11]: 110 ^e	
Supprimé: [24-42]	
Mis en forme	... [244]
Mis en forme	... [250]
Supprimé: 3	... [245]
Supprimé: 73 [60-85] ^f	... [251]
Supprimé: 11	
Mis en forme	... [249]
Supprimé: 13	
Mis en forme	... [248]
Mis en forme	... [246]
Mis en forme	... [247]
Supprimé: 12	
Mis en forme	... [255]
Mis en forme	... [253]
Mis en forme	... [252]
Mis en forme	... [254]
Supprimé: 30	
Mis en forme	... [256]
Supprimé: 34	
Mis en forme	... [258]
Supprimé: [16-53]	
Supprimé: 31 [26-46] ^f	... [260]
Mis en forme	... [262]
Supprimé: [23-35]	
Supprimé: 30 [26-40] ^f	... [265]
Supprimé: 30 [22-36]	
Supprimé: 29 [24-38] ^f	... [270]
Supprimé: 28 [25-32]	
Mis en forme	... [263]
Mis en forme	... [264]
Mis en forme	... [268]
Mis en forme	... [269]
Mis en forme	... [272]
Mis en forme	... [273]
Supprimé: 18...9 [15-20]	... [257]
Mis en forme	... [261]
Supprimé: 15-32	
Supprimé: 14-26] ^f	... [266]
Supprimé: [
Mis en forme	... [259]
Supprimé: 12 [9	
Mis en forme	... [267]
Mis en forme	... [271]
Supprimé: 338 ^f	... [274]
Supprimé: 319 ^f	... [277]
Supprimé: 334 ^f	... [279]
Supprimé: 332 ^f	... [281]
Supprimé: 366 ^f	... [282]
Supprimé: 359 ^f	... [284]
Supprimé: 380 ^f	... [285]
Supprimé: 364 ^f	... [287]
Mis en forme	... [275]

Table 4: Top-down studies used [here](#) with their contribution to the decadal and yearly estimates noted. For decadal means, top down studies must provide at least 8 years of data over the decade to contribute to the estimate. Details on each inverse system and inversions are provided in Table S8 to S11 in the Supplementary Material.

Model	Institution	Observation used	Time period	Number of inversions	2000-2009	2010-2019	2020	References
Carbon Tracker-Europe CH ₄	FMI	Surface stations	2000-2020	4	y	y	y	Suruta et al. (2017)
LMDz-CIE	LSCE/CEA	Surface stations	2000-2020	4	y	y	y	Thanwerdas et al. (2022a)
LMDz-PYVAR	LSCE/CEA/TUHU	GOSAT Leicester v9.0	2010-2020	4	n	y	y	Zheng et al. (2018a, 2018b, 2019)
MIROC4-ACTM	JAMSTEC	Surface stations	2000-2020	5	y	y	y	Patra et al. (2018); Chandra et al. (2021)
NISMON-CH ₄	NIES/MRI	Surface stations	2000-2020	2	y	y	y	Niwa et al. (2022)
NIES-TM-FLEXPART (NTEVAR)	NIES	Surface stations	2000-2020	2	y	y	y	Maksyutov et al. (2020); Wang et al. (2019a)
NIES-TM-FLEXPART (NTEVAR)	NIES	GOSAT NIES L2 v02.95	2010-2020	1	n	y	y	Maksyutov et al. (2020); Wang et al. (2019a)
TM5-CAMS	TNO/VU	Surface stations	2000-2020	1	y	y	y	Segers et al. (2022)
TM5-CAMS	TNO/VU	GOSAT ESA/CCI v2.3.8 (combined with surface observations)	2010-2020	1	n	y	y	Segers et al. (2022)
Total number of runs			24	18	24	24		

- Supprimé: in our new analysis,...ere with their contribution
- Mis en forme ... [360]
- Supprimé: 2008-1 ... [361]
- Supprimé: 2017
- Supprimé: Tsuruta et al. (2017)
- Supprimé: 2017
- Supprimé: 1
- Mis en forme ... [362]
- Supprimé: Carbon Tracker-Europe CH₄ ... [363]
- Supprimé: Yin et al. (2015)
- Mis en forme ... [364]
- Supprimé: PYVAR
- Supprimé: 2010-2016
- Supprimé: 2
- Mis en forme ... [367]
- Supprimé: n
- Mis en forme ... [368]
- Supprimé: n
- Mis en forme ... [365]
- Mis en forme ... [366]
- Mis en forme ... [369]
- Mis en forme ... [370]
- Supprimé: LMDz-PYVAR ... [371]
- Mis en forme ... [372]
- Supprimé: 2
- Supprimé: Zheng et al. (2018b, 2018a)
- Mis en forme ... [376]
- Supprimé: 2017
- Mis en forme ... [375]
- Mis en forme ... [373]
- Supprimé: v7.2
- Mis en forme ... [374]
- Mis en forme ... [377]
- Supprimé: 1
- Mis en forme ... [379]
- Supprimé: n
- Mis en forme ... [380]
- Supprimé: Patra et al. (2016, 2018)
- Mis en forme ... [381]
- Supprimé: 2016
- Mis en forme ... [378]
- Supprimé: NICAM-TM
- Mis en forme ... [383]
- Supprimé: 1
- Mis en forme ... [385]
- Supprimé: Niwa et al. (2017a, 2017b)
- Mis en forme ... [386]
- Mis en forme ... [382]
- Supprimé: 2017
- Mis en forme ... [384]
- Mis en forme ... [387]
- Supprimé: Maksyutov et al. (2020); Wang et al. (2019a)
- Supprimé: 1
- Mis en forme ... [390]

Table 5: Global and latitudinal total methane emissions in Tg CH₄ yr⁻¹, as decadal means (2000-2009 and 2010-2019) and for the year 2020 from this work using bottom-up and top-down approaches. Global and latitudinal emissions for 2000-2009 are also compared with Saunois et al. (2016, 2020) for top-down and bottom-up approaches when available. Uncertainties are reported as [min-max] range. The mean, minimum and maximum values are calculated while discarding outliers, for each category of source and sink. As a result, discrepancies may occur when comparing the sum of categories and their corresponding total due to differences in outlier detections. Differences of 1 Tg CH₄ yr⁻¹ in the totals can also occur due to rounding errors. For the latitudinal breakdown, bottom-up anthropogenic estimates are based only on the gridded products (see Table 1). As a result, the total from the latitudinal breakdown (line called "This work (gridded BU products only)") is slightly different from the values provided in Table 3 and recalled in the line "This work (all BU products)".

Period	2000-2009		2010-2019		2020		
Approach	Bottom-up		Top-down	Bottom-up	Top-down	Bottom-up	Top-down
	Global						
This work (all BU products)	638 [485-813]	543 [526-558]	669 [512-849]	575 [553-586]	685 [540-865]	608 [581-627]	
This work (gridded BU products only)	642 [501-809]		676 [526-845]		691 [565-862]		
S2020	703 [566-842]	547 [524-560]					
S2016	719 [583-861]	552 [535-566]	=	=	=	=	
90°S-30°N							
This work	367 [254-487]	337 [311-361]	388 [275-503]	364 [337-390]	395 [292-521]	386 [353-425]	
S2020	408 [322-532]	346 [320-379]					
S2016	=	356 [334-381]	=	=	=	=	
30°N-60°N							

- Supprimé: 2008-2017
- Mis en forme ... [418]
- Supprimé: 2017, for
- Mis en forme ... [419]
- Supprimé:) and Kirschke et al. (2013... 2020) for top-down
- Mis en forme ... [422]
- Supprimé: 2008-2017
- Mis en forme ... [421]
- Mis en forme ... [423]
- Supprimé: 2017
- Mis en forme ... [424]
- Mis en forme ... [425]
- Mis en forme ... [426]
- Mis en forme ... [427]
- Cellules supprimées ... [433]
- Mis en forme ... [429]
- Cellules supprimées ... [430]
- Cellules supprimées ... [431]
- Cellules supprimées ... [432]
- Cellules supprimées ... [434]
- Cellules supprimées ... [435]
- Mis en forme ... [428]
- Supprimé: This work
- Mis en forme ... [437]
- Mis en forme ... [438]
- Mis en forme ... [439]
- Supprimé:
- Mis en forme ... [440]
- Supprimé:
- Supprimé: 737
- Mis en forme ... [448]
- Mis en forme ... [449]
- Supprimé: 576
- Mis en forme ... [452]
- Supprimé: 747
- Mis en forme ... [454]
- Supprimé: 596
- Mis en forme ... [442]
- Mis en forme ... [451]
- Mis en forme ... [443]
- Mis en forme ... [456]
- Supprimé:
- Mis en forme ... [444]
- Supprimé:
- Mis en forme ... [446]
- Mis en forme ... [457]
- Mis en forme ... [458]
- Cellules supprimées ... [459]
- Cellules supprimées ... [460]
- Cellules supprimées ... [461]
- Cellules supprimées ... [462]
- Cellules supprimées ... [463]
- Cellules supprimées ... [464]
- Supprimé: This work

Period	2000-2009	2010-2019		2020		
Approach	Bottom-up	Top-down	Bottom-up	Top-down	Bottom-up	Top-down
	Global					
This work (all BU products)	638 [485-813]	543 [526-558]	669 [512-849]	575 [553-586]	685 [540-865]	608 [581-627]
This work	234 [169-335]	182 [162-197]	250 [184-345]	187 [160-204]	256 [186-356]	197 [170-215]
S2020	252 [202-342]	178 [159-199]	=	=	=	=
S2016	=	176 [159-195]	=	=	=	=
	60°N-90°N					
This work	42 [22-79]	26 [22-33]	38 [17-73]	24 [18-29]	39 [17-74]	25 [20-32]
S2020	42 [28-70]	23 [17-32]	=	=	=	=
S2016	=	20 [15-25]	=	=	=	=

Supprimé: 2008-2017
Mis en forme ... [493]
Supprimé: 2017
Mis en forme ... [494]
Mis en forme ... [495]
Mis en forme ... [496]
Mis en forme ... [497]
Mis en forme ... [498]
Mis en forme ... [499]
Mis en forme ... [500]
Cellules supprimées ... [503]
Mis en forme ... [501]
Cellules supprimées ... [502]
Cellules supprimées ... [504]
Cellules supprimées ... [505]
Cellules supprimées ... [506]
Cellules supprimées ... [507]
Supprimé: This work
Supprimé: 186
Mis en forme ... [522]
Supprimé: 272
Supprimé: 188
Mis en forme ... [526]
Mis en forme ... [509]
Mis en forme ... [510]
Mis en forme ... [511]
Supprimé:
Mis en forme ... [512]
Supprimé:
Mis en forme ... [514]
Mis en forme ... [520]
Mis en forme ... [515]
Supprimé: 267
Mis en forme ... [524]
Supprimé:
Mis en forme ... [516]
Supprimé:
Mis en forme ... [518]
Mis en forme ... [527]
Mis en forme ... [528]
Supprimé:
Mis en forme ... [529]
Cellules supprimées ... [530]
Cellules supprimées ... [531]
Cellules supprimées ... [532]
Cellules supprimées ... [533]
Cellules supprimées ... [534]
Cellules supprimées ... [535]
Mis en forme ... [536]
Mis en forme ... [537]
Mis en forme ... [540]
Mis en forme ... [541]
Supprimé:
Mis en forme ... [543]

Table 6: Latitudinal methane emissions in Tg CH₄ yr⁻¹ for the last decade **2010-2019**, based on top-down and bottom-up approaches. Uncertainties are reported as [min-max] range of reported studies. **The mean, minimum, and maximum values are calculated while discarding outliers, for each category of source and sink. As a result, discrepancies may occur when comparing the sum of categories and their corresponding total due to differences in outlier detections. Differences of 1 Tg CH₄ yr⁻¹ in the totals can also occur due to rounding errors. For bottom-up approaches, natural and indirect anthropogenic sources are estimated based on available gridded data sets (see text Sect 5.2). As some emissions are missing gridded products (wild animals, permafrost, and hydrates), discrepancies may occur in terms of totals proposed in Table 3. Bottom-up direct anthropogenic estimates are based only on the gridded products (see Table 1).**

Latitudinal band	90°S- 30°N		30°N-60°N		60°-90°N	
	Bottom-up	Top-Down	Bottom-up	Top-Down	Bottom-up	Top-Down
Natural and indirect anthropogenic Sources	178 [95-276]	148 [133-164]	100 [43-188]	42 [36-50]	28 [9-53]	14 [10-21]
Combined wetland and Inland freshwaters	151 [85-234]	128 [112-155]	73 [32-147]	27 [20-42]	24 [9-53]	9 [7-17]
Other natural	27 [11-42]	22 [20-29]	27 [10-41]	19 [16-22]	4 [2-6]	3 [1-5]
Anthropogenic direct sources	210 [180-227]	215 [191-238]	151 [142-157]	144 [121-162]	10 [6-14]	10 [6-16]
Agriculture & Waste	140 [121-150]	150 [135-168]	81 [77-84]	77 [56-88]	1 [1-2]	2 [2-2]
Fossil Fuels	52 [44-65]	46 [36-62]	65 [61-71]	61 [50-69]	7 [4-10]	7 [3-13]
Biomass & biofuel burning	22 [18-30]	19 [16-21]	7 [4-10]	6 [2-7]	1 [0-1]	1 [1-2]
Sum of sources	388 [275-503]	364 [337-390]	250 [184-345]	187 [160-204]	38 [7-73]	24 [18- 29]

- Supprimé: 2008-2017
- Supprimé: other ...atural and indirect anthropogenic sources [557]
- Supprimé: from EDGARv4.3.2 and GAINS.
- Mis en forme ... [558]
- Tableau mis en forme ... [559]
- Mis en forme ... [560]
- Mis en forme ... [561]
- Supprimé: [29-54]
- Mis en forme ... [565]
- Supprimé: 31 [18- 55]
- Supprimé: 16 [11-20]
- Supprimé: 228 [155340]
- Mis en forme ... [562]
- Supprimé: 160 [130-189]
- Mis en forme ... [563]
- Supprimé: 115 [70- 192]
- Mis en forme ... [564]
- Mis en forme ... [566]
- Mis en forme ... [567]
- Mis en forme ... [568]
- Supprimé: Natural Wetland
- Supprimé: 25 [10-43]
- Supprimé: 33 [24-48]
- Supprimé: 13
- Supprimé: 116 [71-146]
- Mis en forme ... [570]
- Supprimé: 135 [116]
- Mis en forme ... [571]
- Supprimé: [2-18]
- Mis en forme ... [575]
- Mis en forme ... [576]
- Supprimé: 16
- Mis en forme ... [572]
- Mis en forme ... [573]
- Mis en forme ... [574]
- Mis en forme ... [577]
- Mis en forme ... [569]
- Mis en forme ... [578]
- Déplacé vers le haut [10]: 112
- Mis en forme ... [579]
- Supprimé: [84-194]
- Mis en forme ... [580]
- Supprimé: 25 [14-36]
- Mis en forme ... [581]
- Supprimé: 90 [60-149]
- Mis en forme ... [582]
- Supprimé: 9 [4-14]
- Mis en forme ... [583]
- Supprimé: 22 [16-37]
- Mis en forme ... [584]
- Supprimé: 2-4
- Mis en forme ... [585]
- Mis en forme ... [586]
- Supprimé: 202 [183-217]

Table 7: Regional methane emissions (regions ranked by continent) in Tg CH₄ yr⁻¹ for the last decade 2010-2019, based on top-down and bottom-up approaches. Uncertainties are reported as [min-max] range of reported studies. Differences of 1 Tg CH₄ yr⁻¹ in the totals can occur due to rounding errors. For bottom-up approaches, natural and indirect anthropogenic sources are estimated based on available gridded data sets (see text Sect 5.2). As some emissions are missing gridded products (wild animals, permafrost, and hydrates), discrepancies may occur in terms of totals proposed in Table 3. Bottom-up direct anthropogenic estimates are based on all products (gridded and per country).

Region	Total emissions		Natural and indirect anthropogenic emissions		Direct anthropogenic emissions	
	Bottom-up	Top-down	Bottom-up	Top-down	Bottom-up	Top-down
USA	49 [27-77]	38 [32-46]	24 [7-43]	12 [7-22]	26 [19-34]	25 [16-31]
Canada	38 [14-71]	20 [17-24]	32 [11-63]	14 [11-22]	6 [3-8]	7 [5-9]
Central America	18 [10-28]	17 [14-19]	8 [3-17]	5 [2-6]	10 [8-12]	12 [11-13]
Northern South America	19 [9-35]	16 [13-20]	10 [3-17]	9 [7-11]	9 [6-17]	7 [6-8]
Brazil	51 [26-79]	47 [41-58]	32 [11-57]	26 [22-36]	19 [16-22]	21 [17-26]
Southwest South America	34 [16-51]	38 [30-48]	21 [6-35]	24 [16-34]	13 [10-16]	14 [12-17]
Europe	42 [29-57]	31 [24-36]	17 [6-30]	7 [5-9]	25 [22-27]	24 [20-31]
Northern Africa	24 [18-33]	25 [23-29]	7 [2-13]	6 [6-8]	18 [16-20]	19 [17-21]
Equatorial Africa	47 [28-83]	47 [39-59]	23 [10-49]	24 [20-30]	24 [19-34]	23 [19-29]
Southern Africa	21 [5-43]	19 [16-24]	11 [2-29]	8 [7-10]	10 [3-14]	11 [10-12]
Russia	48 [24-83]	36 [27-45]	25 [9-47]	14 [11-18]	23 [15-36]	21 [14-29]
Central Asia	15 [6-29]	10 [8-13]	8 [2-19]	1 [0-2]	8 [4-10]	9 [7-11]
Middle East	35 [21-47]	31 [24-39]	9 [3-15]	4 [1-6]	26 [18-31]	28 [20-34]
China	71 [55-99]	57 [37-72]	15 [4-33]	4 [3-7]	57 [51-66]	53 [34-66]
Korean-Japan	6 [4-12]	5 [4-6]	3 [1-7]	1 [1-1]	4 [3-5]	4 [3-5]
South Asia	58 [49-72]	52 [43-60]	13 [5-25]	6 [5-6]	45 [44-47]	45 [37-49]
Southeast Asia	64 [42-93]	63 [52-71]	32 [19-54]	27 [20-34]	32 [23-39]	35 [31-46]
Australasia	16 [9-26]	13 [10-17]	10 [4-19]	6 [4-7]	7 [6-7]	7 [6-7]

Mis en forme : Police :9 pt, Gras

Supprimé: Figure 1: Globally averaged atmospheric CH₄ (ppb) (a) and its annual growth rate G_{ATM} (ppb yr⁻¹) (b) from four measurement programs, National Oceanic and Atmospheric Administration (NOAA), Advanced Global Atmospheric Gases Experiment (AGAGE), Commonwealth Scientific and Industrial Research Organisation (CSIRO), and University of California, Irvine (UCI). Detailed descriptions of methods are given in the supplementary material of Kirschke et al. (2013). <object>... Saut de page </object>

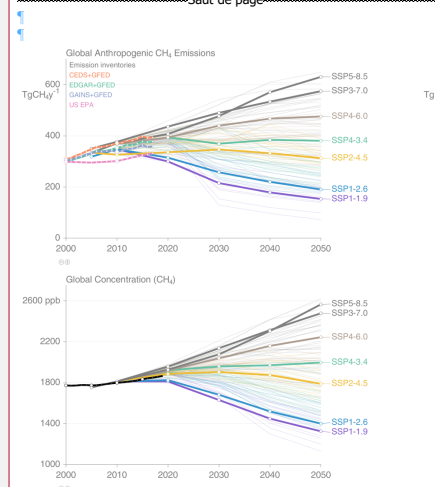


Figure 2: Top: Global anthropogenic methane emissions (including biomass burning) from historical inventories and future projections (in Tg CH₄ yr⁻¹). Top left panel shows inventories and the unharmonized Shared Socioeconomic Pathways (Riahi et al., 2017), with highlighted scenarios representing scenarios assessed in CMIP6 (O'Neill, et al., 2016). Top right panel shows the selected scenarios harmonized with historical emissions (CEDS) for CMIP6 activities (Gidden et al., 2019). USEPA and GAINS estimates have been linearly interpolated from the 5-year original products to yearly values. After 2005, USEPA original estimates are projections. Bottom left: Global methane concentrations for NOAA surface site observations (black) and projections based on SSPs (Riahi et al., 2017) with concentrations estimated using MAGICC (Meinshausen et al., 2011).

... [625]

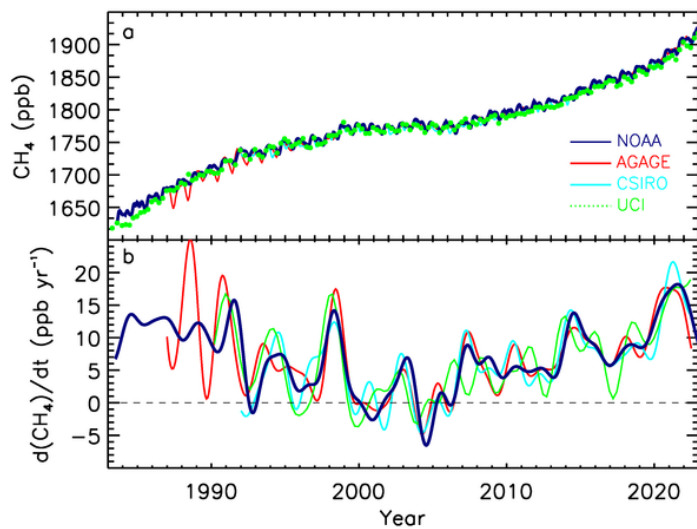


Figure 1: Globally averaged atmospheric CH₄ concentrations (ppb) (a) and annual growth rates G_{ATM} (ppb yr⁻¹) (b) between 1983 and 2022, from four measurement programs, National Oceanic and Atmospheric Administration (NOAA), Advanced Global Atmospheric Gases Experiment (AGAGE), Commonwealth Scientific and Industrial Research Organisation (CSIRO), and University of California, Irvine (UCI). Detailed descriptions of methods are given in the supplementary material of Kirschke et al. (2013).

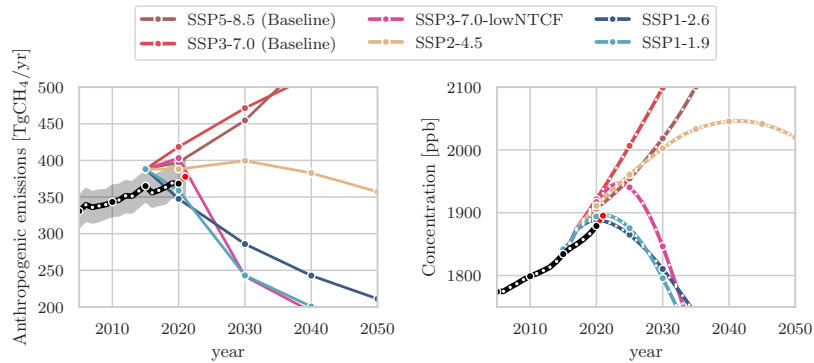


Figure 2: Left: Global anthropogenic methane emissions (including biomass burning) over 2005-2050 from historical inventories (black line and grey shaded area) and future projections (colored lines) (in Tg CH₄ yr⁻¹) from selected scenarios harmonized with historical emissions (CEDS) for CMIP6 activities (Gidden et al., 2019). Historical mean emissions correspond to the average of anthropogenic inventories listed in Table 1 added to the GFEDv4.1s (van der Werf et al., 2017) biomass burning historical emissions. Right: Global atmospheric methane concentrations for NOAA surface site observations (black) and projections based on SSPs (Riahi et al., 2017) with concentrations estimated using MAGICC (Meinshausen et al., 2017, 2020). Red dots show the last year available (2022 for observations).

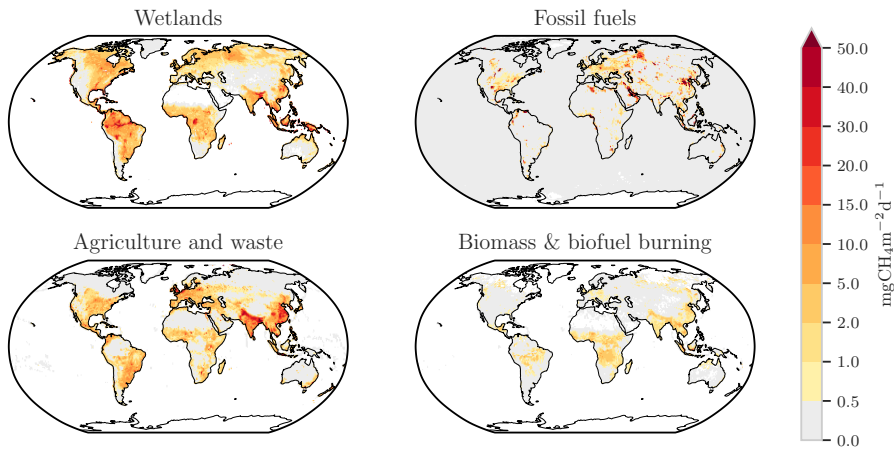


Figure 3: Methane emissions from four source categories: natural wetlands (excluding lakes, ponds, and rivers), biomass and biofuel burning, agriculture and waste, and fossil fuels for the 2010-2019 decade in $\text{mg CH}_4 \text{ m}^{-2} \text{ day}^{-1}$. The wetland emission map represents the mean daily emission average over the 16 biogeochemical models listed in Table 2 and over the 2010-2019 decade. Fossil fuel and Agriculture and Waste emission maps are derived from the mean estimates of gridded CEDS, EDGARv6, EDGARv7 and GAINS models. The biomass and biofuel burning map results from the mean of the biomass burning inventories listed in Table 1 added to the mean of the biofuel estimate from CEDS (O'Rourke et al., 2021), EDGARv6 (Crippa et al., 2021), EDGARv7 (Crippa et al., 2023) and GAINS (Höglund-Isaksson et al., (2020)) models.

- Supprimé: Agriculture
- Supprimé: Waste
- Supprimé: Fossil
- Supprimé: 2008-2017
- Supprimé: 13
- Supprimé: 2008-2017
- Supprimé: EDGARv4.3.2
- Supprimé: , EDGARv4.3.2 and GAINS

Wetlands and Inland Freshwaters Methane Cycle

Million tons of CH₄ per year (Tg CH₄/y), on average 2010-2019

- █ Anthropogenic flux
- █ Natural flux
- █ Anthropogenic and natural flux

Creative Commons BY-SA
Credit must be given to the author. Adaptations must be shared under the same terms.

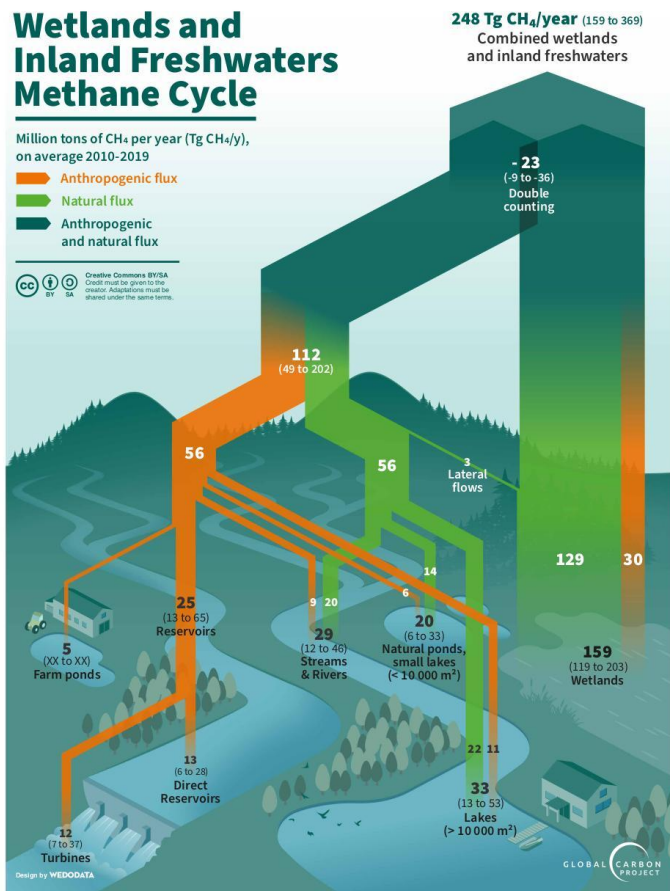
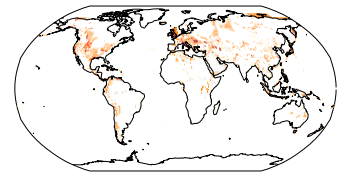
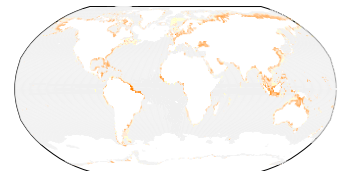


Figure 4: Estimation of wetland and inland freshwater emissions over the 2010-2019 decade in Tg CH₄ yr⁻¹. The fluxes related to voluntary (such as through reservoirs or farm ponds) or involuntary (land use or eutrophication-related) perturbations of the methane cycle are shown here in orange. However, they are accounted for into the “natural and indirect anthropogenic” sources in the Table 3 budget and depicted as natural sources in Fig. 7.

Geological



Ocean



Supprimé:

Mis en forme : Police :10 pt

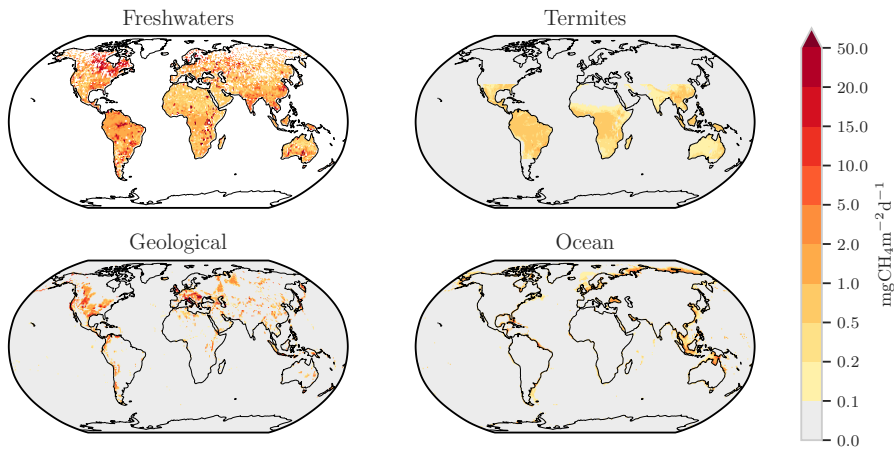


Figure 5: Methane emissions ($\text{mg CH}_4 \text{ m}^{-2} \text{ day}^{-1}$) from **four natural and indirect anthropogenic sources: inland freshwaters (includes lakes, ponds (Johnson et al., 2022.), reservoirs (Johnson et al., 2021) and stream and rivers (Rocher-Ros et al., 2023) with a global total scaled to 89 Tg yr^{-1} , geological (Etiopie et al., 2019), termites (this study) and oceans (Weber et al., 2019).**

Supprimé : three natural sources (left color scale):

Supprimé : , and methane uptake in soils ($\text{mg CH}_4 \text{ m}^{-2} \text{ day}^{-1}$) presented in positive units (right color scale), and based on Murguía-Flores et al. (2018)

Mis en forme : Police :11 pt, Couleur de police : Noir

Mis en forme : Espace Avant : 11 pt, Après : 2 pt, Paragraphes solidaires, Lignes solidaires, Bordure : Haut: (Pas de bordure), Bas: (Pas de bordure), Gauche: (Pas de bordure), Droite: (Pas de bordure), Entre : (Pas de bordure)

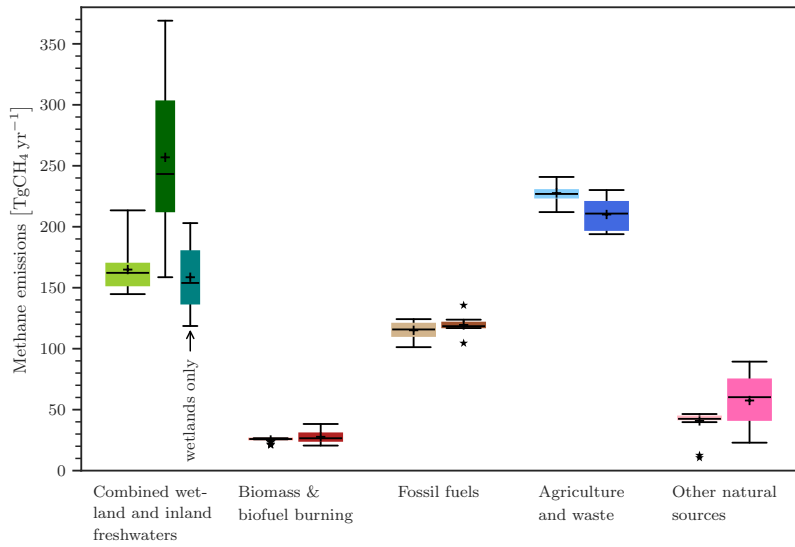
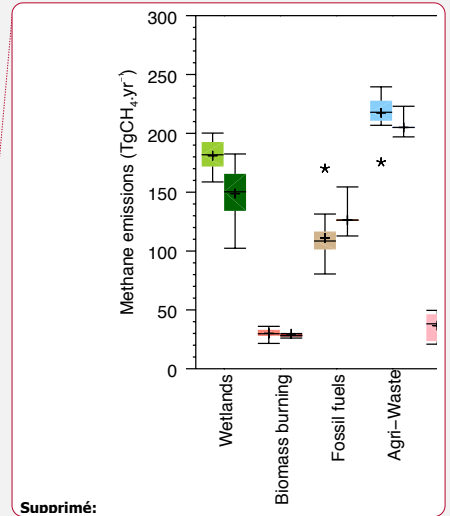


Figure 6: Methane global emissions from five broad categories (see Sect. 2.3) for the 2010-2019 decade for top-down inversion models (left light coloured boxplots) in Tg CH₄ yr⁻¹ and for bottom-up models and inventories (right dark coloured boxplots). For combined wetland and inland freshwaters three estimates are given: left = top-down estimates, middle = bottom-up estimates, right = bottom-up estimates for wetlands only. Median value, first and third quartiles are presented in the boxes. The whiskers represent the minimum and maximum values when suspected outliers are removed (see Sect. 2.2). Suspected outliers are marked with stars. Bottom-up quartiles are not available for bottom-up estimates, except for wetland emissions. Mean values are represented with “+” symbols, these are the values reported in Table 3.



Supprimé:

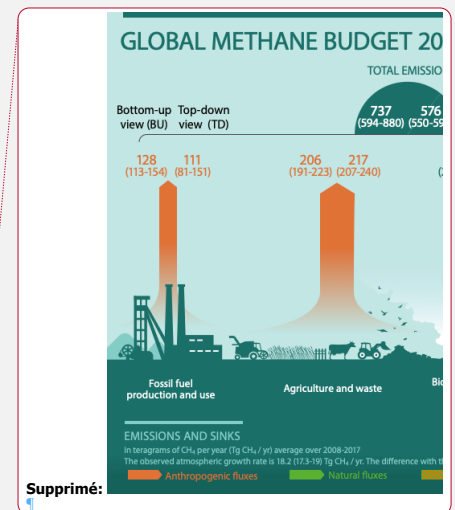
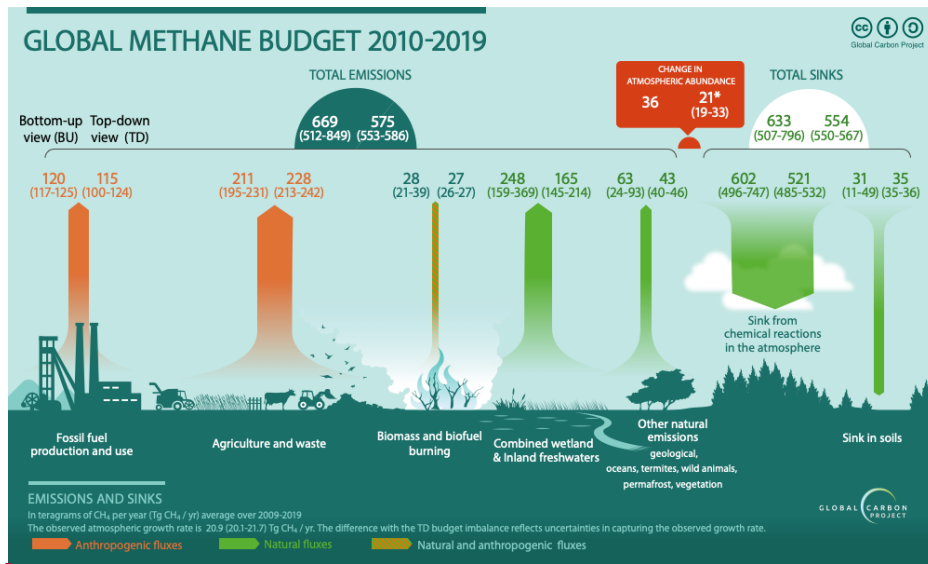
Supprimé: 5

Supprimé: the

Supprimé: 2008-2017

Supprimé: inversions

Supprimé: when existing.



Supprimé:

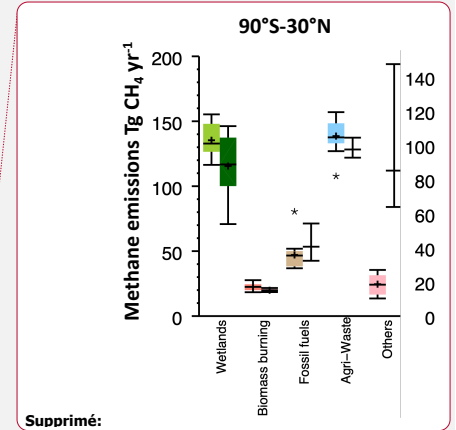
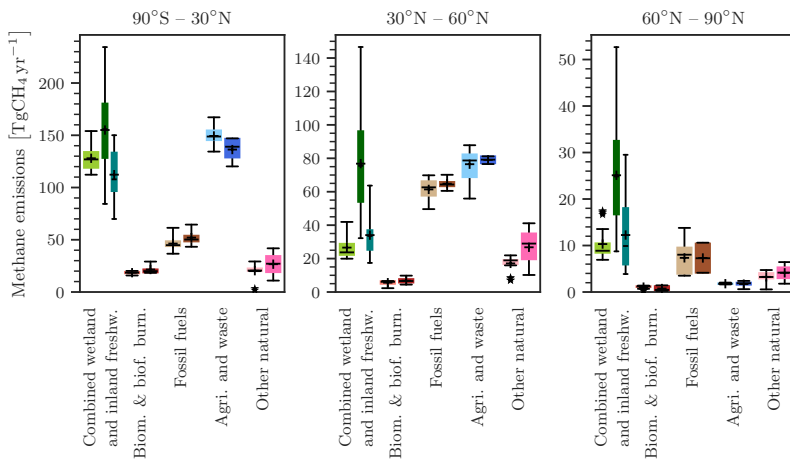
Figure 2: Global Methane Budget for the 2010-2019 decade. Both bottom-up (left) and top-down (right) estimates are provided for each emission and sink category in Tg CH₄ yr⁻¹, as well as for total emissions and total sinks. Biomass and biofuel burning emissions are depicted here as both natural and anthropogenic emissions while they are fully included in anthropogenic emissions in the budget tables and text (Sect. 3.1.5). **Combined wetland and inland freshwaters are depicted as fully natural while part has been attributed an indirect anthropogenic component (Sect. 3.2.2 and Figure 4).**

Supprimé: 6

Supprimé: 2008-2017 decades

Supprimé:).

Mis en forme : Couleur de police : Rouge



Supprimé:

Figure 8: Methane latitudinal emissions from five broad categories (see Sect. 2.3) for the 2010-2019 decade for top-down inversion models (left light coloured boxplots) in $\text{Tg CH}_4 \text{ yr}^{-1}$ and for bottom-up models and inventories (right dark coloured boxplots). For combined wetland and inland freshwaters three estimates are given: left = top-down estimates, middle = bottom-up estimates, right = bottom-up estimates for wetlands only. Median value, first and third quartiles are presented in the boxes. The whiskers represent the minimum and maximum values when suspected outliers are removed (see Sect. 2.2). Suspected outliers are marked with stars. Bottom-up quartiles are not available for bottom-up estimates, except wetland emissions. Mean values are represented with “+” symbols, these are the values reported in Table 6.

Supprimé: 7

Supprimé: the

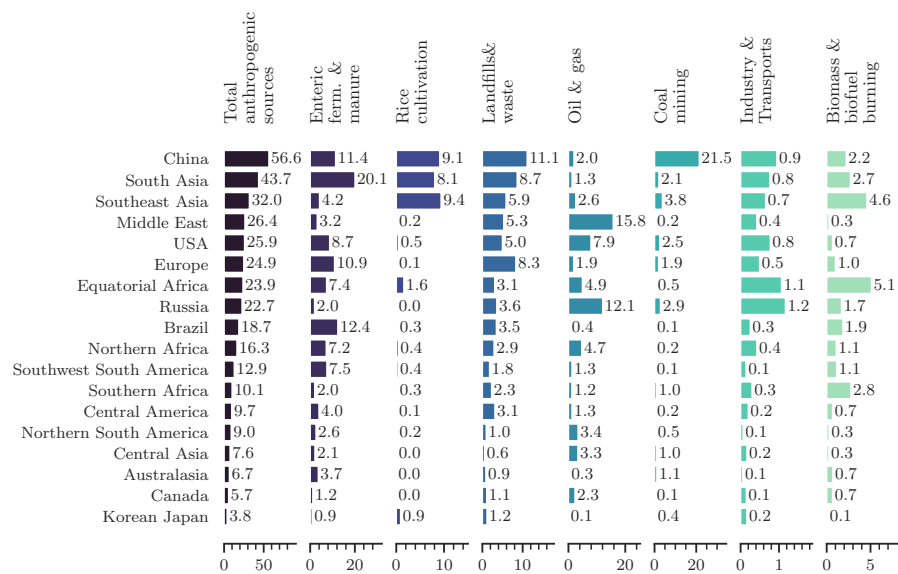
Supprimé: 2008-2017

Supprimé: inversions

Supprimé: as shown

Mis en forme : Police :9 pt, Gras

Mis en forme : Justifié, Espace Après : 10 pt



Supprimé:Saut de section (page suivante).....
Table A1.

Figure 9: Regional anthropogenic emissions for the 2010-2019 decade from bottom-up estimates in Tg CH₄ yr⁻¹. Regions are ranked by their total anthropogenic emissions. Note that each category has its own emission scale.

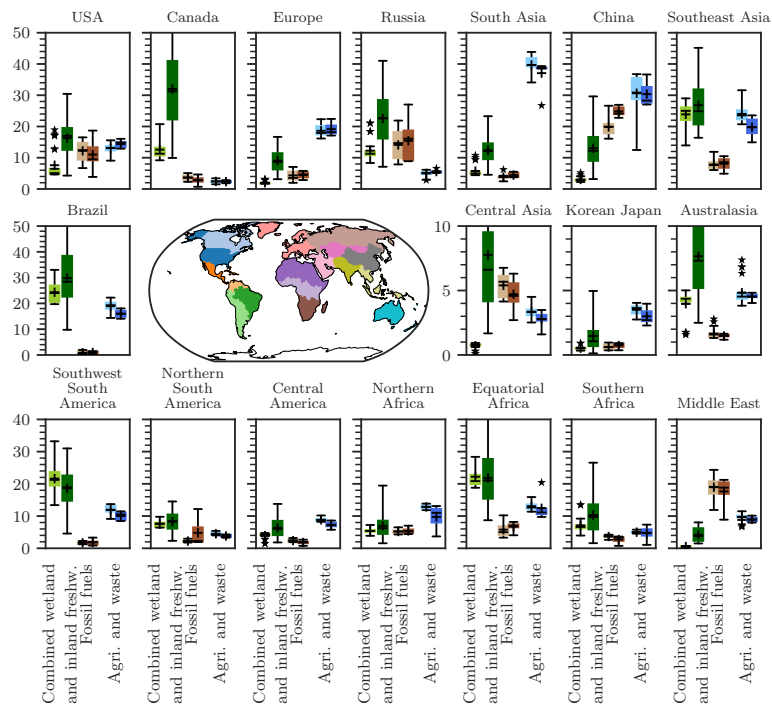


Figure 10: Regional emissions for three broad main emissions categories for the 2010-2019 decade: Combined wetland and inland freshwaters, fossil fuel and agriculture & waste from top-down estimates (left box-plots- and bottom-up estimates (right boxplots). The inner map shows the region's distribution (see also Supplementary material, Table S1 and Fig. S3). More categories are presented in the Supplementary Material in Figure S6.

Table A1. Comparison of terminologies used in this study and previous reports for methane sources.

<u>GCP terminology (This study)</u>		<u>IPCC AR6 (Canadell et al., 2021)</u>	<u>National GHG inventories (used by UNFCCC according to IPCC (2006) and IPCC (2019))</u>	<u>IPCC (2006, 2019) Source sector numbering</u>
<i>Anthropogenic Sources</i>				
<u>Fossil fuels</u>	<u>Coal Mining</u>	<u>Coal Mining</u>	<u>Fugitive emissions from Fuels / Solid fuels</u>	<u>1B1</u>
	<u>Oil and gas</u>	<u>Oil and gas</u>	<u>Fugitive emissions from Fuels / Oil and natural gas</u>	<u>1B2</u>
	<u>Transport</u>	<u>Transport</u>	<u>Transport</u>	<u>1A3</u>
	<u>Industry</u>			<u>Mineral, chemical, metal industry and others</u>
<u>Energy/fuel Combustion activities</u>				<u>1A except 1A3 + 1B3</u>
<u>Agriculture</u>	<u>Enteric fermentation and manure management</u>	<u>Enteric fermentation and manure management</u>	<u>Livestock</u>	<u>3A</u>
	<u>Rice cultivation</u>	<u>Rice cultivation</u>	<u>Rice cultivation</u>	<u>3C7</u>
<u>Waste</u>	<u>Landfills and waste</u>	<u>Landfills and waste</u>	<u>Waste</u>	<u>4</u>
<u>Biofuel and biomass burning</u>	<u>Biofuel burning</u>	<u>Biofuel burning</u>	<u>Biofuel burning</u>	<u>1A4b</u>
	<u>Biomass burning</u>	<u>Biomass burning</u>	<u>Biomass burning</u>	<u>3C1</u>
<i>Natural and indirect sources</i>				
<u>Wetlands</u>	<u>Wetlands</u>	<u>Wetlands</u>	<u>--</u>	<u>--</u>
<u>Inland freshwaters</u>	<u>Reservoirs</u>	<u>included in Inland freshwaters</u>	<u>Land (incl Reservoirs)</u>	<u>in 3B</u>
	<u>Lakes, ponds, and rivers</u>	<u>incl in Inland freshwaters</u>	<u>only canal, ditches and ponds for human uses</u>	<u>in 3B</u>
<u>Other natural sources</u>	<u>Oceans</u>	<u>Oceans</u>	<u>--</u>	<u>--</u>
	<u>Termites</u>	<u>Termites</u>	<u>--</u>	<u>--</u>

	Geological sources	Geological sources	--	--
--	--------------------	--------------------	----	----

Table A2. Summary of methodological changes since the previous budget (Saunois et al., 2020). No significant changes have been applied to the vegetation (Sect. 3.2.8), wild animal (Sect. 3.2.5) and terrestrial permafrost and hydrates (Sect 3.2.7) estimates, though literature has been expanded and/or updated.

	Saunois et al. (2020)	This study
Regions definition (Table S1, Fig S3)	18 continental regions + ocean	same regions except the last region including only Australia and New-Zealand and called Australasia
Anthropogenic global inventories (See Table 1, Sect 3.1.1)	CEDS, EDGARv4.3.2, USEPA (2012), FAO and GAINS ECLIPSE v6	CEDS, EDGARv6 and v7, USEPA (2019), FAO, IIASA GAINS v4 Add estimate of ultra emitters from Lauvaux et al. (2022)
Biomass burning data sets	FINNV1.5, GFASv1.3, GFEDv4.1s, QFEDv2.5	FINNV2.5, GFASv1.3, GFEDv4.1s, QFEDv2.5
Estimate of wetland emissions (See Tables 2 and S3 and Section 3.2.1)	13 land surface models involved, runs with either prescribed areas or based on Hydrological scheme, single meteorological forcing	16 land surface models involved, runs with either prescribed areas or based on Hydrological scheme, two sets of meteorological forcings
Estimate of reservoirs emissions (Sect.3.2.2)	based on Deemer et al. (2016)	based on Johnson et al. (2021), Rosentreter et al. (2021) and Harrison et al. (2021)
Estimate of lakes and ponds emissions (Sect.3.2.2)	based on Bastviken et al. (2011), Wik et al. (2016b) and Tan and Zhuang (2015)	lakes > .1km² : based on Rosentreter et al. (2021), Zhuang et al. (2023) and Johnson et al. (2022) lakes and ponds < 0.1 km² : based on Rosentreter et al. (2021), and Johnson et al. (2022)
Estimates of stream and river emissions (Sect.3.2.2)	From Stanley et al. (2016)	based on Rosentreter et al. (2021) and Rocher-Ros et al. (2023)
Estimates of the anthropogenic perturbation component of inland freshwater emissions (Sect.3.2.2)	---	based on several individual studies on the effect of eutrophication on emissions from lakes, and ponds (See text in Sect. 3.2.2)
Estimate of the double counting in the aquatic systems (Sect.3.2.2)	---	due to the accounting of small lakes and ponds (<0.1km²) in the vegetated wetlands areas used in land surface models and to lateral transport from vegetated wetland to rivers.

Geological sources (Sect 3.2.3) - onshore and offshore	based on Etiope and Schwiezke et al. (2019)	same as in Saunio et al. (2020)
Termite emissions (Sect. 3.2.4)	GPP : Zhang et al. (2017) termite biomass: Jung et al. (2011) EF : Kirshke et al. (2013) and Fraser et al., 1986)	GPP: Wild et al. (2022) termite biomass: based on different studies depending on regions (see text) EF: Sugimoto et al. (1998) Applied a correction factor for mound from Nauer et al. (2018)
Oceanic sources (Sect 3.2.6)	modern biogenic: based on Wuebbles and Hayhoe (2002) , Laruelle et al. (2013) and Rosentreter et al. (2018); geological: based on Etiope (2019)	modern biogenic: based on Rosentreter et al. (2021;2023) and Laruelle et al. (2023) geological: based on Etiope (2019)
Tropospheric OH oxidation (Sect 3.3.2) and stratospheric loss (Sect 3.3.3) (See Supplementary Table S4)	based on results from 11 models contributing to the Chemistry Climate Model Initiative (Morgenstern et al., 2017)	based on results from 11 models contributing to the Chemistry Climate Model Initiative 2022 (Plummer et al., 2021) and the CMIP6 simulations (Collins et al., 2017)
Tropospheric reaction with Cl	based on Hossaini et al. (2016), Wang et al. (2019b) and Gromov (2018)	based on Hossaini et al (2016), Sherwenn et al. (2016), Wang et al (2019b, 2021b) and Gromov (2018)
Soil uptake (See Table S6)	based on Tian et al. (2016)	based on VISIT, JSBACH en MeMo surface models.
Estimates through top-down approaches (See table S7 and S8 to S11)	9 inverse systems contributing, prior fluxes based on EDGARv4.2 or v4.3.2 for most inversions. Most inversion used constant OH.	7 inverse systems contributing, runs with constant and varying OH, prior fluxes based on either EDGARv6 or GAINS

Table A3. Funding supporting the production of the various components of the global methane budget in addition to the authors' supporting institutions (see also acknowledgements).

Funder and grant number (where relevant)	Authors/Simulations/Observations	
Director, Office of Science, Office of Biological and Environmental Research of the US Department of Energy under Contract No. DE-AC02-05CH11231 to Lawrence Berkeley National Laboratory as part of the RUBISCO Scientific Focus Area	WJR, OZ, E3SM/ELM simulations	Mis en forme ... [626] Mis en forme ... [628] Mis en forme ... [627] Mis en forme ... [631] Mis en forme ... [629] Tableau mis en forme ... [630] Supprimé: ARC Linkage project LP150100519 ... [632] Mis en forme ... [633] Tableau mis en forme ... [634] Supprimé: Joseph Canadell
Funded by NASA's Interdisciplinary Research in Earth Science (IDS) Program and the NASA Terrestrial Ecology and Tropospheric Composition Programs	MSJ: lake and reservoir bottom-up methane emission data sets	Mis en forme ... [636] Mis en forme ... [635]
Funded by Agence National de la Recherche through the project Advanced Methane Budget through Multi-constraints and Multi-data streams Modelling (AMB-M ²) - (ANR-21-CE01-0030)	AM, MS	Supprimé: Environment Research and Technology Development Fund ... [637] Supprimé: Naveen Chandra and Prabir K. Patra
The Environment Research and Technology Development Fund (JPMEERF21S20800) of the Environmental Restoration and Conservation Agency provided by Ministry of the Environment of Japan	YN, NISMON-CH ₄	Mis en forme ... [638] Mis en forme ... [639]
Funded by the German Federal Ministry of Education and Research (BMBF) via the "PalMod" project, grant No. 01LP1921A	TK: CH ₄ emission modelling with JSBACH and LPJ-MPI	Mis en forme ... [640] Mis en forme ... [641]
Funded by the Swedish Research Council VR (2020-05338) and Swedish National Space Agency (209/19)	WZ: LPJ-GUESS simulations	Tableau mis en forme ... [642] Mis en forme ... [643] Supprimé: 2-1701
Funded by BELSPO (project FedTwin ReCAP), EU Horizon 2020 project ESM2025 (nr. 101003536) and FRNS PDR project CH4-lake (T.0191.23)	PR: inland water, coastal and oceanic CH ₄ emission synthesis	Mis en forme ... [644] Supprimé: Yosuke Niwa
EU H2020 (725546 ERC METLAKE and 101015825 TRIAGE), Swedish Research Councils VR (2022-03841) and Formas (2018-01794)	DB: inland waters - data and bottom up estimation	Mis en forme ... [646] Supprimé: ,
Supported by the Newton Fund through the Met Office Climate Science for Service Partnership Brazil (CSSP Brazil)	NG: JULES simulations	Mis en forme ... [645] Supprimé: Environment Research and Technology Development Fund ... [647]
Funded by United Nations Environment Programme, Stanford University DTIE21-EN3143	RBJ: inversions and general budget support	Supprimé: Akihiko Ito Mis en forme ... [648] Mis en forme ... [649]
the Joint Fund for Regional Innovation and Development of the National Natural Science Foundation (Grant No. U22A20570); the Natural Sciences and Engineering Research Council of Canada (NSERC, #371706)	Changhui Peng/TRIPLEX-GHG	Supprimé: Environment, Japan Mis en forme ... [650] Mis en forme ... [651] Supprimé: ESA GHG-CCI ... [652] Mis en forme ... [653] Tableau mis en forme ... [654] Mis en forme ... [655] Supprimé: (ERC; grant no. 725546, METLAKE) Supprimé: David Bastviken Mis en forme ... [657] Mis en forme ... [656] Supprimé: Pierre Regnier and Glen P. Peters Supprimé: European Union's Mis en forme ... [658] Mis en forme ... [659] Supprimé: research Mis en forme ... [660] Supprimé: innovation programme under grant agreement ... [661] Mis en forme ... [662] Mis en forme ... [663] Mis en forme ... [664] Supprimé: F.R.S.- FNRS for post-doctoral funding at the ULB ... [665] Mis en forme ... [666] Tableau mis en forme ... [667]
Computing Resources		
LSCE computing resources	Marielle Saunois, Philippe Bousquet, Joël Thanwerdas and Adrien Martinez	
NASA High-End Computing (HEC) Program through the NASA Advanced Supercomputing (NAS) Division at NASA Ames Research Center	Matthew S. Johnson (MSJ)	
Deutsches Klimarechenzentrum (DKRZ), Hamburg, Germany	Thomas Kleinen (TK)	

ALICE High Performance Computing Facility at the University of Leicester
FUJITSU PRIMERGY CX2550M5 at MRI and NEC SX-Aurora TSUBASA at NIES

GOSAT retrievals
Yosuke Niwa (YN)

Support for atmospheric observations

Australian Antarctic Division
 Australian Institute of Marine Science
 Bureau of Meteorology (Australia)
 Commonwealth Scientific and Industrial Research Organisation (CSIRO, Australia)
 Department of Climate Change, Energy, the Environment and Water (DCCEEW, Australia)
 Meteorological Service of Canada
 NASA: grants NAG5-12669, NNX07AE89G, NNX11AF17G, NNX16AC98G and 80NSSC21K1369 to MIT, with subawards to the University of Bristol (for Barbados and Mace Head) and CSIRO (for Kennakoek/Cape Grim); grants NAG5-4023, NNX07AE87G, NNX07AF09G, NNX11AF15G, NNX11AF16G, NNX16AC96G, NNX16AC97G, 80NSSC21K1210 and 80NSSC21K1201 to SIO
 National Oceanic and Atmospheric Administration (NOAA, USA) contract RA133R15CN0008 to the University of Bristol
 NOAA USA
 Refrigerant Reclaim Australia
 UK Department for Business, Energy & Industrial Strategy (BEIS) contract TRN1537/06/2018 and TRN 5488/11/2021 to the University of Bristol
National Oceanic and Atmospheric Administration (NOAA, USA)
 Japanese Ministry of Environment
 Japanese Aerospace Exploration Agency, National Institute for Environmental Studies
NERC UK: grants NE/W004895/1, NE/R016518/1 and NE/X019071/1
The Swedish Research Council VR (2022-04839), European Space Agency projects AMPAC-Net and CCI+ permafrost, European Union's Horizon 2020 Research and Innovation Programme to the Nunataryuk project (no. 773421)

CSIRO flask network
 CSIRO flask network
Kennaok/Cape Grim AGAGE, CSIRO flask network
Kennaok/Cape Grim AGAGE, CSIRO flask network
Kennaok/Cape Grim AGAGE
 CSIRO flask network
AGAGE calibrations and measurements at SIO: La Jolla and AGAGE station operations at Trinidad Head, Mace Head, Barbados, American Samoa, and Kennakoek/Cape Grim
 Barbados
 CSIRO flask network
Kennaok/Cape Grim AGAGE
 Mace Head
Cape Matatula
 GOSAT data, Robert Parker
 GOSAT data, Robert Parker
GOSAT data, Robert Parker
 Permafrost region, Gustaf Hugelius

- Supprimé: Swedish National Infrastructure for
- Supprimé: (SNIC)
- Mis en forme : Espace Après : 6 pt
- Supprimé: Lund
- Supprimé: Centre for Scientific and Technical Computing (Lunarc), project no. 2017/1-423 – Aurora resource
- Supprimé: LPJGUESS Simulations
- Tableau mis en forme
- Mis en forme : Anglais (G.B.)
- Mis en forme : Anglais (G.B.)
- Mis en forme : Police :Gras
- Tableau mis en forme
- Mis en forme : Espace Après : 6 pt
- Mis en forme : Espace Après : 6 pt
- Mis en forme : Espace Après : 6 pt
- Mis en forme : Anglais (G.B.)
- Mis en forme : Espace Après : 6 pt
- Supprimé: Energy (DoEE)
- Mis en forme : Espace Après : 6 pt
- Supprimé: Operation of Mace Head,
- Mis en forme : Espace Après : 6 pt
- Supprimé: and
- Supprimé: ;
- Supprimé: and
- Mis en forme : Anglais (G.B.)
- Supprimé: AGAGE stations and SIO calibration
- Mis en forme : Anglais (G.B.)
- Mis en forme : Espace Après : 6 pt
- Mis en forme : Espace Après : 6 pt
- Mis en forme : Espace Après : 6 pt
- Mis en forme : Espace Après : 6 pt
- Supprimé: ALICE High Performance Computing Facility at the University of Leicester
- Mis en forme : Espace Après : 6 pt
- Supprimé: GOSAT retrievals
- Mis en forme : Espace Après : 6 pt
- Mis en forme : Espace Après : 6 pt
- Supprimé: ¶

Page 1 : [1] Définition du style 03/05/2024 16:41:00

Sous-titre

Page 1 : [1] Définition du style 03/05/2024 16:41:00

Sous-titre

Page 1 : [1] Définition du style 03/05/2024 16:41:00

Sous-titre

Page 1 : [1] Définition du style 03/05/2024 16:41:00

Sous-titre

Page 1 : [1] Définition du style 03/05/2024 16:41:00

Sous-titre

Page 1 : [1] Définition du style 03/05/2024 16:41:00

Sous-titre

Page 1 : [1] Définition du style 03/05/2024 16:41:00

Sous-titre

Page 1 : [1] Définition du style 03/05/2024 16:41:00

Sous-titre

Page 1 : [1] Définition du style 03/05/2024 16:41:00

Sous-titre

Page 1 : [2] Supprimé 03/05/2024 16:41:00

▼

Page 1 : [2] Supprimé 03/05/2024 16:41:00

▼

Page 1 : [3] Supprimé 03/05/2024 16:41:00

▼

Page 1 : [3] Supprimé 03/05/2024 16:41:00

▼

Page 1 : [3] Supprimé 03/05/2024 16:41:00

▼

Page 1 : [4] Supprimé 03/05/2024 16:41:00

Page 1 : [4] Supprimé

03/05/2024 16:41:00



Page 1 : [5] Mis en forme

03/05/2024 16:41:00

Police :12 pt

Page 1 : [5] Mis en forme

03/05/2024 16:41:00

Police :12 pt

Page 1 : [6] Supprimé

03/05/2024 16:41:00



Page 1 : [6] Supprimé

03/05/2024 16:41:00



Page 1 : [6] Supprimé

03/05/2024 16:41:00



Page 1 : [6] Supprimé

03/05/2024 16:41:00



Page 1 : [6] Supprimé

03/05/2024 16:41:00



Page 1 : [6] Supprimé

03/05/2024 16:41:00



Page 1 : [6] Supprimé

03/05/2024 16:41:00



Page 1 : [6] Supprimé

03/05/2024 16:41:00



Page 1 : [6] Supprimé

03/05/2024 16:41:00



Page 1 : [6] Supprimé

03/05/2024 16:41:00



▼
Page 1 : [6] Supprimé

03/05/2024 16:41:00

▼
Page 1 : [7] Supprimé

03/05/2024 16:41:00

▼
Page 1 : [7] Supprimé

03/05/2024 16:41:00

Page 1 : [7] Supprimé **03/05/2024 16:41:00**



Page 1 : [7] Supprimé **03/05/2024 16:41:00**



Page 1 : [7] Supprimé **03/05/2024 16:41:00**



Page 1 : [7] Supprimé **03/05/2024 16:41:00**



Page 1 : [7] Supprimé **03/05/2024 16:41:00**



Page 1 : [7] Supprimé **03/05/2024 16:41:00**



Page 1 : [8] Supprimé **03/05/2024 16:41:00**



Page 1 : [9] Mis en forme **03/05/2024 16:41:00**

Bordure : Haut: (Pas de bordure), Bas: (Pas de bordure), Gauche: (Pas de bordure), Droite: (Pas de bordure), Entre : (Pas de bordure)

Page 1 : [10] Supprimé **03/05/2024 16:41:00**



Page 1 : [11] Mis en forme **03/05/2024 16:41:00**

Bordure : Haut: (Pas de bordure), Bas: (Pas de bordure), Gauche: (Pas de bordure), Droite: (Pas de bordure), Entre : (Pas de bordure)

Page 1 : [12] Mis en forme **03/05/2024 16:41:00**

Droite : 1,32 cm, Bordure : Haut: (Pas de bordure), Bas: (Pas de bordure), Gauche: (Pas de bordure), Droite: (Pas de bordure), Entre : (Pas de bordure)

Page 1 : [13] Supprimé **03/05/2024 16:41:00**



Page 1 : [13] Supprimé **03/05/2024 16:41:00**



Page 1 : [14] Supprimé **03/05/2024 16:41:00**



Page 1 : [15] Mis en forme **03/05/2024 16:41:00**

Bordure : Haut: (Pas de bordure), Bas: (Pas de bordure), Gauche: (Pas de bordure), Droite: (Pas de bordure), Entre

Bordure : Haut: (Pas de bordure), Bas: (Pas de bordure), Gauche: (Pas de bordure), Droite: (Pas de bordure), Entre : (Pas de bordure)

Page 1 : [18] Mis en forme 03/05/2024 16:41:00

Police :Roboto, 9 pt, Couleur de police : Couleur personnalisée(RVB(31;31;31))

Page 1 : [19] Mis en forme 03/05/2024 16:41:00

Police :Roboto, 9 pt, Couleur de police : Couleur personnalisée(RVB(31;31;31))

Page 1 : [20] Supprimé 03/05/2024 16:41:00

Page 2 : [21] Mis en forme 03/05/2024 16:41:00

Couleur de police : Couleur personnalisée(RVB(31;31;31))

Page 2 : [22] Supprimé 03/05/2024 16:41:00

Page 2 : [23] Mis en forme 03/05/2024 16:41:00

Gauche, Retrait : Gauche : 0,04 cm, Droite : 1,32 cm, Autoriser lignes veuves et orphelines, Bordure : Haut: (Pas de bordure), Bas: (Pas de bordure), Gauche: (Pas de bordure), Droite: (Pas de bordure), Entre : (Pas de bordure)

Page 2 : [24] Mis en forme 03/05/2024 16:41:00

Couleur de police : Couleur personnalisée(RVB(31;31;31))

Page 2 : [25] Supprimé 03/05/2024 16:41:00

Page 2 : [26] Mis en forme 03/05/2024 16:41:00

Couleur de police : Couleur personnalisée(RVB(31;31;31))

Page 2 : [26] Mis en forme 03/05/2024 16:41:00

Couleur de police : Couleur personnalisée(RVB(31;31;31))

Page 2 : [27] Supprimé 03/05/2024 16:41:00

Page 2 : [28] Mis en forme 03/05/2024 16:41:00

Bordure : Haut: (Pas de bordure), Bas: (Pas de bordure), Gauche: (Pas de bordure), Droite: (Pas de bordure), Entre : (Pas de bordure)

Page 2 : [29] Supprimé 03/05/2024 16:41:00

Page 2 : [30] Supprimé 03/05/2024 16:41:00

Page 2 : [31] Mis en forme 03/05/2024 16:41:00

Exposant

Page 2 : [34] Mis en forme **03/05/2024 16:41:00**

Retrait : Gauche : 0 cm, Droite : 1,32 cm, Bordure : Haut: (Pas de bordure), Bas: (Pas de bordure), Gauche: (Pas de bordure), Droite: (Pas de bordure), Entre : (Pas de bordure)

Page 2 : [35] Mis en forme **03/05/2024 16:41:00**

Couleur de police : Couleur personnalisée(RVB(31;31;31))

Page 2 : [36] Mis en forme **03/05/2024 16:41:00**

Retrait : Gauche : 0 cm, Bordure : Haut: (Pas de bordure), Bas: (Pas de bordure), Gauche: (Pas de bordure), Droite: (Pas de bordure), Entre : (Pas de bordure)

Page 2 : [37] Mis en forme **03/05/2024 16:41:00**

Couleur de police : Couleur personnalisée(RVB(31;31;31))

Page 2 : [38] Mis en forme **03/05/2024 16:41:00**

Couleur de police : Couleur personnalisée(RVB(31;31;31))

Page 2 : [39] Mis en forme **03/05/2024 16:41:00**

Couleur de police : Couleur personnalisée(RVB(31;31;31))

Page 2 : [40] Mis en forme **03/05/2024 16:41:00**

Bordure : Haut: (Pas de bordure), Bas: (Pas de bordure), Gauche: (Pas de bordure), Droite: (Pas de bordure), Entre : (Pas de bordure)

Page 2 : [41] Supprimé **03/05/2024 16:41:00**

▼

Page 2 : [42] Supprimé **03/05/2024 16:41:00**

▼

Page 2 : [42] Supprimé **03/05/2024 16:41:00**

▼

Page 2 : [43] Supprimé **03/05/2024 16:41:00**

▼

Page 2 : [44] Mis en forme **03/05/2024 16:41:00**

Bordure : Haut: (Pas de bordure), Bas: (Pas de bordure), Gauche: (Pas de bordure), Droite: (Pas de bordure), Entre : (Pas de bordure)

Page 2 : [45] Supprimé **03/05/2024 16:41:00**

▼

Page 2 : [45] Supprimé **03/05/2024 16:41:00**

▼

Page 2 : [45] Supprimé **03/05/2024 16:41:00**

▼

▼
Page 2 : [47] Mis en forme **03/05/2024 16:41:00**

Bordure : Haut: (Pas de bordure), Bas: (Pas de bordure), Gauche: (Pas de bordure), Droite: (Pas de bordure), Entre : (Pas de bordure)

Page 2 : [48] Supprimé **03/05/2024 16:41:00**

▼
Page 2 : [48] Supprimé **03/05/2024 16:41:00**

▼
Page 2 : [49] Mis en forme **03/05/2024 16:41:00**

Couleur de police : Couleur personnalisée(RVB(31;31;31))

Page 3 : [50] Supprimé **03/05/2024 16:41:00**

▼
Page 3 : [51] Mis en forme **03/05/2024 16:41:00**

Bordure : Haut: (Pas de bordure), Bas: (Pas de bordure), Gauche: (Pas de bordure), Droite: (Pas de bordure), Entre : (Pas de bordure)

Page 3 : [52] Mis en forme **03/05/2024 16:41:00**

Police :10 pt

Page 3 : [52] Mis en forme **03/05/2024 16:41:00**

Police :10 pt

Page 3 : [53] Mis en forme **03/05/2024 16:41:00**

Police :10 pt

Page 3 : [54] Mis en forme **03/05/2024 16:41:00**

Police :10 pt

Page 3 : [54] Mis en forme **03/05/2024 16:41:00**

Police :10 pt

Page 3 : [55] Supprimé **03/05/2024 16:41:00**

▼
Page 3 : [56] Mis en forme **03/05/2024 16:41:00**

Couleur de police : Couleur personnalisée(RVB(31;31;31))

Page 3 : [57] Supprimé **03/05/2024 16:41:00**

▼
Page 3 : [58] Mis en forme **03/05/2024 16:41:00**

Anglais (G.B.)

Page 3 : [59] Mis en forme **03/05/2024 16:41:00**

▼
Page 3 : [61] Supprimé **03/05/2024 16:41:00**

▼
Page 3 : [61] Supprimé **03/05/2024 16:41:00**

▼
Page 3 : [62] Mis en forme **03/05/2024 16:41:00**

Couleur de police : Couleur personnalisée(RVB(31;31;31))

Page 3 : [63] Mis en forme **03/05/2024 16:41:00**

Espace Avant : 2 pt, Autoriser lignes veuves et orphelines, Bordure : Haut: (Pas de bordure), Bas: (Pas de bordure), Gauche: (Pas de bordure), Droite: (Pas de bordure), Entre : (Pas de bordure)

Page 3 : [64] Mis en forme **03/05/2024 16:41:00**

Couleur de police : Couleur personnalisée(RVB(31;31;31))

Page 3 : [65] Mis en forme **03/05/2024 16:41:00**

Couleur de police : Couleur personnalisée(RVB(31;31;31))

Page 3 : [66] Supprimé **03/05/2024 16:41:00**

▼
Page 3 : [66] Supprimé **03/05/2024 16:41:00**

▼
Page 3 : [66] Supprimé **03/05/2024 16:41:00**

▼
Page 3 : [67] Mis en forme **03/05/2024 16:41:00**

Police :Roboto, 9 pt, Gras, Couleur de police : Couleur personnalisée(RVB(31;31;31))

Page 3 : [68] Mis en forme **03/05/2024 16:41:00**

Droite : 1,42 cm, Bordure : Haut: (Pas de bordure), Bas: (Pas de bordure), Gauche: (Pas de bordure), Droite: (Pas de bordure), Entre : (Pas de bordure)

Page 3 : [69] Mis en forme **03/05/2024 16:41:00**

Anglais (G.B.)

Page 3 : [70] Supprimé **03/05/2024 16:41:00**

▼
Page 3 : [70] Supprimé **03/05/2024 16:41:00**

▼
Page 3 : [71] Supprimé **03/05/2024 16:41:00**

▼
Page 3 : [71] Supprimé **03/05/2024 16:41:00**

▼
Page 3 : [73] Supprimé

03/05/2024 16:41:00

▼
Page 3 : [73] Supprimé

03/05/2024 16:41:00

▼
Page 3 : [74] Supprimé

03/05/2024 16:41:00

▼
Page 3 : [74] Supprimé

03/05/2024 16:41:00

▼
Page 3 : [74] Supprimé

03/05/2024 16:41:00

▼
Page 3 : [75] Supprimé

03/05/2024 16:41:00

▼
Page 3 : [75] Supprimé

03/05/2024 16:41:00

▼
Page 4 : [76] Supprimé

03/05/2024 16:41:00

Page 4 : [77] Supprimé **03/05/2024 16:41:00**



Page 4 : [77] Supprimé **03/05/2024 16:41:00**



Page 4 : [78] Supprimé **03/05/2024 16:41:00**



Page 4 : [78] Supprimé **03/05/2024 16:41:00**



Page 4 : [78] Supprimé **03/05/2024 16:41:00**



Page 4 : [78] Supprimé **03/05/2024 16:41:00**



Page 4 : [78] Supprimé **03/05/2024 16:41:00**



Page 4 : [78] Supprimé **03/05/2024 16:41:00**



Page 4 : [78] Supprimé **03/05/2024 16:41:00**



Page 4 : [78] Supprimé **03/05/2024 16:41:00**



Page 4 : [78] Supprimé **03/05/2024 16:41:00**



Page 4 : [78] Supprimé **03/05/2024 16:41:00**



Page 4 : [79] Supprimé **03/05/2024 16:41:00**



Page 4 : [79] Supprimé **03/05/2024 16:41:00**



Page 4 : [79] Supprimé **03/05/2024 16:41:00**



Page 4 : [79] Supprimé **03/05/2024 16:41:00**

▼
Page 4 : [80] Supprimé **03/05/2024 16:41:00**

▼
Page 4 : [81] Supprimé **03/05/2024 16:41:00**

▼
Page 4 : [81] Supprimé **03/05/2024 16:41:00**

▼
Page 4 : [82] Supprimé **03/05/2024 16:41:00**

▼
Page 5 : [83] Supprimé **03/05/2024 16:41:00**

▼
Page 9 : [84] Supprimé **03/05/2024 16:41:00**

▼
Page 10 : [85] Supprimé **03/05/2024 16:41:00**

▼
Page 10 : [86] Supprimé **03/05/2024 16:41:00**

▼
Page 14 : [87] Supprimé **03/05/2024 16:41:00**

▼
Page 14 : [88] Mis en forme **03/05/2024 16:41:00**

Normal, Espace Avant : 12 pt, Après : 12 pt, Paragraphes solidaires, Bordure : Haut: (Pas de bordure), Bas: (Pas de bordure), Gauche: (Pas de bordure), Droite: (Pas de bordure), Entre : (Pas de bordure)

Page 14 : [89] Mis en forme **03/05/2024 16:41:00**

▼
Page 25 : [92] Supprimé **03/05/2024 16:41:00**

▼
Page 27 : [93] Supprimé **03/05/2024 16:41:00**

▼
Page 34 : [94] Supprimé **03/05/2024 16:41:00**

▼
Page 37 : [95] Mis en forme **03/05/2024 16:41:00**

Normal, Espace Avant : 12 pt, Après : 12 pt, Paragraphes solidaires, Bordure : Haut: (Pas de bordure), Bas: (Pas de bordure), Gauche: (Pas de bordure), Droite: (Pas de bordure), Entre : (Pas de bordure)

▼
Page 37 : [96] Supprimé **03/05/2024 16:41:00**

▼
Page 37 : [97] Supprimé **03/05/2024 16:41:00**

▼
Page 37 : [98] Supprimé **03/05/2024 16:41:00**

▼
Page 41 : [99] Supprimé **03/05/2024 16:41:00**

▼
Page 41 : [100] Supprimé **03/05/2024 16:41:00**

▼
Page 42 : [101] Supprimé **03/05/2024 16:41:00**

▼
Page 44 : [102] Supprimé **03/05/2024 16:41:00**

▼
Page 47 : [103] Supprimé **03/05/2024 16:41:00**

▼
Page 48 : [104] Supprimé **03/05/2024 16:41:00**

▼
Page 51 : [105] Supprimé **03/05/2024 16:41:00**

▼
Page 53 : [106] Mis en forme **03/05/2024 16:41:00**

Normal, Espace Avant : 12 pt, Après : 12 pt, Paragraphes solidaires, Bordure : Haut: (Pas de bordure), Bas: (Pas de bordure), Gauche: (Pas de bordure), Droite: (Pas de bordure), Entre : (Pas de bordure)

▼
Page 53 : [107] Supprimé **03/05/2024 16:41:00**

▼
Page 53 : [108] Supprimé **03/05/2024 16:41:00**

▼
Page 58 : [109] Supprimé **03/05/2024 16:41:00**

▼
Page 58 : [110] Supprimé **03/05/2024 16:41:00**

Page 64 : [113] Mis en forme **03/05/2024 16:41:00**

Normal, Retrait : Gauche : 0,63 cm, Hiérarchisation + Niveau : 1 + Style de numérotation : Puce + Alignement : 0 cm + Retrait : 0,63 cm, Bordure : Haut: (Pas de bordure), Bas: (Pas de bordure), Gauche: (Pas de bordure), Droite: (Pas de bordure), Entre

Page 64 : [114] Supprimé **03/05/2024 16:41:00**

Page 65 : [115] Supprimé **03/05/2024 16:41:00**

Page 65 : [116] Supprimé **03/05/2024 16:41:00**

Page 66 : [117] Supprimé **03/05/2024 16:41:00**

Page 67 : [118] Supprimé **03/05/2024 16:41:00**

Page 67 : [119] Mis en forme **03/05/2024 16:41:00**

Normal, Espace Avant : 24 pt, Après : 12 pt, Paragraphes solidaires, Bordure : Haut: (Pas de bordure), Bas: (Pas de bordure), Gauche: (Pas de bordure), Droite: (Pas de bordure), Entre : (Pas de bordure)

Page 68 : [120] Supprimé **03/05/2024 16:41:00**

Page 71 : [121] Supprimé **03/05/2024 16:41:00**

Page 123 : [122] Supprimé **03/05/2024 16:41:00**

Page 123 : [123] Supprimé **03/05/2024 16:41:00**

Page 123 : [124] Supprimé **03/05/2024 16:41:00**

Page 124 : [125] Supprimé **03/05/2024 16:41:00**

Page 126 : [126] Supprimé **03/05/2024 16:41:00**

Page 126 : [126] Supprimé **03/05/2024 16:41:00**

Page 126 : [126] Supprimé **03/05/2024 16:41:00**

Page 126 : [128] Mis en forme **03/05/2024 16:41:00**

Police :12 pt

Page 126 : [129] Tableau mis en forme **03/05/2024 16:41:00**

Tableau mis en forme

Page 126 : [130] Mis en forme **03/05/2024 16:41:00**

Droite, Bordure : Haut: (Pas de bordure), Bas: (Pas de bordure), Gauche: (Pas de bordure), Droite: (Pas de bordure), Entre : (Pas de bordure)

Page 126 : [131] Supprimé **03/05/2024 16:41:00**

▼

Page 126 : [132] Mis en forme **03/05/2024 16:41:00**

Bordure : Haut: (Pas de bordure), Bas: (Pas de bordure), Gauche: (Pas de bordure), Droite: (Pas de bordure), Entre : (Pas de bordure)

Page 126 : [133] Mis en forme **03/05/2024 16:41:00**

Police :Non Gras

Page 126 : [134] Supprimé **03/05/2024 16:41:00**

▼

Page 126 : [135] Mis en forme **03/05/2024 16:41:00**

Police :Non Gras

Page 126 : [136] Mis en forme **03/05/2024 16:41:00**

Bordure : Haut: (Pas de bordure), Bas: (Pas de bordure), Gauche: (Pas de bordure), Droite: (Pas de bordure), Entre : (Pas de bordure)

Page 126 : [137] Supprimé **03/05/2024 16:41:00**

▼

Page 126 : [138] Mis en forme **03/05/2024 16:41:00**

Police :Non Gras

Page 126 : [139] Mis en forme **03/05/2024 16:41:00**

Bordure : Haut: (Pas de bordure), Bas: (Pas de bordure), Gauche: (Pas de bordure), Droite: (Pas de bordure), Entre : (Pas de bordure)

Page 126 : [140] Mis en forme **03/05/2024 16:41:00**

Police :Non Gras

Page 126 : [141] Mis en forme **03/05/2024 16:41:00**

Bordure : Haut: (Pas de bordure), Bas: (Pas de bordure), Gauche: (Pas de bordure), Droite: (Pas de bordure), Entre : (Pas de bordure), Taquets de tabulation : Pas à 8,75 cm

Bordure : Haut: (Pas de bordure), Bas: (Pas de bordure), Gauche: (Pas de bordure), Droite: (Pas de bordure), Entre : (Pas de bordure)

Page 126 : [144] Mis en forme **03/05/2024 16:41:00**

Police :Non Gras

Page 126 : [145] Supprimé **03/05/2024 16:41:00**

Page 126 : [146] Mis en forme **03/05/2024 16:41:00**

Police :Non Gras

Page 126 : [147] Mis en forme **03/05/2024 16:41:00**

Bordure : Haut: (Pas de bordure), Bas: (Pas de bordure), Gauche: (Pas de bordure), Droite: (Pas de bordure), Entre : (Pas de bordure)

Page 126 : [148] Supprimé **03/05/2024 16:41:00**

Page 126 : [149] Mis en forme **03/05/2024 16:41:00**

Bordure : Haut: (Pas de bordure), Bas: (Pas de bordure), Gauche: (Pas de bordure), Droite: (Pas de bordure), Entre : (Pas de bordure)

Page 126 : [150] Mis en forme **03/05/2024 16:41:00**

Police :Non Gras

Page 126 : [151] Supprimé **03/05/2024 16:41:00**

Page 126 : [152] Mis en forme **03/05/2024 16:41:00**

Police :Non Gras

Page 126 : [153] Mis en forme **03/05/2024 16:41:00**

Bordure : Haut: (Pas de bordure), Bas: (Pas de bordure), Gauche: (Pas de bordure), Droite: (Pas de bordure), Entre : (Pas de bordure)

Page 126 : [154] Mis en forme **03/05/2024 16:41:00**

Police :9 pt

Page 126 : [155] Supprimé **03/05/2024 16:41:00**

Page 126 : [156] Mis en forme **03/05/2024 16:41:00**

Bordure : Haut: (Pas de bordure), Bas: (Pas de bordure), Gauche: (Pas de bordure), Droite: (Pas de bordure), Entre : (Pas de bordure)

Page 126 : [157] Mis en forme **03/05/2024 16:41:00**

Page 126 : [159] Supprimé **03/05/2024 16:41:00**

Page 126 : [160] Mis en forme **03/05/2024 16:41:00**

Police :Non Gras

Page 126 : [161] Supprimé **03/05/2024 16:41:00**

Page 126 : [162] Mis en forme **03/05/2024 16:41:00**

Police :Non Gras

Page 126 : [163] Supprimé **03/05/2024 16:41:00**

Page 126 : [164] Mis en forme **03/05/2024 16:41:00**

Bordure : Haut: (Pas de bordure), Bas: (Pas de bordure), Gauche: (Pas de bordure), Droite: (Pas de bordure), Entre : (Pas de bordure)

Page 126 : [165] Supprimé **03/05/2024 16:41:00**

Page 126 : [166] Mis en forme **03/05/2024 16:41:00**

Bordure : Haut: (Pas de bordure), Bas: (Pas de bordure), Gauche: (Pas de bordure), Droite: (Pas de bordure), Entre : (Pas de bordure)

Page 126 : [167] Supprimé **03/05/2024 16:41:00**

Page 126 : [168] Mis en forme **03/05/2024 16:41:00**

Bordure : Haut: (Pas de bordure), Bas: (Pas de bordure), Gauche: (Pas de bordure), Droite: (Pas de bordure), Entre : (Pas de bordure)

Page 126 : [169] Supprimé **03/05/2024 16:41:00**

Page 126 : [170] Mis en forme **03/05/2024 16:41:00**

Bordure : Haut: (Pas de bordure), Bas: (Pas de bordure), Gauche: (Pas de bordure), Droite: (Pas de bordure), Entre : (Pas de bordure)

Page 126 : [171] Supprimé **03/05/2024 16:41:00**

Land sources	50 [17-72]		51 [18-73]					
Geological (onshore)	38 [13-53]		38 [13-53]					
Wild animals	2 [1-3]		2 [1-3]					
Termites	9 [3-15]		10 [4-16]					
Wildfires	(**)		(**)					
Permafrost soils (direct)	1 [0-1]		1 [0-1]					
Vegetation	(*)		(*)					

Police :Gras

Page 126 : [174] Supprimé **03/05/2024 16:41:00**

▼
Page 126 : [175] Mis en forme **03/05/2024 16:41:00**

Bordure : Haut: (Pas de bordure), Bas: (Pas de bordure), Gauche: (Pas de bordure), Droite: (Pas de bordure), Entre : (Pas de bordure)

Page 126 : [176] Mis en forme **03/05/2024 16:41:00**

Bordure : Haut: (Pas de bordure), Bas: (Pas de bordure), Gauche: (Pas de bordure), Droite: (Pas de bordure), Entre : (Pas de bordure)

Page 126 : [177] Mis en forme **03/05/2024 16:41:00**

Police :Gras

Page 126 : [178] Supprimé **03/05/2024 16:41:00**

▼
Page 126 : [179] Mis en forme **03/05/2024 16:41:00**

Police :Gras

Page 126 : [180] Mis en forme **03/05/2024 16:41:00**

Gauche

Page 126 : [181] Mis en forme **03/05/2024 16:41:00**

Bordure : Haut: (Pas de bordure), Bas: (Pas de bordure), Gauche: (Pas de bordure), Droite: (Pas de bordure), Entre : (Pas de bordure)

Page 126 : [182] Mis en forme **03/05/2024 16:41:00**

Police :8 pt, Non Gras

Page 126 : [183] Mis en forme **03/05/2024 16:41:00**

Bordure : Haut: (Pas de bordure), Bas: (Pas de bordure), Gauche: (Pas de bordure), Droite: (Pas de bordure), Entre : (Pas de bordure)

Page 126 : [184] Supprimé **03/05/2024 16:41:00**

▼
Page 126 : [185] Mis en forme **03/05/2024 16:41:00**

Police :Gras

Page 126 : [186] Mis en forme **03/05/2024 16:41:00**

Bordure : Haut: (Pas de bordure), Bas: (Pas de bordure), Gauche: (Pas de bordure), Droite: (Pas de bordure), Entre : (Pas de bordure)

Police :Gras

Page 126 : [190] Mis en forme **03/05/2024 16:41:00**

Bordure : Haut: (Pas de bordure), Bas: (Pas de bordure), Gauche: (Pas de bordure), Droite: (Pas de bordure), Entre : (Pas de bordure)

Page 126 : [191] Supprimé **03/05/2024 16:41:00**

Page 126 : [192] Mis en forme **03/05/2024 16:41:00**

Police :Gras

Page 126 : [193] Mis en forme **03/05/2024 16:41:00**

Gauche

Page 126 : [194] Mis en forme **03/05/2024 16:41:00**

Bordure : Haut: (Pas de bordure), Bas: (Pas de bordure), Gauche: (Pas de bordure), Droite: (Pas de bordure), Entre : (Pas de bordure)

Page 126 : [195] Supprimé **03/05/2024 16:41:00**

Page 126 : [196] Mis en forme **03/05/2024 16:41:00**

Police :Gras

Page 126 : [197] Supprimé **03/05/2024 16:41:00**

Page 126 : [198] Mis en forme **03/05/2024 16:41:00**

Police :Gras

Page 126 : [199] Mis en forme **03/05/2024 16:41:00**

Bordure : Haut: (Pas de bordure), Bas: (Pas de bordure), Gauche: (Pas de bordure), Droite: (Pas de bordure), Entre : (Pas de bordure)

Page 126 : [200] Supprimé **03/05/2024 16:41:00**

Page 126 : [201] Mis en forme **03/05/2024 16:41:00**

Interligne : Multiple 1,15 li, Autoriser lignes veuves et orphelines, Bordure : Haut: (Pas de bordure), Bas: (Pas de bordure), Gauche: (Pas de bordure), Droite: (Pas de bordure), Entre : (Pas de bordure)

Page 126 : [202] Supprimé **03/05/2024 16:41:00**

Page 126 : [203] Supprimé **03/05/2024 16:41:00**

Page 126 : [206] Mis en forme **03/05/2024 16:41:00**

Police :Non Gras

Page 126 : [207] Tableau mis en forme **03/05/2024 16:41:00**

Tableau mis en forme

Page 126 : [208] Mis en forme **03/05/2024 16:41:00**

Bordure : Haut: (Pas de bordure), Bas: (Pas de bordure), Gauche: (Pas de bordure), Droite: (Pas de bordure), Entre : (Pas de bordure)

Page 126 : [209] Supprimé **03/05/2024 16:41:00**

▼

Page 126 : [210] Mis en forme **03/05/2024 16:41:00**

Police :Non Gras

Page 126 : [211] Supprimé **03/05/2024 16:41:00**

▼

Page 126 : [212] Mis en forme **03/05/2024 16:41:00**

Bordure : Haut: (Pas de bordure), Bas: (Pas de bordure), Gauche: (Pas de bordure), Droite: (Pas de bordure), Entre : (Pas de bordure)

Page 126 : [213] Mis en forme **03/05/2024 16:41:00**

Police :Non Gras

Page 126 : [214] Mis en forme **03/05/2024 16:41:00**

Bordure : Haut: (Pas de bordure), Bas: (Pas de bordure), Gauche: (Pas de bordure), Droite: (Pas de bordure), Entre : (Pas de bordure)

Page 126 : [215] Supprimé **03/05/2024 16:41:00**

▼

Page 126 : [216] Mis en forme **03/05/2024 16:41:00**

Bordure : Haut: (Pas de bordure), Bas: (Pas de bordure), Gauche: (Pas de bordure), Droite: (Pas de bordure), Entre : (Pas de bordure)

Page 126 : [217] Supprimé **03/05/2024 16:41:00**

▼

Page 126 : [218] Mis en forme **03/05/2024 16:41:00**

Bordure : Haut: (Pas de bordure), Bas: (Pas de bordure), Gauche: (Pas de bordure), Droite: (Pas de bordure), Entre : (Pas de bordure)

Page 126 : [219] Supprimé **03/05/2024 16:41:00**

▼

Page 126 : [222] Mis en forme **03/05/2024 16:41:00**

Bordure : Haut: (Pas de bordure), Bas: (Pas de bordure), Gauche: (Pas de bordure), Droite: (Pas de bordure), Entre : (Pas de bordure)

Page 126 : [223] Supprimé **03/05/2024 16:41:00**

▼

Page 126 : [224] Mis en forme **03/05/2024 16:41:00**

Bordure : Haut: (Pas de bordure), Bas: (Pas de bordure), Gauche: (Pas de bordure), Droite: (Pas de bordure), Entre : (Pas de bordure)

Page 126 : [225] Supprimé **03/05/2024 16:41:00**

▼

Page 126 : [226] Mis en forme **03/05/2024 16:41:00**

Bordure : Haut: (Pas de bordure), Bas: (Pas de bordure), Gauche: (Pas de bordure), Droite: (Pas de bordure), Entre : (Pas de bordure)

Page 126 : [227] Supprimé **03/05/2024 16:41:00**

▼

Page 126 : [227] Supprimé **03/05/2024 16:41:00**

▼

Page 126 : [228] Mis en forme **03/05/2024 16:41:00**

Bordure : Haut: (Pas de bordure), Bas: (Pas de bordure), Gauche: (Pas de bordure), Droite: (Pas de bordure), Entre : (Pas de bordure)

Page 126 : [229] Mis en forme **03/05/2024 16:41:00**

Non Exposant/ Indice

Page 126 : [230] Supprimé **03/05/2024 16:41:00**

▼

Page 126 : [231] Mis en forme **03/05/2024 16:41:00**

Police :8 pt

Page 126 : [232] Supprimé **03/05/2024 16:41:00**

▼

Page 126 : [233] Mis en forme **03/05/2024 16:41:00**

Bordure : Haut: (Pas de bordure), Bas: (Pas de bordure), Gauche: (Pas de bordure), Droite: (Pas de bordure), Entre : (Pas de bordure)

Page 126 : [234] Supprimé **03/05/2024 16:41:00**

▼

Page 126 : [235] Mis en forme **03/05/2024 16:41:00**

Bordure : Haut: (Pas de bordure), Bas: (Pas de bordure), Gauche: (Pas de bordure), Droite: (Pas de bordure), Entre : (Pas de bordure)

Page 126 : [237] Supprimé **03/05/2024 16:41:00**

Page 126 : [237] Supprimé **03/05/2024 16:41:00**

Page 126 : [238] Supprimé **03/05/2024 16:41:00**

Page 126 : [239] Supprimé **03/05/2024 16:41:00**

Page 126 : [240] Supprimé **03/05/2024 16:41:00**

Page 126 : [241] Supprimé **03/05/2024 16:41:00**

Page 126 : [242] Supprimé **03/05/2024 16:41:00**

Page 127 : [243] Supprimé **03/05/2024 16:41:00**

Page 127 : [243] Supprimé **03/05/2024 16:41:00**

Page 127 : [244] Mis en forme **03/05/2024 16:41:00**

Non Exposant/ Indice

Page 127 : [245] Supprimé **03/05/2024 16:41:00**

Page 127 : [246] Mis en forme **03/05/2024 16:41:00**

Bordure : Haut: (Pas de bordure), Bas: (Pas de bordure), Gauche: (Pas de bordure), Droite: (Pas de bordure), Entre : (Pas de bordure)

Page 127 : [247] Mis en forme **03/05/2024 16:41:00**

Non Exposant/ Indice

Page 127 : [248] Mis en forme **03/05/2024 16:41:00**

Police :Non Gras

Page 127 : [249] Mis en forme **03/05/2024 16:41:00**

Bordure : Haut: (Pas de bordure), Bas: (Pas de bordure), Gauche: (Pas de bordure), Droite: (Pas de bordure), Entre : (Pas de bordure)

Bordure : Haut: (Pas de bordure), Bas: (Pas de bordure), Gauche: (Pas de bordure), Droite: (Pas de bordure), Entre : (Pas de bordure)

Page 127 : [253] Mis en forme **03/05/2024 16:41:00**

Bordure : Haut: (Pas de bordure), Bas: (Pas de bordure), Gauche: (Pas de bordure), Droite: (Pas de bordure), Entre : (Pas de bordure)

Page 127 : [254] Mis en forme **03/05/2024 16:41:00**

Bordure : Haut: (Pas de bordure), Bas: (Pas de bordure), Gauche: (Pas de bordure), Droite: (Pas de bordure), Entre : (Pas de bordure)

Page 127 : [255] Mis en forme **03/05/2024 16:41:00**

Police :Non Gras

Page 127 : [256] Mis en forme **03/05/2024 16:41:00**

Bordure : Haut: (Pas de bordure), Bas: (Pas de bordure), Gauche: (Pas de bordure), Droite: (Pas de bordure), Entre : (Pas de bordure)

Page 127 : [257] Supprimé **03/05/2024 16:41:00**

Page 127 : [257] Supprimé **03/05/2024 16:41:00**

Page 127 : [258] Mis en forme **03/05/2024 16:41:00**

Police :Non Gras

Page 127 : [259] Mis en forme **03/05/2024 16:41:00**

Bordure : Haut: (Pas de bordure), Bas: (Pas de bordure), Gauche: (Pas de bordure), Droite: (Pas de bordure), Entre : (Pas de bordure)

Page 127 : [260] Supprimé **03/05/2024 16:41:00**

Page 127 : [261] Mis en forme **03/05/2024 16:41:00**

Bordure : Haut: (Pas de bordure), Bas: (Pas de bordure), Gauche: (Pas de bordure), Droite: (Pas de bordure), Entre : (Pas de bordure)

Page 127 : [262] Mis en forme **03/05/2024 16:41:00**

Police :Non Gras

Page 127 : [263] Mis en forme **03/05/2024 16:41:00**

Police :Non Gras

Page 127 : [264] Mis en forme **03/05/2024 16:41:00**

Bordure : Haut: (Pas de bordure), Bas: (Pas de bordure), Gauche: (Pas de bordure), Droite: (Pas de bordure), Entre : (Pas de bordure)

Page 127 : [267] Mis en forme **03/05/2024 16:41:00**

Bordure : Haut: (Pas de bordure), Bas: (Pas de bordure), Gauche: (Pas de bordure), Droite: (Pas de bordure), Entre : (Pas de bordure)

Page 127 : [268] Mis en forme **03/05/2024 16:41:00**

Police :Non Gras

Page 127 : [269] Mis en forme **03/05/2024 16:41:00**

Bordure : Haut: (Pas de bordure), Bas: (Pas de bordure), Gauche: (Pas de bordure), Droite: (Pas de bordure), Entre : (Pas de bordure)

Page 127 : [270] Supprimé **03/05/2024 16:41:00**

Page 127 : [271] Mis en forme **03/05/2024 16:41:00**

Bordure : Haut: (Pas de bordure), Bas: (Pas de bordure), Gauche: (Pas de bordure), Droite: (Pas de bordure), Entre : (Pas de bordure)

Page 127 : [272] Mis en forme **03/05/2024 16:41:00**

Police :Non Gras

Page 127 : [273] Mis en forme **03/05/2024 16:41:00**

Bordure : Haut: (Pas de bordure), Bas: (Pas de bordure), Gauche: (Pas de bordure), Droite: (Pas de bordure), Entre : (Pas de bordure)

Page 127 : [274] Supprimé **03/05/2024 16:41:00**

Page 127 : [275] Mis en forme **03/05/2024 16:41:00**

Bordure : Haut: (Pas de bordure), Bas: (Pas de bordure), Gauche: (Pas de bordure), Droite: (Pas de bordure), Entre : (Pas de bordure)

Page 127 : [276] Mis en forme **03/05/2024 16:41:00**

Police :Gras

Page 127 : [277] Supprimé **03/05/2024 16:41:00**

Page 127 : [278] Mis en forme **03/05/2024 16:41:00**

Bordure : Haut: (Pas de bordure), Bas: (Pas de bordure), Gauche: (Pas de bordure), Droite: (Pas de bordure), Entre : (Pas de bordure)

Page 127 : [279] Supprimé **03/05/2024 16:41:00**

Page 127 : [280] Mis en forme **03/05/2024 16:41:00**

Police :Non Gras

Page 127 : [283] Mis en forme **03/05/2024 16:41:00**

Police :Non Gras

Page 127 : [284] Supprimé **03/05/2024 16:41:00**

▼

Page 127 : [285] Supprimé **03/05/2024 16:41:00**

▼

Page 127 : [286] Mis en forme **03/05/2024 16:41:00**

Police :Non Gras

Page 127 : [287] Supprimé **03/05/2024 16:41:00**

▼

Page 127 : [288] Tableau mis en forme **03/05/2024 16:41:00**

Tableau mis en forme

Page 127 : [289] Mis en forme **03/05/2024 16:41:00**

Bordure : Haut: (Pas de bordure), Bas: (Pas de bordure), Gauche: (Pas de bordure), Droite: (Pas de bordure), Entre : (Pas de bordure)

Page 127 : [290] Supprimé **03/05/2024 16:41:00**

▼

Page 127 : [291] Mis en forme **03/05/2024 16:41:00**

Bordure : Haut: (Pas de bordure), Bas: (Pas de bordure), Gauche: (Pas de bordure), Droite: (Pas de bordure), Entre : (Pas de bordure)

Page 127 : [292] Mis en forme **03/05/2024 16:41:00**

Bordure : Haut: (Pas de bordure), Bas: (Pas de bordure), Gauche: (Pas de bordure), Droite: (Pas de bordure), Entre : (Pas de bordure)

Page 127 : [293] Mis en forme **03/05/2024 16:41:00**

Bordure : Haut: (Pas de bordure), Bas: (Pas de bordure), Gauche: (Pas de bordure), Droite: (Pas de bordure), Entre : (Pas de bordure)

Page 127 : [294] Supprimé **03/05/2024 16:41:00**

▼

Page 127 : [294] Supprimé **03/05/2024 16:41:00**

▼

Page 127 : [295] Mis en forme **03/05/2024 16:41:00**

Bordure : Haut: (Pas de bordure), Bas: (Pas de bordure), Gauche: (Pas de bordure), Droite: (Pas de bordure), Entre : (Pas de bordure)

Page 127 : [299] Mis en forme **03/05/2024 16:41:00**

Bordure : Haut: (Pas de bordure), Bas: (Pas de bordure), Gauche: (Pas de bordure), Droite: (Pas de bordure), Entre : (Pas de bordure)

Page 127 : [300] Supprimé **03/05/2024 16:41:00**

Page 127 : [301] Mis en forme **03/05/2024 16:41:00**

Bordure : Haut: (Pas de bordure), Bas: (Pas de bordure), Gauche: (Pas de bordure), Droite: (Pas de bordure), Entre : (Pas de bordure)

Page 127 : [302] Supprimé **03/05/2024 16:41:00**

Page 127 : [303] Mis en forme **03/05/2024 16:41:00**

Police :Non Gras

Page 127 : [304] Mis en forme **03/05/2024 16:41:00**

Bordure : Haut: (Pas de bordure), Bas: (Pas de bordure), Gauche: (Pas de bordure), Droite: (Pas de bordure), Entre : (Pas de bordure)

Page 127 : [305] Mis en forme **03/05/2024 16:41:00**

Bordure : Haut: (Pas de bordure), Bas: (Pas de bordure), Gauche: (Pas de bordure), Droite: (Pas de bordure), Entre : (Pas de bordure)

Page 127 : [306] Supprimé **03/05/2024 16:41:00**

Page 127 : [306] Supprimé **03/05/2024 16:41:00**

Page 127 : [307] Mis en forme **03/05/2024 16:41:00**

Police :Non Gras

Page 127 : [308] Mis en forme **03/05/2024 16:41:00**

Police :Gras

Page 127 : [309] Supprimé **03/05/2024 16:41:00**

Page 127 : [309] Supprimé **03/05/2024 16:41:00**

Page 127 : [310] Supprimé **03/05/2024 16:41:00**

Page 127 : [310] Supprimé **03/05/2024 16:41:00**

Page 127 : [311] Mis en forme **03/05/2024 16:41:00**

Page 127 : [313] Supprimé **03/05/2024 16:41:00**

▼
Page 127 : [314] Mis en forme **03/05/2024 16:41:00**

Police :Gras

Page 127 : [315] Mis en forme **03/05/2024 16:41:00**

Bordure : Haut: (Pas de bordure), Bas: (Pas de bordure), Gauche: (Pas de bordure), Droite: (Pas de bordure), Entre : (Pas de bordure)

Page 127 : [316] Mis en forme **03/05/2024 16:41:00**

Bordure : Haut: (Pas de bordure), Bas: (Pas de bordure), Gauche: (Pas de bordure), Droite: (Pas de bordure), Entre : (Pas de bordure)

Page 127 : [317] Supprimé **03/05/2024 16:41:00**

▼
Page 127 : [318] Supprimé **03/05/2024 16:41:00**

▼
Page 127 : [319] Mis en forme **03/05/2024 16:41:00**

Bordure : Haut: (Pas de bordure), Bas: (Pas de bordure), Gauche: (Pas de bordure), Droite: (Pas de bordure), Entre : (Pas de bordure)

Page 127 : [320] Supprimé **03/05/2024 16:41:00**

▼
Page 127 : [321] Tableau mis en forme **03/05/2024 16:41:00**

Tableau mis en forme

Page 127 : [322] Mis en forme **03/05/2024 16:41:00**

Bordure : Haut: (Pas de bordure), Bas: (Pas de bordure), Gauche: (Pas de bordure), Droite: (Pas de bordure), Entre : (Pas de bordure)

Page 127 : [323] Supprimé **03/05/2024 16:41:00**

▼
Page 127 : [324] Mis en forme **03/05/2024 16:41:00**

Police :8 pt, Gras

Page 127 : [325] Supprimé **03/05/2024 16:41:00**

▼
Page 127 : [326] Mis en forme **03/05/2024 16:41:00**

Bordure : Haut: (Pas de bordure), Bas: (Pas de bordure), Gauche: (Pas de bordure), Droite: (Pas de bordure), Entre : (Pas de bordure)

Page 127 : [330] Supprimé **03/05/2024 16:41:00**



Page 127 : [331] Mis en forme **03/05/2024 16:41:00**

Police :Non Gras

Page 127 : [332] Supprimé **03/05/2024 16:41:00**



Page 127 : [333] Supprimé **03/05/2024 16:41:00**



Page 127 : [334] Mis en forme **03/05/2024 16:41:00**

Police :Non Gras

Page 127 : [335] Mis en forme **03/05/2024 16:41:00**

Bordure : Haut: (Pas de bordure), Bas: (Pas de bordure), Gauche: (Pas de bordure), Droite: (Pas de bordure), Entre : (Pas de bordure)

Page 127 : [336] Supprimé **03/05/2024 16:41:00**



Page 127 : [337] Mis en forme **03/05/2024 16:41:00**

Police :Gras

Page 127 : [338] Supprimé **03/05/2024 16:41:00**



Page 127 : [339] Mis en forme **03/05/2024 16:41:00**

Bordure : Haut: (Pas de bordure), Bas: (Pas de bordure), Gauche: (Pas de bordure), Droite: (Pas de bordure), Entre : (Pas de bordure)

Page 127 : [340] Supprimé **03/05/2024 16:41:00**



Page 127 : [341] Mis en forme **03/05/2024 16:41:00**

Bordure : Haut: (Pas de bordure), Bas: (Pas de bordure), Gauche: (Pas de bordure), Droite: (Pas de bordure), Entre : (Pas de bordure)

Page 127 : [342] Mis en forme **03/05/2024 16:41:00**

Police :8 pt, Gras

Page 127 : [343] Supprimé **03/05/2024 16:41:00**



Page 127 : [344] Supprimé **03/05/2024 16:41:00**



Page 127 : [347] Supprimé **03/05/2024 16:41:00**



Page 127 : [348] Mis en forme **03/05/2024 16:41:00**

Bordure : Haut: (Pas de bordure), Bas: (Pas de bordure), Gauche: (Pas de bordure), Droite: (Pas de bordure), Entre : (Pas de bordure)

Page 127 : [349] Mis en forme **03/05/2024 16:41:00**

Couleur de police : Noir

Page 127 : [350] Mis en forme **03/05/2024 16:41:00**

Bordure : Haut: (Pas de bordure), Bas: (Pas de bordure), Gauche: (Pas de bordure), Droite: (Pas de bordure), Entre : (Pas de bordure)

Page 127 : [351] Mis en forme **03/05/2024 16:41:00**

Bordure : Haut: (Pas de bordure), Bas: (Pas de bordure), Gauche: (Pas de bordure), Droite: (Pas de bordure), Entre : (Pas de bordure)

Page 127 : [352] Mis en forme **03/05/2024 16:41:00**

Bordure : Haut: (Pas de bordure), Bas: (Pas de bordure), Gauche: (Pas de bordure), Droite: (Pas de bordure), Entre : (Pas de bordure)

Page 127 : [353] Mis en forme **03/05/2024 16:41:00**

Police :Non Gras

Page 127 : [354] Supprimé **03/05/2024 16:41:00**



Page 127 : [354] Supprimé **03/05/2024 16:41:00**



Page 127 : [355] Supprimé **03/05/2024 16:41:00**



Page 127 : [356] Mis en forme **03/05/2024 16:41:00**

Bordure : Haut: (Pas de bordure), Bas: (Pas de bordure), Gauche: (Pas de bordure), Droite: (Pas de bordure), Entre : (Pas de bordure)

Page 127 : [357] Mis en forme **03/05/2024 16:41:00**

Bordure : Haut: (Pas de bordure), Bas: (Pas de bordure), Gauche: (Pas de bordure), Droite: (Pas de bordure), Entre : (Pas de bordure)

Page 127 : [358] Supprimé **03/05/2024 16:41:00**



Page 127 : [358] Supprimé **03/05/2024 16:41:00**

Page 128 : [360] Mis en forme 03/05/2024 16:41:00

Couleur de police : Rouge

Page 128 : [361] Supprimé 03/05/2024 16:41:00

Page 128 : [362] Mis en forme 03/05/2024 16:41:00

Anglais (G.B.)

Page 128 : [363] Supprimé 03/05/2024 16:41:00

Page 128 : [364] Mis en forme 03/05/2024 16:41:00

Anglais (G.B.)

Page 128 : [365] Mis en forme 03/05/2024 16:41:00

Anglais (G.B.)

Page 128 : [366] Mis en forme 03/05/2024 16:41:00

Anglais (G.B.)

Page 128 : [367] Mis en forme 03/05/2024 16:41:00

Anglais (G.B.)

Page 128 : [368] Mis en forme 03/05/2024 16:41:00

Anglais (G.B.)

Page 128 : [369] Mis en forme 03/05/2024 16:41:00

Anglais (G.B.)

Page 128 : [370] Mis en forme 03/05/2024 16:41:00

Anglais (G.B.)

Page 128 : [371] Supprimé 03/05/2024 16:41:00

Page 128 : [372] Mis en forme 03/05/2024 16:41:00

Anglais (G.B.)

Page 128 : [373] Mis en forme 03/05/2024 16:41:00

Anglais (G.B.)

Page 128 : [374] Mis en forme 03/05/2024 16:41:00

Anglais (G.B.)

Page 128 : [375] Mis en forme 03/05/2024 16:41:00

Anglais (G.B.)

Page 128 : [376] Mis en forme 03/05/2024 16:41:00

Anglais (G.B.)

Page 128 : [379] Mis en forme 03/05/2024 16:41:00

Anglais (G.B.)

Page 128 : [380] Mis en forme 03/05/2024 16:41:00

Anglais (G.B.)

Page 128 : [381] Mis en forme 03/05/2024 16:41:00

Anglais (G.B.)

Page 128 : [382] Mis en forme 03/05/2024 16:41:00

Anglais (G.B.), Indice

Page 128 : [383] Mis en forme 03/05/2024 16:41:00

Anglais (G.B.)

Page 128 : [383] Mis en forme 03/05/2024 16:41:00

Anglais (G.B.)

Page 128 : [384] Mis en forme 03/05/2024 16:41:00

Anglais (G.B.)

Page 128 : [385] Mis en forme 03/05/2024 16:41:00

Anglais (G.B.)

Page 128 : [386] Mis en forme 03/05/2024 16:41:00

Anglais (G.B.)

Page 128 : [387] Mis en forme 03/05/2024 16:41:00

Anglais (G.B.)

Page 128 : [388] Mis en forme 03/05/2024 16:41:00

Anglais (G.B.)

Page 128 : [389] Mis en forme 03/05/2024 16:41:00

Anglais (G.B.)

Page 128 : [390] Mis en forme 03/05/2024 16:41:00

Anglais (G.B.)

Page 128 : [391] Mis en forme 03/05/2024 16:41:00

Anglais (G.B.)

Page 128 : [392] Mis en forme 03/05/2024 16:41:00

Anglais (G.B.)

Page 128 : [393] Mis en forme 03/05/2024 16:41:00

Anglais (G.B.)

Page 128 : [396] Mis en forme 03/05/2024 16:41:00

Anglais (G.B.)

Page 128 : [397] Mis en forme 03/05/2024 16:41:00

Anglais (G.B.)

Page 128 : [398] Mis en forme 03/05/2024 16:41:00

Anglais (G.B.)

Page 128 : [399] Supprimé 03/05/2024 16:41:00



Page 128 : [400] Mis en forme 03/05/2024 16:41:00

Anglais (G.B.)

Page 128 : [401] Mis en forme 03/05/2024 16:41:00

Anglais (G.B.)

Page 128 : [402] Mis en forme 03/05/2024 16:41:00

Anglais (G.B.)

Page 128 : [403] Supprimé 03/05/2024 16:41:00



Page 128 : [404] Mis en forme 03/05/2024 16:41:00

Anglais (G.B.)

Page 128 : [405] Mis en forme 03/05/2024 16:41:00

Droite

Page 128 : [406] Mis en forme 03/05/2024 16:41:00

Anglais (G.B.)

Page 128 : [407] Mis en forme 03/05/2024 16:41:00

Autoriser lignes veuves et orphelines

Page 128 : [408] Mis en forme 03/05/2024 16:41:00

Anglais (G.B.)

Page 128 : [409] Mis en forme 03/05/2024 16:41:00

Anglais (G.B.)

Page 128 : [410] Mis en forme 03/05/2024 16:41:00

Anglais (G.B.)

Page 128 : [413] Mis en forme 03/05/2024 16:41:00

Anglais (G.B.)

Page 128 : [414] Cellules supprimées 03/05/2024 16:41:00

Cellules supprimées

Page 128 : [415] Cellules supprimées 03/05/2024 16:41:00

Cellules supprimées

Page 128 : [416] Cellules supprimées 03/05/2024 16:41:00

Cellules supprimées

Page 128 : [417] Supprimé 03/05/2024 16:41:00

Page 129 : [418] Mis en forme 03/05/2024 16:41:00

Anglais (G.B.)

Page 129 : [419] Mis en forme 03/05/2024 16:41:00

Anglais (G.B.)

Page 129 : [420] Supprimé 03/05/2024 16:41:00

Page 129 : [420] Supprimé 03/05/2024 16:41:00

Page 129 : [421] Mis en forme 03/05/2024 16:41:00

Police :9 pt

Page 129 : [422] Mis en forme 03/05/2024 16:41:00

Retrait : Première ligne : 0 cm, Bordure : Haut: (Pas de bordure), Bas: (Pas de bordure), Gauche: (Pas de bordure), Droite: (Pas de bordure), Entre : (Pas de bordure)

Page 129 : [423] Mis en forme 03/05/2024 16:41:00

Police :9 pt

Page 129 : [424] Mis en forme 03/05/2024 16:41:00

Autoriser lignes veuves et orphelines

Page 129 : [425] Mis en forme 03/05/2024 16:41:00

Police :9 pt

Page 129 : [426] Mis en forme 03/05/2024 16:41:00

Police :9 pt

Page 129 : [427] Mis en forme 03/05/2024 16:41:00

Page 129 : [429] Mis en forme **03/05/2024 16:41:00**

Centré, Bordure : Haut: (Pas de bordure), Bas: (Pas de bordure), Gauche: (Pas de bordure), Droite: (Pas de bordure), Entre : (Pas de bordure)

Page 129 : [430] Cellules supprimées **03/05/2024 16:41:00**

Cellules supprimées

Page 129 : [431] Cellules supprimées **03/05/2024 16:41:00**

Cellules supprimées

Page 129 : [432] Cellules supprimées **03/05/2024 16:41:00**

Cellules supprimées

Page 129 : [433] Cellules supprimées **03/05/2024 16:41:00**

Cellules supprimées

Page 129 : [434] Cellules supprimées **03/05/2024 16:41:00**

Cellules supprimées

Page 129 : [435] Cellules supprimées **03/05/2024 16:41:00**

Cellules supprimées

Page 129 : [436] Supprimé **03/05/2024 16:41:00**

Page 129 : [437] Mis en forme **03/05/2024 16:41:00**

Bordure : Haut: (Pas de bordure), Bas: (Pas de bordure), Gauche: (Pas de bordure), Droite: (Pas de bordure), Entre : (Pas de bordure)

Page 129 : [438] Mis en forme **03/05/2024 16:41:00**

Police :9 pt, Gras, Non Italique, Anglais (G.B.)

Page 129 : [439] Mis en forme **03/05/2024 16:41:00**

Police :9 pt, Non Gras, Italique

Page 129 : [440] Mis en forme **03/05/2024 16:41:00**

Police :9 pt, Non Gras, Italique

Page 129 : [440] Mis en forme **03/05/2024 16:41:00**

Police :9 pt, Non Gras, Italique

Page 129 : [441] Supprimé **03/05/2024 16:41:00**

Page 129 : [442] Mis en forme **03/05/2024 16:41:00**

Police :9 pt

Page 129 : [444] Mis en forme 03/05/2024 16:41:00

Police :9 pt, Italique

Page 129 : [445] Supprimé 03/05/2024 16:41:00

Page 129 : [446] Mis en forme 03/05/2024 16:41:00

Police :9 pt, Non Gras, Italique

Page 129 : [447] Supprimé 03/05/2024 16:41:00

Page 129 : [448] Mis en forme 03/05/2024 16:41:00

Autoriser lignes veuves et orphelines

Page 129 : [449] Mis en forme 03/05/2024 16:41:00

Police :9 pt, Gras

Page 129 : [450] Supprimé 03/05/2024 16:41:00

Page 129 : [451] Mis en forme 03/05/2024 16:41:00

Autoriser lignes veuves et orphelines, Bordure : Haut: (Pas de bordure), Bas: (Pas de bordure), Gauche: (Pas de bordure), Droite: (Pas de bordure), Entre : (Pas de bordure)

Page 129 : [452] Mis en forme 03/05/2024 16:41:00

Police :9 pt, Gras

Page 129 : [453] Supprimé 03/05/2024 16:41:00

Page 129 : [454] Mis en forme 03/05/2024 16:41:00

Police :9 pt, Gras

Page 129 : [454] Mis en forme 03/05/2024 16:41:00

Police :9 pt, Gras

Page 129 : [455] Supprimé 03/05/2024 16:41:00

Page 129 : [456] Mis en forme 03/05/2024 16:41:00

Police :9 pt, Gras

Page 129 : [456] Mis en forme 03/05/2024 16:41:00

Police :9 pt, Gras

Page 129 : [457] Mis en forme 03/05/2024 16:41:00

Police :9 pt

Page 129 : [458] Mis en forme 03/05/2024 16:41:00

Centré, Bordure : Haut: (Pas de bordure), Bas: (Pas de bordure), Gauche: (Pas de bordure), Droite: (Pas de

Cellules supprimées

Page 129 : [461] Cellules supprimées 03/05/2024 16:41:00

Cellules supprimées

Page 129 : [462] Cellules supprimées 03/05/2024 16:41:00

Cellules supprimées

Page 129 : [463] Cellules supprimées 03/05/2024 16:41:00

Cellules supprimées

Page 129 : [464] Cellules supprimées 03/05/2024 16:41:00

Cellules supprimées

Page 129 : [465] Supprimé 03/05/2024 16:41:00

Page 129 : [466] Mis en forme 03/05/2024 16:41:00

Bordure : Haut: (Pas de bordure), Bas: (Pas de bordure), Gauche: (Pas de bordure), Droite: (Pas de bordure), Entre : (Pas de bordure)

Page 129 : [467] Mis en forme 03/05/2024 16:41:00

Police :9 pt, Gras

Page 129 : [468] Mis en forme 03/05/2024 16:41:00

Police :9 pt, Non Gras, Italique

Page 129 : [469] Mis en forme 03/05/2024 16:41:00

Police :9 pt, Italique

Page 129 : [470] Supprimé 03/05/2024 16:41:00

Page 129 : [471] Mis en forme 03/05/2024 16:41:00

Police :9 pt, Italique

Page 129 : [472] Mis en forme 03/05/2024 16:41:00

Police :9 pt, Non Gras, Italique

Page 129 : [473] Mis en forme 03/05/2024 16:41:00

Police :9 pt, Italique

Page 129 : [474] Supprimé 03/05/2024 16:41:00

Page 129 : [475] Mis en forme 03/05/2024 16:41:00

Police :9 pt, Non Gras, Italique

Page 129 : [478] Supprimé 03/05/2024 16:41:00

▼ **Page 129 : [479] Mis en forme** 03/05/2024 16:41:00

Police :9 pt

Page 129 : [479] Mis en forme 03/05/2024 16:41:00

Police :9 pt

Page 129 : [480] Supprimé 03/05/2024 16:41:00

▼ **Page 129 : [481] Mis en forme** 03/05/2024 16:41:00

Police :9 pt, Gras

Page 129 : [481] Mis en forme 03/05/2024 16:41:00

Police :9 pt, Gras

Page 129 : [482] Supprimé 03/05/2024 16:41:00

▼ **Page 129 : [483] Mis en forme** 03/05/2024 16:41:00

Police :9 pt

Page 129 : [484] Mis en forme 03/05/2024 16:41:00

Police :9 pt

Page 129 : [485] Mis en forme 03/05/2024 16:41:00

Centré, Bordure : Haut: (Pas de bordure), Bas: (Pas de bordure), Gauche: (Pas de bordure), Droite: (Pas de bordure), Entre : (Pas de bordure)

Page 129 : [486] Mis en forme 03/05/2024 16:41:00

Police :9 pt, Non Gras, Italique

Page 129 : [487] Cellules supprimées 03/05/2024 16:41:00

Cellules supprimées

Page 129 : [488] Cellules supprimées 03/05/2024 16:41:00

Cellules supprimées

Page 129 : [489] Cellules supprimées 03/05/2024 16:41:00

Cellules supprimées

Page 129 : [490] Cellules supprimées 03/05/2024 16:41:00

Cellules supprimées

Page 129 : [491] Cellules supprimées 03/05/2024 16:41:00

Cellules supprimées

Page 129 : [492] Cellules supprimées 03/05/2024 16:41:00

Retrait : Première ligne : 0 cm, Bordure : Haut: (Pas de bordure), Bas: (Pas de bordure), Gauche: (Pas de bordure), Droite: (Pas de bordure), Entre : (Pas de bordure)

Page 148 : [495] Mis en forme **03/05/2024 16:41:00**

Police :9 pt

Page 130 : [496] Mis en forme **03/05/2024 16:41:00**

Autoriser lignes veuves et orphelines

Page 148 : [497] Mis en forme **03/05/2024 16:41:00**

Police :9 pt

Page 148 : [498] Mis en forme **03/05/2024 16:41:00**

Police :9 pt

Page 148 : [499] Mis en forme **03/05/2024 16:41:00**

Bordure : Haut: (Pas de bordure), Bas: (Pas de bordure), Gauche: (Pas de bordure), Droite: (Pas de bordure), Entre : (Pas de bordure)

Page 148 : [500] Mis en forme **03/05/2024 16:41:00**

Police :9 pt

Page 148 : [501] Mis en forme **03/05/2024 16:41:00**

Centré, Bordure : Haut: (Pas de bordure), Bas: (Pas de bordure), Gauche: (Pas de bordure), Droite: (Pas de bordure), Entre : (Pas de bordure)

Page 148 : [502] Cellules supprimées **03/05/2024 16:41:00**

Cellules supprimées

Page 148 : [503] Cellules supprimées **03/05/2024 16:41:00**

Cellules supprimées

Page 148 : [504] Cellules supprimées **03/05/2024 16:41:00**

Cellules supprimées

Page 148 : [505] Cellules supprimées **03/05/2024 16:41:00**

Cellules supprimées

Page 148 : [506] Cellules supprimées **03/05/2024 16:41:00**

Cellules supprimées

Page 148 : [507] Cellules supprimées **03/05/2024 16:41:00**

Cellules supprimées

Page 130 : [508] Supprimé **03/05/2024 16:41:00**

Police :9 pt, Gras

Page 130 : [511] Mis en forme 03/05/2024 16:41:00

Police :9 pt, Non Gras, Italique

Page 130 : [511] Mis en forme 03/05/2024 16:41:00

Police :9 pt, Non Gras, Italique

Page 130 : [512] Mis en forme 03/05/2024 16:41:00

Police :9 pt, Italique

Page 130 : [513] Supprimé 03/05/2024 16:41:00



Page 130 : [514] Mis en forme 03/05/2024 16:41:00

Police :9 pt, Non Gras, Italique

Page 130 : [515] Mis en forme 03/05/2024 16:41:00

Police :9 pt, Italique

Page 130 : [516] Mis en forme 03/05/2024 16:41:00

Police :9 pt, Italique

Page 130 : [517] Supprimé 03/05/2024 16:41:00



Page 130 : [518] Mis en forme 03/05/2024 16:41:00

Police :9 pt, Italique

Page 130 : [519] Supprimé 03/05/2024 16:41:00

Page 130 : [520] Mis en forme 03/05/2024 16:41:00

Police :10 pt, Gras

Page 130 : [521] Supprimé 03/05/2024 16:41:00

Page 130 : [522] Mis en forme 03/05/2024 16:41:00

Police :10 pt, Gras

Page 130 : [522] Mis en forme 03/05/2024 16:41:00

Police :10 pt, Gras

Page 130 : [523] Supprimé 03/05/2024 16:41:00

Page 130 : [524] Mis en forme 03/05/2024 16:41:00

Police :10 pt, Gras

Page 130 : [524] Mis en forme 03/05/2024 16:41:00

Page 130 : [527] Mis en forme 03/05/2024 16:41:00

Police :9 pt

Page 130 : [528] Mis en forme 03/05/2024 16:41:00

Centré, Bordure : Haut: (Pas de bordure), Bas: (Pas de bordure), Gauche: (Pas de bordure), Droite: (Pas de bordure), Entre : (Pas de bordure)

Page 130 : [529] Mis en forme 03/05/2024 16:41:00

Police :9 pt, Non Gras, Italique

Page 130 : [530] Cellules supprimées 03/05/2024 16:41:00

Cellules supprimées

Page 130 : [531] Cellules supprimées 03/05/2024 16:41:00

Cellules supprimées

Page 130 : [532] Cellules supprimées 03/05/2024 16:41:00

Cellules supprimées

Page 130 : [533] Cellules supprimées 03/05/2024 16:41:00

Cellules supprimées

Page 130 : [534] Cellules supprimées 03/05/2024 16:41:00

Cellules supprimées

Page 130 : [535] Cellules supprimées 03/05/2024 16:41:00

Cellules supprimées

Page 130 : [536] Mis en forme 03/05/2024 16:41:00

Police :9 pt

Page 130 : [537] Mis en forme 03/05/2024 16:41:00

Bordure : Haut: (Pas de bordure), Bas: (Pas de bordure), Gauche: (Pas de bordure), Droite: (Pas de bordure), Entre : (Pas de bordure)

Page 130 : [538] Supprimé 03/05/2024 16:41:00

Page 130 : [539] Mis en forme 03/05/2024 16:41:00

Police :9 pt, Gras

Page 130 : [540] Mis en forme 03/05/2024 16:41:00

Police :9 pt

Page 130 : [541] Mis en forme 03/05/2024 16:41:00

Autoriser lignes veuves et orphelines

Page 130 : [544] Supprimé **03/05/2024 16:41:00**



Page 130 : [545] Mis en forme **03/05/2024 16:41:00**

Bordure : Haut: (Pas de bordure), Bas: (Pas de bordure), Gauche: (Pas de bordure), Droite: (Pas de bordure), Entre : (Pas de bordure)

Page 130 : [546] Mis en forme **03/05/2024 16:41:00**

Police :9 pt

Page 130 : [546] Mis en forme **03/05/2024 16:41:00**

Police :9 pt

Page 130 : [547] Supprimé **03/05/2024 16:41:00**



Page 130 : [548] Mis en forme **03/05/2024 16:41:00**

Police :9 pt

Page 130 : [549] Supprimé **03/05/2024 16:41:00**



Page 130 : [550] Mis en forme **03/05/2024 16:41:00**

Police :9 pt

Page 130 : [551] Supprimé **03/05/2024 16:41:00**



Page 130 : [552] Mis en forme **03/05/2024 16:41:00**

Police :9 pt

Page 130 : [553] Supprimé **03/05/2024 16:41:00**



Page 130 : [554] Mis en forme **03/05/2024 16:41:00**

Police :9 pt

Page 130 : [555] Supprimé **03/05/2024 16:41:00**



Page 130 : [556] Mis en forme **03/05/2024 16:41:00**

Police :9 pt, Non Gras

Page 131 : [557] Supprimé **03/05/2024 16:41:00**



Page 131 : [557] Supprimé **03/05/2024 16:41:00**

Police :10 pt

Page 131 : [559] Tableau mis en forme 03/05/2024 16:41:00

Tableau mis en forme

Page 131 : [560] Mis en forme 03/05/2024 16:41:00

Police :10 pt

Page 131 : [561] Mis en forme 03/05/2024 16:41:00

Police :10 pt

Page 131 : [561] Mis en forme 03/05/2024 16:41:00

Police :10 pt

Page 131 : [562] Mis en forme 03/05/2024 16:41:00

Police :10 pt

Page 131 : [563] Mis en forme 03/05/2024 16:41:00

Police :10 pt

Page 131 : [564] Mis en forme 03/05/2024 16:41:00

Police :10 pt

Page 131 : [565] Mis en forme 03/05/2024 16:41:00

Police :10 pt, Gras

Page 131 : [565] Mis en forme 03/05/2024 16:41:00

Police :10 pt, Gras

Page 131 : [566] Mis en forme 03/05/2024 16:41:00

Police :10 pt

Page 131 : [567] Mis en forme 03/05/2024 16:41:00

Police :10 pt

Page 131 : [568] Mis en forme 03/05/2024 16:41:00

Police :10 pt

Page 131 : [569] Mis en forme 03/05/2024 16:41:00

Police :10 pt, Non Gras

Page 131 : [570] Mis en forme 03/05/2024 16:41:00

Police :10 pt

Page 131 : [571] Mis en forme 03/05/2024 16:41:00

Police :10 pt

Page 131 : [574] Mis en forme **03/05/2024 16:41:00**

Police :10 pt

Page 131 : [575] Mis en forme **03/05/2024 16:41:00**

Police :10 pt

Page 131 : [576] Mis en forme **03/05/2024 16:41:00**

Police :10 pt

Page 131 : [577] Mis en forme **03/05/2024 16:41:00**

Police :10 pt

Page 131 : [578] Mis en forme **03/05/2024 16:41:00**

Police :10 pt, Non Gras

Page 131 : [579] Mis en forme **03/05/2024 16:41:00**

Police :8 pt

Page 131 : [580] Mis en forme **03/05/2024 16:41:00**

Police :10 pt

Page 131 : [581] Mis en forme **03/05/2024 16:41:00**

Police :10 pt

Page 131 : [582] Mis en forme **03/05/2024 16:41:00**

Police :10 pt

Page 131 : [583] Mis en forme **03/05/2024 16:41:00**

Police :10 pt

Page 131 : [584] Mis en forme **03/05/2024 16:41:00**

Police :10 pt

Page 131 : [585] Mis en forme **03/05/2024 16:41:00**

Police :10 pt

Page 131 : [586] Mis en forme **03/05/2024 16:41:00**

Police :10 pt

Page 131 : [586] Mis en forme **03/05/2024 16:41:00**

Police :10 pt

Page 131 : [587] Mis en forme **03/05/2024 16:41:00**

Police :10 pt

Page 131 : [588] Mis en forme **03/05/2024 16:41:00**

Police :10 pt, Gras

Page 131 : [590] Mis en forme 03/05/2024 16:41:00

Police :10 pt, Gras

Page 131 : [591] Mis en forme 03/05/2024 16:41:00

Police :10 pt

Page 131 : [592] Mis en forme 03/05/2024 16:41:00

Police :10 pt

Page 131 : [593] Mis en forme 03/05/2024 16:41:00

Police :10 pt, Gras

Page 131 : [593] Mis en forme 03/05/2024 16:41:00

Police :10 pt, Gras

Page 131 : [594] Mis en forme 03/05/2024 16:41:00

Police :10 pt, Non Gras

Page 131 : [595] Mis en forme 03/05/2024 16:41:00

Police :10 pt

Page 131 : [596] Mis en forme 03/05/2024 16:41:00

Police :10 pt

Page 131 : [597] Mis en forme 03/05/2024 16:41:00

Police :10 pt

Page 131 : [598] Mis en forme 03/05/2024 16:41:00

Police :10 pt

Page 131 : [599] Mis en forme 03/05/2024 16:41:00

Police :10 pt

Page 131 : [600] Mis en forme 03/05/2024 16:41:00

Police :10 pt

Page 131 : [601] Mis en forme 03/05/2024 16:41:00

Police :10 pt

Page 131 : [602] Mis en forme 03/05/2024 16:41:00

Police :10 pt, Non Gras

Page 131 : [603] Mis en forme 03/05/2024 16:41:00

Police :10 pt

Page 131 : [606] Mis en forme **03/05/2024 16:41:00**

Police :10 pt

Page 131 : [607] Mis en forme **03/05/2024 16:41:00**

Police :10 pt

Page 131 : [608] Mis en forme **03/05/2024 16:41:00**

Police :10 pt

Page 131 : [609] Mis en forme **03/05/2024 16:41:00**

Police :10 pt

Page 131 : [609] Mis en forme **03/05/2024 16:41:00**

Police :10 pt

Page 131 : [610] Mis en forme **03/05/2024 16:41:00**

Police :10 pt, Non Gras

Page 131 : [611] Mis en forme **03/05/2024 16:41:00**

Police :10 pt

Page 131 : [612] Mis en forme **03/05/2024 16:41:00**

Police :10 pt

Page 131 : [613] Mis en forme **03/05/2024 16:41:00**

Police :10 pt

Page 131 : [614] Mis en forme **03/05/2024 16:41:00**

Police :10 pt

Page 131 : [615] Mis en forme **03/05/2024 16:41:00**

Police :10 pt

Page 131 : [616] Mis en forme **03/05/2024 16:41:00**

Police :10 pt

Page 131 : [617] Mis en forme **03/05/2024 16:41:00**

Police :10 pt

Page 131 : [618] Mis en forme **03/05/2024 16:41:00**

Police :10 pt

Page 131 : [619] Mis en forme **03/05/2024 16:41:00**

Police :10 pt, Gras

Page 131 : [619] Mis en forme **03/05/2024 16:41:00**

Police :10 pt

Page 131 : [622] Mis en forme 03/05/2024 16:41:00

Police :10 pt

Page 131 : [623] Mis en forme 03/05/2024 16:41:00

Police :10 pt

Page 131 : [624] Mis en forme 03/05/2024 16:41:00

Police :10 pt

Page 132 : [625] Supprimé 03/05/2024 16:41:00

Page 147 : [626] Mis en forme 03/05/2024 16:41:00

Normal, Bordure : Haut: (Pas de bordure), Bas: (Pas de bordure), Gauche: (Pas de bordure), Droite: (Pas de bordure), Entre : (Pas de bordure)

Page 147 : [627] Mis en forme 03/05/2024 16:41:00

Forcer une largeur de colonne identique

Page 147 : [628] Mis en forme 03/05/2024 16:41:00

Anglais (G.B.)

Page 147 : [628] Mis en forme 03/05/2024 16:41:00

Anglais (G.B.)

Page 147 : [628] Mis en forme 03/05/2024 16:41:00

Anglais (G.B.)

Page 147 : [629] Mis en forme 03/05/2024 16:41:00

Police :Gras, Anglais (G.B.)

Page 147 : [630] Tableau mis en forme 03/05/2024 16:41:00

Tableau mis en forme

Page 147 : [631] Mis en forme 03/05/2024 16:41:00

Retrait : Gauche : 0,25 cm

Page 147 : [632] Supprimé 03/05/2024 16:41:00

Director, Office of Science, Office of Biological and Environmental Research of the US Department of Energy under Contract No. DE-AC02-05CH11231 to Lawrence Berkeley National Laboratory as part of the RUBISCO Scientific Focus Area,

WJR, OZ, E3SM/ELM simulations

Page 147 : [633] Mis en forme 03/05/2024 16:41:00

Espace Après : 6 pt

Page 147 : [636] Mis en forme 03/05/2024 16:41:00

Police :+Corps (Times New Roman), Anglais (G.B.)

Page 147 : [637] Supprimé 03/05/2024 16:41:00

▼

Page 147 : [638] Mis en forme 03/05/2024 16:41:00

Espace Après : 6 pt

Page 147 : [639] Mis en forme 03/05/2024 16:41:00

Police :+Corps (Times New Roman), Anglais (G.B.)

Page 147 : [640] Mis en forme 03/05/2024 16:41:00

Police :+Corps (Times New Roman), Anglais (G.B.)

Page 147 : [641] Mis en forme 03/05/2024 16:41:00

Espace Après : 6 pt

Page 147 : [642] Tableau mis en forme 03/05/2024 16:41:00

Tableau mis en forme

Page 147 : [643] Mis en forme 03/05/2024 16:41:00

Police :+Corps (Times New Roman)

Page 147 : [644] Mis en forme 03/05/2024 16:41:00

Police :+Corps (Times New Roman)

Page 147 : [644] Mis en forme 03/05/2024 16:41:00

Police :+Corps (Times New Roman)

Page 147 : [645] Mis en forme 03/05/2024 16:41:00

Police :+Corps (Times New Roman)

Page 147 : [645] Mis en forme 03/05/2024 16:41:00

Police :+Corps (Times New Roman)

Page 147 : [646] Mis en forme 03/05/2024 16:41:00

Police :+Corps (Times New Roman), Anglais (G.B.), Indice

Page 147 : [647] Supprimé 03/05/2024 16:41:00

▼

Page 147 : [648] Mis en forme 03/05/2024 16:41:00

Espace Après : 6 pt

Page 147 : [649] Mis en forme 03/05/2024 16:41:00

Police :+Corps (Times New Roman)

Page 147 : [650] Mis en forme 03/05/2024 16:41:00

Police :+Corps (Times New Roman), Anglais (G.B.)

Page 147 : [651] Mis en forme 03/05/2024 16:41:00

Police :+Corps (Times New Roman), Anglais (G.B.)

Page 147 : [652] Supprimé 03/05/2024 16:41:00

[Funded by the Swedish Research Council VR \(2020-05338\) and Swedish National Space Agency \(209/19\)](#) [WZ: LPJ-GUESS simulations](#)

Page 147 : [653] Mis en forme 03/05/2024 16:41:00

Espace Après : 6 pt

Page 147 : [654] Tableau mis en forme 03/05/2024 16:41:00

Tableau mis en forme

Page 147 : [655] Mis en forme 03/05/2024 16:41:00

Police :+Corps (Times New Roman)

Page 147 : [656] Mis en forme 03/05/2024 16:41:00

Police :+Corps (Times New Roman)

Page 147 : [656] Mis en forme 03/05/2024 16:41:00

Police :+Corps (Times New Roman)

Page 147 : [657] Mis en forme 03/05/2024 16:41:00

Police :+Corps (Times New Roman), Anglais (G.B.)

Page 147 : [658] Mis en forme 03/05/2024 16:41:00

Espace Après : 6 pt

Page 147 : [659] Mis en forme 03/05/2024 16:41:00

Police :+Corps (Times New Roman)

Page 147 : [660] Mis en forme 03/05/2024 16:41:00

Police :+Corps (Times New Roman)

Page 147 : [661] Supprimé 03/05/2024 16:41:00

Page 147 : [662] Mis en forme 03/05/2024 16:41:00

Police :+Corps (Times New Roman), Anglais (G.B.)

Page 147 : [663] Mis en forme 03/05/2024 16:41:00

EU H2020 (725546 ERC METLAKE and 101015825 TRIAGE) , Swedish Research Councils VR (2022-03841) and Formas (2018-01794)

DB; inland waters - data and bottom up estimation

Page 147 : [666] Mis en forme 03/05/2024 16:41:00

Espace Après : 6 pt

Page 147 : [667] Tableau mis en forme 03/05/2024 16:41:00

Tableau mis en forme

Page 147 : [668] Mis en forme 03/05/2024 16:41:00

Police :+Corps (Times New Roman), Anglais (G.B.)

Page 147 : [669] Supprimé 03/05/2024 16:41:00

Page 147 : [670] Mis en forme 03/05/2024 16:41:00

Police :+Corps (Times New Roman), Anglais (G.B.)

Page 147 : [671] Supprimé 03/05/2024 16:41:00

Page 147 : [672] Mis en forme 03/05/2024 16:41:00

Espace Après : 6 pt

Page 147 : [673] Tableau mis en forme 03/05/2024 16:41:00

Tableau mis en forme

Page 147 : [674] Mis en forme 03/05/2024 16:41:00

Police :+Corps (Times New Roman)

Page 147 : [674] Mis en forme 03/05/2024 16:41:00

Police :+Corps (Times New Roman)

Page 147 : [675] Mis en forme 03/05/2024 16:41:00

Police :+Corps (Times New Roman), 12 pt, Anglais (G.B.)

Page 147 : [676] Mis en forme 03/05/2024 16:41:00

Espace Après : 6 pt

Page 147 : [677] Supprimé 03/05/2024 16:41:00

Funded by United Nations Environment Programme, Stanford University DTIE21-EN3143

RBJ; inversions and general budget support

Page 147 : [678] Mis en forme 03/05/2024 16:41:00

Espace Après : 6 pt

Page 147 : [679] Tableau mis en forme 03/05/2024 16:41:00

Tableau mis en forme

Page 147 : [682] Supprimé

03/05/2024 16:41:00

the Joint Fund for Regional Innovation and Development of the National Natural Science Foundation (Grant No. U22A20570); the Natural Sciences and Engineering Research Council of Canada (NSERC, #371706), Changhui Peng/TRIPLEX-GHG

Page 147 : [683] Mis en forme

03/05/2024 16:41:00

Espace Avant : 12 pt, Après : 6 pt

Page 147 : [684] Tableau mis en forme

03/05/2024 16:41:00

Tableau mis en forme

Page 147 : [685] Mis en forme

03/05/2024 16:41:00

Police :+Corps (Times New Roman)

Page 147 : [685] Mis en forme

03/05/2024 16:41:00

Police :+Corps (Times New Roman)

Page 147 : [686] Mis en forme

03/05/2024 16:41:00

Police :+Corps (Times New Roman)

Page 147 : [686] Mis en forme

03/05/2024 16:41:00

Police :+Corps (Times New Roman)

Page 147 : [687] Mis en forme

03/05/2024 16:41:00

Retrait : Gauche : -0,21 cm, Espace Avant : 12 pt, Après : 6 pt

Page 147 : [688] Mis en forme

03/05/2024 16:41:00

Police :+Corps (Times New Roman), Anglais (G.B.)

Page 147 : [689] Supprimé

03/05/2024 16:41:00

Page 147 : [690] Mis en forme

03/05/2024 16:41:00

Police :Gras

Page 147 : [691] Tableau mis en forme

03/05/2024 16:41:00

Tableau mis en forme

Page 147 : [692] Supprimé

03/05/2024 16:41:00

Page 147 : [693] Mis en forme

03/05/2024 16:41:00

Espace Après : 6 pt

Page 147 : [694] Tableau mis en forme

03/05/2024 16:41:00

Tableau mis en forme

Page 147 : [695] Mis en forme

03/05/2024 16:41:00

Francia

Page 147 : [698] Supprimé

03/05/2024 16:41:00

NASA High-End Computing (HEC) Program through the NASA Advanced Supercomputing (NAS) Division at NASA Ames Research Center

Matthew S. Johnson (MSJ)

Page 147 : [699] Mis en forme

03/05/2024 16:41:00

Espace Après : 6 pt

Page 147 : [700] Tableau mis en forme

03/05/2024 16:41:00

Tableau mis en forme